Dissertation zur Erlangung des Doktorgrades
der Fakultät für Chemie und Pharmazie
der Ludwig-Maximilians-Universität München

Regulation of Kindlin-2 function by protein-protein interaction and post-translational modifications

Marina Theodosiou

aus Pafos, Zypern

2018

Erklärung

Diese Dissertation wurde im Sinne von § 7 der Promotionsordnung vom 28. November 2011 von Herrn Prof. Dr. Reinhard Fässler betreut.

Eidesstattliche Versicherung

Diese Dissertation wurde selbstständig, ohne unerlaubte Hilfe erarbeitet.

München, 02.11.2018

Marina Theodosiou

Dissertation eingereicht am 02.11.2018

1. Gutachter Prof. Dr. Reinhard Fässler
2. Gutachter Prof. Dr. Olivier Gires

Mündliche Prüfung am 17.12.2018

To Anastasia & Kimon

Table of Contents

Summary

Integrins are heterodimeric transmembrane receptors composed by non-covalently linked α and β subunits. They are involved in cell extracellular matrix adhesions through binding to extracellular matrix molecules such as fibronectin, collagen, laminin. Integrins heterodimer consists of large extracellular domains which mediate ligand binding, single-span transmembrane domains and short cytoplasmic tails. Conformational changes, which affect the entire integrin molecule regulate integrin ligand binding affinity. Integrins shift from a low affinity state/bent-closed (BC) and extended-close (EC) conformations to a high affinity state/extended-open (EO) conformation. For the transition to high-affinity state/EO conformation transmembrane and tail domains are separated and the headpiece is opened increasing the ligand binding affinity.

Talin and kindlin bind β integrin cytoplasmatic tail and play a pivotal role in the process of integrin activation and signaling. Talin binding to the integrin tail induces conformation changes shifting integrin to the high affinity state/ EO conformation. Kindlin cooperates with talin in the process of integrin activation; however, the exact mechanism of action is still not well-defined. Regardless the mechanisms of action, talin and kindlin are essential for the process of integrin activation. However, conflicting results exist if both proteins have to be co-expressed for proper integrin activation in non-hematopoietic cells. Furthermore, while several studies have shown how talin can be activated (release of the autoinhibition state) and recruited to the plasma membrane through the interaction with different proteins and second messengers, similar studies about kindlin regulation are missing. For this purpose, further studies are essential to understand how different interactors or post-translation modifications regulate kindlin function.

In the **first manuscript**, I analyzed the role of kindlin-2 tyrosine phosphorylation. In an attempt to identify possible tyrosine kinases that phosphorylate kindlin-2, we performed a kinase screening. I identified Abelson (Abl) tyrosine kinases and mapped the Abl phosphorylation site at tyrosine 179 of kindlin-2. Expression of phosphomimetic (Y179E) and phosphodeficient (Y179F) mutant kindlin-2 in kindlin knockout fibroblasts as well as in kindlin-2 depleted ILK fl/fl cells (experiments in ILK fl/fl cells were done by Dr. Ralph T. Böttcher) revealed that Y179 phosphorylation is important for circular dorsal ruffle formation. Furthermore, I performed a mass-spectrometry based screening to identify specific interacting partners for phosphomimetic (Y179E) and phosphodeficient (Y179F) kindlin-2

that will help unravel the underlying molecular mechanism of the kindlin-2 Y179 phosphorylation in these cells.

In the **first publication**, we analyzed how kindlin and talin contribute to integrin activation and signaling in non-hematopoietic cells. For this purpose, we generated mouse kidney fibroblasts lacking kindlin-1/2 or talin-1/2. These cells are unable to activate their integrins and to adhere. Re-expression of either kindlin or talin failed to rescue the phenotype, demonstrating that both proteins have to be co-expressed to activated integrins in non-hematopoietic cells. In contrast to talin-deficient cells, kindlin-deficient cells were not able to initiate isotropic spreading on fibronectin after Mn^{2+}-assisted integrin activation. To identify binding partner(s) of kindlin-2 that could explain the phenotype we performed a Yeast Two Hybrid screening (Y2H) and identified paxillin family members as novel binding partners of kindlin-2. Mechanistically we were able to show that upon integrin activation, kindlin recruits paxillin to nascent adhesions which binds focal adhesion kinase (FAK) resulting in its activation, which in turn facilitates cell spreading, proliferation and survival.

As a continuation of the second paper, in the **second publication** we further characterized the kindlin-2-paxillin interaction using crosslinking proteomics and cell biology by introducing kindlin-1/2 and talin-1/2-deficient (quadruple null) cells that I personally generated. We characterised two paxillin binding sites located in kindlin-2 PH and F0 domain. Both sites contribute to paxillin binding and mediate paxillin recruitment to integrin adhesion sites. Reconsitution of the quadruple cells with kindlin-2 (wildtype or deletion variants) or talin-1 allowed us to analyze both proteins and different kindlin-2 variants in the same cellular background. In the previous paper, we proposed that kindlin-2/paxillin complex in nascent adhesions activates Rac1 to induce isotropic spreading. In this paper, we overexpressed constitutively active Rac1 and tested if it will induce cell spreading in kindlin-2 as well as talin-1 reconstituted cell lines. Interestingly, only the kindlin-2 expressing cells were able to spread upon overexpression of constitutively active Rac1 suggesting that kindlin-2 must have additional function during cell spreading that talin-1 is unable to perform. Using mass spectrometry-based interaction studies I was able to show that kindlin-2 interacts with the Arp2/3 complex. Additional cell biology experiments lead us to the conclusion that kindlin-2 associates with paxillin to activate Rac1 and with the Arp2/3 complex to induce membrane protrusions.

Abbreviations

ABS	Actin binding site
ADMIDAS	Adjacent to metal-ion-dependent adhesion site
AJ	Adherent junction
BC	Bent-closed
Cdc42	Cell division cycle 42
CDRs	Circular dorsal ruffles
Coll	Collagen
CP	Capping protein
DD	Dimerization domain
DLC1	Deleted in liver cancer 1
Dock180	Dedicator of cytokinesis 180
EB	Epidermolysis bullosa
EC	Extended-close
ECM	Extracellular Matrix
EGF	Epidermal growth factor
EGFR	Epidermal growth factor receptor
ELMO1	Engulfment and motility 1
EMT	Epithelial to Mesenchymal Transition
EO	Extended-open
ERK	Extracellular-signal regulated kinase
FA	Focal adhesion
FAK	Focal adhesion kinase
FB	Fibrillar adhesion
FERM	Band 4.1/ Ezrin/ Radixin/ Moesin
FHL	Four-and-a-half LIM protein
FN	Fibronectin
GAP	GTPase activating proteins
GDI	Guanine nucleotide dissociation inhibitors
GEF	Guanine nucleotide exchange factor
GFOER	Glycine (G), phenylalanine (F),hydroxyproline (O), glutamic acid (E), arginine(R)
GFR	Growth factor receptor

GM-CSF	Granulocyte macrophage colony stimulating factor
GSK	Glycogen synthase kinase
HGF	Hepatocyte Growth Factor
IBS	Integrin binding site
ICAM	Intercellular adhesion molecule 1
ICAP	Integrin cytoplasmic domain-associated protein-1
I-EGF	Integrin epidermal growth factor-like
IGFR	Insulin growth factor receptor
ILK	Integrin-linked kinase
IMC	Inner molecular clasp
IPP	ILK-parvin-pinch
JNK	c-Jun n-terminal kinase
KS	Kindler syndrome
LAD	Leukocyte adhesion deficiency
LDV	Leucine(L), aspartate (D), Valine (V)
LFA-1	Lymphocyte function-associated antigen 1
LN	Laminin
MAdCAM-1	Mucosal addressin cell adhesion molecule-1
MIDAS	Metal ion dependent adhesion site
NA	Nascent adhesion
OMC	Outer membrane clasp
PDGF	Platelet derived growth factor
PDGFR	Platelet derived growth factor receptor
PH	Pleckstrin homology domain
PI3K	Phosphatidylinositol 3-kinase
PIP_3	Phospholipid phosphatidylinositol (3,4,5)-trisphosphate
PIPKIγ	Phosphatidylinositol phosphates kinase type Iγ
PKB	Protein kinase B
PKC	Protein kinase C
PSI	Plexin/semaphoring/integrin
PTB	Phosphotyrosine binding
Rac1	Ras related C3 botulinum toxin substrate 1
RGD	Arginine(R),glycine(G),aspartate(D)

RhoA	Ras homologous
RhoGDIa	Rho GDP-dissociation inhibitor α
RIAM	Rap1-GTP interacting adapter molecule
ROCK	Rho-associate kinase
SDL	Specificity determining loop
Smad	Small body size mothers against decapentaplegic
SOS	Son of sevenless
SCC	Squamous cell carcinoma
SyMBS	Synergistic metal ion binding site
TGFβ	Transforming growth factor β
TMD	Transmembrane domain
VASP	Vasodilator-stimulated phosphoproteins
VBS	Vinculin binding site
VCAM1	Vascular cell adhesion molecule 1
VEGFR	Vascular endothelial growth factor receptor
VN	Vitronectin
WASP	Wiskott-Aldrich syndrome protein

1. Introduction

1.1. Integrin receptor family and adhesion

Tightly regulated mechanisms of cell adhesion to extracellular matrix (ECM) and cell-cell interaction were the prerequisite for metazoan evolution from their unicellular ancestors. These cell communication mechanisms are important for the establishment of multicellular sophisticated structures such as circulatory and immune systems that are required for proper metazoans development. One of the most characterised family of receptor involved in these functions is the integrin family (Johnson et al., 2009). Integrins are transmembrane proteins that mediate the linkage between the ECM and the cytoskeleton (Burke, 1999; Hynes, 2002; van der Flier and Sonnenberg, 2001). The regulation of their affinity by inside-out and outside-in signaling is an important feature for a plethora of biological phenomena such as cell adhesion, migration, proliferation, apoptosis, gene expression and differentiation (Giancotti and Ruoslahti, 1999).

1.1.1. Integrin subtypes and functions

In general, all multicellular organisms express integrins and homologous sequences have also been identified in prokaryotes (Sebe-Pedros et al., 2010). Integrins are heterodimeric transmembrane proteins composed of non-covalently linked α and β subunits. - Human genome contains 18 α and 8 β subunit genes leading to 24 different α-β protein pairs. Each pair can recognize and bind to a specific set of ECM proteins. Based on their ligand specificity and the presences of I domain in their α subunit, integrins can be categorized into different groups (Figure 1) (Hynes, 2002).

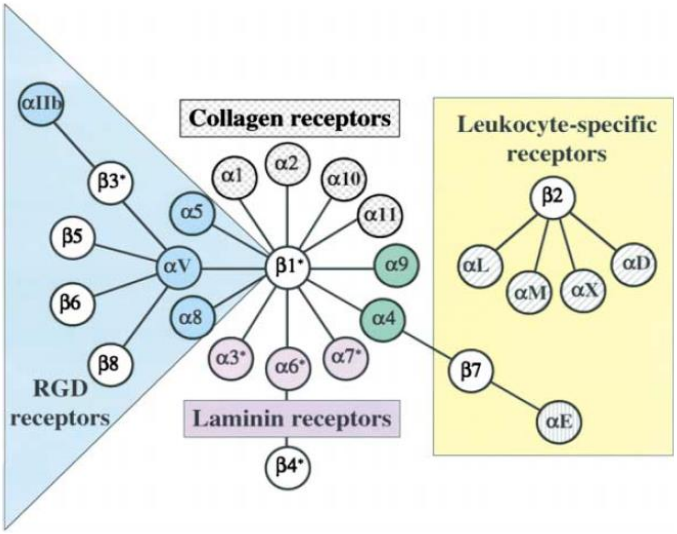

Figure 1: Classification of integrin receptor family. 24 α-β heterodimers are characterized until now. Lines indicate the combinations. Gray hatching or stippling indicate the a subunits which contain I domain. *Picture is adapted from (Hynes, 2002).*

αV containing heterodimers (αvβ1, αvβ3, αvβ5 αvβ6 and αvβ8) together with the α5β1, α8β1 and αIIbβ3, recognize the tripeptide amino acid sequence Arg-Gly-Asp (RGD). This peptide motif can be found in fibronectin (FN), fibrinogen, vitronectin (VN), osteopontin and thrombospondin as well as in Latency-Associated Protein (LAP) complex which is part of inactive transforming growth factor β (TGFβ). This subset of integrin heterodimers recognizes the RGD motif in this variety of ligands with different affinities and specificities. In particular, α3β1, α6β1, α7β1 and α6β4 are the major laminin (LN) receptors. These receptors bind to different regions/motifs of LN and show differences in specificity and affinity along the fifteen isoforms of LN (Humphries et al., 2006; Nishiuchi et al., 2006). The collagen (Coll) binding integrins are the α1β1, α2β1, α10β1 and α11β1 heterodimers thatrecognize the triple-helical Gly-Phe-Hyp-Gly-Glu-Arg (GFOGER) peptide sequence in the different Coll types. α4β1, α4β7, α9β1, the leukocyte specific receptors (αLβ2, αMβ2, αXβ2, αDβ2) and αEβ7 heterodimers bind related sequence in their ligand (Ley et al., 2007). α4β1, α4β7, α9β1 bind to Leu-Asp-Val (LDV) peptide sequence which can be found in FN, vascular cell adhesion molecule 1 (VCAM1) and mucosal addressin cell adhesion molecule-1 (MAdCAM1). The β2 heterodimers αLβ2, αMβ2, αXβ2, αDβ2 bind specifically to intercellular adhesion molecule 1 (ICAM1), VCAM1 and FN while αEβ7 to E-cadherin. VCAM1, MAdCAM1 and ICAM1 are surface proteins expressed by endothelial cells enabling leukocytes to bind to the endothelial layer and transmigrate into the tissue (Humphries et al., 2006).

The expression pattern of integrin heterodimers varies among the different cell types and tissues. For instance, β2 and β7 heterodimers are restricted to hematopoietic system in contrast to β1 heterodimers which can be found in almost all the tissues. Furthermore, the integrin repertoire of the cells can vary based on the developmental age and changes in the micro-environmental conditions.

Several studies using mouse genetics shed a light on the functional role of these proteins in the development and tissue homeostasis as well as in disease progression (Table 1). Integrin knockout mice fall into three different categories based on their phenotypes which are: (a) embryonic lethality, (b) perinatal lethality and (c) no obvious or mild defects. Deletion of β1 integrin, which is ubiquitously expressed and pairs with multiple α partners, causes embryonic lethality at embryonic day 6.5 due to preimplantation developmental defects (Fassler et al., 1995; Stephens et al., 1995). Deletion of α3 and α6 integrin leads to branching defects of the lung and kidney and severe delamination defects of the skin and cortex organization, respectively, causing perinatal lethality. On the other hand, deletion of

collagen receptors results in minor abnormalities without affecting fertility and viability, indicating asignificant redundancy and compensation among collagen receptors (Bouvard et al., 2001; Bouvard et al., 2013).

Integrin subunit	Mouse phenotype	Effects of loss	Link to human disease
α1	Viable, fertile	Defects in collagen synthesis, tumour angiogenesis, small kidneys, skin hardening	Unknown
α2	Viable, fertile	Defects in platelet adhesion, mammary ductal branching and kidney development	Unknown
α3	Perinatal lethal	Defects in kidney and lung development, skin blistering	Interstitial lung disease, nephrotic syndrome, epidermolysis bullosa
α4	Embryonic lethal	Defects in placenta formation, cardiac development and haematopoietic cell maintenance and homing	Unknown
α5	Embryonic lethal	Defects in neural crest cell survival and mesoderm formation	Unknown
α6	Perinatal lethal	Defects in brain cortex organization, skin blistering	Junctional epidermolysis bullosa with pyloric stenosis
α7	Perinatal lethal	Defects in vascular development and placenta formation, muscular dystrophy	Muscular dystrophy
α8	Perinatal lethal	Kidney defects, deafness	Unknown
α9	Perinatal lethal	Defects in lymphatic valve formation and in the development of the lymphatic system, congenital chylothorax*	Congenital chylothorax
α10	Viable, fertile	Dwarfism, mild chondrodysplasia	Unknown
α11	Viable, fertile	Dwarfism, increase mortality, defective incisor eruption	Unknown
αv	Embryonic or perinatal lethal	Defects in placenta formation and in CNS and GI blood cell development, cleft palate	Unknown
αx	Viable, fertile	T cell defects, increased susceptibility to bacterial infections	Systemic lupus erythematosus
αL	Viable, fertile	Impaired leucocyte recruitment and tumour rejection, defects in osteoclast development	Psoriasis
αD	Viable, fertile	Increased susceptibility to bacterial infections	Unknown
αM	Viable, fertile	Impaired phagocytosis and PMN apoptosis, obesity, defective mast cell development	Systemic lupus erythematosus
αE	Viable, fertile	Reduced lymphocyte numbers	Unknown
αIIb	Viable, fertile	Platelet abnormalities	Glanzmann's thrombasthenia, thrombocytopenia
β1	Embryonic lethal	Inner cell mass deterioration	Unknown
β2	Viable, fertile	Impaired leucocyte migration, skin infections, osteoporosis	LADI
β3	Viable, fertile	Platelet abnormalities, bone defects	Glanzmann's thrombasthenia, thrombocytopenia
β4	Perinatal lethal	Skin blistering	Epidermolysis bullosa
β5	Viable, fertile	No apparent phenotype	Unknown
β6	Viable, fertile	TGFβ activation defect, juvenile baldness, asthma, periodontal disease	Asthma
β7	Viable, fertile	Immunological defects	Inflammatory bowel disease
β8	Embryonic or perinatal lethal	Defects in placenta and in CNS and GI blood cell development, cleft palate	Unknown

CNS, central nervous system; GI, gastrointestinal tract; LADI, leucocyte adhesion deficiency type I; PMN, polymorphonuclear neutrophil; TGFβ, transforming growth factor-β. A fully referenced version of this table is available in supplementary information S1 (table).*Lymphatic fluid accumulation in the pleural cavity.

Table 1: Phenotypes of integrin knockout mice and their link to human diseases. *Table is adapted from (Bouvard et al., 2013).*

Human diseases have been associated with alteration in integrin expression or functionality. The lack of the β2 subunit gene or point mutations of the gene lead to the development of Leukocyte Adhesion Deficiency type I (LAD I). LAD I is a rare autosomal recessivly inherited disease characterized by recurring life-threatening infections, impaired wound healing and severe gingivitis and periodontitis (Schmidt et al., 2013). Mutations in either αIIβ or β3 subunits are associated with Glanzmann's thrombasthenia, a severe platelet

dysfunction and bleeding disorder (Hogg and Bates, 2000). Moreover, mutations in α6 or β4 integrin result in Epidermolysis Bullosa (EB) which is characterized by severe skin blistering and fragility (Takizawa et al., 1997; Vidal et al., 1995).

1.2. Integrin structure and activity

1.2.1. Structure of Integrins

Integrin α and β subunits are type I transmembrane glycoproteins with large extracellular domains (approx. 1104 amino acids for α and 800 amino acids for β subunits), single spanning transmembrane domains (TMD, 25-29 amino acids) and short cytoplasmic tails. The short cytoplasmic domains have lengths of 20-70 amino acids with the exception of β4 cytoplasmic tail being around 1000 amino acids (Wegener and Campbell, 2008).

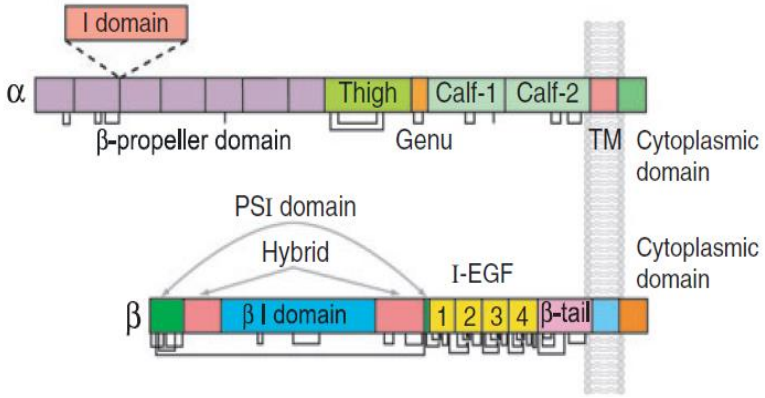

Figure 2: Schematic organization of integrin domains. Nine α-subunits contain an I domain. Cysteines and disulfides are depicted as lines below the stick figures *Picture is adapted from (Luo et al., 2007).*

1.2.1.1. Extracellular domain

The α subunit ectodomain can be subdivided into membrane proximal leg domain and distal ligand binding head domain. The N-terminal structure of the α ectodomain folds into a seven-bladed β-propeller domain while the α subunit leg domain contains an Ig-like Thigh domain and two extended β-sandwich domains named Calf-1 and Calf-2. Thigh and Calf-1 domain are connected by a small Ca^{2+}-binding loop which serves as a point for switchblade extension of the α subunit and is termed as genu. Additionally, 9 of the 18 α integrin subunits are characterized by the presence of αI domain (von Willebrand factor type A) of about 200 amino acids, which is inserted between the blades 2 and 3 of the β-propeller domain. The αI domain has five β-sheets surrounded by seven helices forming a divalent cation-binding site

at the top of the domain, which binds Mg^{+2} (Arnaout et al., 2007; Campbell and Humphries, 2011).

Similar to the α subunit, the head piece of β subunit is comprised of the plexin/semaphoring/integrin (PSI) which is interrupted by a β sandwich hybrid domain containing the βI domain of about 240 amino acids, that is homologous to αI domain. Specifically, the βI domain can be divided into two parts: the first allows the formation of the interface with the β-propeller of the α subunit and the second is essential for specific ligand binding, known as the specificity determining loop (SDL). The lower β subunit leg is characterized by four cysteine-rich integrin epidermal growth factor-like (I-EGF) 1-4 domains and a short disulfide-bonded β-sheet tail (β-tail). A flexible region is located between the I-EGF domains 1 and 2 (β-knee) and is adjacent to the α leg genu (Figure 2) (Arnaout et al., 2007; Luo et al., 2007).

As mentioned above, 9 of the 18 α subunits are characterized by the presence of the αI domain which mediates the binding to the ligand. In αI-less integrins, the ligand binding site called the integrin head is formed between the β-propeller domain of the α subunit and the βI domain of the β subunit (Zhu et al., 2013). αI and βI domains are structurally homologous and undergo similar conformational changes to regulate ligand binding affinity. Divalent cations bound at the metal ion-dependent adhesion sites (MIDAS) motif of the αI domain or βI domain regulate integrins ligand binding (Xia and Springer, 2014). In the βI domain, two additional Ca^{2+} binding sites can be found: (a) SyMBS (synergistic metal ion binding site) and (b) AdMIDAS (adjacent to MIDAS) which participate in integrin-ligand affinity regulation. Due to the presence of these sites integrin activation is influenced by divalent cations (Springer et al., 2008; Xia and Springer, 2014).

1.2.1.2. Transmembrane and cytosolic domain

The single spanning TMDs of integrins are characterized by the presence of 20 hydrophobic amino acids at their N-terminus, followed by a positively charged Arg or Lys, and a batch of hydrophobic amino acids at the C-terminus (membrane proximal region), which are highly conserved among species (Kim et al., 2011). Structural studies, using mainly αIIbβ3 integrin as a model, characterized two interaction sites termed as inner and outer membrane clasps. The outer membrane clasp (OMC) is mediated by the interaction of conserved glycine residues in the αIIb G972/G976 and β3 G708 allowing close packing of

the TMDs. The inner membrane clasp (IMC), is established by hydrophobic interaction of Phe residues (αIIb F992-F993) against the β3 TMD (β3 L712, W715, K716, I719) which promotes the electrostatic interaction between αIIb R995 and β3 D723 residues (Lau et al., 2009). Furthermore, structural analysis of aIIbβ3 TMD dimer embedded in bicelles revealed a 25° crossing angle between α-TMD and β-TMD with the β-TMD tilted in the membrane (Lau et al., 2009). TMD tilting is required for the formation of the IMC and OMC. Mutations leading to the disruption of the IMC (R995D or D723R) or OMC (G972L or G976L) destabilize the association of aIIb and β3 TMDs resulting in a constitutively active integrin (Hughes et al., 1996; Luo et al., 2005). It is widely accepted that TMD interaction stabilizes αIIβ3 in low affinity stage. Other studies, however, question whether this model can be applied to all integrin heterodimers, especially for β1 integrin (Czuchra et al., 2006; Lu et al., 2016), highlighting the importance of further research in this area.

Integrin cytoplasmatic domains/tails mediate integrin signaling and establish the connection to the actin cytoskeleton. Lacking any enzymatic activity, cytoplasmic tails perform their functions through the recruitment of adaptor proteins. The results from different structural studies propose that cytoplasmic tails are rather flexible and adapt certain structure in the presence of binding proteins (Campbell and Humphries, 2011). Membrane proximal NPxY and the membrane distal NxxY motifs are the hot-spot binding sites in β integrin tails. Both motifs are recognition sites for phosphotyrosine binding (PTB) domain containing proteins and mice carrying mutations in these motifs die at early embryonic stages due to impaired integrin function (Czuchra et al., 2006). Contrary to the β integrin tails, the sequences of α subunits are highly divergent except for a conserved GFFKR motif close to the TMD, which is part of the IMC. Due to the sequence diversity of α subunits, specific interacting proteins have been assigned for distinct subunits. Among them, SHARPIN and MDGI (mammary-derived growth inhibitor) were shown to inhibit integrin activation by binding to the highly conserved region of α integrin tails (Bouvard et al., 2013; Rantala et al., 2011).

1.2.2. Conformational regulation of integrins

It is widely accepted that integrins undergo large conformational changes. The three major conformational states of integrins are: the bent-closed conformation (BC), the extended-closed conformation (EC) and extended-open conformation (EO). Integrins can reversibly shift between the different states with BC to be the most abuntant on the cell

surface (Figure 3) (Li and Springer, 2018; Li et al., 2017b; Moore et al., 2018; Nishida et al., 2006; Springer and Dustin, 2012).

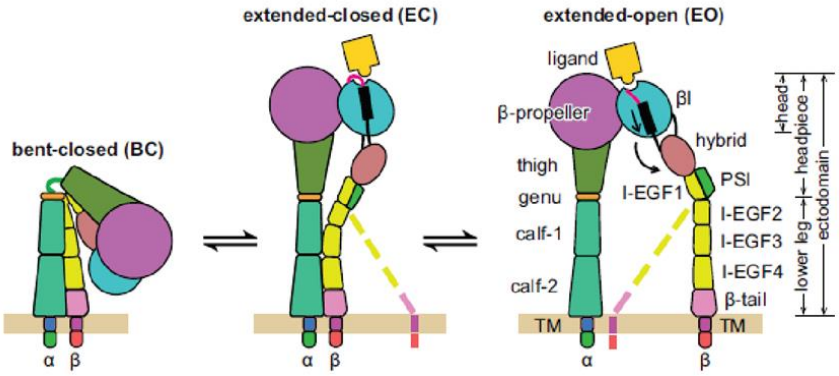

Figure 3: Schematic representation of conformational changes of integrins. In the BC state, no ligand binding can occur due to the orientation and closed conformation of the headpiece. This conformation is stabilized by tight interactions of the hybrid domain and the integrin leg piece regions. The EC is the result of a and b knees extension which raises the headpiece away from the cell membrane. Conformational changes in the headpiece, resulting in an EO and this change is coupled to the hybrid domain via pistoning of the βI-α7-helix (black cylinder), leading to hybrid domain swing out and stabilization of the high affinity conformation. *Picture is adapted from (Li et al., 2017b).*

The BC conformation is primarily stabilized by multiple contacts, between the headpiece/ hybrid domain and the lower legs, between the lower α and β legs (Calf-2 and β tail domain, EGF-2/3 domains with Calf-1) and between the α and β transmembrane and cytoplasmic domains. The overall contacts can be easily disrupted shifting integrin towards extension and separation (Luo et al., 2007; Takagi et al., 2003). In the BC, which represents a resting or inactive state of integrin, the ligand binding site is not in the optimal orientation (towards the cell membrane) for binding extracellular ligands. Thus, BC is characterized by lower ligand binding affinity than the EO form (Li et al., 2017b; Moore et al., 2018).

Extension of the α and β knees raises the integrin headpiece away from the plasma membrane leading to the trasition from a BC to EC conformation. However, further conformational changes in the headpiece cause an increase in the ligand binding affinity (4000-6000 fold for α5β1 and 600-800 fold for α4β1 increase) (Li and Springer, 2017; Li and Springer, 2018). More precisely, a swing-out of the hybrid domain away from the α subunit pulls downwards on the α7 helix of the βA domain promoting the upward movement of the α1 helix shifting the βA domain to a high affinity conformation (Luo et al., 2004; Xiao et al., 2004; Yang et al., 2004). A recent study showed that α5β1 integrin extension requires a free energy of about 4 kcal/mol while headpiece opening is energetically favored after extension, thereby concluding that extension is the major energy obstacle in integrin activation process

(Li and Springer, 2017). To favor integrin EO over EC, force (range of 0-4pN) by actomyosin system should be applied on ligand bound integrin through adaptor proteins which are bound to the β subunit cytoplasmic domain (Astrof et al., 2006; Li and Springer, 2017; Li and Springer, 2018; Puklin-Faucher et al., 2006).

1.3. Talin and kindlin roles in integrin activation process

Talin and kindlin bind integrin cytoplasmic tail. Talin binding to the integrin tail induces conformational changes towards the high affinity integrin state (EO state). How kindlin exactly contributes to integrin activation is not well understood (Kim et al., 2011; Shattil et al., 2010). It is suggested that kindlin promotes integrin clustering (Ye et al., 2013). Notably, a recent study, by Li and Springer showed that the role of talin and/or kindlin in the integrin activation process is to stabilize the EO conformation of ligand-bound integrin (Li and Springer, 2017). Regardless of the exact underlying mechanisms of action, talin and kindlin are essential for integrin activation since deletion of these proteins leads to severe integrin activation, adhesion and spreading defects (Calderwood et al., 2013; Theodosiou et al., 2016; Zhang et al., 2008).

1.3.1. Talin

Vertebrates contain two talin genes that encode the closely related proteins with distinct expression pattern, talin1 and talin2 (74% identity). Talin-1 is ubiquitously expressed while talin-2 is expressed in cardiac, skeletal muscles and in brain tissues (Critchley and Gingras, 2008). *Talin-1* knockout mice die at E8.5-9.5 due to arrested gastrulation (Monkley et al., 2000),while *talin-2* knockout mice are viable and fertile (Debrand et al., 2012).

1.3.1.1. Talin structure

Talin is a 270 kDa membrane associated protein, composed by two main regions, a 47 kDa N-terminal head and a 220 kDa C-terminal rod. The talin head is an atypical FERM (Band 4.1/ Ezrin/ Radixin/ Moesin) domain with an F0 domain additional to the F1, F2 and F3 subdomains and an extra insertion in the F1 domain. Through the PTB domain of the F3 subdomain, talin binds the membrane proximal NPxY domain of β integrin tails. Through the same site, it also binds Focal Adhesion Kinase (FAK), T-Cell Lymphoma Invasion and

Metastasis 1 (TIAM1), layilin (a hyaluronan receptor) and Phosphatidylinositol phosphates kinase type Iγ (PIPKIγ). The talin head is linked with the talin rod through an unstructured linker region. The talin rod is made up of 13 4-helix or 5-helix bundles (R1-R13) and a single helix dimerization domain (DD).

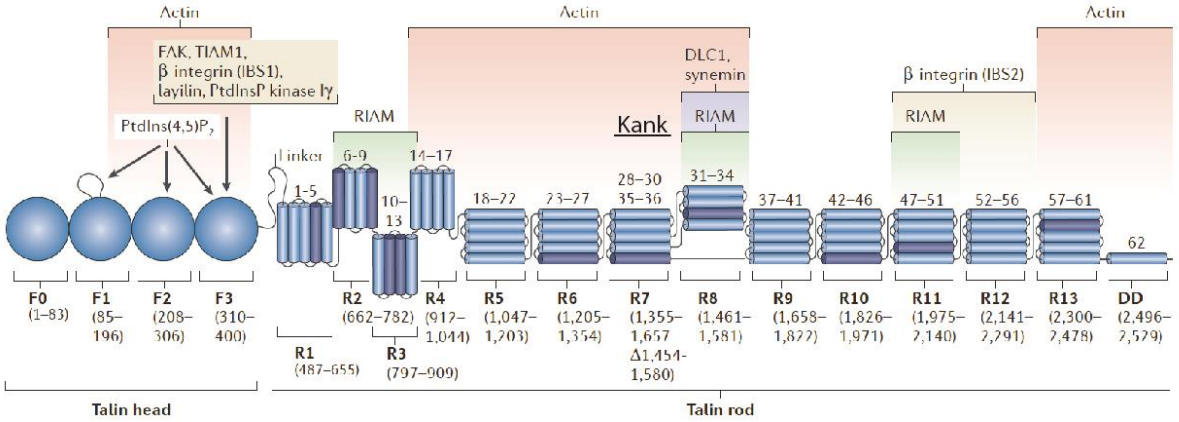

Figure 4: Domain organization of full-length talin. The scheme shows a hypothetical structure of talin and the interaction sites for talin binding proteins. Domains are indicated; F0-3represents FERM sub-domains 0-3, R1-13 represents rod domains 1-13, DD stands for dimerization domain. *Picture is modified from (Calderwood et al., 2013).*

The rod domain contains eleven identified vinculin binding sites (VBS), at least two actin binding sites (ABS2 and ABS3), a second integrin binding site (IBS2), several binding sites for Rap1-GTP interacting adaptor molecule (RIAM), binding site for KN motif and Ankyrin repeat domains (Kank) proteins, and binding sites for the tumor suppressor protein, Deleted in liver cancer 1 (DLC1) and for the intermediate filament protein, synemin (Figure 4) (Calderwood et al., 2013; Critchley and Gingras, 2008; Klapholz and Brown, 2017; Sun et al., 2016a).

1.3.2. Talin binding to integrin tail

Talin interacts with β integrin tails and disrupts the association of TMD between α and β integrins by changing the title angle of β integrin TMD. More specifically, thetalin F3 domain interacts with the membrane proximal NPxY motif and forms a salt bridge with the conserved aspartic acid residue in the membrane proximal region of the β integrin tail. Furthermore, interactions between conserved basic residues, in the F2 (Anthis et al., 2009b) and in the F1 loop (Goult et al., 2010) of talin with the acidic phospholipids in the plasma membrane play a key role in membrane binding and proper orientation of talin FERM

domain which contribute to the tilting of β integrin TMD (Figure 5). Phosphorylation or mutation of the tyrosine in the NPxY motif or the presence of proteins which compete with talin for integrin binding, such as Dedicator Of Cytokinesis 180 (Dock180) or filamin, interfere with talin-mediated integrin activation (Anthis et al., 2009a; Kiema et al., 2006; Oxley et al., 2008).

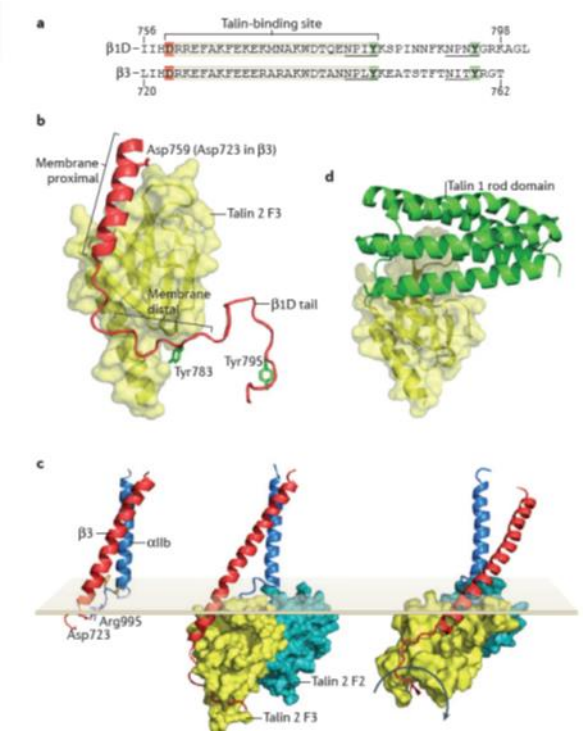

Figure 5: Structural basis of talin integrin binding . (a) Talin interaction sites are highlighted in β1A and β3 integrin cytoplasmic domain. (b) Crystal structure of talin in complex with the 1D tail. Talin interaction with Asp-759 and Tyr-783 are important for talin-integrin interaction and talin-dependent integrin activation (c) Talin binding to integrin modulates β integrin TMD topology. TMD dimerization by innermembrane clasp (IMC, Asp-723 and Arg-995) and transmembrane interaction stabilize integrin in inactive state (left); Talin binding to Asp-723 on β3 integrin tail disrupts the IMC (middle); talin binding to plasma membrane tilts β-TMD, induces TMD separation at outer membrane side and promotes conformation change in ectodomain (right). (d) Crystal structure of the autoinhibitory interaction between talin-F3 domain and R9 domain. *Picture is adapted from (Calderwood et al., 2013)*

The binding of talin to integrin tail is tightly regulated by different mechanisms. In general, talin is mainly localized in the cytosol in an autoinhibited state. The talin F3 domain binds the R9 domain in the talin rod, and thus the binding of F3 domain to the integrin tail is masked (Figure 5d). Disruption of the talin autoinhibition state and translocation to the plasma membrane can be regulated by several factors. The positively charged residues in the F3 domain, which interact with the negatively charged residues in the R9 domain can also interact with acidic membrane phospholipids (PtdIns(4,5)P_2) leading to talin activation (Goksoy et al., 2008). Of note, disruption of the F3-R9 interaction is not enough to recruit talin to the plasma membrane, additional targeting sequence in the FERM domain are masked by the interaction between the F2-F3 FERM and R1-R2 rod domains (Banno et al., 2012). Furthermore, vinculin binds to the rod domain of talin releasing the autoinhibition and promoting its membrane targeting (Banno et al., 2012). Membrane targeting of talin and subsequently integrin activation can be mediated through the small GTPase Rap1 and its effector protein RIAM. Rap1 becomes activated upon protease-activated receptor (PAR)

stimulation or through Protein Kinase C (PKC). Activated Rap1 recruits RIAM together with its binding partner talin to the cell membrane in a PtdIns(4,5)P_2 dependent manner. Interestingly, it has been shown that the lack of kindlin inhibits the Rap1-RIAM-mediated talin activation (Kahner et al., 2012). Another family of proteins, which mediates talin activation, is Kank. Kank proteins bind directly to the talin R7 domain through their evolutionarily conserved KN motif, promoting talin activation in a force-and Filamentous-actin (F-actin) independent manner (Bouchet et al., 2016; Sun et al., 2016b). In addition, talin can regulate its own activation through its binding to the PIPKIγ. In particular, talin F3 domain binds the PIPKIγ leading to its activation and recruitment to the plasma membrane (Di Paolo et al., 2002; Ling et al., 2002). Thus, more PtdIns(4,5)P_2 are locally synthesized, facilitating the proper orientation of talin head leading to integrin activation (Anthis et al., 2009b; Martel et al., 2001). Additionally, depletion of PIKIγ, specifically at focal adhesions (FAs), leads to slower recruitment of talin and vinculin to FAs (Legate et al., 2011).

Talin as cytoplasmic adaptor protein links actin cytoskeleton to integrin at the plasma membrane. It functions as mechanosensor as it undergoes conformational changes under forces transduced through the actin cytoskeleton. Early studies showed that forces (range of piconewton) on talin leads to the stretching of protein and the exposure of cryptic VBS which further promote the recruitment of vinculin leading to the stabilization of adhesions (del Rio et al., 2009; Jiang et al., 2003).

In summary, talin interacts simultaneously with integrin and actin and has a fundamental role in integrin activation and in the establishment of stable integrin-actin linkage.

1.3.3. Kindlin

Over the last decade, it has become clear that kindlin plays a key role in integrin activation and signaling (Montanez et al., 2008; Moser et al., 2009a; Moser et al., 2008; Ussar et al., 2008). Kindlin can directly bind to the integrin tail, and mutations that impair this binding abolish integrin activation (Bottcher et al., 2012). For more details about the kindlin family members and their molecular functions see section 1.6.

1.3.3.1. Kindlin structure

Kindlin, like talin, is characterized by the presence of a FERM domain thatconsists of F1, F2 and F3 subdomains. However, a recently solved crystal structure of kindlin showed

that unlike talin, which is characterized by an extended conformation (Elliott et al., 2010; Goult et al., 2010), kindlin adopts the expected cloverleaf-like arrangement for FERM domains (Li et al., 2017a). Additionaly as a unique attribute of kindlin, the F2 domain harbors one pleckstrin homology domain (PH), which enables interaction with multiple phosphoinositides at cell membranes (Lai-Cheong et al., 2010; Lemmon, 2008). The short positively charged region in the N-terminal, called F0 domain (ubiquitin like) and the unstructured loop in the F1 domain, are also required for kindlin binding to the plasma membrane (Bouaouina et al., 2012; Perera et al., 2011). Furthermore, based on bioinformatic analysis, kindlin possess nuclear export (NES) and nuclear localization (NLS) signals (Ussar et al., 2006).

Kindlin binds the β integrin tail through its F3 domain at three different sites: **(1)** the membrane distal NxxY motif **(2)** the serine/threonine motif presents N-terminal to the NxxY motif (TTV for β1 and STF for β3) and **(3)** the C-terminus region of β integrin tail (Figure 6) (Bottcher et al., 2012; Fitzpatrick et al., 2014; Harburger et al., 2009; Li et al., 2017a). How is the binding of kindlin to the integrin tail regulated? Does kindlin require an activation step prior the binding to the integrin tail like talins? It is still unclear if kindlin has to undergo an activation step to enable its binding to the integrin tail. While a study in *C.elegans* suggested that ILK (Integrin Linked Kinase) binding to kindlin can induce conformational changes promoting its binding to the integrin tail (Qadota et al., 2012), studies using mammalian kindlins were not able to confirm this mechanism (Fukuda et al., 2014; Huet-Calderwood et al., 2014). Competitive binding of other proteins to the kindlin-binding sites at the integrin tail such as Integrin Cytoplasmic domain-Associated Protein-1 (ICAP1) and filamin as well as phosphorylation of the tyrosine in the membrane distal NxxY motif can regulate kindlin binding to integrin tail (Bledzka et al., 2010; Calderwood et al., 2013; Liu et al., 2013). Furthermore, it is still mechanistically uncharacterised how kindlin contributes to integrin activation/stabilization of the EO conformation. It is suggested that kindlin controls integrin ligand binding by inducing integrin clustering however the underlyingunderling mechanism remains unclear (Ye et al., 2013) (for details about integrin clustering see section 1.4.1.). Interestingly, a recent study suggested that kindlin dimer formation promotes integrin clustering (Li et al., 2017a). However, further investigation is needed to understand the exact function of kindlin in theintegrin activation process.

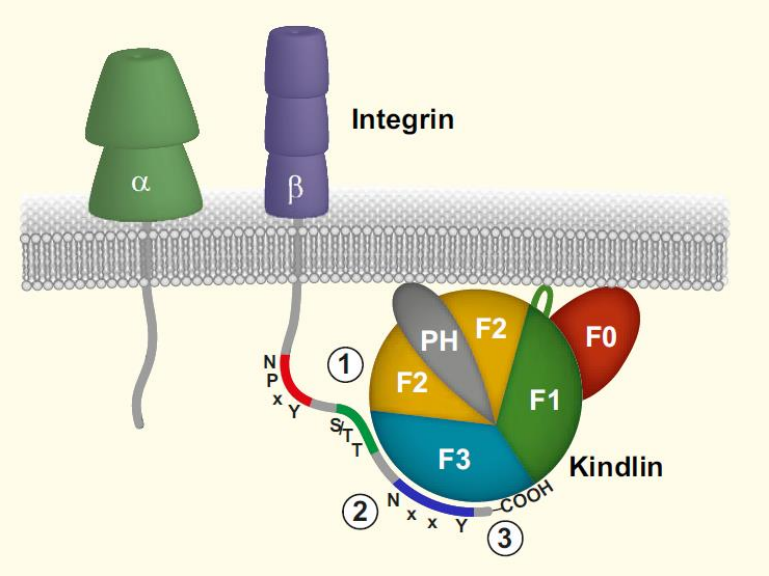

Figure 6: Integrin-kindlin binding sites. Kindlin through the F3 subdomains binds to three different motifs at the β integrin tails: 1) a serine/threonine motif 2) the membrane distal NxxY 3) and the C-terminus. *Picture is adapted from (Rognoni et al., 2016).*

1.3.4. Kindlin and talin binding to the integrin tail

Despite the plethora of studies concerning integrin activation and signaling, it is still unclear whether kindlin and talin bind consecutively or jointly the integrin tails. Three different binding models have been proposed: **1) Sequential binding model.** Based on a recent study in which the authors used a fluorescence fluctuation method, kindlin-2 unlike talin, is constantly associated with the β1 integrin tail in developing nascent adhesion (NA). This observation suggests a sequential binding of integrin activators and that kindlin binding facilitates talin recruitment (Bachir et al., 2014). **2) Cis co-operation model**. Based on NMR, size-exclusion chromatography, SPR (Surface Plasmon Resonance) experiments and ultracentrifugation studies both activators can bind simultaneously to β integrin cytoplasmatic tails (Bledzka et al., 2012; Yates et al., 2012). Thus formation of a ternary complex could induce the integrin activation. **3) Trans co-operation model**, kindlin and talin could be engaged at different integrin tails and cooperate in trans in integrin nanocluster (Figure 7) (Moser et al., 2009b).

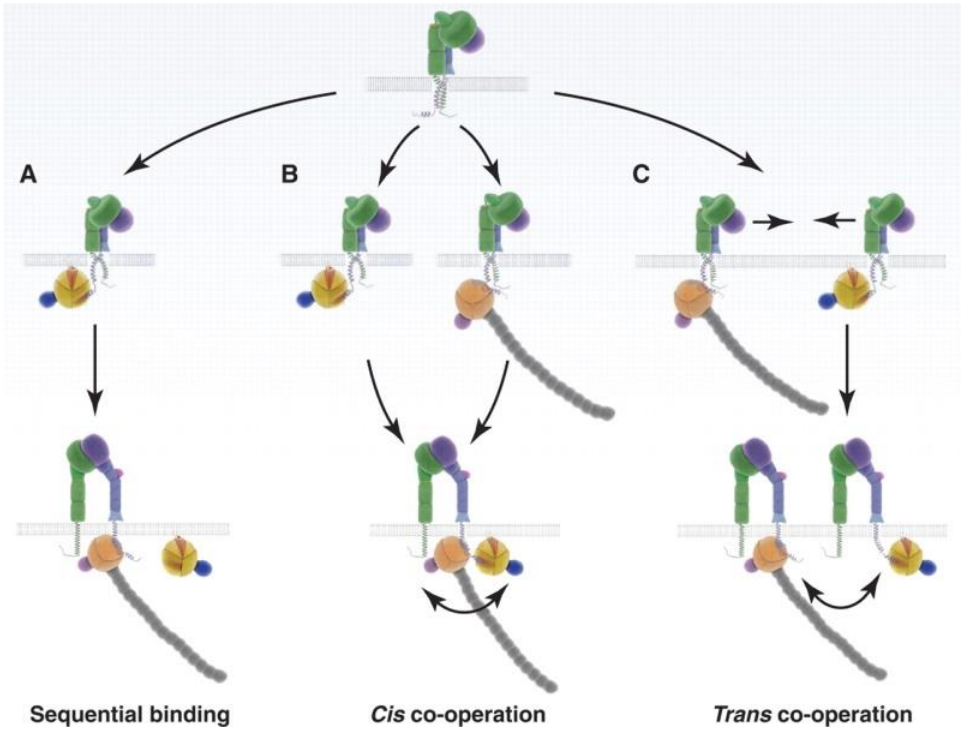

Figure 7: Putative binding modes of kindlin and talin binding to the β integrin tail. *Picture is adapted from (Moser et al., 2009b).*

1.4. Control of integrin-mediated adhesion

The ability of cells to adhere and simultaneously to probe their mechano-chemical environment is critical for development, wound healing, immunity and cancer. Integrin-mediated adhesion to the ECM plays a central role in these processes. Below I discuss how integrin ligand affinity can be modulated (integrin clustering, catch bond), how integrin adhesion structures transduce mechanical information (mechanotransduction) and describe the different adhesion structures that are present in cells.

1.4.1. Integrin clustering and catch bond formation contribute to adhesion strengthening

Adhesion strengthening of the integrin-ligand complexes can be mediated through integrin clustering and catch bond formation. Conformational changes in integrin receptors increase their affinity for the ligands. Since a single integrin-ligand interaction is not sufficient to establish cell adhesion to the ECM, lateral association of integrins (integrin

clustering) increases the overall strength of cellular adhesiveness (avidity) in a synergistic manner (Roca-Cusachs et al., 2009; Shi and Boettiger, 2003).

The underling mechanism of integrin clustering is still unknown; however, according to a recent model, clustering of integrins can be regulated by the mechanical resistance of the glycocalyx (Boettiger, 2012; Paszek et al., 2009). The model is based on the fact that integrins at the plasma membrane are surrounded by bulky membrane-bound glycoproteins, known as glycocalyx, which impede ECM access to integrins. The initial contact formation between integrin and ECM requires local removal and compression of glycocalyx as well as deformation of the cell membrane. After the initial integrin-ligand interactions, the cell surface will be closer to the ECM (due to the compression of glycocalyx) facilitating integrin clustering (Paszek et al., 2009; Paszek et al., 2014). The force generated through the compression of the surrounding glycocalyx imposes a pulling force on integrins promoting integrin extension, clustering and FA maturation (Figure 8). Furthermore, integrin associated proteins have been implicated in integrin clustering including talin (Ellis et al., 2014), kindlin (Ye et al., 2013) and α-actinin (Bachir et al., 2014; Roca-Cusachs et al., 2009).

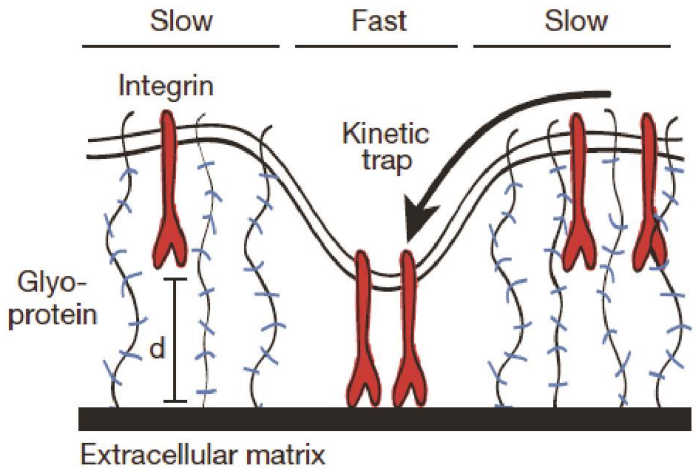

Figure 8: The role of glycocalyx in integrin clustering. The glycocalyx is a layer of glycoproteins bound to the cell surface (blue/black lines). Because of the height of glycocalyx, integrins (red) cannot reach the ECM. Local compression of glycocalyx and membrane deformation are required for the initial contact. After the initial contact is formed it brings the cell surface closer to the ECM facilitating integrin clustering. *Picture is adapted from (Paszek et al., 2014).*

The stability of bonds between cell adhesion molecules and ligands is mainly regulated by mechanical force. Generally, the lifetime of receptor-ligand bonds decreases with increasing applied force (slip-bond). Interestingly, catch bonds show opposite behavior as lifetime increases with tensile force applied to the bond (Thomas, 2008). The catch bond functions as a mechanical allostery altering molecular conformation and increasing stability of adhesive bonds (Friedland et al., 2009). *In vitro* Atomic Force Microscopy (AFM) methods, revealed catch bond behavior between FN fragment and α5β1 integrin in the range of 10-30 pN (Kong et al., 2009). Such catch bond behavior has not been observed for αIIbβ3

(Litvinov et al., 2011) or αvβ3 integrins (Jiang et al., 2003; Roca-Cusachs et al., 2009). Additionally, stretching of the bond between α5β1 integrin and FN by repeated application of mechanical forces (∼10 pN), significantly prolongs the bond lifetime in a process called "cyclic mechanical reinforcement" (Kong et al., 2013).

1.4.2. Integrin-mediated mechanotransduction and integrin-actin connection

Reciprocal interactions between the cells and their surrounding environment are important for fundamental biological processes such as organ development, tissue homeostasis, and also for pathogenesis. Cells are able to detect and react to mechanical cues from the surrounded ECM in a process termed as mechanosensing and mechanoresponse respectively, through integrin adhesion sites (Hoffman et al., 2011). In particular, at these sites, integrins connect the ECM with actin cytoskeleton and can transfer intracellular traction force, generated by the actin retrograde flow and myosin II to the ECM. In addition, extracellular mechanical cues, such as substrate stiffness and shear stress, can be sensed and translated into biochemical signals through integrin related signaling pathways (Sun et al., 2016a). Thus, adhesion sites serve as bidirectional mechanotransduction machineries for the cells.

During mechanotransduction, force induces changes in protein conformation, protein binding affinity or enzymatic reactions which in turn induce biochemical signals. Among the most important mechanosensitive adhesion proteins are talin, vinculin, α-actinin and filamins. These proteins can directly bind actin and the integrin tail, with the exception of vinculin, which interacts with integrin via talin.

Talin is a direct integrin interactor with several actin-binding sites and establishes the initial linkage between integrin and actin filaments with slip bonds of 2-pN amplitude (Jiang et al., 2003). Talin-depleted fibroblasts initially spread normally, but at later time points round up and are unable to form mature FAs. This phenotype can only be rescued after the overexpression of full length talin, but not by talin head (lack all C-terminal actin binding sites), showing that force transmitted between integrins and actin has a key role in integrin mechanosensing (Austen et al., 2015; Zhang et al., 2008). Furthermore, mechanical stretching of talin reveals cryptic binding sites for vinculin (del Rio et al., 2009). Talin has 11 VBS with the consensus sequence of LxxAAxxVAxxVxxLIxxA. Vinculin recruitment and interaction with talin strengthens the connection between talin and actin by further recruiting F-actin (Humphries et al., 2007).

Vinculin, a 117 kDa protein, consists of three main domains, an N-terminal head domain, a flexible proline-rich hinge region and the C-terminal tail domain (Goldmann, 2016; Peng et al., 2011). Vinculin exists in an inactive conformation in the cytosol and upon recruitment to FAs, it switches to an extended activated form. The presence of talin is a prerequisite for its recruitment to FAs and activation (Zhang et al., 2008; Ziegler et al., 2006). The process of activation is important for the interaction of vinculin with different proteins, such as α-actinin, VASP (Vasodilator-Stimulated Phosphoproteins), the Arp2/3 complex, paxillin and F-actin (Atherton et al., 2016). Vinculin knockout cells spread less, have fewer and smaller FAs and they show increase migration rate (Saunders et al., 2006; Xu et al., 1998). Further studies, showed that vinculin is required to strengthen and stabilize the talin-actin interaction by binding directly to both proteins (Gallant et al., 2005; Humphries et al., 2007).

The talin-vinculin axis is a major contributor for the integrin-actin linkage. Once a force is generated, another actin binding protein, α-actinin, is recruited to FAs (Laukaitis et al., 2001) via interactions with vinculin, talin and integrin. α-actinin is a key actin crosslinker forming an anti paraller dimer which connects bundles of F-actin fibers (Ribeiro Ede et al., 2014; Sjoblom et al., 2008). Knockdown of α-actinin leads to short actin filaments that are randomly oriented. As a consequence of the change in actin organization punctate adhesions are formed, near the leading edge,which are unable to mature. Thus, α-actinin has a key role in FAs maturation and actin cytoskeletal stability (Choi et al., 2008)

Furthermore, additional integrin bound proteins, which indirectly associate with or regulate actin cytoskeleton, contribute to the establishment and maintenance of the integrin-actin linkage such as ILK, kindlins, paxillin, tensin, and FAK. For example, ILK directly or via kindlin interacts with β integrin tail and connects to actin through parvin, forming the (ILK/ pinch/ parvin) IPP protein complex (Wickstrom et al., 2010).

In summary, integrin-actin connection is established and stabilized through different proteins at adhesion sites. This connection is essential for the transduction of mechanical information at adhesion sites.

1.4.3. Assembly of integrin-dependent adhesion structures

Integrin-based adhesions are higly complex structures that function as signaling centers. Differences in the protein composition, morphology, dynamics and localization of the adhesome structures can further subdivide these structures into nascent adhesions (NAs),

focal adhesions (FAs), fibrillar adhesions (FBs), podosomes and others (Figure 9) (Parsons et al., 2010).

Once a lamellipodium forms the first contact with the ECM, integrins are activated by the recruitment of talin and kindlin (inside-out signaling) and thus stabilize the connection of integrins with ECM. This is followed by integrin clustering and the initiation of NAs nucleation. These initial adhesion structures are dot-shaped, transient structures (lifetime ~ 60s) with less than 1 mm in diameter, which are formed in the lamellipodium region behind the leading edge of the cell (Geiger and Yamada, 2011; Sun et al., 2014). Their assembly and stability are myosin II independent but require Arp2/3 complex-mediated actin polymerization (Alexandrova et al., 2008). NAs are active adhesive signaling complexes as defined by the presence of highly tyrosine phosphorylated proteins such as paxillin, FAK and talin. They can either disassemble very fast or mature in an actomyosin dependent manner into FAs (Choi et al., 2008).

FAs are 1-5 µm long and have a lifetime up to 20 minutes. They are characterized by an elongated morphology and are generally found at the ends of actin filament bundles or stress fibers. Blebbistatin (myosin II inhibitor) treatment prevents adhesion maturation and increases the number of NAs. Myosin IIA overexpression increases NA maturation to FAs (Vicente-Manzanares et al., 2008). More specifically, generation of tension by myosin II induces conformational changes of focal adhesion proteins, leading to exposure of cryptic binding sites for other proteins or sites for post-translational modifications (Parsons et al., 2010). One such example is talin: conformational changes at the tailin rod domain, by force of the range of piconewton, promote the recruitment and binding of vinculin (del Rio et al., 2009). Thus vinculin is recruited to FAs in a force-dependent manner and further reinforces the connection between integrins and F-actin (Cohen et al., 2006; Humphries et al., 2007).

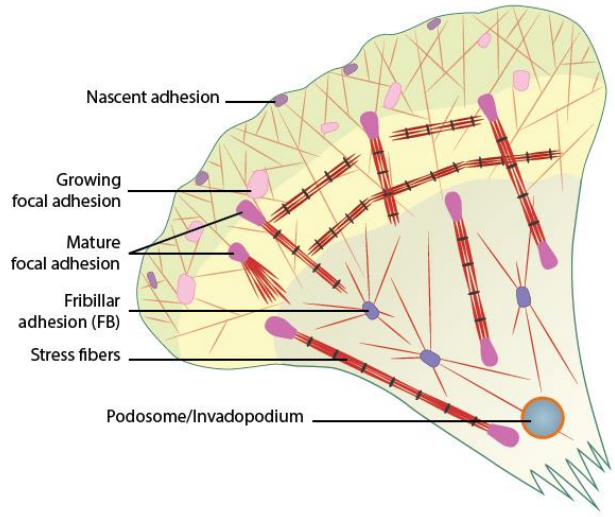

Figure 9: Different types of adhesion complexes. Initial contacts to the ECM are established in the lamellipodium supported by Arp2/3 that induce dendritic actin network leading to the formation of NAs. NAs undergo either disassembly or force-dependent maturation into FA. FAs are connected to thick stress fibers and can further mature into fibrillar adhesions. Podosomes/Invadopodium are other adhesion structures usually found in higly migratory cells, such as osteoclasts and cancer cells, respectively. *Picture is modified from MBInfo Wiki.*.

In fibroblasts, FAs can further mature into fibrillar adhesions (FBs). FBs are elongated structures with a lifetime of several hours and are found around the cell center. The maturation process is characterized by the recruitment of tensin as well as centripetal translocation of α5β1 integrin containing FAs, accompanied by the stretching of FN fibrils (Pankov et al., 2000). FBs have an active role in remodeling ECM and fibrilogenesis.

Podosomes are another adhesion structures mainly observed in highly migratory cells such as leukocytes, osteoclasts and endothelial cells. They are small, ring-shaped, highly dynamic adhesions (lifetime 2-10 minutes) characterized by a central actin core surrounded by adhesion-associated proteins. They function as sites of localized protease secretion and ECM degradation (Gimona et al., 2008).

1.5. Integrin signaling

Integrins can signal bi-directionally: information can flow from extracellular stimuli leading to intracellular changes (outside-in), but also intracellular stimuli can induce extracellular changes (inside-out signaling). Integrins lack any enzymatic activity and in order to perform their bi-directional signaling task, a multiprotein complex forms around the cytoplasmic tails called integrin adhesome. Until now, more than 200 adhesome proteins have been identified (Winograd-Katz et al., 2014). Some of these adhesion proteins serve as a scaffold for the physical connection of the integrin tails to the cytoskeleton and others are involved in adhesion-mediated signaling.

1.5.1. Integrin-mediated intracellular effects

Integrin activation leads to a series of intracellular changes. These changes can be divided based on time into different categories **1)** Immediate effects (first 10 minutes) **2)** Short term effects (10-60 minutes) and **3)** Long term effects (Figure 10).

The immediate consequences of integrin activation are mainly: **(1)** the upregulation of lipid kinases activity, including Phosphatidylinositol 3-kinase (PI3K) and PIPKIγ, which lead to the increased production of lipid second messengers PtdIns(4,5)P2 and PtdIns(3,4,5)P3 and **(2)** the rapid phosphorylation of different proteins. This local increase in the production of PtdIns(4,5)P2 can also promote talin activation and recruitment to the plasma membrane (see section 1.3.2.). Furthermore, phosphorylation of the integrin bound proteins creates binding sites for additional proteins at NAs. One of the immediate phosphorylation events after

integrin-mediated adhesion is the autophosphorylation of FAK at tyrosine 397, which enables the interaction with Src family kinases through the Src-homology 2 domain (SH2). Following this interaction Src phosphorylates FAK at additional tyrosine residues and maximizes its kinase activity (Mitra and Schlaepfer, 2006). This active FAK-Src complex phosphorylates various adhesion proteins such as paxillin and p130Cas, thereby activating several signal transduction cascades. The immediate responses lead to the activation of Ras homolog (Rho) family GTPases and other actin regulatory proteins that drive the rearrangement of the actin cytoskeleton and myosin-mediated force generation, allowing changes in cell morphology and migration. In addition, as a short term effect of integrin activation, Protein Kinase B (PKB also known as Akt), Glycogen Synthase Kinase (GSK), Extracellular-signal Regulated Kinases 1/2 (ERK1/2) and c-Jun n-terminal kinase (JNK) are activated. Finally, long-term attachment to ECM causes changes in gene expression and signaling pathways that influence survival, proliferation and differentiation (Legate et al., 2009).

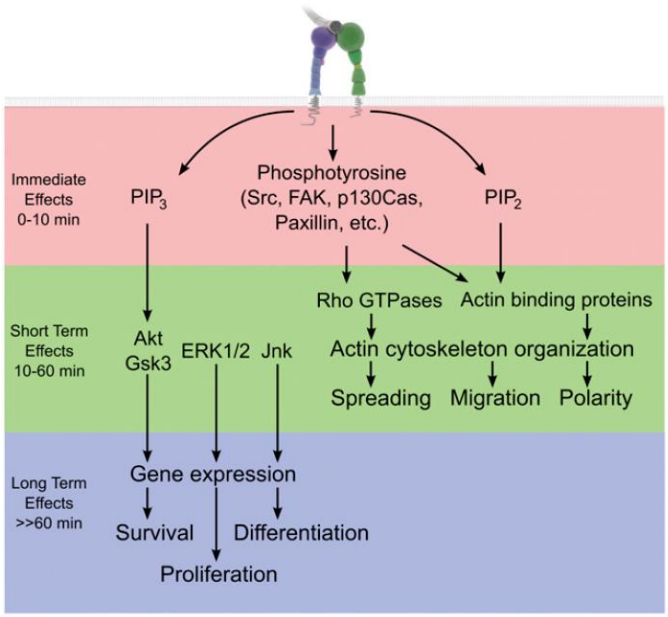

Figure 10: Consequence of integrin activation. The three temporal stages of integrin downstream signaling. *Picture is adapted from (Legate et al., 2009).*

The most essential components of integrin-mediated signaling are kindlins, FAK and paxillin. The role of these molecules will further discussed below (for kindins see section 1.6).

1.5.2. FAK

FAK is a non-receptor tyrosine kinase with a central role in integrin downstream signaling. The structure of FAK consists of an N-terminal FERM domain, a central kinase domain, prolin-rich regions and a C-terminal focal adhesion targeting domain (FAT) (Kleinschmidt and Schlaepfer, 2017; Mitra et al., 2005; Sulzmaier et al., 2014).

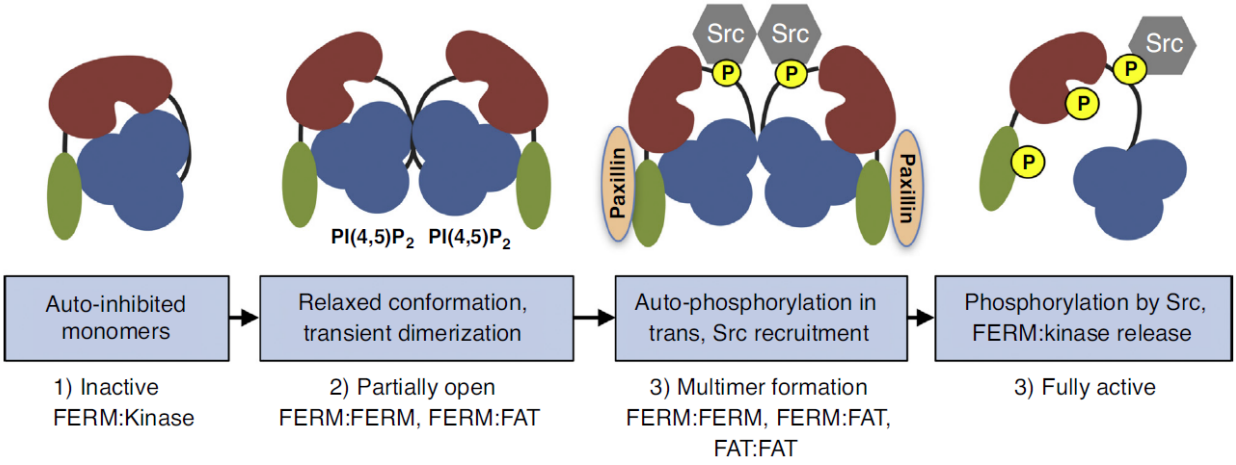

Figure 11: FAK activation proposed mechanism. 1) FAK autoinhibited state maintained by interactions between the FERM (blue) and kinase (brown) domains. 2) FERM binding to phosphatidylinositol-4,5-biphosphate [PI(4,5)P2] induces a relaxed conformation leading to FAK dimers through transient FERM:FERM and FAT:FAT interaction. 3) FERM:FERM and FAT:FAT dimerization allows FAK autophosphorylation at Y397 in trans (yellow) and thus exposing a binding site for Src. Paxillin reinforces FERM:FAT (FAT shown in green) interaction. 4) Src further phosphorylates FAK leading to FAK full activation. *Picture is adapted from (Kleinschmidt and Schlaepfer, 2017).*

FAK resides in the cytosol in an autoinhibited state through an intramolecular interaction between the FERM and kinase domains. Upon integrin engagement, paxillin binding to FAK facilities its recruitment to integrins. Locally enriched FAK molecules favor dimerization through the association of their FERM domains, while interaction between FAT and FERM domains further stabilize FAK dimers (Brami-Cherrier et al., 2014). These events cause FAK autophosphorylation at Y397, following recruitment and activation of Src kinase. Src kinase further phosphorylates FAK (Y576 and Y577) resulting in the formation and activation of FAK-Src complex (Figure 11) (Kleinschmidt and Schlaepfer, 2017).

Activated FAK functions both as a scaffold and as a kinase for many FAs proteins and plays a major role in actin and FAs dynamics thereby modulating in cell migration (Mitra et al., 2005; Sieg et al., 2000). Additionally, overexpression of FAK has been correlated with the invasive and metastatic potential of several tumors, while FAK knockout embryonic fibroblasts show an overabundance of FAs and decrease cell migration (Ilic et al., 1995;

Sulzmaier et al., 2014). FAK regulates actin dynamics mediated by Rac activation through its interaction with p130CAS-Crk-Dock180 and paxillin-GIT-PIX complexes. Binding of FAK to PI3K and Grb7 were also shown to promote cell migration (Mitra et al., 2005). Furthermore, FAK induces actin polymerization through its interaction with Arp2/3 complex and N-WASP (Serrels et al., 2007).

1.5.3. Paxillin

Paxillin is one of the early components of NAs and a major schaffold protein of FAs. Through its interaction with various adaptor proteins, kinases and phosphatases paxillin modulates integrin signaling controlling cell adhesion, spreading and migration. The Paxillin family is comprised of three members: paxillin (PXN), Hic-5 (TGFB1l1) and leupaxin (LPX), which share similar protein structure and interacting proteins but differ in their tissue expression pattern (Figure 12) (Deakin et al., 2012; Deakin and Turner, 2008).

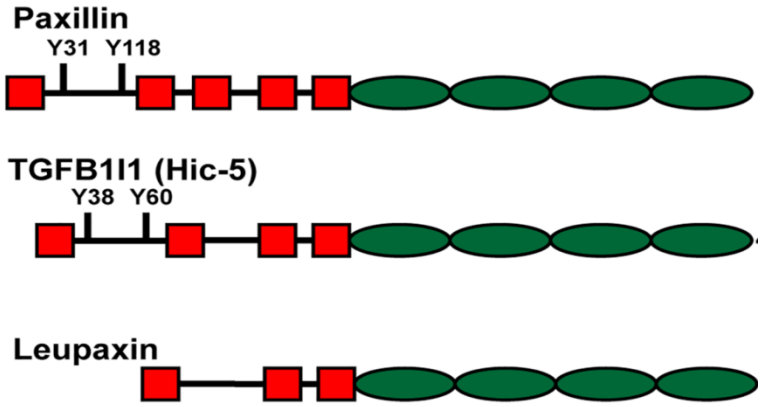

Figure 12: Paxillin family members and domain structure (LD motifs-red, LIM domains-green). *Picture is adapted from (Jacob et al., 2016).*

The C-terminus of paxillin consists of four LIM (Lin-11, Isl-1, Mec-3) domains, which are double zinc finger motifs. These motifs are mainly protein-binding domains, with the LIM-2/3 domains being essential for the targeting of paxillin to the plasma membrane (Brown et al., 1996). However, the underlying mechanism of paxillin recruitment to the plasma membrane remains unclear. Furthermore, paxillin LIM domains are binding sites for microtubules and tyrosine phosphatase PTP-PEST, and these interactions are important for adhesion dynamics and cell migration (Deakin and Turner, 2008; Efimov et al., 2008). The N-terminus characterized by the presences of leucine-rich (LD) domains.

Upon integrin adhesion to ECM, paxillin is phosphorylated. Paxillin phosphorylation regulates its binding to FA proteins including FAK, vinculin, PAK, ILK, talin, GIT and ARF.

Additionally, paxillin regulates the spatiotemporal activation of RhoGTPases by recruiting GEFs (Guanine nucleotide Exchange Factors), GAPs (GTPase Activating Proteins) and GDIs (Guanine nucleotide Dissociation Inhibitors) through its interactor partners to FAs. For instance, upon paxillin tyrosine phosphorylation (Y-31, Y-118) by the FAK/Src complex, the CrkII-DOCK180-ELMO complex can interact with paxillin through CrkII SH2 domain and thus promoting Rac1 activation (Valles et al., 2004). In addition, phosphorylated paxillin interacts with p120RasGAP, eliminating the binding between p120RasGAP and p190RhoGAP at the plasma mebrane and thereby inhibiting RhoA activation (Tsubouchi et al., 2002).

To sum up, FAK and paxillin are central integrin signaling components that play a major role in integrin downstream signaling and cell migration.

1.5.4. Integrin and growth factor cross-talk

Integrins and growth factor receptors (GFRs) collaborate at many different levels. The interplay of two receptors leads to changes, in the activity of integrin or GFRs associated signaling proteins or effectors. It still remains unknown if the cooperation between the receptors is achieved by direct interaction or through common effector-binding proteins. Signaling coordination between integrins and GFRs can be described as concomitant when both receptors can trigger, independently, the same signaling pathways (Ivaska and Heino, 2011; Legate et al., 2009). The best example is FAK activation. FAK autophosphorylation at tyrosine 397 is one of the earliest responses of integrin activation. This induces an interaction with Src, which leads to stabilization of Src catalytic activity and further phosphorylation of FAK kinase. However, FAK autophosphorylation can also be induced by growth factor signaling (Sieg et al., 2000). In either ways, FAK activation leads to the activation of downstream signaling such as the ERK and JNK/MAPK pathways (Figure 13). Another example of receptor crosstalk is the direct activation of GFRs by integrins in the absence of growth-factor stimulation. In fact, αVβ3 and β1 integrins can induce Epidermal Growth Factor Receptor (EGFR) phosphorylation in the absence of epidermal growth factor (EGF) (Moro et al., 1998). In addition, αVβ3 integrins mediate growth factor independent clustering of GFRs, such as the Vascular Endothelial Growth Factor Receptor 2 (VEGFR2) (Soldi et al., 1999), Platelet Derived Growth Factor Receptor (PDGFR) and Insulin Growth Factor Receptor-1 (IGFR-1) (Borges et al., 2000; DeMali et al., 1999; Schneller et al., 1997).

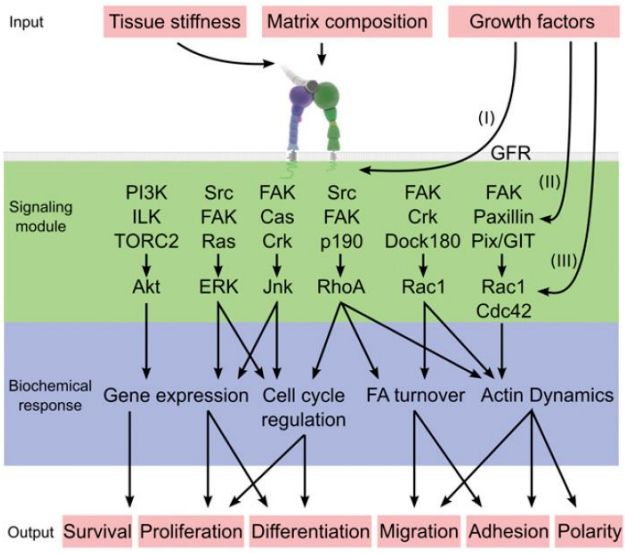

Figure 13: Integrin signaling and influence of growth factor environment and receptors. Integrin-mediated signaling interacts with growth factor signaling on multiple level: (I) integrin affinity for ligands, (II) the activity of the integrin-associated signaling proteins (FAK, Src, and PI3K), and (III) the activity of the downstream effectors (ERK, Akt, JNK, and the Rho GTPases). *Picture is adapted from (Legate et al., 2009).*

1.6. Kindlin family

In mammals, three kindlin paralogues can be found: *kindlin-1* (FERMT1; chromosome 20p12.3), *kindlin-2* (FERMT2; chromosome 14q22.1) and *kindlin-3* (FERMT3; chromosome 11q13.1). Genomic studies showed that all metazoans, but not premetazoans, have at least one *kindlin* gene. Based on phylogenetic analysis on vertebrate kindlins, *kindlin-2* appears to have the lowest rate of evolution and most likely maintained the ancestral features, while *kindlin-1* and *kindlin-3* originate from *kindlin-2* gene duplication (Khan et al., 2011; Meller et al., 2015). Although all three proteins share a high degree of similarity, around 60% amino acid sequence identity, protein specific functions and expression pattern have been -assigned to each member. Kindlin-1 expression is restricted to epithelial cells while kindlin-2 is ubiquitously expressed, with the exception of hematopoietic cells. Kindlin-3 is found in the hematopoietic system and also possibly expressed in endothelial and breast cancer cells (Bialkowska et al., 2010; Karakose et al., 2010; Meves et al., 2009; Sossey-Alaoui et al., 2014).

1.6.1. Kindlin-1 and kindlin-3

Mutations of the *kindlin-1* gene in humans are associated with Kindler Syndrome (KS), an autosomal recessive skin disease. Patients suffering from Kindler´s syndromeare characterized by skin blistering, skin atrophy with progressive poikilodermia, ulcerative colitis-like defect of the digestive system, photosensitivity and high risk for skin cancer development (Has et al., 2011). Keratinocytes from human patients display adhesion, spreading and migration defects (Herz et al., 2006). Knockout mice for *kindlin-1* die postnatally due to intestinal epithelial dysfunction and develop severe skin atrophy as a consequence of impaired integrin activation (Ussar et al., 2008). Despite the expression of kindlin-1 and kindlin-2 in keratinocytes, kindlin-2 cannot compensate the loss of kindlin-1 suggesting that these proteins exert similar but also specific functions (Bandyopadhyay et al., 2012; He et al., 2011; Ussar et al., 2008).

Deletion of *kindlin-1* specifically in skin epithelial cells in mice leads to skin blistering, basement membrane defects and skin inflammation, defects that can be attributed to the defective integrin-mediated adhesions (Rognoni et al., 2014). Interestingly, mice lacking kindlin-1 in skin epithelial cells are also characterized by an aberrant hair development and hair follicles cycles, enlarged stem cells compartments, hyperproliferative bulge stem cells and skin tumor development. These defects were attributed to αvβ6 integrin activation impairement resulting in a reduction in TGF-β signaling and in increased canonical Wnt/β-catenin signaling caused by enhanced transcription levels of Wnt ligands and receptors (Bandyopadhyay et al., 2012; Rognoni et al., 2014). Mechanistically, kindlin-1 binds to the β6 integrin tail leading to αvβ6 activation. Activated αvβ6 binds the RGD motif of LAP resulting in TGF-β release and TGF-β receptor signaling. The levels of Wnt signaling are controlled by kindlin-1 through an integrin-independent mechanism. Loss of kindlin-1 induces the nuclear translocation of β-catenin/LEF which leads to increase Wnt ligand and receptor transcription, and induction of canonical Wnt signaling. The authors suggest that kindlin-1 binds and retains a transcription factor in the cytoplasm thus controlling the transcription of Wnt ligands and receptors (Rognoni et al., 2014). Kindlin-1 has been shown to regulate TGF-β/Smad3 signaling in colorectal cancer cells. Kindlin-1 acts as an adaptor molecule for the formation of TGF-β receptor type I , Smad anchor for receptor activation (SARA), and Small body size Mothers Against Decapentaplegic (Smad3) complex and is required for the phosphorylation and nuclear translocation of Smad3 (Kong et al., 2016). Additionally, kindlin-1-deficient keratinocytes and squamous cell carcinoma (SCC) cells

have been shown to be more sensitive to DNA damage following oxidative stress. The authors, attribute the defects to kindlin-1-dependent activation of ERK and thus protection from DNA damage, a function of kindlin-1 which depends on its integrin binding ability (Emmert et al., 2017). Notably, kindlin-1 is not only localized at FAs. A recent study has shown that kindlin-1 trans-locates to centrosome, in an integrin- and phosphorylation-dependent manner, where it plays a role in the assembly of the mitotic spindle (Patel et al., 2013).

Kindlin-3, as the only member of the kindlin family expressed in hematopoietic system, binds β1, β2 and β3 integrin tails. Recent findings suggest the expression of kindlin-3 outside the hematopoietic system, specifically in epithelial and breast cancer cells, raising questions about the function of kindlin-3 in these cells and how kindlin-3 interferes with other kindlin isoforms expressed in these cells (Bialkowska et al., 2010; Sossey-Alaoui et al., 2014).

Loss of *kindlin-3* expression in humans leads to LADIII, a very rare autosomal recessive disease characterized by leukocyte adhesion defects, severe bleeding and osteopetrosis caused by defects in β1, β2, and β3 integrin activation in neutrophils, lymphocytes, platelets and osteoclasts (Schmidt et al., 2013; Svensson et al., 2009). Mice lacking *kindlin-3* die within the first week after birth. They are characterized by severe bleeding due to platelet dysfunction resultant from the inability of kindlin-3-deficient platelets to activate integrins (Moser et al., 2008). Furthermore, defects in the inflammatory responses and in adhesion and spreading of bone-resorbing osteoclasts upon kindlin-3 loss are due to impaired β2 integrin activation in leukocytes (Moser et al., 2009a) and β1, β2, and β3 integrin activation in osteoclasts (Schmidt et al., 2011).

In vitro experiments using kindlin-3-deficient hematopoetic cells used as a tool to further characterized the important function of kindlin-3. In effector T cells kindlin-3 is particularly important for the induction and stabilization of integrin-ligand bonds (α4β1 and αLβ2) when the ligand levels are low (Moretti et al., 2013). In B cells, kindlin-3 is not only required for the early transient integrin LFA-1 (Lymphocyte function-associated antigen 1) dependent adhesions but also for the final stable adhesions generated under flow conditions (Willenbrock et al., 2013). In dentritic cells kindlin-3 is required for the stabilization of LFA-1:ICAM bonds which are critical for lymphocyte arrest and spreading on dendritic cells. Impairment of kindlin-3 - β2 integrin interaction leads to increased granulocyte-macrophage colonystimulating factor (GM-CSF) receptor/Syk signaling which is associated with an accumulation of migratory dendritic cells in lymphoid organs and an increased Th1 immune

responses *in vivo* (Morrison et al., 2014). Interestingly, erythrocytes of kindlin-3-deficient mice are characterized by abnormal shape. Since integrins are not expressed in theses cells, this observation implies that kindlin-3 has functions that are not integrin-dependent (Kruger et al., 2008).

1.6.2. Kindlin-2

Kindlin-2 is the most widely expressed member of the kindlin family. Not surprisingly, ablation of kindlin-2 in mice causes peri-implantation lethality as a result of attachment failure between endoderm and epiblast to the basement membrane (Montanez et al., 2008). In adherent cells, kindlin-2 is mainly localized at FAs and cytoplasm. However, it can be detected in the cell-cell junctions of differentiated keratinocytes and epithelial cells as well as in the nucleus of chondrocytes, smooth muscle and tumor cells (Dowling et al., 2008a; Ussar et al., 2008; Wu et al., 2015; Yu et al., 2013; Yu et al., 2012). The localization of kindlin-2 in different cellular compartments, in combination with recent studies concerning its different functions, expand the role of kindlin-2 beyond integrin activation and cell-matrix adhesion.

Kindlin-2 is highly expressed in cardiac and skeletal muscles and is required for myocyte elongation and fusion (Dowling et al., 2008a; Dowling et al., 2008b). Mechanistically, during myogenic differentiation kindlin-2 forms a complex with a β-catenin and TCF4, binds to myogenic promoter and enhances its expression (Yu et al., 2013). In tubular epithelial cells, kindlin-2 has been shown to interact with TGFβ receptor type I and Smad3 leading to the activation of TGF-β/Smad signaling (Wei et al., 2013). Moreover, kindlin-2 promotes Epithelial to Mesenchymal Transition (EMT) in tubular epithelial cells through its interaction with Son of Sevenless homolog 1 (SOS-1), which promotes Ras activation and activates ERK1/2 and Akt signaling (Wei et al., 2014). Deletion of kindlin-2 in chondrocytes leads to progressive dwarfism, severe kyphosis, low bone mass and neonatal lethality. The defects in chondrocyte numbers and organization were due to reduction of Sox9 expression and inhibition of TGF-β1 induced Smad2 phosphorylation caused by kindlin-2 ablation (Wu et al., 2015). Kindlin-2 has been recently shown to be important for adherent junctions (AJs) formation, more precisesly kindlin-2 acts as a stabilizing linker of AJs by binding directly and simultaneously to β- or γ- catenin and actin (Pluskota et al., 2017). Kindlin-2 has been shown to implicate in EGFR signaling. Kindlin-2 interacts with EGFR

promoting EGF-induced breast cancer cell migration and also stabilizes EGFR protein by blocking its ubiquitination and degradation (Guo et al., 2015). Additionally kindlin-2 has been connected with tumor invasion. In fact, kindlin-2 in breast cancer cells was shown to form a transcriptional complex with active β-catenin and TCF4 and thus promoting Wnt signaling (Yu et al., 2012). Through the same signaling pathway, kindlin-2 also promotes hepatocellular carcinoma invasion and metastasis (Lin et al., 2017).

Kindlin-2 binds to β1, β2 and β3 integrin tails and plays an important role in recruitment of other focal adhesion proteins, such as ILK and migfilin (Montanez et al., 2008; Tu et al., 2003). Its direct interaction with ILK mediates the connection of kindlin-2 to the actin cytoskeleton through the IPP complex. However, a recent study has shown a direct interaction between kindlin-2 and actin, mapping an ABS in the F0 domain of kindlin-2. Through this direct interaction with actin, kindlin-2 supports cell spreading and actin organization (Bledzka et al., 2016). Additionally, kindlin-2 associates with Rho GDP-dissociation inhibitor α (RhoGDIα) and FHL1 (Four-and-a-half LIM protein 1) (Sun et al., 2017; Wang et al., 2018). Research in our laboratory (part of this PhD thesis) identified paxillin and Arp2/3 as kindlin-2 direct interactor partners (Bottcher et al., 2017; Theodosiou et al., 2016) (Figure14).

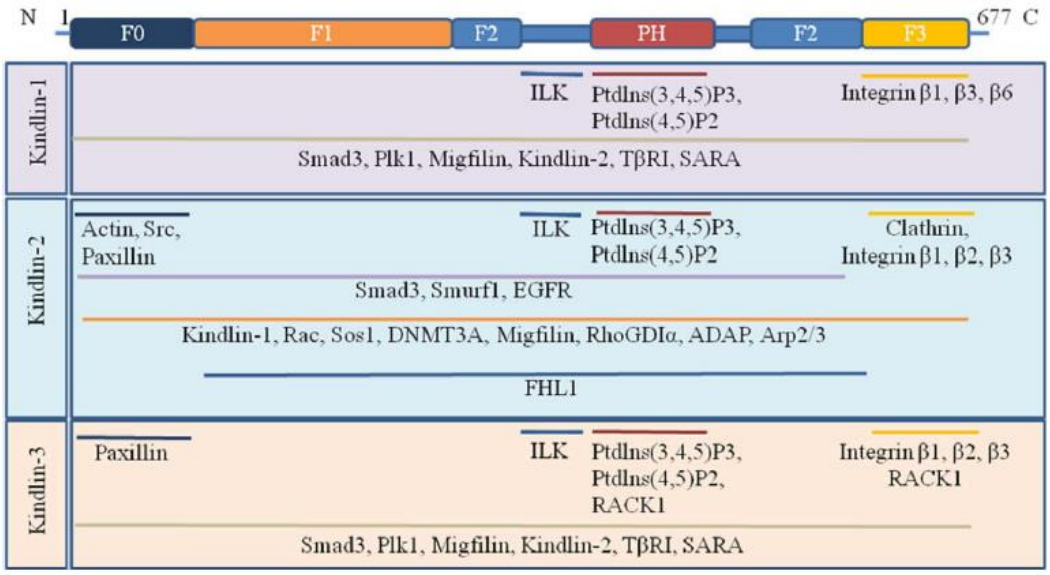

Figure 14: A shematic representation of kindlin family interactor partners. *Picture is adapted from (Zhan and Zhang, 2018).*

To sum up, kindlins together with talin play an essential role in the integrin activation process. Interestingly, recent studies strongly suggest that the role of kindlins extends beyond integrin-mediated adhesion.

1.6.3. Post-translational modification of kindlins

It still remains unclear how the functions as well as the localization of kindlins can be exactly regulated. Recent evidences suggest that post-translational modifications are important to regulate kindlins' localization and function.

Phosphorylation of kindlin-1 by Polo-like kinase (Plk) at Thr30 leads to its recruitment to the centrosomes where it interacts with different pericentriolar proteins and plays a role in the formation of the mitotic spindles (Patel et al., 2013). It has been shown that kindlin-2 tyrosine phosphorylation increases upon adhesion of the human podocytes to FN. Under these conditions, Src activity induces tyrosine phosphorylation of kindlin-2 as well as the formation of Src-kindlin-2 complex (Qu et al., 2014). On the other hand, another group has shown that Src can directly phosphorylate kindlin-2 at Tyr193, increasing its binding affinity towards migfilin and the recruitment of migfilin to FAs (Liu et al., 2015). More recently, another elegant study has shown that kindlin-2 serine phosphorylation induces the formation of invadopodia. The authors found a different phosphorylation status of kindlin-2 comparing the phosphorylation status of cancer cells plated either on gelatin or on high dense fibrillary collagen, a potent inducer of invadopodia formation (Artym et al., 2015). Additionaly, kindlin-2 levels were shown to be regulated by ubiquitination. More precisely, the E3 ligase Smurf1 interacts with the proline rich domain of kindlin-2 through its WW domain, ubiquitinates kindlin-2, leading to its proteosomal degradation, thus regulating integrin activation (Wei et al., 2017). Stimulation of platelets and HEL cells increases the phosphorylation of kindlin-3 at Thr482 and Ser484 sites, which are present only in kindlin-3. Mutation of these sites leads to a decrease in the soluble ligand binding and spreading of the cells on fibrinogen (Bialkowska et al., 2015).

Furthermore, calpain cleavage of kindlin-3 was shown to regulate the dynamics of integrin-kindlin-3 interaction. Stimulation of platelets and leukocytes lead to calpain-mediated cleavage of kindlin-3 at Tyr373. Calpain-resistant mutant kindlin-3-expressing cells are characterized by stronger adhesion and decreased migration rate as a result of the stabilized association of kindlin-3 with the integrin tail (Zhao et al., 2012). In addition, kindlin-3 has been shown to be a substrate of caspase-3 in a screening of proteolysis at the early stages of cutaneous wound healing. The authors mapped the site of kindlin-3 cleavage after Asp344 residue and suggested potential implications of cleavage in the apoptosis of hematopoietic cells during wound healing (Sabino et al., 2015).

1.7. Molecular pathways implicated in actin distribution and dynamics.

Dynamic actin polymerization and actomyosin contraction not only facilitate the assembly and maturation of FAs but also provide the driving force for the establishment of cell protrusion/retraction, thus enabling cell migration (Parsons et al., 2010). Cells construct actin based membrane protrusions that enable them to adhere, spread, migrate and degrade the ECM. Examples of these distinct structructes are the following: **Lamellipodia** are transient broad flat protrusions forming at the leading edge of cells. They are characterized by a dendritic, Arp2/3 complex-dependent actin network. **Filopodia** are finger-like protrusions which originate from the dentritic actin network of lamellipodia. They can support residual slow migration in the absence of lamellipodia. **Dorsal ruffles** are F-actin membrane projections on the apical cell surface and appear as highly dynamic rings. **Invadopodia** are protrusions of tumor cells that locally secrete proteases to degrade ECM, thereby enabling them to invade the BM. All of these structures contribute to migration depending on the specific circumstances (Krause and Gautreau, 2014).

1.7.1. Actin modulators

Various actin-binding proteins regulate actin polymerization, structure/morphology and stability. G-actin polymerization into F-actin produces polar double helix filaments with fast growing barbed and pointed ends.

The **Arp2/3** complex is the major actin nucleator in the lamellipodium and is higly conserved among the eukatyotes. It consists of seven different subunits. The Arp2/3 complex binds the side of preexisting actin filaments and generates new actin branches with a characteristic angle of 70^{o} (Goley and Welch, 2006; Pollard, 2007). Deletion of Arp2/3 complex members results in loss of lamellipodia formation and reduced cell migration (Suraneni et al., 2012; Wu et al., 2012). Nucleation-Promoting Factors (NPFs) are required for the activation of the Arp2/3 complex. Wiskott-Aldrich Syndrome protein (WASP) family members (N-WASP, WAVE1-3, WASH) interact through their VCA (Verprolin homology Connencting Acidic) domain with the Arp2/3 complex leading to its activation (Krause and Gautreau, 2014). Furthermore, small GTPase Rac and the phospholipid phosphatidylinositol (3,4,5)-trisphosphate (PIP_3), cooperate for the recruitment and activation of the SCAR–WAVE regulatory complex at the leading edge of lamellipodia upstream of Arp2/3 (Lebensohn and Kirschner, 2009). Arp2/3 actin nucleator activity and NAs are tightly

coupled and depend on each other. Several studies have shown that Arp2/3 is recruited to NAs through transient interactions with vinculin (Chorev et al., 2014; DeMali et al., 2002) and/or FAK (Serrels et al., 2007; Swaminathan et al., 2016).

Once the actin branching point is established by the Arp2/3 complex, new actin filaments can be elongated by two types of protein elongators: **ENA/VASP** and **formins**. These proteins associate with F-actin barded ends, thereby preventing binding of capping proteins and promoting the elongation of the filament by recruiting profilin-G-actin. In vertebrates, the ENA/VASP family proteins is composed of three members: MENA, EVL and VASP (Krause et al., 2002). They localize in growing free barbed ends of actin filaments of lamellipodia or filopodia. Cells lacking ENA/VASP proteins display shorter but highly branched actin filaments and lamellipodia. In contrast, overexpression of ENA/VASP leads to longer, less branched actin filaments and lamellipodia (Bear et al., 2002). Formins are characterized by the presences of two formin homology domains, FH1and FH2, which can nucleate linear actin filaments by staying associated with barbed ends. Therefore formins prevent capping (FH2) and promote processive elongation with the help of profilin (FH1) (Goode and Eck, 2007; Schonichen and Geyer, 2010). Another actin binding protein which plays a role in filopodia formation is fascin. **Fascin** is the major actin bundling protein, which localizes at the tip of filopodia and is required for their stability. Depletion of fascin results in a significant reduction of filopodia formation (Vignjevic et al., 2006).

Other actin interacting proteins that play a role in filaments stability are the **capping protein (CP)**, **cofilin** and **cortactin**. The actin CP is a heterodimeric protein composed of α and β subunits, which binds actin filaments at barded end inhibiting de-polymerization or elongation, leading to their stabilization (Wear and Cooper, 2004). Depletion of CP, resulted in loss of lamellipodia and increase in filopodia formation. Thus, CP plays an important role in lamellipodia and filopodia dynamics (Mejillano et al., 2004). Cortactin is a scaffold protein which stabilizes branched actin networks and inhibits de-branching through its interaction with the Arp2/3 complex and F-actin (Weaver et al., 2001). It mainly localizes at sites of dynamic actin assembly such as lamellipodia and invadopodia (Kirkbride et al., 2011). Study of cortactin knockdown cells has shown that cortactin promotes cell migration by increasing lamellipodia persistence and also adhesion assembly (Bryce et al., 2005). Cofilin belongs to the ADF/Cofilin family of actin-binding proteins, which have a central role in controlling actin dynamics (Bravo-Cordero et al., 2013). Cofilin depolymerizes actin filaments by providing free barbed ends for further polymerization increasing the off-rate of actin monomers from the barbed ends. By severing the existing actin filaments, cofilin creates new

barbed ends and hence new filaments, to which the Arp2/3 complex can then bind and stimulate branching (Ichetovkin et al., 2002).

All in all, the above proteins regulate actin polymerization, structure and stability and play major roles in the formation of actin-rich structures, which are important for cell migration.

1.7.2. RhoGTPases

All the actin modulators mentioned above are controlled by several signaling molecules. One of the key regulators of these proteins are members of the Rho family of small GTPases (Rho GTPases). Rho GTPases are ubiquitously expressed and more than 20 members have been identified in mammals. They act as molecular switches to control signal transduction by cycling between an active GTP-bound to an inactive GDP-bound conformation. Three types of regulatory proteins control this cycle: GEFs, GAPs and GDIs. Interaction with GEFs facilitates the exchange of GDP to GTP (activation) while GAP enhances the intrinsic GTPase activity (inactivation) of the Rho GTPases. GDIs sequester the GDP-bound form of some GTPases in the cytosol preventing their activation by GEFs.

The Rho family GTPases RhoA (Ras homologous), Rac1 (Ras related C3 botulinum toxin substrate 1) and Cdc42 (cell division cycle 42) are the best characterized members of the family and they have been associated with cytoskeleton rearrangements (Raftopoulou and Hall, 2004; Spiering and Hodgson, 2011). Rac1 and Cdc42 are required for the generation of actin-rich protrusions at the leading edge, namely lamellipodia (dendritic actin network) for Rac1 and filopodia (parallel linear actin filaments) for Cdc42. Despite the distinct actin architecture of these structures, they both initiate peripheral actin polymerization through the Arp2/3 complex. In contrast, RhoA stimulates actin polymerization through formins (mDia1). Furthermore, RhoA activates ROCK (Rho- associate kinase) leading to the phosphorylation and inactivation of myosin light chain phosphatase, thereby increasing myosin II-mediated contraction and bundling of actin (Huveneers and Danen, 2009; Parsons et al., 2010) (Figure 15).

RhoGTPases play an important role in cellular processes such as cell adhesion and migration. While regulating these cellular functions the members of the Rho family cooperate or antagonize each other (Guilluy et al., 2011). For instance, RhoA and Rac play antagonistic roles during cell adhesion. Rac promotes formation of NAs at the leading edge while RhoA-dependent contractility leads to FAs maturation. Initial adhesion and spreading are associated

with transient Rac activation and inhibition of RhoA, while the later adhesion is characterized by gradual RhoA activation and Rac inhibition (Choi et al., 2008; Price et al., 1998; Ren et al., 1999). Thus, the balance between Rac and RhoA activity seems to control the fate of adhesions.

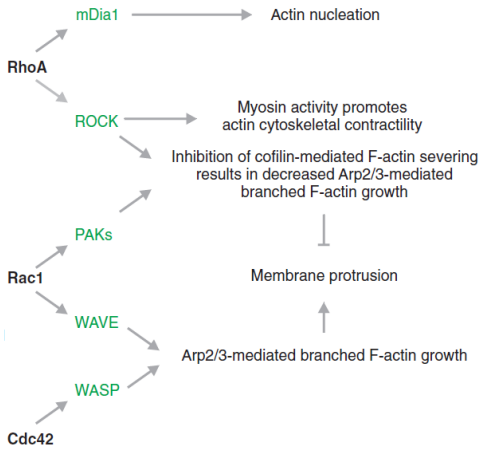

Figure 15: RhoA, Rac1 and Cdc42 through the recruitment of different effector proteins (green) regulate the actin cytoskeleton dynamics that are required for membrane protrusions and/or cytoskeletal contractility. *Picture is modified from (Huveneers and Danen, 2009).*

Integrins regulate Rho GTPase activity by recruiting different GEFs and GAPs to the adhesion sites. Initial cell adhesion and integrin activation induces FAK activation and the formation of Src/FAK complex. This active complex recruits and phosphorylates p130Cas, which leads to the recruitment of a complex composed of Dock180 (180 kDa protein downstream of CRK) and ELMO1 (engulfment and motility 1). The Dock180-ELMO1 complex serves as unconventional GEF for Rac, which promotes formation of membrane protrusions and subsequently cell migration (Brugnera et al., 2002). Furthermore, Src/FAK complex phosphorylates paxillin, which recruits a complex consisting of the ArfGAP PKL (paxillin-kinase linker)/GIT (G-protein-coupled receptor kinase interacting protein) and β-PIX (PAK-interacting exchange factor-beta), acting as a GEF for Rac1 (ten Klooster et al., 2006). In addition, FAK activation and phosphorylation promote SH2-mediated binding of p120RasGAP to FAK and FAK-mediated p190A tyrosine phosphorylation, leading to the formation of a FAK-p120RasGAP-p190A complex. FAK activity induces the recruitment of the complex to the leading edge FAs causing transient inhibition of RhoA activity (Tomar et al., 2009).

All in all, the tight regulation of Rho GTPases activity through different GEFs, GAPs and GDIs controls the actin polymerization and thereby plays a crucial role in adhesion and migration.

1.7.3. Circular dorsal ruffles

Growth factor stimulation can induce robust changes in the cytoskeleton beneath the plasma membrane leading to the formation of membrane ruffles. Membrane ruffles are small fin-shaped F-actin-enriched structures which are subdivided into peripheral and circular dorsal ruffles (CDRs) and can occur independently of each other (Chhabra and Higgs, 2007). Peripheral ruffles are persistent bending structures of the cell membrane at the leading edge which form immediately after growth factor stimulation. On the other hand, CDRs are transient, ring shaped structures found at the dorsal plasma membrane of cells, forming after 2 min of stimulation and disappearing within 30 min (Figure 16) (Buccione et al., 2004).

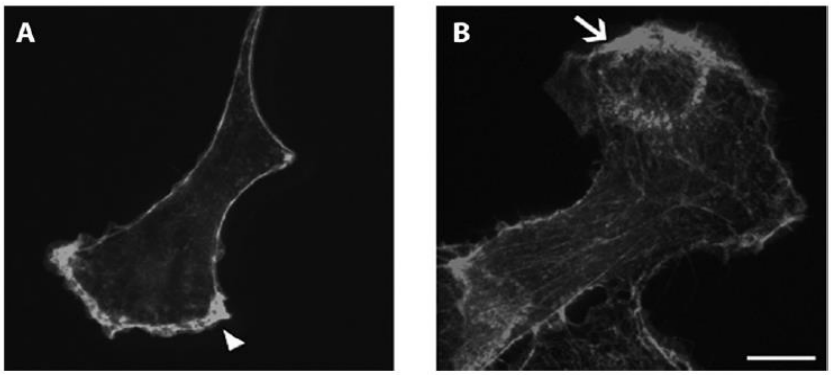

Figure 16: NIH 3T3 cells stained with phalloidin characterized by the presences of A) peripheral and B) dorsal ruffles. *Picture is adapted from (Hoon et al., 2012).*

CDRs play a role in internalization of transmembrane proteins and in the preparation of the cell for migration with the two functions to be interconnected. Cells shift to a motile state upon growth factor stimulation by rearanging their actin cytoskeleton. There is a high correlation between the site of CDRs formation and that of lamellipodium extension. Actin stress fibers are rapidly disassembled at CDRs leaving a fine cortical actin meshwork which is useful for lamellipodium formation (Hoon et al., 2012; Krueger et al., 2003). Intriguing studies have shown that CDRs composed an important platform for a clathrin-caveolin independent sequestration and internalization of receptor tyrosine kinases (RTKs) which specifically induce CDRs formation, for example the EGFR (Orth et al., 2006). Furthermore, upon growth factor stimulation integrins localize at CDRs where they are also internalized and recycled back to newly formed adhesions at the leading edge of migratory cells (Gu et al., 2011). CDRs are implicated also in macropynocytosis (Buccione et al., 2004; Hoon et al., 2012). Macropynocytosis describes the non-specific endocytosis of extracellular liquid and molecules of the cell (Bloomfield and Kay, 2016). It is an actin driven process which was

hypothesized to be dependent on CDRs formation (Dharmawardhane et al., 2000). Macropinosomes were shown to form at the site where CDRs disappear. Formation of CDRs in the cells was connected with an increased micropinocytosis activity (Dowrick et al., 1993). The two cellular processes have many proteins in common such as actin, PI3K. However, studies have shown that macropynocytosis is not exclusively dependent on CDRs formation questioning the necessity of CDRs in macropynocytosis (Suetsugu et al., 2003)

Different signaling proteins have been found to localize and/or regulate the formation of these actin-rich circular structures. It is well established that actin polymerization proteins, membrane-deforming proteins (BAR/F-BAR containing proteins), protein kinases and small GTPases are involved in the formation of CDRs.

Proteins involve in actin polymerization are implicated in CDRs formation. Among them N-WASP protein, an Arp2/3 activator, has been shown to be important for CDRs formation. Depletion of N-WASP or expression of a truncated form which is unable to bind Arp2/3 lead to a massive decrease of CDRs formation (Legg et al., 2007). Another Ap2/3 activator protein, cortactin, localizes to CDRs upon PDGF stimulation and is also necessary for their formation (Krueger et al., 2003). However, the role of WAVE1 and WAVE2, which also activate Arp2/3, in the formation of CDRs remains controversial. While Suetsugu and colleagues have shown that WAVE1 is responsible for CDRs formation and WAVE2 for peripheral ruffles formation, Legg and colleagues suggest that neither WAVE2 nor WAVE1 are essential for CDRs formation (Legg et al., 2007; Suetsugu et al., 2003). Additionally, actin associated proteins and adaptor proteins are important for CDRs formation. Actin-binding protein-1 not only localizes at CDRs but it also necessary for their formation upon PDGF stimulation, through its interaction with WIP (Cortesio et al., 2010). Nck is an adaptor molecule which has been shown to localize at CDRs. Nck knockout cells exhibit almost no CDRs after PDGF stimulation (Rivera et al., 2006; Ruusala et al., 2008). Nck, through its SH3 domains interacts with proteins such as N-WASP, WAVE, Gab1, PAK1 and PINCH1, and is also capable to activate N-WASP resulting the Arp2/3-mediated actin polymerization leading to CDRs formation (Ruusala et al., 2008)

Membrane-deforming proteins play a crucial role in the formation of CDRs. Dynamin 2 (Dyn2) is localized to CDRs and its depletion leads to inhibition of CDRs formation (Krueger et al., 2003). Notably, Dyn2 interacts through its proline-rich domain with BAR/I-BAR (Bin-Amphiphysin-Rvs) and F-BAR (Fer-CIP4 homology-BAR) containing proteins. These proteins are curved proteins and they have dual functions in membrane remodeling and actin dynamics. Sorting nexin 9 (Snx9), a BAR containing protein, is a known interactor of

Dyn2 which is essential for the clathrin-dependent endocytosis. Interestingly, Snx9 is critical for CDRs formation and can be also localized at CDRs. It also accosiates with N-WASP and stimulates N-WASP/Arp2/3-mediated actin polymerization. The PIP_2 at the plasma membrane promote SNX9 oligomerization and modulate its ability to stimulate polymerization through N-WASP/Arp2/3- (Yarar et al., 2007). Tuba and IRSp53 are two other curved proteins which interact with N-WASP and WAVE1, respectively, and have been shown to localize and control the formation of CDRs (Peleg et al., 2011). Another interesting protein is the SH3YL1, which can be localized at CDRs after PDGF stimulation and through its SH3 domain SYLF interacts with phospholipids (especially PIP_3). Additionaly, SH3YL1 interacts with 5-phosphatase src-homology 2–containing inositol-5-phosphatase 2 (SHIP2), which is also important for CDRs formation. Through these interactions SH3YL1 regulates the production of PIP2 which correlates with CDRs formation (Hasegawa et al., 2011). All together, these studies highlight the importance of membrane dynamics in the morphogenesis of CDRs.

Additionally, several signaling pathways that are involved in the regulation of actin polymerization and thereby in CDR formation include several protein kinases and small GTPases. Upon PDGF stimulation activated PAK1 localized with F-actin at CDRs. Overexpression of activated PAK1 was shown to induce CDRs formation. PAK1 interacts with Arp2/3 and PI3K, proteins essential for CDR formation (Dharmawardhane et al., 2000; Zhao et al., 1998). Rac and Rab5, members of the Ras superfamily, are necessary for CDR formation. Cells lacking Rac1 are unable to form CDRs (Ladwein and Rottner, 2008). Activated Rac1 recruits WAVE1 to ruffles resulting in WAVE complex activation, which leads to Arp2/3 dependent actin reorganization (Eden et al., 2002). Rab5, which also functions in the regulation of endocytosis pathway, has been shown to regulate CDRs formation. Through its endocytosis function, Rab5 leads to the trafficking of Rac1 together with Tiam1 to early endosomes, where Rac1 undergoes activation and thus is recycled to the plasma membrane leading to CDRs formation (Palamidessi et al., 2008). Additionaly, Rab5, through its interaction with the Rab5 GTPase-activating protein RN-tre, associates with actinin-4 and F-actin and modulates actin dynamics and therefore CDRs formation (Lanzetti et al., 2004). Treatment of cells with worthmanin leads to a reduction of CDRs formation, underscoring the involment of PI3K kinase in this cellular process (Wymann and Arcaro, 1994). Regardless the undefined exact role of PI3K in CDRs formation, PI3K and phosphoinosites (PIP2 and PIP3) are implicated at different stages in the processs of CDR formation. PI3K activation by RTKs has been shown to modulate Rac1 activation while

phosphoinosites interact and recruit BAR-containing proteins/curved proteins to the membranes (Hasegawa et al., 2011; Innocenti et al., 2003).

Abelson (Abl) kinases localize to CDRs and play a major role in their formation (Plattner et al., 1999; Sini et al., 2004). *Abl1*$^{-/-}$ knockout embryonic mouse fibroblasts do not form CDRs upon PDGF stimulation and this can be rescued after the re-expresion of the kinases in these cells (Boyle et al., 2007; Sini et al., 2004). How exactly Abl kinases promote the formation of CDRs is not well understood. Different studies suggest that Abl kinases phosphorylate cortactin and WAVE2 enhancing their ability to activate the Arp2/3 complex leading to CDRs formation (Antoku and Mayer, 2009; Boyle et al., 2007; Hernandez et al., 2004; Stuart et al., 2006). Abl1 has been also showed to phosphorylate the GEF SOS-1 which promotes Rac activation thereby inducing the formation of CDRs (Sini et al., 2004).

1.8. Abl Kinases

The Abelson (Abl) non-receptor protein tyrosine kinases family is composed by two members Abl1 and Abl2/Arg. Studies of the Abelson murine lymphosarcoma virus led to the discovery of cellular Ableson (Abl) non-receptor protein kinases more than 40 years ago (Abelson and Rabstein, 1970; Goff et al., 1980). Subsequent studies revealed that chromosomal translocations of human *Abl1* associates with diferrent types of human cancers. Charactreristic example is the chromosomal translocation, identified in chronic myelogenous leukemia (CML), which results in the creation of the Philadelpia (Ph) chromosome and the production of the hyper-active kinase BCR-ABL1(Colicelli, 2010; Greuber et al., 2013).

While upnormal kinase activity of Abl kinases is associated with leukemias, the enzymatic activity of endogenous Abl kinases is tightly regulated by different stimuli that vary from growth factors, DNA damage, oxidative stress to adhesion receptors and microbial pathogens (Kharbanda et al., 1995; Khatri et al., 2016; Lewis et al., 1996; Plattner et al., 1999). Upon activation, Abl kinases regulate several biological processes such as cell migration, adhesion, invasion, polarity, endocytosis, cell survival and proliferation (Colicelli, 2010; Khatri et al., 2016). Abnormally activated Abl kinases have been linked to leukemias, several solid tumors, neurogenerative diseases and inflammatory disorders. Recently, Abl kinases have been shown to be required for bacterial and viral entry in mammalian cells (Khatri et al., 2016).

Abl and Abl2 kinases are ubiquitously expressed and share high sequence and structure similarities. The N-terminal regulatory and catalytic domains are over 90% identical between Abl1 and Abl2, containing a tyrosine kinase Src homology1 (SH1) domain and regulatory SH2 and SH3 domains. Conserved PxxP motifs are shared between the Abl kinases which mediate the binding to SH3 domain containing proteins. The C-terminal domain of both kinases contains a conserved calponin homology (CH) (F)-actin-binding domain. In Abl1 a globular (G)-actin-binding domain and a DNA binding domain precedes the F-actin domain. The DNA binding domain, the three nuclear localization signal (NLS) motifs and the one nuclear export signal (NES) at the C-terminus of Abl1 are consistent with its nucleo-cytoplasmic localization. In contrast, Abl2 has a [I/L]WEQ F-actin-binding domain (F)-actin binding domain and microtubules (MT) binding motif in the C-terminus which are responsible for its localization to the cytoplasm, its accumulation at F-actin rich sites in the cell periphery and its ability to crosslink MT and F-actin in vitro (Miller et al., 2004). Alternative splicing of the first exons of Abl1 and Abl2 leads to the production of different variants with different N-terminal sequences. The human 1β and mouse type IV variant contain an N-terminal glycine which is myristoylated (Figure 17) (Colicelli, 2010).

Abl kinases activity is highly regulated by intermolecular and intramolecular interactions as well as post-translational modifications that lead to changes in the conformation of the kinase domain corresponding either to an autoinhibited or an active state. Intramolecular interaction of the Abl SH3 and SH2 domain, more precisely between the SH3 domain and the N-terminal lobe of the kinase domain, acts as a clamp switch and holds the kinase in an inactive conformation (Barila and Superti-Furga, 1998; Hantschel, 2012). Furthermore, the SH2 domain forms an extensive interaction interface with the C-terminal lobe of the kinase domain that is stabilized by an interlocking network of hydrogen bonds (Nagar et al., 2003). Myristoylation is also involved in regulating Abl kinase activity. The N-terminal myristoyl modification of Abl1β and Abl2β binds to a deep hydrophobic pocket in the C-lobe of the kinase domain and induces conformational changes contributing to autoinhibitory fold (Nagar et al., 2003). In addition, an amino-terminal Cap sequence interacts with the several regions along the Abl1 protein and stabilizes its inactive conformation (Pluk et al., 2002).

Tyrosine phosphorylation is needed to further enhance the enzymatic activity of Abl kinases. Abl phosphorylation prevents its reversion to the locked conformation and properly orients the catalytic sites. This modification can occur either in trans for both Abl1 and Abl2 (autophosphorylation) or by Src, PDGFR and EGFR (Sirvent et al., 2008). Tyrosine

phosphorylation of Abl1-Y245 (Abl2-Y272) in the SH2-kinase domain linker region leads to proper orientation of the catalytic site, while phosphorylation at Abl1-Y412 (Abl2-Y439) , which resides in the activation loop of the kinase domain, prevents the reversion to the locked conformation leading to full kinase activation (Brasher and Van Etten, 2000; Dorey et al., 2001; Tanis et al., 2003).

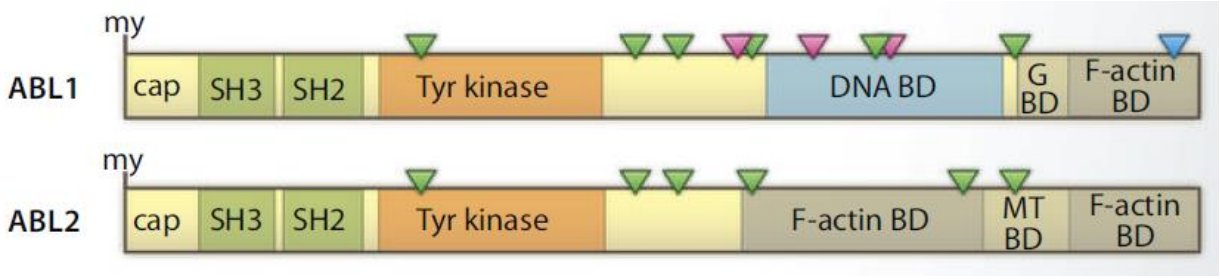

Figure 17: Human Abl kinases (Abl1 and Abl2) domain structure. My, myristoylation site; cap: N-terminal region of Abl kinases; Tyr, tyrosine; G BD, G-actin–binding domain; MT BD, microtubule-binding domain. Green triangle, PxxP motif, blue triangle, NES; magenta triangle, NLS. *Picture is adapted from (Colicelli, 2010).*

Not surprisingly, genetic inactivation of *Abl1* and *Abl2* in mice revealed that the two kinases have unique and common physiological roles. Ablation of *Abl1* gene causes embryonic and neonatal lethality with variable penetrance depending on the strain background. *Abl1* knockout mice exhibit splenic and thymic atrophy, reduced numbers of B and T cells, cardiac abnormalities and osteoporosis linked to defective osteoblasts proliferation and premature senescence (Kua et al., 2012; Li et al., 2000; Moresco et al., 2005; Schwartzberg et al., 1991; Tybulewicz et al., 1991). On the other hand, *Abl2* knockout mice are viable and exhibit neuronal defects that include age related dendrite destabilization and regression (Gourley et al., 2009; Koleske et al., 1998; Moresco et al., 2005). *Abl1*$^{-/-}$ *Abl2*$^{-/-}$ mice are embryonic lethal (embryonic day 11), further supporting the redundant and essential functions of these kinases during development (Koleske et al., 1998).

1.8.1. Abl kinases and cytoskeleton

Abl1 and Abl2 are the only mammalian tyrosine non-receptor kinases that can directly interact with cytoskeleton. Not surprisingly the best defined function of these kinases is their ability to regulate cytoskeletal dynamics and function (Bradley et al., 2006; Khatri et al., 2016). Abl kinases act downstream of growth factor and cell surface receptors, such as

integrins and cadherins, promoting cytoskeletal changes required for lamellipodial protrusions, CDRs formation, cell migration and invasion.

Upon PDGF stimulation *Abl1*$^{-/-}$ fibroblasts showed a dramatic reduction of CDRs formation, a reduction that can be restored by re-expression of Abl1 in the cells (Plattner et al., 1999; Wennstrom et al., 1994). Additionaly, cells deficient for both Abl kinases are unable to form peripheral ruffles or CDRs upon PDGF or EGF stimulation (Boyle et al., 2007; Sini et al., 2004). Adhesion of fibroblasts to FN lead to lamellipodial and filopodial formation. Abl1 reconstituted *Abl1*$^{-/-}$ *Abl2*$^{-/-}$ fibroblasts characterized by increased number of filopodia and F-actin microspikes formation upon adhesion to FN (Woodring et al., 2002). Abl1 is shown to localize at the tips of these filopodia. Moreover, Abl1 kinase activity increases during the first 30 min of integrin mediated adhesion and Abl1 has been shown to translocate from nucleus to FAs during the initial time of integrin-mediated adhesion (Lewis et al., 1996). On the other hand, *Abl2*$^{-/-}$ fibroblasts characterized by a reduction in lamellipodial dynamics and Abl2 is localized with F-actin at the lamellipodial structures (Miller et al., 2004). Interestingly, a recent study from the Koleske group suggests a direct interaction of Abl2 with integrin β1 tail. Abl2 is activated by this direct interaction and activated Abl2 phosphorylates integrin β1 tail at Tyr-783 leading to changes in cell shape and motility (Simpson et al., 2015). All in all Abl kinases coordinate membrane ruffles and cell protrusions downstream of growth factor and integrin adhesions receptors.

Regulation of actin cytoskeletal dynamics is mediated by active Abl kinases throughthe phosphorylation of key substrates. Abl kinases modulate actin cytoskeleton in part by controlling the activity of Rho family GTPases Rho and Rac and/or by modulating the function Arp2/3 complex regulators. Interestingly, the C-terminus of Abl family kinases has been shown to regulate the structure of the F-actin and microtubule cytoskeletons in a kinase-independent manner (Miller et al., 2004).

Abl kinases modulate Rho family GTPases activity through the phosphorylation of key substrates such as SOS-1, Crk and p190RhoGAP.

Sos-1

Son of Sevenless 1 (Sos-1) is a dual GEF for small GTPases Rac and Ras. Sos-1 protein characterized by the presence of histone-like (HD) and the Dbl homology (DH) domain at the N-terminus (Rojas et al., 2011). Through inter molecular interactions in DH-HD domains, its Rac GEF activity is inhibited. Sos-1 can be can be activated either through its interaction with Abi and Eps8 or though its tyrosine phosphorylation by Abl1 (Gerboth et al., 2018; Sini et al., 2004). More precisely, Abl1 phosphorylates Sos-1 at Y1196, elicitating

its Rac-GEF activity. Phosphorylation of Sos-1 by Abl1 is required Rac activation and Rac-dependent actin modulation and cell migration induced after PDGF stimulation (Gerboth et al., 2018).

CrkII

CrkII belongs to a family of adaptor molecules consisting predominantly of Src homology 2 (SH2) and SH3 domains, with no obvious catalytic function, that couples to effector proteins including p130Cas, C3G, Sos, Eps15, Dock180 (Bell and Park, 2012). Association of CrkII with p130Cas induces cell migration and invasion through a Rac-dependent mechanism (Klemke et al., 1998). Experiments using *Abl*$^{-/-}$*Abl2*$^{-/-}$ fibroblast cells showed increase CrkII-p130Cas coupling and motility. Reconstitution of the cells with constitutive active Abl1 kinase prevents CrkII-Cas coupling and inhibits cell migration (Kain and Klemke, 2001). This is mediated through the phosphorylation of CrkII by Abl kinases at Y221. This phosphorylation leads to intramolecular interaction in CrkII preventing its interaction with p130Cas and Dock180 and thus Rac activation (Feller et al., 1994). However, experiments using COS-7 cells showed that the Y221 phosphorylation of CrkII regulates Rac membrane translocation upon cell adhesion and this is necessary for Rac activation and downstream signaling (Abassi and Vuori, 2002).

p190RhoGAP

The Rho-specific GTPase-activating protein p190RhoGAP is a substrate of Abl2. Integrin mediated cell adhesion induces Abl2 activation resulting p190RhoGAP phosphorylation. The phosphorylation of p190RhoGAP promotes its binding to p120RasGAP and the recruitment of p190:p120 complex to the cell periphery where it can inhibit Rho (Bradley et al., 2006). On the other hand, when *Abl2*$^{-/-}$ fibroblasts are plated on FN not only is there a reduction of p190 phosphorylation but also a significant elevation of active Rho and increased F-actin stress fibers (Bradley et al., 2006; Peacock et al., 2007).

Additionaly, Abl kinases phosphorylate and interact with several actin regulators and thus can modulate cytoskeletal dynamics. Among the actin regulators which can be phosphorylated by Abl kinases are WASP, WAVE proteins and Cortactin.

WASP and WAVE

In mammals, the WASP and WAVE family are composed of five members: the hematopoietic-specific WASP, the ubiquitous N-WASP, WAVE1, WAVE2 and WAVE3. Their activation leads to a burst of actin polymerization and the formation of numerous actin-based structures, such as lamellipodia, filopodia, podosomes and dorsal ruffles. Through their C-terminal VCA (verprolin-homoly domain (V), the cofilin homology domain (C) and the

acidic domain (A)) these proteins bind to an actin monomer and to the Arp2/3 comlpex resulting in its activation and actin polymerization (Pollitt and Insall, 2009).

WASP proteins are predominantly found in an autoinhibited conformation in which the C-terminus of the protein interacts with its N-terminus. Competitive binding of different proteins for instance, Cdc42, WIP, TOCA1 releases this autoinhibition (Bell and Park, 2012; Pollitt and Insall, 2009; Takenawa and Suetsugu, 2007). Additionaly, phosphorylation of N-WASP by Abl kinases inhibits its transition to autoinhibition state thereby enchancing actin polymerization (Burton et al., 2005).

WAVE proteins are not autoinhibited but they form part of a larger WAVE regulatory complex (WRC) that contains four other proteins named: SRA1/PIR121, Nap1, Abi and HSPC300. The ability of WAVE to interact with Arp2/3 complex and mediate actin polymerization is inhibited with in the WRC complex. Optimal activity of the WRC complex can be achieved by its recruitment to the plasma membrane and the release of WAVE inhibition (Takenawa and Suetsugu, 2007) In mammals Abl1 kinase, though its interaction with Abi, phosphorylates WAVE2 in response to growth factors or adhesion to FN leading to its localization to the leading edge and promoting its activity (Leng et al., 2005; Stuart et al., 2006). Additionaly, Abl1 has shown to interact and phosphorylate WAVE3 in respond to PDGF, resulting WAVE3 recruitment to the plasma membane. Phosphorylation of WAVE3 by Abl1 is important for lamellipodia formation and cell migration (Sossey-Alaoui et al., 2007).

Cortactin

Cortactin is an actin promoting nucleator factor that binds the Arp3 subunit of the Arp2/3 complex leading to its weak activation and as a consequence the stimulation of actin polymerization and the formation of branched actin-filament networks (Weaver et al., 2001). It can also synergize with N-WASP to greatly enhance actin polymerization (Kowalski et al., 2005). Phosphorylation of cortactin by Abl kinases upon PDGF stimulation is essential for their ability to induce the formation of dorsal ruffles in fibroblasts (Boyle et al., 2007). Cortactin phosphorylation by Abl2 upon integrin adhesion leads to lamellipodial formation. Abl2 acts as a kinase as well as binding protein scaffold and both functions are required to promote adhesion-dependent cell edge protrusion (Lapetina et al., 2009).

Taken together Abl tyrosine kinases through their direct connection with actin cytoskeleton, as well as the phosphorylation of proteins which are either directly or indirectly implicated in the control of actin polymerization, play an important role in cell adhesion and migration.

2. Aim of the thesis

Kindlin is a key regulatory molecule in the integrin activation process and in bidirectional signaling, but it also fulfills functions beyond integrin activation. Despite the importance of kindlin, it is still unclear how kindlin function is regulated. Recent evidence suggests a role of post-translational modifications and specific kindlin-interacting proteins in the regulation of kindlin localization and function. However, the mechanisms which trigger kindlin localization to different cellular compartments, as well as the way its integrin-dependent and independent functions can be regulated, remain largely unknown. It becomes apparent that studies are needed to specify kindlin regulation/activation mechanisms.

In order to get an insight into the regulation mechanisms of kindlin-2 functions my **first aim** was to investigate how **post-translational modifications and especially phosphorylation can regulate kindlin-2 function and localization**. In order to achieved this aim a kinase screening (ProQinase) was performed. Additionally, I performed mass spectroscopy based studies to identify and characterize possible kinases and the corresponding phosphorylation sites on kindlin-2. Furthermore, I analysed the functional role of kindlin-2 phosphorylation.

The **second aim** of my thesis was to **identify novel binding proteins of kindlin-2** and **investigate the role of these interactions in the regulation of kidlin-2 functions**. For this purpose a yeast two hybrid study was performed. Additionally, I performed mass spectroscopy based interactor studies.

Furthermore, for a better comparative analysis of kindlin and talin functions **I generated quadruple null fibroblasts that lack talin-1/2 and kindlin-1/2**. These cells allow the functional characterization of kindlin and talin in the same cellular background excluding any artifacts that arise by using cells derived from different parental cell lines.

3. Short summaries of manuscripts

3.1. Tyrosine phosphorylation of Kindlin-2 by Abl kinases controls growth factor-triggered circular dorsal ruffle formation (manuscript in preparation)

Marina Theodosiou, Ralph T. Böttcher, Maik Veelders, Reinhard Fässler

Kindlin-2 is a key molecule in the integrin activation process and integrin downstream signaling. Recent studies suggest a role of phosphorylation in the regulation of kindlin-2 function as mediator of integrin downstream signaling. In this manuscript we show that Abl kinases phosphorylate kindlin-2 *in vivo* and *in vitro* at tyrosine 179. Expression of phosphomimetic (myc-Kind2Y179E) and phosphodeficient (myc-Kind2Y179F) kindlin-2 in kindlin-2 knockout fibroblasts implicates kindlin-2 Y179 phosphorylation in dorsal ruffles formation. This study assigns a previously unknown function of kindlin-2 in CDRs formation which is controlled by phosphorylation.

3.2. Kindlin-2 cooperates with talin to activate integrins and induces cell spreading by directly binding paxillin

Marina Theodosiou, Moritz Widmaier, Ralph T. Böttcher, Emanuel Rognoni, Maik Veelders, Mitasha Bharadwaj, Armin Lambacher, Katharina Austen, Daniel Müller, Roy Zent, Reinhard Fässler

It is widely establish that kindlin and talin contribute to integrin activation and signaling in hematopoietic cells. However the lack of similar studies in non-hematopoietic cells prompted us to generate mouse kidney fibroblasts lacking kindlin-1/2 or talin-1/2 and study the role of the single protein in integrin activation and signaling. Kindlin-1/2 or talin-1/2 knockout fibroblasts fail to activate integrins and to adhere demostrating that both proteins are essential for integrin activation. When we partially bypass integrin activation using Mn^{2+} we observed isotropic cell spreading on FN of talin-deficient cells but not kindlin-deficient cells. To obtain a mechanistic explanation for this observation we performed a Yeast Two Hybrid screening (Y2H) to identify kindlin-2 interactors and identified paxillin family members as novel binding partners of kindlin-2. In this study, we show that kindlin recruits paxillin to nascent adhesions which binds FAK resulting in its activation and lamellipodia formation.

3.3. Kindlin-2 recruits paxillin and Arp2/3 to promote membrane protrusions during initial cell spreading

Ralph T. Böttcher, Maik Veelders, Pascaline Rombaut, Jan Faix, Marina Theodosiou, Theresa E.Stradal, Klemens Rottner, Roy Zent, Franz Herzog, Reinhard Fässler

Cell adhesion and spreading is a process which involves integrin binding to ECM and complex rearrangements of actin cytoskeleton. Kindlin-2 is a major integrin activator which also plays a cental role in cell spreading. In our previous paper we showed that kindlin-2 directly binds and recruits paxillin to nascent adhesions, which activates FAK and Rac1 inducing cells isotropic spreading. In this paper we further characterized the kindlin-2-paxillin interaction by mapping another binding site located in the F0 domain of kindlin-2. Additionally, we showed a direct binding of kindlin-2 to the Arp2/3 complex which is important for membrane protrusions and cell spreading. The key finding of the study is that kindlin-2 through its binding to paxillin and the Arp2/3 complex mediates the induction of membrane protrusions.

4. References

Abassi, Y.A., and K. Vuori. 2002. Tyrosine 221 in Crk regulates adhesion-dependent membrane localization of Crk and Rac and activation of Rac signaling. *EMBO J*. 21:4571-4582.

Abelson, H.T., and L.S. Rabstein. 1970. Lymphosarcoma: virus-induced thymic-independent disease in mice. *Cancer Res*. 30:2213-2222.

Alexandrova, A.Y., K. Arnold, S. Schaub, J.M. Vasiliev, J.J. Meister, A.D. Bershadsky, and A.B. Verkhovsky. 2008. Comparative dynamics of retrograde actin flow and focal adhesions: formation of nascent adhesions triggers transition from fast to slow flow. *PLoS One*. 3:e3234.

Anthis, N.J., J.R. Haling, C.L. Oxley, M. Memo, K.L. Wegener, C.J. Lim, M.H. Ginsberg, and I.D. Campbell. 2009a. Beta integrin tyrosine phosphorylation is a conserved mechanism for regulating talin-induced integrin activation. *J Biol Chem*. 284:36700-36710.

Anthis, N.J., K.L. Wegener, F. Ye, C. Kim, B.T. Goult, E.D. Lowe, I. Vakonakis, N. Bate, D.R. Critchley, M.H. Ginsberg, and I.D. Campbell. 2009b. The structure of an integrin/talin complex reveals the basis of inside-out signal transduction. *EMBO J*. 28:3623-3632.

Antoku, S., and B.J. Mayer. 2009. Distinct roles for Crk adaptor isoforms in actin reorganization induced by extracellular signals. *J Cell Sci*. 122:4228-4238.

Arnaout, M.A., S.L. Goodman, and J.P. Xiong. 2007. Structure and mechanics of integrin-based cell adhesion. *Curr Opin Cell Biol*. 19:495-507.

Artym, V.V., S. Swatkoski, K. Matsumoto, C.B. Campbell, R.J. Petrie, E.K. Dimitriadis, X. Li, S.C. Mueller, T.H. Bugge, M. Gucek, and K.M. Yamada. 2015. Dense fibrillar collagen is a potent inducer of invadopodia via a specific signaling network. *J Cell Biol*. 208:331-350.

Astrof, N.S., A. Salas, M. Shimaoka, J. Chen, and T.A. Springer. 2006. Importance of force linkage in mechanochemistry of adhesion receptors. *Biochemistry*. 45:15020-15028.

Atherton, P., B. Stutchbury, D. Jethwa, and C. Ballestrem. 2016. Mechanosensitive components of integrin adhesions: Role of vinculin. *Exp Cell Res*. 343:21-27.

Austen, K., P. Ringer, A. Mehlich, A. Chrostek-Grashoff, C. Kluger, C. Klingner, B. Sabass, R. Zent, M. Rief, and C. Grashoff. 2015. Extracellular rigidity sensing by talin isoform-specific mechanical linkages. *Nat Cell Biol*. 17:1597-1606.

Bachir, A.I., J. Zareno, K. Moissoglu, E.F. Plow, E. Gratton, and A.R. Horwitz. 2014. Integrin-associated complexes form hierarchically with variable stoichiometry in nascent adhesions. *Curr Biol*. 24:1845-1853.

Bandyopadhyay, A., G. Rothschild, S. Kim, D.A. Calderwood, and S. Raghavan. 2012. Functional differences between kindlin-1 and kindlin-2 in keratinocytes. *J Cell Sci*. 125:2172-2184.

Banno, A., B.T. Goult, H. Lee, N. Bate, D.R. Critchley, and M.H. Ginsberg. 2012. Subcellular localization of talin is regulated by inter-domain interactions. *J Biol Chem*. 287:13799-13812.

Barila, D., and G. Superti-Furga. 1998. An intramolecular SH3-domain interaction regulates c-Abl activity. *Nat Genet*. 18:280-282.

Bear, J.E., T.M. Svitkina, M. Krause, D.A. Schafer, J.J. Loureiro, G.A. Strasser, I.V. Maly, O.Y. Chaga, J.A. Cooper, G.G. Borisy, and F.B. Gertler. 2002. Antagonism between Ena/VASP proteins and actin filament capping regulates fibroblast motility. *Cell*. 109:509-521.

Bell, E.S., and M. Park. 2012. Models of crk adaptor proteins in cancer. *Genes Cancer*. 3:341-352.

Bialkowska, K., T.V. Byzova, and E.F. Plow. 2015. Site-specific phosphorylation of kindlin-3 protein regulates its capacity to control cellular responses mediated by integrin alphaIIbbeta3. *J Biol Chem*. 290:6226-6242.

Bialkowska, K., Y.Q. Ma, K. Bledzka, K. Sossey-Alaoui, L. Izem, X. Zhang, N. Malinin, J. Qin, T. Byzova, and E.F. Plow. 2010. The integrin co-activator Kindlin-3 is expressed and functional in a non-hematopoietic cell, the endothelial cell. *J Biol Chem*. 285:18640-18649.

Bledzka, K., K. Bialkowska, H. Nie, J. Qin, T. Byzova, C. Wu, E.F. Plow, and Y.Q. Ma. 2010. Tyrosine phosphorylation of integrin beta3 regulates kindlin-2 binding and integrin activation. *J Biol Chem*. 285:30370-30374.

Bledzka, K., K. Bialkowska, K. Sossey-Alaoui, J. Vaynberg, E. Pluskota, J. Qin, and E.F. Plow. 2016. Kindlin-2 directly binds actin and regulates integrin outside-in signaling. *J Cell Biol*. 213:97-108.

Bledzka, K., J. Liu, Z. Xu, H.D. Perera, S.P. Yadav, K. Bialkowska, J. Qin, Y.Q. Ma, and E.F. Plow. 2012. Spatial coordination of kindlin-2 with talin head domain in interaction with integrin beta cytoplasmic tails. *J Biol Chem*. 287:24585-24594.

Bloomfield, G., and R.R. Kay. 2016. Uses and abuses of macropinocytosis. *J Cell Sci*. 129:2697-2705.

Boettiger, D. 2012. Mechanical control of integrin-mediated adhesion and signaling. *Curr Opin Cell Biol*. 24:592-599.

Borges, E., Y. Jan, and E. Ruoslahti. 2000. Platelet-derived growth factor receptor beta and vascular endothelial growth factor receptor 2 bind to the beta 3 integrin through its extracellular domain. *J Biol Chem*. 275:39867-39873.

Bottcher, R.T., C. Stremmel, A. Meves, H. Meyer, M. Widmaier, H.Y. Tseng, and R. Fassler. 2012. Sorting nexin 17 prevents lysosomal degradation of beta1 integrins by binding to the beta1-integrin tail. *Nat Cell Biol*. 14:584-592.

Bottcher, R.T., M. Veelders, P. Rombaut, J. Faix, M. Theodosiou, T.E. Stradal, K. Rottner, R. Zent, F. Herzog, and R. Fassler. 2017. Kindlin-2 recruits paxillin and Arp2/3 to promote membrane protrusions during initial cell spreading. *J Cell Biol*. 216:3785-3798.

Bouaouina, M., B.T. Goult, C. Huet-Calderwood, N. Bate, N.N. Brahme, I.L. Barsukov, D.R. Critchley, and D.A. Calderwood. 2012. A conserved lipid-binding loop in the kindlin FERM F1 domain is required for kindlin-mediated alphaIIbbeta3 integrin coactivation. *J Biol Chem*. 287:6979-6990.

Bouchet, B.P., R.E. Gough, Y.C. Ammon, D. van de Willige, H. Post, G. Jacquemet, A.M. Altelaar, A.J. Heck, B.T. Goult, and A. Akhmanova. 2016. Talin-KANK1 interaction controls the recruitment of cortical microtubule stabilizing complexes to focal adhesions. *Elife*. 5.

Bouvard, D., C. Brakebusch, E. Gustafsson, A. Aszodi, T. Bengtsson, A. Berna, and R. Fassler. 2001. Functional consequences of integrin gene mutations in mice. *Circ Res*. 89:211-223.

Bouvard, D., J. Pouwels, N. De Franceschi, and J. Ivaska. 2013. Integrin inactivators: balancing cellular functions in vitro and in vivo. *Nat Rev Mol Cell Biol*. 14:430-442.

Boyle, S.N., G.A. Michaud, B. Schweitzer, P.F. Predki, and A.J. Koleske. 2007. A critical role for cortactin phosphorylation by Abl-family kinases in PDGF-induced dorsal-wave formation. *Curr Biol*. 17:445-451.

Bradley, W.D., S.E. Hernandez, J. Settleman, and A.J. Koleske. 2006. Integrin signaling through Arg activates p190RhoGAP by promoting its binding to p120RasGAP and recruitment to the membrane. *Mol Biol Cell*. 17:4827-4836.

Brami-Cherrier, K., N. Gervasi, D. Arsenieva, K. Walkiewicz, M.C. Boutterin, A. Ortega, P.G. Leonard, B. Seantier, L. Gasmi, T. Bouceba, G. Kadare, J.A. Girault, and S.T. Arold. 2014. FAK dimerization controls its kinase-dependent functions at focal adhesions. *EMBO J*. 33:356-370.

Brasher, B.B., and R.A. Van Etten. 2000. c-Abl has high intrinsic tyrosine kinase activity that is stimulated by mutation of the Src homology 3 domain and by autophosphorylation at two distinct regulatory tyrosines. *J Biol Chem*. 275:35631-35637.

Bravo-Cordero, J.J., M.A. Magalhaes, R.J. Eddy, L. Hodgson, and J. Condeelis. 2013. Functions of cofilin in cell locomotion and invasion. *Nat Rev Mol Cell Biol*. 14:405-415.

Brown, M.C., J.A. Perrotta, and C.E. Turner. 1996. Identification of LIM3 as the principal determinant of paxillin focal adhesion localization and characterization of a novel motif on paxillin directing vinculin and focal adhesion kinase binding. *J Cell Biol*. 135:1109-1123.

Brugnera, E., L. Haney, C. Grimsley, M. Lu, S.F. Walk, A.C. Tosello-Trampont, I.G. Macara, H. Madhani, G.R. Fink, and K.S. Ravichandran. 2002. Unconventional Rac-GEF activity is mediated through the Dock180-ELMO complex. *Nat Cell Biol*. 4:574-582.

Bryce, N.S., E.S. Clark, J.L. Leysath, J.D. Currie, D.J. Webb, and A.M. Weaver. 2005. Cortactin promotes cell motility by enhancing lamellipodial persistence. *Curr Biol*. 15:1276-1285.

Buccione, R., J.D. Orth, and M.A. McNiven. 2004. Foot and mouth: podosomes, invadopodia and circular dorsal ruffles. *Nat Rev Mol Cell Biol*. 5:647-657.

Burke, R.D. 1999. Invertebrate integrins: structure, function, and evolution. *Int Rev Cytol*. 191:257-284.

Burton, E.A., T.N. Oliver, and A.M. Pendergast. 2005. Abl kinases regulate actin comet tail elongation via an N-WASP-dependent pathway. *Mol Cell Biol*. 25:8834-8843.

Calderwood, D.A., I.D. Campbell, and D.R. Critchley. 2013. Talins and kindlins: partners in integrin-mediated adhesion. *Nat Rev Mol Cell Biol*. 14:503-517.

Campbell, I.D., and M.J. Humphries. 2011. Integrin structure, activation, and interactions. *Cold Spring Harb Perspect Biol*. 3.

Chhabra, E.S., and H.N. Higgs. 2007. The many faces of actin: matching assembly factors with cellular structures. *Nat Cell Biol*. 9:1110-1121.

Choi, C.K., M. Vicente-Manzanares, J. Zareno, L.A. Whitmore, A. Mogilner, and A.R. Horwitz. 2008. Actin and alpha-actinin orchestrate the assembly and maturation of nascent adhesions in a myosin II motor-independent manner. *Nat Cell Biol*. 10:1039-1050.

Chorev, D.S., O. Moscovitz, B. Geiger, and M. Sharon. 2014. Regulation of focal adhesion formation by a vinculin-Arp2/3 hybrid complex. *Nat Commun*. 5:3758.

Cohen, D.M., B. Kutscher, H. Chen, D.B. Murphy, and S.W. Craig. 2006. A conformational switch in vinculin drives formation and dynamics of a talin-vinculin complex at focal adhesions. *J Biol Chem*. 281:16006-16015.

Colicelli, J. 2010. ABL tyrosine kinases: evolution of function, regulation, and specificity. *Sci Signal*. 3:re6.

Cortesio, C.L., B.J. Perrin, D.A. Bennin, and A. Huttenlocher. 2010. Actin-binding protein-1 interacts with WASp-interacting protein to regulate growth factor-induced dorsal ruffle formation. *Mol Biol Cell*. 21:186-197.

Critchley, D.R., and A.R. Gingras. 2008. Talin at a glance. *J Cell Sci*. 121:1345-1347.

Czuchra, A., H. Meyer, K.R. Legate, C. Brakebusch, and R. Fassler. 2006. Genetic analysis of beta1 integrin "activation motifs" in mice. *J Cell Biol*. 174:889-899.

Deakin, N.O., J. Pignatelli, and C.E. Turner. 2012. Diverse roles for the paxillin family of proteins in cancer. *Genes Cancer*. 3:362-370.

Deakin, N.O., and C.E. Turner. 2008. Paxillin comes of age. *J Cell Sci*. 121:2435-2444.

Debrand, E., F.J. Conti, N. Bate, L. Spence, D. Mazzeo, C.A. Pritchard, S.J. Monkley, and D.R. Critchley. 2012. Mice carrying a complete deletion of the talin2 coding sequence are viable and fertile. *Biochem Biophys Res Commun*. 426:190-195.

del Rio, A., R. Perez-Jimenez, R. Liu, P. Roca-Cusachs, J.M. Fernandez, and M.P. Sheetz. 2009. Stretching single talin rod molecules activates vinculin binding. *Science*. 323:638-641.

DeMali, K.A., E. Balciunaite, and A. Kazlauskas. 1999. Integrins enhance platelet-derived growth factor (PDGF)-dependent responses by altering the signal relay enzymes that are recruited to the PDGF beta receptor. *J Biol Chem*. 274:19551-19558.

DeMali, K.A., C.A. Barlow, and K. Burridge. 2002. Recruitment of the Arp2/3 complex to vinculin: coupling membrane protrusion to matrix adhesion. *J Cell Biol*. 159:881-891.

Dharmawardhane, S., A. Schurmann, M.A. Sells, J. Chernoff, S.L. Schmid, and G.M. Bokoch. 2000. Regulation of macropinocytosis by p21-activated kinase-1. *Mol Biol Cell*. 11:3341-3352.

Di Paolo, G., L. Pellegrini, K. Letinic, G. Cestra, R. Zoncu, S. Voronov, S. Chang, J. Guo, M.R. Wenk, and P. De Camilli. 2002. Recruitment and regulation of phosphatidylinositol phosphate kinase type 1 gamma by the FERM domain of talin. *Nature*. 420:85-89.

Dorey, K., J.R. Engen, J. Kretzschmar, M. Wilm, G. Neubauer, T. Schindler, and G. Superti-Furga. 2001. Phosphorylation and structure-based functional studies reveal a positive and a negative role for the activation loop of the c-Abl tyrosine kinase. *Oncogene*. 20:8075-8084.

Dowling, J.J., E. Gibbs, M. Russell, D. Goldman, J. Minarcik, J.A. Golden, and E.L. Feldman. 2008a. Kindlin-2 is an essential component of intercalated discs and is required for vertebrate cardiac structure and function. *Circ Res*. 102:423-431.

Dowling, J.J., A.P. Vreede, S. Kim, J. Golden, and E.L. Feldman. 2008b. Kindlin-2 is required for myocyte elongation and is essential for myogenesis. *BMC Cell Biol*. 9:36.

Dowrick, P., P. Kenworthy, B. McCann, and R. Warn. 1993. Circular ruffle formation and closure lead to macropinocytosis in hepatocyte growth factor/scatter factor-treated cells. *Eur J Cell Biol*. 61:44-53.

Eden, S., R. Rohatgi, A.V. Podtelejnikov, M. Mann, and M.W. Kirschner. 2002. Mechanism of regulation of WAVE1-induced actin nucleation by Rac1 and Nck. *Nature*. 418:790-793.

Efimov, A., N. Schiefermeier, I. Grigoriev, R. Ohi, M.C. Brown, C.E. Turner, J.V. Small, and I. Kaverina. 2008. Paxillin-dependent stimulation of microtubule catastrophes at focal adhesion sites. *J Cell Sci*. 121:196-204.

Elliott, P.R., B.T. Goult, P.M. Kopp, N. Bate, J.G. Grossmann, G.C. Roberts, D.R. Critchley, and I.L. Barsukov. 2010. The Structure of the talin head reveals a novel extended conformation of the FERM domain. *Structure*. 18:1289-1299.

Ellis, S.J., E. Lostchuck, B.T. Goult, M. Bouaouina, M.J. Fairchild, P. Lopez-Ceballos, D.A. Calderwood, and G. Tanentzapf. 2014. The talin head domain reinforces integrin-mediated adhesion by promoting adhesion complex stability and clustering. *PLoS Genet*. 10:e1004756.

Emmert, H., H. Patel, and V.G. Brunton. 2017. Kindlin-1 protects cells from oxidative damage through activation of ERK signalling. *Free Radic Biol Med*. 108:896-903.

Fassler, R., M. Pfaff, J. Murphy, A.A. Noegel, S. Johansson, R. Timpl, and R. Albrecht. 1995. Lack of beta 1 integrin gene in embryonic stem cells affects morphology, adhesion, and migration but not integration into the inner cell mass of blastocysts. *J Cell Biol*. 128:979-988.

Feller, S.M., B. Knudsen, and H. Hanafusa. 1994. c-Abl kinase regulates the protein binding activity of c-Crk. *EMBO J*. 13:2341-2351.

Fitzpatrick, P., S.J. Shattil, and A.J. Ablooglu. 2014. C-terminal COOH of integrin beta1 is necessary for beta1 association with the kindlin-2 adapter protein. *J Biol Chem*. 289:11183-11193.

Friedland, J.C., M.H. Lee, and D. Boettiger. 2009. Mechanically activated integrin switch controls alpha5beta1 function. *Science*. 323:642-644.

Fukuda, K., K. Bledzka, J. Yang, H.D. Perera, E.F. Plow, and J. Qin. 2014. Molecular basis of kindlin-2 binding to integrin-linked kinase pseudokinase for regulating cell adhesion. *J Biol Chem*. 289:28363-28375.

Gallant, N.D., K.E. Michael, and A.J. Garcia. 2005. Cell adhesion strengthening: contributions of adhesive area, integrin binding, and focal adhesion assembly. *Mol Biol Cell*. 16:4329-4340.

Geiger, B., and K.M. Yamada. 2011. Molecular architecture and function of matrix adhesions. *Cold Spring Harb Perspect Biol*. 3.

Gerboth, S., E. Frittoli, A. Palamidessi, F.C. Baltanas, M. Salek, J. Rappsilber, C. Giuliani, F. Troglio, Y. Rolland, G. Pruneri, S. Kreutmair, I. Pallavicini, M. Zobel, M. Cinquanta, S. Minucci, C. Gomez, E. Santos, A.L. Illert, and G. Scita. 2018. Phosphorylation of SOS1 on tyrosine 1196 promotes its RAC GEF activity and contributes to BCR-ABL leukemogenesis. *Leukemia*. 32:820-827.

Giancotti, F.G., and E. Ruoslahti. 1999. Integrin signaling. *Science*. 285:1028-1032.

Gimona, M., R. Buccione, S.A. Courtneidge, and S. Linder. 2008. Assembly and biological role of podosomes and invadopodia. *Curr Opin Cell Biol*. 20:235-241.

Goff, S.P., E. Gilboa, O.N. Witte, and D. Baltimore. 1980. Structure of the Abelson murine leukemia virus genome and the homologous cellular gene: studies with cloned viral DNA. *Cell*. 22:777-785.

Goksoy, E., Y.Q. Ma, X. Wang, X. Kong, D. Perera, E.F. Plow, and J. Qin. 2008. Structural basis for the autoinhibition of talin in regulating integrin activation. *Mol Cell*. 31:124-133.
Goldmann, W.H. 2016. Role of vinculin in cellular mechanotransduction. *Cell Biol Int*. 40:241-256.
Goley, E.D., and M.D. Welch. 2006. The ARP2/3 complex: an actin nucleator comes of age. *Nat Rev Mol Cell Biol*. 7:713-726.
Goode, B.L., and M.J. Eck. 2007. Mechanism and function of formins in the control of actin assembly. *Annu Rev Biochem*. 76:593-627.
Goult, B.T., M. Bouaouina, P.R. Elliott, N. Bate, B. Patel, A.R. Gingras, J.G. Grossmann, G.C. Roberts, D.A. Calderwood, D.R. Critchley, and I.L. Barsukov. 2010. Structure of a double ubiquitin-like domain in the talin head: a role in integrin activation. *EMBO J*. 29:1069-1080.
Gourley, S.L., A.J. Koleske, and J.R. Taylor. 2009. Loss of dendrite stabilization by the Abl-related gene (Arg) kinase regulates behavioral flexibility and sensitivity to cocaine. *Proc Natl Acad Sci U S A*. 106:16859-16864.
Greuber, E.K., P. Smith-Pearson, J. Wang, and A.M. Pendergast. 2013. Role of ABL family kinases in cancer: from leukaemia to solid tumours. *Nat Rev Cancer*. 13:559-571.
Gu, Z., E.H. Noss, V.W. Hsu, and M.B. Brenner. 2011. Integrins traffic rapidly via circular dorsal ruffles and macropinocytosis during stimulated cell migration. *J Cell Biol*. 193:61-70.
Guilluy, C., R. Garcia-Mata, and K. Burridge. 2011. Rho protein crosstalk: another social network? *Trends Cell Biol*. 21:718-726.
Guo, B., J. Gao, J. Zhan, and H. Zhang. 2015. Kindlin-2 interacts with and stabilizes EGFR and is required for EGF-induced breast cancer cell migration. *Cancer Lett*. 361:271-281.
Hantschel, O. 2012. Structure, regulation, signaling, and targeting of abl kinases in cancer. *Genes Cancer*. 3:436-446.
Harburger, D.S., M. Bouaouina, and D.A. Calderwood. 2009. Kindlin-1 and -2 directly bind the C-terminal region of beta integrin cytoplasmic tails and exert integrin-specific activation effects. *J Biol Chem*. 284:11485-11497.
Has, C., D. Castiglia, M. del Rio, M.G. Diez, E. Piccinni, D. Kiritsi, J. Kohlhase, P. Itin, L. Martin, J. Fischer, G. Zambruno, and L. Bruckner-Tuderman. 2011. Kindler syndrome: extension of FERMT1 mutational spectrum and natural history. *Hum Mutat*. 32:1204-1212.
Hasegawa, J., E. Tokuda, T. Tenno, K. Tsujita, H. Sawai, H. Hiroaki, T. Takenawa, and T. Itoh. 2011. SH3YL1 regulates dorsal ruffle formation by a novel phosphoinositide-binding domain. *J Cell Biol*. 193:901-916.
He, Y., P. Esser, A. Heinemann, L. Bruckner-Tuderman, and C. Has. 2011. Kindlin-1 and -2 have overlapping functions in epithelial cells implications for phenotype modification. *Am J Pathol*. 178:975-982.
Hernandez, S.E., M. Krishnaswami, A.L. Miller, and A.J. Koleske. 2004. How do Abl family kinases regulate cell shape and movement? *Trends Cell Biol*. 14:36-44.
Herz, C., M. Aumailley, C. Schulte, U. Schlotzer-Schrehardt, L. Bruckner-Tuderman, and C. Has. 2006. Kindlin-1 is a phosphoprotein involved in regulation of polarity, proliferation, and motility of epidermal keratinocytes. *J Biol Chem*. 281:36082-36090.
Hoffman, B.D., C. Grashoff, and M.A. Schwartz. 2011. Dynamic molecular processes mediate cellular mechanotransduction. *Nature*. 475:316-323.
Hogg, N., and P.A. Bates. 2000. Genetic analysis of integrin function in man: LAD-1 and other syndromes. *Matrix Biol*. 19:211-222.
Hoon, J.L., W.K. Wong, and C.G. Koh. 2012. Functions and regulation of circular dorsal ruffles. *Mol Cell Biol*. 32:4246-4257.
Huet-Calderwood, C., N.N. Brahme, N. Kumar, A.L. Stiegler, S. Raghavan, T.J. Boggon, and D.A. Calderwood. 2014. Differences in binding to the ILK complex determines kindlin isoform adhesion localization and integrin activation. *J Cell Sci*. 127:4308-4321.

Hughes, P.E., F. Diaz-Gonzalez, L. Leong, C. Wu, J.A. McDonald, S.J. Shattil, and M.H. Ginsberg. 1996. Breaking the integrin hinge. A defined structural constraint regulates integrin signaling. *J Biol Chem*. 271:6571-6574.

Humphries, J.D., A. Byron, and M.J. Humphries. 2006. Integrin ligands at a glance. *J Cell Sci*. 119:3901-3903.

Humphries, J.D., P. Wang, C. Streuli, B. Geiger, M.J. Humphries, and C. Ballestrem. 2007. Vinculin controls focal adhesion formation by direct interactions with talin and actin. *J Cell Biol*. 179:1043-1057.

Huveneers, S., and E.H. Danen. 2009. Adhesion signaling - crosstalk between integrins, Src and Rho. *J Cell Sci*. 122:1059-1069.

Hynes, R.O. 2002. Integrins: bidirectional, allosteric signaling machines. *Cell*. 110:673-687.

Ichetovkin, I., W. Grant, and J. Condeelis. 2002. Cofilin produces newly polymerized actin filaments that are preferred for dendritic nucleation by the Arp2/3 complex. *Curr Biol*. 12:79-84.

Ilic, D., Y. Furuta, S. Kanazawa, N. Takeda, K. Sobue, N. Nakatsuji, S. Nomura, J. Fujimoto, M. Okada, and T. Yamamoto. 1995. Reduced cell motility and enhanced focal adhesion contact formation in cells from FAK-deficient mice. *Nature*. 377:539-544.

Innocenti, M., E. Frittoli, I. Ponzanelli, J.R. Falck, S.M. Brachmann, P.P. Di Fiore, and G. Scita. 2003. Phosphoinositide 3-kinase activates Rac by entering in a complex with Eps8, Abi1, and Sos-1. *J Cell Biol*. 160:17-23.

Ivaska, J., and J. Heino. 2011. Cooperation between integrins and growth factor receptors in signaling and endocytosis. *Annu Rev Cell Dev Biol*. 27:291-320.

Jacob, A.E., C.E. Turner, and J.D. Amack. 2016. Evolution and Expression of Paxillin Genes in Teleost Fish. *PLoS One*. 11:e0165266.

Jiang, G., G. Giannone, D.R. Critchley, E. Fukumoto, and M.P. Sheetz. 2003. Two-piconewton slip bond between fibronectin and the cytoskeleton depends on talin. *Nature*. 424:334-337.

Johnson, M.S., N. Lu, K. Denessiouk, J. Heino, and D. Gullberg. 2009. Integrins during evolution: evolutionary trees and model organisms. *Biochim Biophys Acta*. 1788:779-789.

Kahner, B.N., H. Kato, A. Banno, M.H. Ginsberg, S.J. Shattil, and F. Ye. 2012. Kindlins, integrin activation and the regulation of talin recruitment to alphaIIbbeta3. *PLoS One*. 7:e34056.

Kain, K.H., and R.L. Klemke. 2001. Inhibition of cell migration by Abl family tyrosine kinases through uncoupling of Crk-CAS complexes. *J Biol Chem*. 276:16185-16192.

Karakose, E., H.B. Schiller, and R. Fassler. 2010. The kindlins at a glance. *J Cell Sci*. 123:2353-2356.

Khan, A.A., A. Janke, T. Shimokawa, and H. Zhang. 2011. Phylogenetic analysis of kindlins suggests subfunctionalization of an ancestral unduplicated kindlin into three paralogs in vertebrates. *Evol Bioinform Online*. 7:7-19.

Kharbanda, S., R. Ren, P. Pandey, T.D. Shafman, S.M. Feller, R.R. Weichselbaum, and D.W. Kufe. 1995. Activation of the c-Abl tyrosine kinase in the stress response to DNA-damaging agents. *Nature*. 376:785-788.

Khatri, A., J. Wang, and A.M. Pendergast. 2016. Multifunctional Abl kinases in health and disease. *J Cell Sci*. 129:9-16.

Kiema, T., Y. Lad, P. Jiang, C.L. Oxley, M. Baldassarre, K.L. Wegener, I.D. Campbell, J. Ylanne, and D.A. Calderwood. 2006. The molecular basis of filamin binding to integrins and competition with talin. *Mol Cell*. 21:337-347.

Kim, C., F. Ye, and M.H. Ginsberg. 2011. Regulation of integrin activation. *Annu Rev Cell Dev Biol*. 27:321-345.

Kirkbride, K.C., B.H. Sung, S. Sinha, and A.M. Weaver. 2011. Cortactin: a multifunctional regulator of cellular invasiveness. *Cell Adh Migr*. 5:187-198.

Klapholz, B., and N.H. Brown. 2017. Talin - the master of integrin adhesions. *J Cell Sci*. 130:2435-2446.

Kleinschmidt, E.G., and D.D. Schlaepfer. 2017. Focal adhesion kinase signaling in unexpected places. *Curr Opin Cell Biol*. 45:24-30.

Klemke, R.L., J. Leng, R. Molander, P.C. Brooks, K. Vuori, and D.A. Cheresh. 1998. CAS/Crk coupling serves as a "molecular switch" for induction of cell migration. *J Cell Biol*. 140:961-972.
Koleske, A.J., A.M. Gifford, M.L. Scott, M. Nee, R.T. Bronson, K.A. Miczek, and D. Baltimore. 1998. Essential roles for the Abl and Arg tyrosine kinases in neurulation. *Neuron*. 21:1259-1272.
Kong, F., A.J. Garcia, A.P. Mould, M.J. Humphries, and C. Zhu. 2009. Demonstration of catch bonds between an integrin and its ligand. *J Cell Biol*. 185:1275-1284.
Kong, F., Z. Li, W.M. Parks, D.W. Dumbauld, A.J. Garcia, A.P. Mould, M.J. Humphries, and C. Zhu. 2013. Cyclic mechanical reinforcement of integrin-ligand interactions. *Mol Cell*. 49:1060-1068.
Kong, J., J. Du, Y. Wang, M. Yang, J. Gao, X. Wei, W. Fang, J. Zhan, and H. Zhang. 2016. Focal adhesion molecule Kindlin-1 mediates activation of TGF-beta signaling by interacting with TGF-betaRI, SARA and Smad3 in colorectal cancer cells. *Oncotarget*. 7:76224-76237.
Kowalski, J.R., C. Egile, S. Gil, S.B. Snapper, R. Li, and S.M. Thomas. 2005. Cortactin regulates cell migration through activation of N-WASP. *J Cell Sci*. 118:79-87.
Krause, M., J.E. Bear, J.J. Loureiro, and F.B. Gertler. 2002. The Ena/VASP enigma. *J Cell Sci*. 115:4721-4726.
Krause, M., and A. Gautreau. 2014. Steering cell migration: lamellipodium dynamics and the regulation of directional persistence. *Nat Rev Mol Cell Biol*. 15:577-590.
Krueger, E.W., J.D. Orth, H. Cao, and M.A. McNiven. 2003. A dynamin-cortactin-Arp2/3 complex mediates actin reorganization in growth factor-stimulated cells. *Mol Biol Cell*. 14:1085-1096.
Kruger, M., M. Moser, S. Ussar, I. Thievessen, C.A. Luber, F. Forner, S. Schmidt, S. Zanivan, R. Fassler, and M. Mann. 2008. SILAC mouse for quantitative proteomics uncovers kindlin-3 as an essential factor for red blood cell function. *Cell*. 134:353-364.
Kua, H.Y., H. Liu, W.F. Leong, L. Li, D. Jia, G. Ma, Y. Hu, X. Wang, J.F. Chau, Y.G. Chen, Y. Mishina, S. Boast, J. Yeh, L. Xia, G.Q. Chen, L. He, S.P. Goff, and B. Li. 2012. c-Abl promotes osteoblast expansion by differentially regulating canonical and non-canonical BMP pathways and p16INK4a expression. *Nat Cell Biol*. 14:727-737.
Ladwein, M., and K. Rottner. 2008. On the Rho'd: the regulation of membrane protrusions by Rho-GTPases. *FEBS Lett*. 582:2066-2074.
Lai-Cheong, J.E., M. Parsons, and J.A. McGrath. 2010. The role of kindlins in cell biology and relevance to human disease. *Int J Biochem Cell Biol*. 42:595-603.
Lanzetti, L., A. Palamidessi, L. Areces, G. Scita, and P.P. Di Fiore. 2004. Rab5 is a signalling GTPase involved in actin remodelling by receptor tyrosine kinases. *Nature*. 429:309-314.
Lapetina, S., C.C. Mader, K. Machida, B.J. Mayer, and A.J. Koleske. 2009. Arg interacts with cortactin to promote adhesion-dependent cell edge protrusion. *J Cell Biol*. 185:503-519.
Lau, T.L., C. Kim, M.H. Ginsberg, and T.S. Ulmer. 2009. The structure of the integrin alphaIIbbeta3 transmembrane complex explains integrin transmembrane signalling. *EMBO J*. 28:1351-1361.
Laukaitis, C.M., D.J. Webb, K. Donais, and A.F. Horwitz. 2001. Differential dynamics of alpha 5 integrin, paxillin, and alpha-actinin during formation and disassembly of adhesions in migrating cells. *J Cell Biol*. 153:1427-1440.
Lebensohn, A.M., and M.W. Kirschner. 2009. Activation of the WAVE complex by coincident signals controls actin assembly. *Mol Cell*. 36:512-524.
Legate, K.R., S. Takahashi, N. Bonakdar, B. Fabry, D. Boettiger, R. Zent, and R. Fassler. 2011. Integrin adhesion and force coupling are independently regulated by localized PtdIns(4,5)2 synthesis. *EMBO J*. 30:4539-4553.
Legate, K.R., S.A. Wickstrom, and R. Fassler. 2009. Genetic and cell biological analysis of integrin outside-in signaling. *Genes Dev*. 23:397-418.
Legg, J.A., G. Bompard, J. Dawson, H.L. Morris, N. Andrew, L. Cooper, S.A. Johnston, G. Tramountanis, and L.M. Machesky. 2007. N-WASP involvement in dorsal ruffle formation in mouse embryonic fibroblasts. *Mol Biol Cell*. 18:678-687.

Lemmon, M.A. 2008. Membrane recognition by phospholipid-binding domains. *Nat Rev Mol Cell Biol*. 9:99-111.

Leng, Y., J. Zhang, K. Badour, E. Arpaia, S. Freeman, P. Cheung, M. Siu, and K. Siminovitch. 2005. Abelson-interactor-1 promotes WAVE2 membrane translocation and Abelson-mediated tyrosine phosphorylation required for WAVE2 activation. *Proc Natl Acad Sci U S A*. 102:1098-1103.

Lewis, J.M., R. Baskaran, S. Taagepera, M.A. Schwartz, and J.Y. Wang. 1996. Integrin regulation of c-Abl tyrosine kinase activity and cytoplasmic-nuclear transport. *Proc Natl Acad Sci U S A*. 93:15174-15179.

Ley, K., C. Laudanna, M.I. Cybulsky, and S. Nourshargh. 2007. Getting to the site of inflammation: the leukocyte adhesion cascade updated. *Nat Rev Immunol*. 7:678-689.

Li, B., S. Boast, K. de los Santos, I. Schieren, M. Quiroz, S.L. Teitelbaum, M.M. Tondravi, and S.P. Goff. 2000. Mice deficient in Abl are osteoporotic and have defects in osteoblast maturation. *Nat Genet*. 24:304-308.

Li, H., Y. Deng, K. Sun, H. Yang, J. Liu, M. Wang, Z. Zhang, J. Lin, C. Wu, Z. Wei, and C. Yu. 2017a. Structural basis of kindlin-mediated integrin recognition and activation. *Proc Natl Acad Sci U S A*. 114:9349-9354.

Li, J., and T.A. Springer. 2017. Integrin extension enables ultrasensitive regulation by cytoskeletal force. *Proc Natl Acad Sci U S A*. 114:4685-4690.

Li, J., and T.A. Springer. 2018. Energy landscape differences among integrins establish the framework for understanding activation. *J Cell Biol*. 217:397-412.

Li, J., Y. Su, W. Xia, Y. Qin, M.J. Humphries, D. Vestweber, C. Cabanas, C. Lu, and T.A. Springer. 2017b. Conformational equilibria and intrinsic affinities define integrin activation. *EMBO J*. 36:629-645.

Lin, J., W. Lin, Y. Ye, L. Wang, X. Chen, S. Zang, and A. Huang. 2017. Kindlin-2 promotes hepatocellular carcinoma invasion and metastasis by increasing Wnt/beta-catenin signaling. *J Exp Clin Cancer Res*. 36:134.

Ling, K., R.L. Doughman, A.J. Firestone, M.W. Bunce, and R.A. Anderson. 2002. Type I gamma phosphatidylinositol phosphate kinase targets and regulates focal adhesions. *Nature*. 420:89-93.

Litvinov, R.I., V. Barsegov, A.J. Schissler, A.R. Fisher, J.S. Bennett, J.W. Weisel, and H. Shuman. 2011. Dissociation of bimolecular alphaIIbbeta3-fibrinogen complex under a constant tensile force. *Biophys J*. 100:165-173.

Liu, W., K.M. Draheim, R. Zhang, D.A. Calderwood, and T.J. Boggon. 2013. Mechanism for KRIT1 release of ICAP1-mediated suppression of integrin activation. *Mol Cell*. 49:719-729.

Liu, Z., D. Lu, X. Wang, J. Wan, C. Liu, and H. Zhang. 2015. Kindlin-2 phosphorylation by Src at Y193 enhances Src activity and is involved in Migfilin recruitment to the focal adhesions. *FEBS Lett*. 589:2001-2010.

Lu, Z., S. Mathew, J. Chen, A. Hadziselimovic, R. Palamuttam, B.G. Hudson, R. Fassler, A. Pozzi, C.R. Sanders, and R. Zent. 2016. Implications of the differing roles of the beta1 and beta3 transmembrane and cytoplasmic domains for integrin function. *Elife*. 5.

Luo, B.H., C.V. Carman, and T.A. Springer. 2007. Structural basis of integrin regulation and signaling. *Annu Rev Immunol*. 25:619-647.

Luo, B.H., C.V. Carman, J. Takagi, and T.A. Springer. 2005. Disrupting integrin transmembrane domain heterodimerization increases ligand binding affinity, not valency or clustering. *Proc Natl Acad Sci U S A*. 102:3679-3684.

Luo, B.H., J. Takagi, and T.A. Springer. 2004. Locking the beta3 integrin I-like domain into high and low affinity conformations with disulfides. *J Biol Chem*. 279:10215-10221.

Martel, V., C. Racaud-Sultan, S. Dupe, C. Marie, F. Paulhe, A. Galmiche, M.R. Block, and C. Albiges-Rizo. 2001. Conformation, localization, and integrin binding of talin depend on its interaction with phosphoinositides. *J Biol Chem*. 276:21217-21227.

Mejillano, M.R., S. Kojima, D.A. Applewhite, F.B. Gertler, T.M. Svitkina, and G.G. Borisy. 2004. Lamellipodial versus filopodial mode of the actin nanomachinery: pivotal role of the filament barbed end. *Cell*. 118:363-373.

Meller, J., I.B. Rogozin, E. Poliakov, N. Meller, M. Bedanov-Pack, E.F. Plow, J. Qin, E.A. Podrez, and T.V. Byzova. 2015. Emergence and subsequent functional specialization of kindlins during evolution of cell adhesiveness. *Mol Biol Cell*. 26:786-796.

Meves, A., C. Stremmel, K. Gottschalk, and R. Fassler. 2009. The Kindlin protein family: new members to the club of focal adhesion proteins. *Trends Cell Biol*. 19:504-513.

Miller, A.L., Y. Wang, M.S. Mooseker, and A.J. Koleske. 2004. The Abl-related gene (Arg) requires its F-actin-microtubule cross-linking activity to regulate lamellipodial dynamics during fibroblast adhesion. *J Cell Biol*. 165:407-419.

Mitra, S.K., D.A. Hanson, and D.D. Schlaepfer. 2005. Focal adhesion kinase: in command and control of cell motility. *Nat Rev Mol Cell Biol*. 6:56-68.

Mitra, S.K., and D.D. Schlaepfer. 2006. Integrin-regulated FAK-Src signaling in normal and cancer cells. *Curr Opin Cell Biol*. 18:516-523.

Monkley, S.J., X.H. Zhou, S.J. Kinston, S.M. Giblett, L. Hemmings, H. Priddle, J.E. Brown, C.A. Pritchard, D.R. Critchley, and R. Fassler. 2000. Disruption of the talin gene arrests mouse development at the gastrulation stage. *Dev Dyn*. 219:560-574.

Montanez, E., S. Ussar, M. Schifferer, M. Bosl, R. Zent, M. Moser, and R. Fassler. 2008. Kindlin-2 controls bidirectional signaling of integrins. *Genes Dev*. 22:1325-1330.

Moore, T.I., J. Aaron, T.L. Chew, and T.A. Springer. 2018. Measuring Integrin Conformational Change on the Cell Surface with Super-Resolution Microscopy. *Cell Rep*. 22:1903-1912.

Moresco, E.M., S. Donaldson, A. Williamson, and A.J. Koleske. 2005. Integrin-mediated dendrite branch maintenance requires Abelson (Abl) family kinases. *J Neurosci*. 25:6105-6118.

Moretti, F.A., M. Moser, R. Lyck, M. Abadier, R. Ruppert, B. Engelhardt, and R. Fassler. 2013. Kindlin-3 regulates integrin activation and adhesion reinforcement of effector T cells. *Proc Natl Acad Sci U S A*. 110:17005-17010.

Moro, L., M. Venturino, C. Bozzo, L. Silengo, F. Altruda, L. Beguinot, G. Tarone, and P. Defilippi. 1998. Integrins induce activation of EGF receptor: role in MAP kinase induction and adhesion-dependent cell survival. *EMBO J*. 17:6622-6632.

Morrison, V.L., M.J. James, K. Grzes, P. Cook, D.G. Glass, T. Savinko, H.S. Lek, C. Gawden-Bone, C. Watts, O.R. Millington, A.S. MacDonald, and S.C. Fagerholm. 2014. Loss of beta2-integrin-mediated cytoskeletal linkage reprogrammes dendritic cells to a mature migratory phenotype. *Nat Commun*. 5:5359.

Moser, M., M. Bauer, S. Schmid, R. Ruppert, S. Schmidt, M. Sixt, H.V. Wang, M. Sperandio, and R. Fassler. 2009a. Kindlin-3 is required for beta2 integrin-mediated leukocyte adhesion to endothelial cells. *Nat Med*. 15:300-305.

Moser, M., K.R. Legate, R. Zent, and R. Fassler. 2009b. The tail of integrins, talin, and kindlins. *Science*. 324:895-899.

Moser, M., B. Nieswandt, S. Ussar, M. Pozgajova, and R. Fassler. 2008. Kindlin-3 is essential for integrin activation and platelet aggregation. *Nat Med*. 14:325-330.

Nagar, B., O. Hantschel, M.A. Young, K. Scheffzek, D. Veach, W. Bornmann, B. Clarkson, G. Superti-Furga, and J. Kuriyan. 2003. Structural basis for the autoinhibition of c-Abl tyrosine kinase. *Cell*. 112:859-871.

Nishida, N., C. Xie, M. Shimaoka, Y. Cheng, T. Walz, and T.A. Springer. 2006. Activation of leukocyte beta2 integrins by conversion from bent to extended conformations. *Immunity*. 25:583-594.

Nishiuchi, R., J. Takagi, M. Hayashi, H. Ido, Y. Yagi, N. Sanzen, T. Tsuji, M. Yamada, and K. Sekiguchi. 2006. Ligand-binding specificities of laminin-binding integrins: a comprehensive survey of laminin-integrin interactions using recombinant alpha3beta1, alpha6beta1, alpha7beta1 and alpha6beta4 integrins. *Matrix Biol*. 25:189-197.

Orth, J.D., E.W. Krueger, S.G. Weller, and M.A. McNiven. 2006. A novel endocytic mechanism of epidermal growth factor receptor sequestration and internalization. *Cancer Res*. 66:3603-3610.

Oxley, C.L., N.J. Anthis, E.D. Lowe, I. Vakonakis, I.D. Campbell, and K.L. Wegener. 2008. An integrin phosphorylation switch: the effect of beta3 integrin tail phosphorylation on Dok1 and talin binding. *J Biol Chem*. 283:5420-5426.

Palamidessi, A., E. Frittoli, M. Garre, M. Faretta, M. Mione, I. Testa, A. Diaspro, L. Lanzetti, G. Scita, and P.P. Di Fiore. 2008. Endocytic trafficking of Rac is required for the spatial restriction of signaling in cell migration. *Cell*. 134:135-147.

Pankov, R., E. Cukierman, B.Z. Katz, K. Matsumoto, D.C. Lin, S. Lin, C. Hahn, and K.M. Yamada. 2000. Integrin dynamics and matrix assembly: tensin-dependent translocation of alpha(5)beta(1) integrins promotes early fibronectin fibrillogenesis. *J Cell Biol*. 148:1075-1090.

Parsons, J.T., A.R. Horwitz, and M.A. Schwartz. 2010. Cell adhesion: integrating cytoskeletal dynamics and cellular tension. *Nat Rev Mol Cell Biol*. 11:633-643.

Paszek, M.J., D. Boettiger, V.M. Weaver, and D.A. Hammer. 2009. Integrin clustering is driven by mechanical resistance from the glycocalyx and the substrate. *PLoS Comput Biol*. 5:e1000604.

Paszek, M.J., C.C. DuFort, O. Rossier, R. Bainer, J.K. Mouw, K. Godula, J.E. Hudak, J.N. Lakins, A.C. Wijekoon, L. Cassereau, M.G. Rubashkin, M.J. Magbanua, K.S. Thorn, M.W. Davidson, H.S. Rugo, J.W. Park, D.A. Hammer, G. Giannone, C.R. Bertozzi, and V.M. Weaver. 2014. The cancer glycocalyx mechanically primes integrin-mediated growth and survival. *Nature*. 511:319-325.

Patel, H., J. Zich, B. Serrels, C. Rickman, K.G. Hardwick, M.C. Frame, and V.G. Brunton. 2013. Kindlin-1 regulates mitotic spindle formation by interacting with integrins and Plk-1. *Nat Commun*. 4:2056.

Peacock, J.G., A.L. Miller, W.D. Bradley, O.C. Rodriguez, D.J. Webb, and A.J. Koleske. 2007. The Abl-related gene tyrosine kinase acts through p190RhoGAP to inhibit actomyosin contractility and regulate focal adhesion dynamics upon adhesion to fibronectin. *Mol Biol Cell*. 18:3860-3872.

Peleg, B., A. Disanza, G. Scita, and N. Gov. 2011. Propagating cell-membrane waves driven by curved activators of actin polymerization. *PLoS One*. 6:e18635.

Peng, X., E.S. Nelson, J.L. Maiers, and K.A. DeMali. 2011. New insights into vinculin function and regulation. *Int Rev Cell Mol Biol*. 287:191-231.

Perera, H.D., Y.Q. Ma, J. Yang, J. Hirbawi, E.F. Plow, and J. Qin. 2011. Membrane binding of the N-terminal ubiquitin-like domain of kindlin-2 is crucial for its regulation of integrin activation. *Structure*. 19:1664-1671.

Plattner, R., L. Kadlec, K.A. DeMali, A. Kazlauskas, and A.M. Pendergast. 1999. c-Abl is activated by growth factors and Src family kinases and has a role in the cellular response to PDGF. *Genes Dev*. 13:2400-2411.

Pluk, H., K. Dorey, and G. Superti-Furga. 2002. Autoinhibition of c-Abl. *Cell*. 108:247-259.

Pollard, T.D. 2007. Regulation of actin filament assembly by Arp2/3 complex and formins. *Annu Rev Biophys Biomol Struct*. 36:451-477.

Pollitt, A.Y., and R.H. Insall. 2009. WASP and SCAR/WAVE proteins: the drivers of actin assembly. *J Cell Sci*. 122:2575-2578.

Price, L.S., J. Leng, M.A. Schwartz, and G.M. Bokoch. 1998. Activation of Rac and Cdc42 by integrins mediates cell spreading. *Mol Biol Cell*. 9:1863-1871.

Puklin-Faucher, E., M. Gao, K. Schulten, and V. Vogel. 2006. How the headpiece hinge angle is opened: New insights into the dynamics of integrin activation. *J Cell Biol*. 175:349-360.

Qadota, H., D.G. Moerman, and G.M. Benian. 2012. A molecular mechanism for the requirement of PAT-4 (integrin-linked kinase (ILK)) for the localization of UNC-112 (Kindlin) to integrin adhesion sites. *J Biol Chem*. 287:28537-28551.

Qu, H., Y. Tu, J.L. Guan, G. Xiao, and C. Wu. 2014. Kindlin-2 tyrosine phosphorylation and interaction with Src serve as a regulatable switch in the integrin outside-in signaling circuit. *J Biol Chem*. 289:31001-31013.

Raftopoulou, M., and A. Hall. 2004. Cell migration: Rho GTPases lead the way. *Dev Biol*. 265:23-32.

Rantala, J.K., J. Pouwels, T. Pellinen, S. Veltel, P. Laasola, E. Mattila, C.S. Potter, T. Duffy, J.P. Sundberg, O. Kallioniemi, J.A. Askari, M.J. Humphries, M. Parsons, M. Salmi, and J. Ivaska. 2011. SHARPIN is an endogenous inhibitor of beta1-integrin activation. *Nat Cell Biol*. 13:1315-1324.

Ren, X.D., W.B. Kiosses, and M.A. Schwartz. 1999. Regulation of the small GTP-binding protein Rho by cell adhesion and the cytoskeleton. *EMBO J*. 18:578-585.

Ribeiro Ede, A., Jr., N. Pinotsis, A. Ghisleni, A. Salmazo, P.V. Konarev, J. Kostan, B. Sjoblom, C. Schreiner, A.A. Polyansky, E.A. Gkougkoulia, M.R. Holt, F.L. Aachmann, B. Zagrovic, E. Bordignon, K.F. Pirker, D.I. Svergun, M. Gautel, and K. Djinovic-Carugo. 2014. The structure and regulation of human muscle alpha-actinin. *Cell*. 159:1447-1460.

Rivera, G.M., S. Antoku, S. Gelkop, N.Y. Shin, S.K. Hanks, T. Pawson, and B.J. Mayer. 2006. Requirement of Nck adaptors for actin dynamics and cell migration stimulated by platelet-derived growth factor B. *Proc Natl Acad Sci U S A*. 103:9536-9541.

Roca-Cusachs, P., N.C. Gauthier, A. Del Rio, and M.P. Sheetz. 2009. Clustering of alpha(5)beta(1) integrins determines adhesion strength whereas alpha(v)beta(3) and talin enable mechanotransduction. *Proc Natl Acad Sci U S A*. 106:16245-16250.

Rognoni, E., R. Ruppert, and R. Fassler. 2016. The kindlin family: functions, signaling properties and implications for human disease. *J Cell Sci*. 129:17-27.

Rognoni, E., M. Widmaier, M. Jakobson, R. Ruppert, S. Ussar, D. Katsougkri, R.T. Bottcher, J.E. Lai-Cheong, D.B. Rifkin, J.A. McGrath, and R. Fassler. 2014. Kindlin-1 controls Wnt and TGF-beta availability to regulate cutaneous stem cell proliferation. *Nat Med*. 20:350-359.

Rojas, J.M., J.L. Oliva, and E. Santos. 2011. Mammalian son of sevenless Guanine nucleotide exchange factors: old concepts and new perspectives. *Genes Cancer*. 2:298-305.

Ruusala, A., T. Pawson, C.H. Heldin, and P. Aspenstrom. 2008. Nck adapters are involved in the formation of dorsal ruffles, cell migration, and Rho signaling downstream of the platelet-derived growth factor beta receptor. *J Biol Chem*. 283:30034-30044.

Sabino, F., O. Hermes, F.E. Egli, T. Kockmann, P. Schlage, P. Croizat, J.N. Kizhakkedathu, H. Smola, and U. auf dem Keller. 2015. In vivo assessment of protease dynamics in cutaneous wound healing by degradomics analysis of porcine wound exudates. *Mol Cell Proteomics*. 14:354-370.

Saunders, R.M., M.R. Holt, L. Jennings, D.H. Sutton, I.L. Barsukov, A. Bobkov, R.C. Liddington, E.A. Adamson, G.A. Dunn, and D.R. Critchley. 2006. Role of vinculin in regulating focal adhesion turnover. *Eur J Cell Biol*. 85:487-500.

Schmidt, S., M. Moser, and M. Sperandio. 2013. The molecular basis of leukocyte recruitment and its deficiencies. *Mol Immunol*. 55:49-58.

Schmidt, S., I. Nakchbandi, R. Ruppert, N. Kawelke, M.W. Hess, K. Pfaller, P. Jurdic, R. Fassler, and M. Moser. 2011. Kindlin-3-mediated signaling from multiple integrin classes is required for osteoclast-mediated bone resorption. *J Cell Biol*. 192:883-897.

Schneller, M., K. Vuori, and E. Ruoslahti. 1997. Alphavbeta3 integrin associates with activated insulin and PDGFbeta receptors and potentiates the biological activity of PDGF. *EMBO J*. 16:5600-5607.

Schonichen, A., and M. Geyer. 2010. Fifteen formins for an actin filament: a molecular view on the regulation of human formins. *Biochim Biophys Acta*. 1803:152-163.

Schwartzberg, P.L., A.M. Stall, J.D. Hardin, K.S. Bowdish, T. Humaran, S. Boast, M.L. Harbison, E.J. Robertson, and S.P. Goff. 1991. Mice homozygous for the ablm1 mutation show poor viability and depletion of selected B and T cell populations. *Cell*. 65:1165-1175.

Sebe-Pedros, A., A.J. Roger, F.B. Lang, N. King, and I. Ruiz-Trillo. 2010. Ancient origin of the integrin-mediated adhesion and signaling machinery. *Proc Natl Acad Sci U S A*. 107:10142-10147.

Serrels, B., A. Serrels, V.G. Brunton, M. Holt, G.W. McLean, C.H. Gray, G.E. Jones, and M.C. Frame. 2007. Focal adhesion kinase controls actin assembly via a FERM-mediated interaction with the Arp2/3 complex. *Nat Cell Biol*. 9:1046-1056.

Shattil, S.J., C. Kim, and M.H. Ginsberg. 2010. The final steps of integrin activation: the end game. *Nat Rev Mol Cell Biol*. 11:288-300.

Shi, Q., and D. Boettiger. 2003. A novel mode for integrin-mediated signaling: tethering is required for phosphorylation of FAK Y397. *Mol Biol Cell*. 14:4306-4315.

Sieg, D.J., C.R. Hauck, D. Ilic, C.K. Klingbeil, E. Schaefer, C.H. Damsky, and D.D. Schlaepfer. 2000. FAK integrates growth-factor and integrin signals to promote cell migration. *Nat Cell Biol*. 2:249-256.

Simpson, M.A., W.D. Bradley, D. Harburger, M. Parsons, D.A. Calderwood, and A.J. Koleske. 2015. Direct interactions with the integrin beta1 cytoplasmic tail activate the Abl2/Arg kinase. *J Biol Chem*. 290:8360-8372.

Sini, P., A. Cannas, A.J. Koleske, P.P. Di Fiore, and G. Scita. 2004. Abl-dependent tyrosine phosphorylation of Sos-1 mediates growth-factor-induced Rac activation. *Nat Cell Biol*. 6:268-274.

Sirvent, A., C. Benistant, and S. Roche. 2008. Cytoplasmic signalling by the c-Abl tyrosine kinase in normal and cancer cells. *Biol Cell*. 100:617-631.

Sjoblom, B., A. Salmazo, and K. Djinovic-Carugo. 2008. Alpha-actinin structure and regulation. *Cell Mol Life Sci*. 65:2688-2701.

Soldi, R., S. Mitola, M. Strasly, P. Defilippi, G. Tarone, and F. Bussolino. 1999. Role of alphavbeta3 integrin in the activation of vascular endothelial growth factor receptor-2. *EMBO J*. 18:882-892.

Sossey-Alaoui, K., X. Li, and J.K. Cowell. 2007. c-Abl-mediated phosphorylation of WAVE3 is required for lamellipodia formation and cell migration. *J Biol Chem*. 282:26257-26265.

Sossey-Alaoui, K., E. Pluskota, G. Davuluri, K. Bialkowska, M. Das, D. Szpak, D.J. Lindner, E. Downs-Kelly, C.L. Thompson, and E.F. Plow. 2014. Kindlin-3 enhances breast cancer progression and metastasis by activating Twist-mediated angiogenesis. *FASEB J*. 28:2260-2271.

Spiering, D., and L. Hodgson. 2011. Dynamics of the Rho-family small GTPases in actin regulation and motility. *Cell Adh Migr*. 5:170-180.

Springer, T.A., and M.L. Dustin. 2012. Integrin inside-out signaling and the immunological synapse. *Curr Opin Cell Biol*. 24:107-115.

Springer, T.A., J. Zhu, and T. Xiao. 2008. Structural basis for distinctive recognition of fibrinogen gammaC peptide by the platelet integrin alphaIIbbeta3. *J Cell Biol*. 182:791-800.

Stephens, L.E., A.E. Sutherland, I.V. Klimanskaya, A. Andrieux, J. Meneses, R.A. Pedersen, and C.H. Damsky. 1995. Deletion of beta 1 integrins in mice results in inner cell mass failure and peri-implantation lethality. *Genes Dev*. 9:1883-1895.

Stuart, J.R., F.H. Gonzalez, H. Kawai, and Z.M. Yuan. 2006. c-Abl interacts with the WAVE2 signaling complex to induce membrane ruffling and cell spreading. *J Biol Chem*. 281:31290-31297.

Suetsugu, S., D. Yamazaki, S. Kurisu, and T. Takenawa. 2003. Differential roles of WAVE1 and WAVE2 in dorsal and peripheral ruffle formation for fibroblast cell migration. *Dev Cell*. 5:595-609.

Sulzmaier, F.J., C. Jean, and D.D. Schlaepfer. 2014. FAK in cancer: mechanistic findings and clinical applications. *Nat Rev Cancer*. 14:598-610.

Sun, Y., C. Guo, P. Ma, Y. Lai, F. Yang, J. Cai, Z. Cheng, K. Zhang, Z. Liu, Y. Tian, Y. Sheng, R. Tian, Y. Deng, G. Xiao, and C. Wu. 2017. Kindlin-2 Association with Rho GDP-Dissociation Inhibitor alpha Suppresses Rac1 Activation and Podocyte Injury. *J Am Soc Nephrol*. 28:3545-3562.

Sun, Z., S.S. Guo, and R. Fassler. 2016a. Integrin-mediated mechanotransduction. *J Cell Biol*. 215:445-456.

Sun, Z., A. Lambacher, and R. Fassler. 2014. Nascent adhesions: from fluctuations to a hierarchical organization. *Curr Biol*. 24:R801-803.

Sun, Z., H.Y. Tseng, S. Tan, F. Senger, L. Kurzawa, D. Dedden, N. Mizuno, A.A. Wasik, M. Thery, A.R. Dunn, and R. Fassler. 2016b. Kank2 activates talin, reduces force transduction across integrins and induces central adhesion formation. *Nat Cell Biol*. 18:941-953.

Suraneni, P., B. Rubinstein, J.R. Unruh, M. Durnin, D. Hanein, and R. Li. 2012. The Arp2/3 complex is required for lamellipodia extension and directional fibroblast cell migration. *J Cell Biol*. 197:239-251.

Svensson, L., K. Howarth, A. McDowall, I. Patzak, R. Evans, S. Ussar, M. Moser, A. Metin, M. Fried, I. Tomlinson, and N. Hogg. 2009. Leukocyte adhesion deficiency-III is caused by mutations in KINDLIN3 affecting integrin activation. *Nat Med*. 15:306-312.

Swaminathan, V., R.S. Fischer, and C.M. Waterman. 2016. The FAK-Arp2/3 interaction promotes leading edge advance and haptosensing by coupling nascent adhesions to lamellipodia actin. *Mol Biol Cell*. 27:1085-1100.

Takagi, J., K. Strokovich, T.A. Springer, and T. Walz. 2003. Structure of integrin alpha5beta1 in complex with fibronectin. *EMBO J*. 22:4607-4615.

Takenawa, T., and S. Suetsugu. 2007. The WASP-WAVE protein network: connecting the membrane to the cytoskeleton. *Nat Rev Mol Cell Biol*. 8:37-48.

Takizawa, Y., H. Shimizu, T. Nishikawa, N. Hatta, L. Pulkkinen, and J. Uitto. 1997. Novel ITGB4 mutations in a patient with junctional epidermolysis bullosa-pyloric atresia syndrome and altered basement membrane zone immunofluorescence for the alpha6beta4 integrin. *J Invest Dermatol*. 108:943-946.

Tanis, K.Q., D. Veach, H.S. Duewel, W.G. Bornmann, and A.J. Koleske. 2003. Two distinct phosphorylation pathways have additive effects on Abl family kinase activation. *Mol Cell Biol*. 23:3884-3896.

ten Klooster, J.P., Z.M. Jaffer, J. Chernoff, and P.L. Hordijk. 2006. Targeting and activation of Rac1 are mediated by the exchange factor beta-Pix. *J Cell Biol*. 172:759-769.

Theodosiou, M., M. Widmaier, R.T. Bottcher, E. Rognoni, M. Veelders, M. Bharadwaj, A. Lambacher, K. Austen, D.J. Muller, R. Zent, and R. Fassler. 2016. Kindlin-2 cooperates with talin to activate integrins and induces cell spreading by directly binding paxillin. *Elife*. 5:e10130.

Thomas, W. 2008. Catch bonds in adhesion. *Annu Rev Biomed Eng*. 10:39-57.

Tomar, A., S.T. Lim, Y. Lim, and D.D. Schlaepfer. 2009. A FAK-p120RasGAP-p190RhoGAP complex regulates polarity in migrating cells. *J Cell Sci*. 122:1852-1862.

Tsubouchi, A., J. Sakakura, R. Yagi, Y. Mazaki, E. Schaefer, H. Yano, and H. Sabe. 2002. Localized suppression of RhoA activity by Tyr31/118-phosphorylated paxillin in cell adhesion and migration. *J Cell Biol*. 159:673-683.

Tu, Y., S. Wu, X. Shi, K. Chen, and C. Wu. 2003. Migfilin and Mig-2 link focal adhesions to filamin and the actin cytoskeleton and function in cell shape modulation. *Cell*. 113:37-47.

Tybulewicz, V.L., C.E. Crawford, P.K. Jackson, R.T. Bronson, and R.C. Mulligan. 1991. Neonatal lethality and lymphopenia in mice with a homozygous disruption of the c-abl proto-oncogene. *Cell*. 65:1153-1163.

Ussar, S., M. Moser, M. Widmaier, E. Rognoni, C. Harrer, O. Genzel-Boroviczeny, and R. Fassler. 2008. Loss of Kindlin-1 causes skin atrophy and lethal neonatal intestinal epithelial dysfunction. *PLoS Genet*. 4:e1000289.

Ussar, S., H.V. Wang, S. Linder, R. Fassler, and M. Moser. 2006. The Kindlins: subcellular localization and expression during murine development. *Exp Cell Res*. 312:3142-3151.

Valles, A.M., M. Beuvin, and B. Boyer. 2004. Activation of Rac1 by paxillin-Crk-DOCK180 signaling complex is antagonized by Rap1 in migrating NBT-II cells. *J Biol Chem*. 279:44490-44496.

van der Flier, A., and A. Sonnenberg. 2001. Function and interactions of integrins. *Cell Tissue Res*. 305:285-298.

Vicente-Manzanares, M., M.A. Koach, L. Whitmore, M.L. Lamers, and A.F. Horwitz. 2008. Segregation and activation of myosin IIB creates a rear in migrating cells. *J Cell Biol*. 183:543-554.
Vidal, F., D. Aberdam, C. Miquel, A.M. Christiano, L. Pulkkinen, J. Uitto, J.P. Ortonne, and G. Meneguzzi. 1995. Integrin beta 4 mutations associated with junctional epidermolysis bullosa with pyloric atresia. *Nat Genet*. 10:229-234.
Vignjevic, D., S. Kojima, Y. Aratyn, O. Danciu, T. Svitkina, and G.G. Borisy. 2006. Role of fascin in filopodial protrusion. *J Cell Biol*. 174:863-875.
Wang, X., X. Wei, Y. Yuan, Q. Sun, J. Zhan, J. Zhang, Y. Tang, F. Li, L. Ding, Q. Ye, and H. Zhang. 2018. Src-mediated phosphorylation converts FHL1 from tumor suppressor to tumor promoter. *J Cell Biol*.
Wear, M.A., and J.A. Cooper. 2004. Capping protein: new insights into mechanism and regulation. *Trends Biochem Sci*. 29:418-428.
Weaver, A.M., A.V. Karginov, A.W. Kinley, S.A. Weed, Y. Li, J.T. Parsons, and J.A. Cooper. 2001. Cortactin promotes and stabilizes Arp2/3-induced actin filament network formation. *Curr Biol*. 11:370-374.
Wegener, K.L., and I.D. Campbell. 2008. Transmembrane and cytoplasmic domains in integrin activation and protein-protein interactions (review). *Mol Membr Biol*. 25:376-387.
Wei, X., X. Wang, Y. Xia, Y. Tang, F. Li, W. Fang, and H. Zhang. 2014. Kindlin-2 regulates renal tubular cell plasticity by activation of Ras and its downstream signaling. *Am J Physiol Renal Physiol*. 306:F271-278.
Wei, X., X. Wang, J. Zhan, Y. Chen, W. Fang, L. Zhang, and H. Zhang. 2017. Smurf1 inhibits integrin activation by controlling Kindlin-2 ubiquitination and degradation. *J Cell Biol*. 216:1455-1471.
Wei, X., Y. Xia, F. Li, Y. Tang, J. Nie, Y. Liu, Z. Zhou, H. Zhang, and F.F. Hou. 2013. Kindlin-2 mediates activation of TGF-beta/Smad signaling and renal fibrosis. *J Am Soc Nephrol*. 24:1387-1398.
Wennstrom, S., P. Hawkins, F. Cooke, K. Hara, K. Yonezawa, M. Kasuga, T. Jackson, L. Claesson-Welsh, and L. Stephens. 1994. Activation of phosphoinositide 3-kinase is required for PDGF-stimulated membrane ruffling. *Curr Biol*. 4:385-393.
Wickstrom, S.A., A. Lange, E. Montanez, and R. Fassler. 2010. The ILK/PINCH/parvin complex: the kinase is dead, long live the pseudokinase! *EMBO J*. 29:281-291.
Willenbrock, F., D. Zicha, A. Hoppe, and N. Hogg. 2013. Novel automated tracking analysis of particles subjected to shear flow: kindlin-3 role in B cells. *Biophys J*. 105:1110-1122.
Winograd-Katz, S.E., R. Fassler, B. Geiger, and K.R. Legate. 2014. The integrin adhesome: from genes and proteins to human disease. *Nat Rev Mol Cell Biol*. 15:273-288.
Woodring, P.J., E.D. Litwack, D.D. O'Leary, G.R. Lucero, J.Y. Wang, and T. Hunter. 2002. Modulation of the F-actin cytoskeleton by c-Abl tyrosine kinase in cell spreading and neurite extension. *J Cell Biol*. 156:879-892.
Wu, C., S.B. Asokan, M.E. Berginski, E.M. Haynes, N.E. Sharpless, J.D. Griffith, S.M. Gomez, and J.E. Bear. 2012. Arp2/3 is critical for lamellipodia and response to extracellular matrix cues but is dispensable for chemotaxis. *Cell*. 148:973-987.
Wu, C., H. Jiao, Y. Lai, W. Zheng, K. Chen, H. Qu, W. Deng, P. Song, K. Zhu, H. Cao, D.L. Galson, J. Fan, H.J. Im, Y. Liu, J. Chen, D. Chen, and G. Xiao. 2015. Kindlin-2 controls TGF-beta signalling and Sox9 expression to regulate chondrogenesis. *Nat Commun*. 6:7531.
Wymann, M., and A. Arcaro. 1994. Platelet-derived growth factor-induced phosphatidylinositol 3-kinase activation mediates actin rearrangements in fibroblasts. *Biochem J*. 298 Pt 3:517-520.
Xia, W., and T.A. Springer. 2014. Metal ion and ligand binding of integrin alpha5beta1. *Proc Natl Acad Sci U S A*. 111:17863-17868.
Xiao, T., J. Takagi, B.S. Coller, J.H. Wang, and T.A. Springer. 2004. Structural basis for allostery in integrins and binding to fibrinogen-mimetic therapeutics. *Nature*. 432:59-67.
Xu, W., H. Baribault, and E.D. Adamson. 1998. Vinculin knockout results in heart and brain defects during embryonic development. *Development*. 125:327-337.

Yang, W., M. Shimaoka, J. Chen, and T.A. Springer. 2004. Activation of integrin beta-subunit I-like domains by one-turn C-terminal alpha-helix deletions. *Proc Natl Acad Sci U S A*. 101:2333-2338.

Yarar, D., C.M. Waterman-Storer, and S.L. Schmid. 2007. SNX9 couples actin assembly to phosphoinositide signals and is required for membrane remodeling during endocytosis. *Dev Cell*. 13:43-56.

Yates, L.A., A.K. Fuzery, R. Bonet, I.D. Campbell, and R.J. Gilbert. 2012. Biophysical analysis of Kindlin-3 reveals an elongated conformation and maps integrin binding to the membrane-distal beta-subunit NPXY motif. *J Biol Chem*. 287:37715-37731.

Ye, F., B.G. Petrich, P. Anekal, C.T. Lefort, A. Kasirer-Friede, S.J. Shattil, R. Ruppert, M. Moser, R. Fassler, and M.H. Ginsberg. 2013. The mechanism of kindlin-mediated activation of integrin alphaIIbbeta3. *Curr Biol*. 23:2288-2295.

Yu, Y., L. Qi, J. Wu, Y. Wang, W. Fang, and H. Zhang. 2013. Kindlin 2 regulates myogenic related factor myogenin via a canonical Wnt signaling in myogenic differentiation. *PLoS One*. 8:e63490.

Yu, Y., J. Wu, Y. Wang, T. Zhao, B. Ma, Y. Liu, W. Fang, W.G. Zhu, and H. Zhang. 2012. Kindlin 2 forms a transcriptional complex with beta-catenin and TCF4 to enhance Wnt signalling. *EMBO Rep*. 13:750-758.

Zhan, J., and H. Zhang. 2018. Kindlins: Roles in development and cancer progression. *Int J Biochem Cell Biol*.

Zhang, X., G. Jiang, Y. Cai, S.J. Monkley, D.R. Critchley, and M.P. Sheetz. 2008. Talin depletion reveals independence of initial cell spreading from integrin activation and traction. *Nat Cell Biol*. 10:1062-1068.

Zhao, Y., N.L. Malinin, J. Meller, Y. Ma, X.Z. West, K. Bledzka, J. Qin, E.A. Podrez, and T.V. Byzova. 2012. Regulation of cell adhesion and migration by Kindlin-3 cleavage by calpain. *J Biol Chem*. 287:40012-40020.

Zhao, Z.S., E. Manser, X.Q. Chen, C. Chong, T. Leung, and L. Lim. 1998. A conserved negative regulatory region in alphaPAK: inhibition of PAK kinases reveals their morphological roles downstream of Cdc42 and Rac1. *Mol Cell Biol*. 18:2153-2163.

Zhu, J., J. Zhu, and T.A. Springer. 2013. Complete integrin headpiece opening in eight steps. *J Cell Biol*. 201:1053-1068.

Ziegler, W.H., R.C. Liddington, and D.R. Critchley. 2006. The structure and regulation of vinculin. *Trends Cell Biol*. 16:453-460.

5. Acknowledgements

First, I would like to thank my PhD thesis supervisor, Prof. Reinhard Fässler for giving me the opportunity to work in his laboratory and in Max Planck Institute. I would like to thank him for his support and encouragement thoughout the entire period of my study.

Second, I would like to thank my TAC committee members Prof. Olivier Gires (also my second thesis referee) and Dr. Andreas Pichlmair. They were always availiable not only for scientific but also for personal discussions. I want also to thank Prof. Matin Biel, Prof. Markus Sperandio, Prof. Julian Stingele and Dr. Gregor Witte for their willingness and time to evaluate my work.

Third, I would like to thank Dr. Moritz Widmaier my initial supervisor when I started working on my PhD. A big thank goes to Dr. Ralph Böttcher who helped me a lot during the last period of my PhD and supported my work while I was on maternity leave. I want also to thank Dr. Maik Veelders and Dr. Lambacher Armin for the nice collaboration we had, as well as Dr. Nagarjuna Nagaraj from corefacility for the help with mass spectrometry data analysis. I would also like to thank Dr. Markus Moser and Dr. Peter Krenn for their help with the FACS machine.

I would like to thank the lab girls, Dr. Georgina Colo, Dr. Valeria Samareli, Dr. Franziska Kundrat and Dr. Maria Benito for creating such a nice working environment. Additionally, I want to thank Hildegard Reiter (Mischa), Ursula Kuhn, Ines Lach-Kusevic, Klaus Weber and Lidia Wimmer for creating a family feeling in the lab.

Last but not least, I would like to thank Kimon who was and is always there for me, even during the most difficult periods of this work, and of course my daughter Anastasia, who came and gave another meaning to my life.

6. Appendix

In the following, papers I to III are reprinted.

I. **Marina Theodosiou**, Ralph T Böttcher, Maik Veelders and Reinhard Fässler. **Tyrosine phosphorylation of Kindlin-2 by Abl kinases controls growth factor-triggered circular dorsal ruffle formation.** (manuscript in progress)

II. **Marina Theodosiou,** Moritz Widmaier, Ralph T Böttcher, Emanuel Rognoni, Maik Veelders, Mitasha Bharadwaj, Armin Lambacher, Katharina Austen, Daniel Müller, Roy Zent, Reinhard Fässler. **Kindlin-2 cooperated with talin to activate integrins and induces cell spreading by directly binding paxillin**. *eLife*. 5:e10130

III. Ralph T. Böttcher, Maik Veelders, Pascaline Rombaut, Jan Faix, **Marina Theodosiou**, Theresa E.Stradal, Klemens Rottner, Roy Zent, Franz Herzog, Reinhard Fässler. **Kindlin-2 recruits paxillin and Arp2/3 to promote membrane protrusions during initial cell spreading**. *JCB*. Vol.216 no.11

Tyrosine phosphorylation of Kindlin-2 by Abl kinases controls growth factor-triggered circular dorsal ruffle formation

Marina Theodosiou[1], Ralph T. Böttcher[1], Maik Veelders[1], and Reinhard Fässler[1]

[1]Department of Molecular Medicine, Max Planck Institute of Biochemistry, 82152 Martinsried, Germany

Corresponding author: Reinhard Fässler (faessler@biochem.mpg.de)

Abstract

Kindlin-2 plays a key role in integrin activation and signaling; however, the mechanisms regulating kindlin-2 functions are incompletely understood. Here we show that Abl kinases phosphorylate kindlin-2 at tyrosine 179. Upon epidermal growth factor stimulation cells expressing the phospho-deficient mutant form of kindlin-2 showed a reduction in circular dorsal ruffles formation, actin rich-ring shaped structures involved in receptor internalization and cell migration. In the current study we uncover a previously unknown function of kindlin-2 in circular dorsal ruffles formation, which is controlled by tyrosine phosphorylation.

Introduction

Integrins are transmembrane receptors composed by non-covalently linked α and β subunits, which mediate cell adhesion to the extracellular matrix (ECM) and to other cells (Burke, 1999; Hynes, 2002; van der Flier and Sonnenberg, 2001). In addition to establishing a mechanical link to the actin cytoskeleton, integrin-mediated adhesions lead to the assembly of large protein complexes, which induce various signaling pathways (Legate et al., 2009; Parsons et al., 2010; Winograd-Katz et al., 2014). Integrin-mediated signaling controls a plethora of biological phenomena such as cell adhesion, migration, proliferation, apoptosis, gene expression and differentiation (Giancotti and Ruoslahti, 1999).

Kindlin-2 is a key molecule in integrin activation process and integrin-mediated cell adhesion (Montanez et al., 2008; Theodosiou et al., 2016). Increasing amount of evidence assigns functions to kindlin-2 beyond integrin activation and signaling (Wei et al., 2014; Wei et al., 2013; Wu et al., 2015; Yu et al., 2012). Interestingly, post-translational modifications of kindlin-2 have been shown to modulate integrin downstream signaling (Artym et al., 2015; Liu et al., 2015; Qu et al., 2014). More precisely, kindlin-2 tyrosine phosphorylation and its association with Src have been shown to increase upon cell adhesion to fibronectin and be required for paxillin phosphorylation (Qu et al., 2014). Src has been shown to directly phosphorylate kindlin-2 at tyrosine 193. Phosphorylation of tyrosine 193 increased the binding affinity of kindlin-2 towards migfilin and thus its recruitment to focal adhesions (Liu et al., 2015). Furthermore, kindlin-2 serine phosphorylation has been shown to act as inducer of invadopodia formation (Artym et al., 2015).

The Abelson (Abl) family of non-receptor tyrosine kinases consist of two ubiquitously expressed members Abl1 and Abl2/Arg. Ablation of *Abl1* gene causes embryonic and neonatal lethality (Kua et al., 2012; Li et al., 2000; Moresco et al., 2005; Schwartzberg et al., 1991; Tybulewicz et al., 1991), while *Abl2* knockout mice are viable and exhibit neuronal

defects that include age related dendrite destabilization and regression (Gourley et al., 2009; Koleske et al., 1998; Moresco et al., 2005). *Abl1*$^{-/-}$ *Abl2*$^{-/-}$ mice are embryonic lethal (embryonic day 11), supporting the redundant and essential functions of these kinases during development (Koleske et al., 1998). Abl kinases can be activated by growth factor stimulation and integrin engagement (Boyle et al., 2007; Lewis et al., 1996; Woodring et al., 2002) and are implicated in cellular responses downstream of integrin-mediated adhesion. Activated Abl kinases not only interact directly with actin, but also with phosphorylate key proteins, which induce actin cytoskeletal remodelling important for the formation of membrane dorsal ruffles and lamellipodia (Boyle et al., 2007).

Circular dorsal ruffles (CDRs) are transient, ring shaped, actin enriched structures that form at the dorsal plasma membrane in response to growth factors stimulation (Itoh and Hasegawa, 2013). CDRs have a critical function in receptor internalization, integrin trafficking, cell migration and macropinocytosis (Abella et al., 2010; Dharmawardhane et al., 2000; Gu et al., 2011; Hoon et al., 2012; Krueger et al., 2003; Orth et al., 2006). CDRs formation requires the co-signaling of α5β1 integrin and epidermal growth factor receptor (EGFR) (Azimifar et al., 2012). Additionally, different proteins have been shown to regulate CDRs formation; among them are known focal adhesion proteins (paxillin, ILK, β1 integrin, Src), proteins involved in actin polymerization (WAVE1, WAVE2, N-WASP, cortactin) different kinases (Abl, PAK1, PI3K) and membrane deforming proteins (Snx-9, Tuba, IRSp53) (Hoon et al., 2012; Stuart et al., 2006; Suetsugu et al., 2003).

To further understand the role of kindlin-2 phosphorylation in the regulation of kindlin-2 function we performed a kinase screening. We found that Abl kinases phosphorylate kindlin-2 exclusively at tyrosine 179 inducing CDRs formation.

Results

Kindlin-2 is tyrosine phosphorylated by Abl kinases

To investigate the kindlin-2 phosphorylation status we first performed endogenous immunoprecipitation assays for kindlin-2 using adherent fibroblast, breast cancer (MDA-MB-231) and melanoma (B16-F1) cells which were cultured in the presences of serum. After immunoprecipitation of endogenous kindlin-2, lysates were probed with antibodies against p-Tyr. In agreement with previous studies (Liu et al., 2015; Qu et al., 2014), kindlin-2 was found to be tyrosine phosphorylated in all cell lines tested (Figure 1A). Furthermore, we analyzed the endogenous immunoprecipitated kindlin-2 from adherent fibroblast by mass spectroscopy (MS). Interestingly, kindlin-2 was found to be phosphorylated at 5 different serine sites (S159, S351, S666, S180, S181) (FigureS1A). Phosphorylation of kindlin-2 at the sites S159, S180, S666 was already shown to be implicated in invadopodia formation (Artym et al., 2015). Since the majority of the identified serine phosphorylation sites of kindlin-2 were already identified and functionally characterized by others we decided to focus further studies on the role of kindlin-2 tyrosine phosphorylation.

To identify kinases involved in kindlin-2 tyrosine phosphorylation a company (ProQinase) performed a tyrosine kinase screening using recombinant kindlin-2. Recombinant kindlin-2 expression and purification was performed as previously described (Bottcher et al., 2017; Theodosiou et al., 2016) (Figure S1B). The commercial tyrosine kinase library consisted of 94 tyrosine kinases, 70 of which were recombinant wild type kinases of the overall 90 tyrosine kinases identified in the human tyrosine-specific kinome (Robinson et al., 2000). The library also contained 16 frequently mutated kinases. Among the tyrosine kinases, which gave the highest score for kindlin-2 phosphorylation was Abl1 kinase (Figure 1B, S1C), whereas Abl2, the other family member, gave a lower score (Figure 1B). Interestingly, c-Src

kinase did not show a high score, although a recent publication reported that c-Src phosphorylates kindlin-2 at Y193 (Liu et al., 2015). The discrepancy between our screening results and the published data may be due to the different experimental approaches used. We specifically used recombinant kindlin-2 expressed in *Escherichia coli* Rosetta cells, the purity of which was tested (Figure S1B) (Bottcher et al., 2017; Theodosiou et al., 2016), to perform the *in vitro* kinase assay, while Liu et al. (2015) used imunnoprecipitated flag-kindlin-2 over-expressed in 293T cells. To further validate the results from the kinase screening we performed *in vitro* kinase assay using recombinant kindlin-2 and recombinant Abl1 and Abl2 kinases in combination with western blot analysis or Liquid Chromatography-Mass Spectrometry (LC-MS). Using Western blot analysis we showed that the addition of kinases in the reactions resulted in tyrosine phosphorylation of kindlin-2. With the LC-MS method we calculated kindlin-2 mass before and after the addition of the kinases in the reaction. Using the mass difference we were able to calculate how many tyrosine residues of the kindlin-2 are phosphorylated by WT Abl kinases. Our experiments showed that WT-Abl1 and WT-Abl2 phosphorylate kindlin-2 at one tyrosine. Both methods confirmed the tyrosine phosphorylation of kindlin-2 by Abl and Abl2 *in vitro* (Figure 1C, 2B). Notably, immunoprecipitation of overexpressed myc-tagged kindlin-2 together with Abl1 or Abl2 wild type (WT), Constitutive Active (PP) or Kinase Dead (KD) in HEK293T cells. The experiments showed a decrease in tyrosine phosphorylation of kindlin-2 when Abl1 KD or Abl2 KD were overexpressed, while expectedly, Abl1WT, Abl1 PP and Abl2WT overexpression induced high levels of kindlin-2 tyrosine phosphorylation (Figure 1D, 1E). Interestingly, overexpression of Abl kinases resulted the appearance of two or even three bands of tyrosine phosphorylated kindlin-2. We speculate that the difference in the molecular weight of kindlin-2 correspond to differentially highly post-translational modified kindlin-2. Interestingly, tyrosine phosphorylation of proteins has been shown to create a binding site for

ubiquitin ligases (Cooper et al., 2015). Further experiments and analysis are needed to examine if tyrosine phosphorylation of kindlin-2 can induce kindlin-2 ubiquitination or if the difference in the molecular weight correspond to other post-translational modifications. Collectively, these results showed that Abl kinases can phosphorylate kindlin-2.

Abl family kinases phosphorylate kindlin-2 at Y179

Mouse kindlin-2 sequence analysis revealed 21 tyrosine residues most of which, based on the published structures of kindlin-2, are on the protein surface (Li et al., 2017; Liu et al., 2011; Perera et al., 2011) (Figure S2A). Using PHOSIDA (http://141.61.102.18/phosida/index.aspx), an online post-translational modification database, we were able to identify a single canonical c-Abl binding motif (I/V/LYXXP/F) in mouse kindlin-2 sequence corresponding to tyrosine at position 179 (Figure 2A). Tyrosine Y179 is located in the F1 domain of kindlin-2, which belongs to a flexible loop that was shown to mediate binding of kindlin-2 to the plasma membrane (Bouaouina et al., 2012). To validate this observation we first expressed recombinant kindlin-2 bearing a phospho-deficient mutation (Y179F) (Figure S2B) and performed *in vitro* kinase assays using recombinant WT-kindlin-2 and Y179F-kindlin-2 (Y179F)). Using the LC-MS method, we were able to confirm based on the mass deference, which was only observed in WT-kindlin-2 and not in the Y179F-kindlin-2, that WT-Abl1 and WT-Abl2 phosphorylate kindlin-2 at one residue, the tyrosine Y179 (Figure 2B). Furthermore, we compared the tyrosine phosphorylation of kindlin-2 after immunoprecipitations in HEK293T cells overexpressing either myc-Kind2WT or myc-Kind2Y179F together with Abl1 or Abl2 WT and found that the phosphorylation levels of myc-Kind2Y179F were dramatically decreased compared to the levels of myc-Kind2WT (Figure 2C, 2D).

To further confirm these findings, we took advantage of *Abl1*$^{-/-}$ *Abl2*$^{-/-}$ fibroblasts (Finn et al., 2003), which constitute the best cellular system to directly prove that Abl kinases are required for kindlin-2 tyrosine phosphorylation. In agreement with our overexpression results and *in vitro* kinase assays, the kindlin-2 tyrosine phosphorylation levels in *Abl1*$^{-/-}$ *Abl2*$^{-/-}$ fibroblasts were very low and increased upon overexpression of WT-Abl1. Interestingly, WT-Abl2 overexpression did not increase tyrosine phosphorylation of kindlin-2, showing that kindlin-2 constitutes a better cellular substrate for Abl1 than for Abl2 (Figure 2E). We also investigated whether overexpressed Abl1 phosphorylates all kindlin family members by immunoprecipitation followed by anti-pY Western blotting in HEK293T cells overexpressing either GFP-tagged kindlin-1, kindlin-2 or kindlin-3 (Figure S2C). The results of these experiments revealed that Abl1 overexpression exclusively leads to a size shift and phosphorylation of kindlin-2. This conclusion is in line with the sequence analysis of kindlins showing that tyrosine Y179 embedded in the canonical Abl phospho-motif is not conserved between kindlin family members (Figure S2D).

Collectively, these findings demonstrate that Abl1 and Abl2 phosphorylate kindlin-2 at tyrosine Y179 *in vitro*, with kindlin-2 to be a better substrate for Abl1 in cells.

Kindlin-2 Y179 phosphorylation is important for dorsal ruffles formation

In order to characterize the functions of this phosphorylation site we generated mouse *kindlin-1/2* out fibroblasts stably expressing phospho-deficient (myc-Kind2Y179F) or phospho-mimetic (myc-Kind2Y179E) (Theodosiou et al., 2016) (Figure S3A). Single clones were picked and FACS sorted for equal kindlin-2 expression levels. Western blots showed that myc-tagged kindlins were overexpressed compared to the kindlin floxed control cells. Importantly, however, the immunoblots confirmed equal expression of myc-tagged kindlins (Figure S3B). Immunostainings of the cells showed the expected localization of kindlin-2

with paxillin in focal adhesions (Figure S3C). Abl kinases control actin cytoskeleton dynamics and the induction of circular dorsal membrane ruffles (CDRs) upon growth factors stimulation (Boyle et al., 2007; Hernandez et al., 2004). F-actin distribution was similar between the myc-tagged kindlin-2 overexpressing cells and CDRs were not apparent before EGF treatment. Already 3 minutes after epidermal growth factor (EGF) treatment, however, CDRs peaked in all cell lines and began fading 5 minutes after treatment. Interestingly, both 3 and 5 minutes after EGF treatment significantly fewer cells expressing phospho-deficient myc-Kind2Y179F showed CDRs compared to cells expressing mycKind2WT or phosphomimetic myc-Kind2Y179E (Figure 3A, 3B). We also siRNA-depleted kindlin-2 in a ILK fl/fl cells (Azimifar et al., 2012), and re-expressed GFP-Kind2WT, GFP-Kind2Y179F and GFP-Kind2Y179E. The efficiency of kindlin-2 siRNA was around 50%, while the re-expression of GFP-kindlin forms where not equal in all cell lines used (Figure S3D). Interestingly, treatment of the cells with EGF, also showed that fewer GFP-Kind2Y179F expressing cells developed CDRs confirming the importance of Y179 phosphorylation for CDRs formation (Figure S3E). The reduction in the CDRs formation was not due to reduced Epidermal Growth Factor Receptor (EGFR) activation or downstream signaling as ERK and Src activation were similar in all cell lines (Figure 3C).

These findings indicate kindlin-2 phosphorylation at Y179 plays a role in dorsal ruffles formation.

Search for pY179-kindlin-2 interactors

To obtain insight into the underlying molecular mechanisms of how kindlin-2 Y179 phosphorylation is implicated in CDR formation, we performed a MS-based interactor screen in which we compared the interactors between the phosphomimetic (Y179E) and phosphodeficient (Y179F) kindlin-2. To this end, starved myc-Kind2WT, myc-Kind2Y179F

and myc-Kind2Y179E expressing cells seeded on FN were stimulated with EGF for 3 min at 37°C to induce CDR formation. Subsequently, cells were incubated with dithiobis (succinimidyl propionate) (DSP) in order to capture transient kindlin-2 interactors. Following cell lysis and immunoprecipitation, samples were further processed for LC-MS/MS analysis (Figure 4A).

Hierarchical clustering of the 131 ANOVA significant interactors of kindlin-2 allowed the identification of protein clusters, which preferentially bound either myc-Kind2Y179E or myc-Kindl2Y179F, and a group of proteins which bound to Kind2WT, Kind2Y179F and Kind2Y179E. Furthermore, a student's t-test between myc and myc-Kind2WT samples reveals 48 specific interactors for kindlin-2, among them ILK and integrin β1 which are known kindlin-2 binding proteins. Only 18 proteins showed differential binding between myc-Kind2Y179F and myc-Kind2Y179E (Figure S4B). Among the proteins which showed a preferential binding to myc-Kind2Y179E, in comparison to myc-Kind2Y179F, were Dspysl2/CRMP2 (Dihydropyrimidinase-related protein 2/Collapsin Response Mediator Protein-2) and Nme2/NM23-H2 (Nucleoside diphosphate kinase B). CRMP-2 is a cytosolic tetrameric protein which belongs to the CRMP family. It is implicated in neuronal development (Myllykoski et al., 2017; Zhang et al., 2016). Nme2 is a nucleoside diphosphate kinase (NDPK) which catalyzes the transfer of a phosphate from nucleoside triphosphates (NTPs) to nucleoside diphosphates (NDPs) (Boissan et al., 2018). Nme family proteins have been associated with tumor metastasis suppression, endocytosis and membrane remodeling (Boissan et al., 2014; Boissan et al., 2018; Polanski et al., 2011). Despite the lack of any study that directly connects CRMP2 or Nme2 with CDRs, these proteins are reported to associate with proteins connect with actin cytoskeleton dynamics (Fournier et al., 2002; Sarhan et al., 2017; Yoneda et al., 2012). Future studies are needed to explore the connection of CRMP2 and Nme2 with kindlin-2 and circular ruffles formation.

Discussion

Kindlin-2 plays a key role in integrin activation process (Montanez et al., 2008; Theodosiou et al., 2016) and downstream signaling (Qu et al., 2014; Theodosiou et al., 2016). Tyrosine and serine phosphorylation of kindlin-2 is induced upon integrin-mediated adhesion and implicated in integrin downstream signaling (Artym et al., 2015; Liu et al., 2015; Qu et al., 2014). In the present study we provide evidence that kindlin-2 is phosphorylated at Y179 by Abl kinases and that this phosphorylation controls the formation of CDRs.

Abl kinases are implicated in CDR formation (Plattner et al., 1999; Sini et al., 2004). Upon their activation by integrin engagement or growth factor stimulation, Abl kinases phosphorylate different proteins that modulate the actin cytoskeleton (Antoku and Mayer, 2009; Boyle et al., 2007; Hernandez et al., 2004; Stuart et al., 2006). In the current study we show that Abl kinases phosphorylate kindlin-2 *in vivo* as well as *in vitro*. We also mapped the phosphorylation site to Y179. Using cell lines lacking endogenous kindlin-2 and expressing phosphomimetic myc-Kind2Y179E or phosphodeficient myc-Kind2Y179F, we were able to uncover a novel role of kindlin-2 phosphorylation in the formation of CDRs. To our knowledge this is the first time that kindlin-2 is implicated in the formation of these actin rich structures. How kindlin-2 regulates the formation of these structures is currently unknown. It is possible that kindlin-2 phosphorylation by Abl changes kindlin-2 localization or the interaction of kindlin-2 with specific set of proteins.

Beside kindlin-2, other focal adhesion proteins have also been implicated in CDRs formation. Previous study by our group showed that integrin β1-ILK and EGF signaling cooperate to mediate cytoskeletal rearrangements leading to CDRs formation (Azimifar et al., 2012). Integrin β1, paxillin and Src are well-known focal adhesion proteins, which are implicated in

CDRs formation (Buccione et al., 2004; King et al., 2011; Sero et al., 2011). In the current study we observed that tyrosine phosphorylation of kindlin-2 is required for CDRs formation.

We also report an MS based interactor study, which led to the identification of Dspysl2/CRMP2 (Dihydropyrimidinase-related protein 2/Collapsin Response Mediator Protein-2) and NDPK/Nme2/NM23 (Nucleoside diphosphate kinase B) as potential kindlin-2 interacting proteins that preferentially binds to the phosphomimetic Y179E form of kindlin-2. CRMP2 is a ubiquitously expressed protein with highest expression in the nervous system (Tan et al., 2014). Most of the studies about CRMP2 deal with its role in the nervous system where it is implicated in various neuronal processes such as neurite outgrowth, neuronal polarity and differentiation through its microtubules assembly and trafficking functions (Hensley et al., 2011; Inagaki et al., 2001). Recent studies by Wewer and colleagues showed that a splice variant of CRMP2 is expressed in epithelial cells where it acts as a substrate and inhibitor of ROCKII and thus regulates cell motility and extracellular matrix assembly (Yoneda et al., 2012). Interestingly, CRMP2 and ROCKII also co-localize to cortical membrane ruffles of cells (Yoneda et al., 2012). Additionally, it has recently been showed that CRMP2 is required for Platelet derived growth factor (PDGF)-induced cell migration (Sarhan et al., 2017). On the other hand, Nme2 is ubiquitously expressed protein which localizes in the cytosol, at the plasma membrane and can also translocate in the nucleus where it regulates gene expression (Boissan et al., 2018). It belongs to the Nucleoside diphosphate kinases (NDPK), also named NME, superfamily, which consist of ten genes (Boissan et al., 2018). Nme2 possesses not only a nucleoside diphosphate kinase activity (NDPK) but also a histidine kinase activity (Fuhs and Hunter, 2017). Most of the research is focused on the function of Nme1, another NDPK family member, as tumor metastasis suppressor (McCorkle et al., 2014). However, the function of Nme2 in tumor metastasis remains controversial and not well examined (Boissan et al., 2018; Thakur et al., 2011).

Additionally, Nme1 and Nme2 proteins have been shown to interact with dynamin and regulate dynamin-dependent endocytosis and membrane fission (Boissan et al., 2014). Notably, Nme2 has been shown to directly interact with ICAP-1α. In cells, Nme2 co-localized with ICAP-1 at lamellipodia during initial adhesion and spreading (Fournier et al., 2002). However, the functional role of this interaction remains unknown. Unfortunately, I did not have the time to confirm the interaction of kindlin-2 with CRMP2 and Nme2 and to further analyze the implication of these interactions in actin dynamics and cellular functions such as cell migration, integrin uptake. These studies are needed to clarify a potential role CRMP2 and Nme2 in CDRs formation and the connection with kindlin-2.

In conclusion, we here show that Abl kinases phosphorylate kindlin-2 at Y179. We also show that kindlin-2 controls CDRs formation in a tyrosine-179 phosphorylation-dependent manner. Future work is needed to provide insights about how kindlin-2 controls CDRs formation and how phosphorylation of Y179 modulates this function. This occurs probably through controlling its interaction with other proteins including CRMP2 and Nme2.

Material and Methods

Cell lines generation and cell culture

The kindlin-1flox/flox kindlin-2flox/flox mouse fibroblasts have been described in (Theodosiou et al., 2016). Cells were stably transfected with the sleeping beauty transposase system using ITR-Puro (+) plasmid containing the myc-mouse kindlin-2 cDNA. Following selection using puromycin, cells were infected with an adenovirus to transduce the Cre recombinase. Single clones were picked and checked for the efficiency of kindlin-2 endogenous deletion using genotyping PCR and Western blot. *Abl1*$^{-/-}$*Abl2*$^{-/-}$ fibroblasts were kindly provided by Prof. Koleske J. Anthony, Yale University (Finn et al., 2003). GFP-Kind2WT cells were previously described (Theodosiou et al., 2016). All cells were cultured under standard cell culture conditions using Dulbecco's modified Eagle's medium (DMEM) supplemented with 8% fetal calf serum (FCS) and Penicillin/Streptomycin.

Antibodies and reagents

The following antibodies were used: kindlin-2 (MAB2617, Millipore) WB: 1:1000, IF: 1:500; GFP (A11122, Invitrogen) WB: 1:2000, IF: 1:1000; 4G10 (05-321, Millipore) WB: 1:1000, myc (05-724, Millipore) WB: 1:1000, β-actin (A2228, Sigma) WB: 1:1000, Paxillin (32084, Abcam) IF: 1:300, Paxillin (610051, BD Transduction Laboratories) IF: 1:400; Cortactin (05-180, Millipore) IF: 1:250, Phalloidin-TRITC (P1951, Sigma,) IF: 1:300; Abl1 (2862, Cell Signaling) WB: 1:1000; Src (2108, Cell Signaling) WB: 1:1000, pY416 Src (6943, Cell Singaling) 1:1000; EGFR (2232, Cell Signaling) WB: 1:1000, pY845 EGFR (2231, Cell Signaling) WB: 1:1000, pY992 EGFR (2235, Cell Signaling) WB: 1:1000, ERK1/2 (9102, Cell Signaling) WB:1:1000, p T202 Y204 ERK1/2 (4376, Cell Signaling) WB: 1:1000, Arg (from Koleske lab) WB: 1:2000.

Recombinant mouse Abl1 was purchased from Enzonase and recombinant human Arg was purchased from Invitrogen (PV3266). Recombinant human EGF was purchased from Millipore and used at 50 ng/ml final concentration.

Expression and purification of recombinant kindlin-2

The recombinant expression of kindlin-2 wild type and Y179F in *Escherichia coli* Rosetta cells was induced with 1 mM or 0.2 mM IPTG, respectively, at 18°C for 22 hr. After cell lysis and clarification of the supernatant, kindlin-2 was purified by Ni-NTA affinity chromatography. Eluate fractions containing kindlin-2 were pooled, cleaved with SenP2 protease and purified by size-exclusion chromatography yielding unmodified murine kindlin-2. In order to perform kinase assay using the recombinant kindlin-2 the buffer was changed to 50mM HEPES pH 7.5, 5% Glycerol, 150mM NaCl and 1mM DTT.

Tyrosine kinase screening

The tyrosine kinase screening was conducted by ProQinase GmbH in Freiburg, Germany. Most of the 94 tyrosine kinases were expressed, purified and functionally tested by ProQinase GmbH. Recombinant kindlin-2 was provided in 50mM HEPES pH 7.5, 5% Glycerol, 150mM NaCl and 1mM DTT at the concentration of 1 mg/ml. 96-well plates were used for the reactions each of them contained 10 µl of kinase solution and 40 µl of buffer/ ATP/ test sample mixture. One well of each assay plate was used for a buffer/substrate control containing no enzyme. The reaction mixture contained 60 mM HEPES-NaOH, pH 7.5, 3 mM MgCl2, 3 mM MnCl2, 3 µM Na-orthovanadate, 1.2 mM DTT, 50 µg/ml PEG20000, 1 µM ATP/[γ-33P]-ATP (0.7 x 1005 cpm per well), protein kinase (1-400 ng/50µl) and kindlin-2 protein (5 µg/50 µl). The assay plates were incubated at 30° C for 60 minutes. Subsequently, the reactions were stopped with 20 µl of 10% (v/v) H3PO4 and then

transferred into 96-well glass-fiber filter plates (MultiScreen MSFC, Millipore), pre-wetted with 150 mM H3PO4, followed by 10 min incubation at room temperature. The filter plates were washed three times with 250 µl of 150 mM H3PO4 and once with 20 µl of 100% ethanol. After drying the plates for 30 min at 40° C, 50 µl of scintillator (Rotiszint Eco plus, Roth) were added to each well and incorporation of 33Pi ("counting of cpm") was determined with a microplate scintillation counter (Microbeta, Perkin Elmer). For evaluation of the results of the glass-fiber filter assays, the autophosphorylation activity of each kinase was used to normalize the value in the current experiment. Additionally, the background value of kindlin-2 sample was subtracted from each raw value.

Kinase assay

For the kinase assay, 100ng of each kinase, Abl1 (BML-SE5630, Enzonase) and Abl2 (PV3266, Invitrogen), was incubated together with 1 µg of recombinant kindlin-2 in the presences of 100µM ATP in the reaction buffer (20mM Tris, pH7.5, 10mM $MgCl_2$, 0.3mM Na_3VO_4, 5mM β-glycerol phosphate, 0.5mM EGTA, 1mM DTT). Reactions were incubated for 45 min at 30°C. Reactions were stopped either by adding 1µl 1M EDTA following boiling for 10 min at 95°C in 2x loading buffer for western blot analysis or by adding 1% TFA for the LC/MS analysis.

Immunostainings

For immunostainings cells were cultured on glass coverslips coated with 5ug/ml FN (Calbiochem). In the case of CDR induction, cells were serum-starved overnight in DMEM containing 0.2% FCS before plating on FN coated coverslips (5 µg/ml) for 45 min. CDRs formation was induced after 3 min EGF (50 ng/ml) stimulation of the cells. Afterwards, cells were fixed with 4% PFA for 10 min at RT and permeabilized for 10 min with 0.2% Triton X-100/PBS at RT. 3% BSA in PBS was used for 1h at RT to block background signals.

Subsequently, they were incubated in the dark with primary and secondary antibodies diluted in 3% BSA, 0.2% Triton X-100/PBS. The fluorescent images were acquired with a laser scanning confocal microscope (Leica SP5).

Constructs

Constitutive active (PP), Kinase Dead (KD) and Wild Type (WT) human Abl1 cDNA was a generous gift from Prof. Hantschel Oliver, Swiss Institute for Experimental Cancer Research (ISREC), CH-1015 Lausanne, Switzerland. Abl1 cDNA were subcloned into EGFP-C1 vector. Kind1-GFP, Kind2-GFP and Kind3-GFP constructs have been described (Moser et al., 2008; Theodosiou et al., 2016; Ussar et al., 2008). To subclone the myc-Kind2 cDNA BamHI-myc-EcoRV-K2 5'ggatccatggaacaaaaacttatttctgaagaagatctggatatcatggctctggacgggataaggat-3' and NotI-K2 5'gcggccgctcacacccaaccactggtgagtttg-3' primers were cloned into the ITR-Puro (+) plasmid to obtain a kindlin-2 version that is fused with myc at N-terminus. YFP- Abl2 wild type (WT) mouse cDNA was provided by Prof. Koleske J. Anthony, Yale University.

Site directed mutagenesis

Point mutations for myc-Kind2 cDNA were introduced using the following primers K2Y179Ffw 5'-GAT CAG GAA GCA TAT TTT CAA GCC CGG GAC-3' and K2Y179Frv 5'-GTC CCG GGC TTG AAA ATA TGC TTC CTG ATC-3' for the Y179F mutation and K2Y179Efw 5'-GCC TGG ATC AGG AAG CAT AGA ATC AAG CCC GGG ACT TTA TAG-3' K2Y179Erv 5'-CTA TAA AGT CCC GGG CTT GAT TCT ATG CTT CCT GAT CCA GGC-3' for the Y179E mutation. For YFP-Abl2 KD, point mutations were introduced using the following primers Abl2KD-fw 5'-CTT ACA GTG GCT GTG AGA ACA CTG

AAG GAA GAC-3', Abl2KD-rv 5'-GTC TTC CTT CAG TGT TCT CAC AGC CAC TGT AAG-3'.

All reactions were carried out following the Quick Change Site-Directed kit (Stratagene).

Transient transfections

Cells were transiently transfected with Lipofectamine 2000 (Invitrogen) according to the manufacturer's protocol.

Immunoprecipitations

For immunoprecipitation of GFP and myc-tagged proteins, cells were lysed and immunoprecipitated using the μMACS GFP Isolation Kit (130-091-288 from Miltenyi Biotec) or myc Isolation Kit (130-091-284 from Miltenyi Biotec) respectively, following the manufacturer's protocol.

For immunoprecipitation of kindlin-2, the different cell lines were lysed in lysis buffer (50 mM Tris, pH 8.0, 150 mM NaCl, 1% Triton X-100, 0.05% sodium deoxycholate, 10 mM EDTA) and incubated with kindlin2 antibodies for 2 hr at 4°C while rotating. Isotype-matched IgG was used as a negative control. Lysates were then incubated with 50 μl protein A/G Plus Agarose (Santa Cruz) for 2 hr at 4°C. Following repeated washes with lysis buffer, proteins were eluted from the beads using Laemmli buffer and analyzed by western blotting.

Mass spectrometry

For the kindlin-2 interactome analysis by mass spectrometry (MS), cells were starved overnight in DMEM containing 0.2% FCS before plating on FN coated dishes (5 μg/ml) for 45 min. Following 3 min EGF (50 ng/ml) stimulation the cells were incubated for 5 min 0.5 M dithiobis(succinimidyl propionate) (DSP) at RT and washed with 0.5 mM Tris, pH 7.5 for

15 min. Cell lysis and myc-IPs were performed using the μ-MACS anti-myc magnetic beads and following the supplier instructions (130-091-284 from Miltenyi).

The samples were separated by SDS-PAGE gels and each sample/lane was cut into three bands and digested by the standard in-gel Trypsin digestion protocol (Shevchenko et al., 2006). The peptides were purified using C18 StageTips (Rappsilber et al., 2007). The samples were loaded 19 on a 15 cm column packed with 1.9 micron C18 beads from Dr Maisch GmbH via the Thermo nanoLC-1200 autosampler and sprayed directly into Q Exactive HF mass spectrometer. The mass spectrometer was operated in data dependent mode with Top N acquisition method. The raw data were processed using MaxQuant computational platform (Cox and Mann, 2008). The peak lists generated were searched with initial precursor and fragment mass tolerance of 7 and 20 ppm respectively. Carbamidomethylation of cysteine was used as static modification and oxidation of methionine and protein N–terminal acetylation was used as variable modification. Since the samples were cross-linked with DSP and later subjected to reduction and alkylation, carbamidomethylation of DSP were also included in the database search. The peak lists were searched against the Uniprot Mouse database the proteins and peptides were filtered at 1% false discovery rate. Proteins were quantified using the MaxLFQ algorithm in MaxQuant (Cox et al., 2014).

For the kindlin-2 phosphorylation analysis by mass spectrometry (MS), cells were cultured under normal conditions. Cell lysis and kindlin-2 immunoprecipitations were performed as described above. The samples were separated by SDS-PAGE gels and the sample was cut into two bands and digested by the standard in-gel Trypsin digestion protocol (Shevchenko et al., 2006).

Statistical analysis

All statistical significances (*P<0.05; **P<0.01; ***P<0.001) were determined by two-tailed unpaired *t*-test. Statistical analysis were performed with Prism (GraphPad, La Jolla, USA). All statistical analysis for MS data were performed using Perseus bioinformatics. Student t-test and ANOVA were used to compare the samples.

Figure Legends

Figure 1: Kindlin-2 is tyrosine phosphorylated by Abl kinases. (A) Immunoprecipitation of endogenous kindlin-2 from different cell lines fibroblasts (Fibro.), MDA-MB-231, B16-F1, show tyrosine phosphorylation of kindlin-2. **(B)** Kinase screening identifies Abl kinases among the kinases that phosphorylate kindlin-2. **(C)** *In vitro* kinase assay using recombinant kindlin-2 (asterisk) and recombinant Abl1 and Abl2 (asterisks), confirm that both kinase phosphorylate kindlin-2. **(D)** myc-IPs of lysates from HEK 293T cells overexpressing GFP-tagged Abl1 WT (wild type), PP (constitutive active), KD (kinase dead) and myc-kindlin-2. **(E)** myc-IPs of lysates from HEK 293T cells overexpressing YFP-tagged Abl2 WT and KD and myc-kindlin-2. pY, phosphotyrosine; GFP-Abl1, green fluorescent protein tagged Abl1; YFP-Abl2, yellow fluorescent protein tagged Abl2.

Figure 2: Abl kinases phosphorylate kindlin-2 at Y179. (A) In silico analysis reveals one binding motif of Abl kinase on mouse kindlin-2 sequence. **(B)** LC-MS of *in vitro* kinase assay using recombinant mouse kindlin-2 WT or Y197F together with mouse Abl1 or human Abl2. Samples where 10% TFA (Trifluoroacetic acid) is added serve as a control. **(C)** myc-IPs of lysates from HEK 293T cells overexpressing GFP-tagged Abl1 WT (wild type) and myc-kindlin-2 WT or Y179F. **(D)** myc-IPs of lysates from HEK 293T cells overexpressing YFP-tagged Abl2 WT (wild type) and myc-kindlin-2 WT or Y179F. **(E)** myc-IPs of lysates from $Abl1^{-/-}$ $Abl2^{-/-}$ cells overexpressing myc-kindlin-2 WT or Y179F and GFP-Abl1 or YFP-Abl2.

Figure 3: Kindlin-2 tyrosine phosphorylation at Y179 induces dorsal ruffles formation. (A) Fibroblasts expressing myc-Kind2WT, myc-Kind2Y179F and myc-Kind2Y179E seeded on FN and stimulated with EGF for 3 min. Cells stained for actin, paxillin and cortactin. **(B)**

Quantification of CDRs formation after EGF stimulation for 0, 3 and 5 minutes (n=3 independent experiments; two-tailed unpaired t-test (**P<0.01, ***P<0.001); error bars indicate standard deviation). **(C)** Downstream signaling of EGF stimulation for 3, 5 and 15 minutes of fibroblasts expressing myc-Kind2WT, myc-Kind2Y179F and myc-Kind2Y179E. Bar, 10µm.

Figure 4: Analysis of kindlin-2 tyrosine dependent interactors. (A) Representation of the myc-IPs interactor screening strategy. **(B)** Hierarchical cluster analysis of 131 ANOVA significant interactors (n=3).

Figure Supplement 1

(A) Immunoprecipitation of endogenous kindlin-2 (Coomassie gel) combined with MS-analysis showed phosphorylation of kindlin-2 at different serines. The graph shows the intensity of the four phosphorylated peptides identified under these experimental settings. **(B)** Coomassie gel of the purification process of recombinant kindlin-2. Kindlin-2 protein was eluted in the fraction 4 (Asterisk). PL= cell pellet, DF= Flow-through, F0= soluble protein fraction, F1-5= eluted fractions. **(C)** Table of tyrosine kinases with score more than 2,5 after the performance of tyrosine kinase screening using recombinant kindlin-2 protein.

Figure Supplement 2

(A) Analysis of kindlin-2 tyrosines position using PyMol (http://www.pymol.org/) based on the published 3D structure of kindlin-2. (**B)** Coomassie gel of the purification process of recombinant kindlin-2 Y179F. Kindlin-2 Y179F protein was eluted in the fraction 4 (Asterisk). PL= cell pellet, DF= Flow-through, F0= soluble protein fraction, F1-5= eluted fractions **(C)** GFP-IPs of lysates from HEK 293T cells overexpressing GFP-tagged kindlin-1,

kindlin-2 and kindlin-3 together with Abl1 WT. **(D)** Sequence alignment of mouse kindlins shows the lack of conservation of Y179 through kindlin family members.

Figure Supplement 3

(A) Sequencing of the final ITR-myc-kindlin-2 vector bearing the TAT-GAA (Y-E) and TAT-TTT (Y-F) mutation. **(B)** Expression levels of myc-Kind2WT, myc-Kind2Y179F and myc-Y179E after FACS sorting for similar expression levels. **(C)** Fibroblasts expressing myc-Kind2WT, myc-Kind2Y179F and myc-Kind2Y179E seeded on FN and stained for actin, paxillin and kindlin-2. **(D)** Re-expression of GFP-Kind2WT, GFP-Kind2Y179F and GFP-Kind2Y179E in ILK fl/fl cells after siRNA-depletion of endogenous kindlin-2. **(E)** Fibroblasts expressing GFP-Kind2WT, GFP-Kind2Y179F and GFP-Kind2Y179E seeded on FN and stimulated with EGF for 3 min. Cells stained for actin and GFP; Bar, 10µm, 20 µm.

Figure Supplement 4

(A) Volcano plots showing interactors of myc-Kind2WT and **(B)** proteins which differentially bind to myc-Kind2Y179F and myc-Kind2Y179E; (FDR: 0.1, S0:0.5)

References

Abella, J.V., C.A. Parachoniak, V. Sangwan, and M. Park. 2010. Dorsal ruffle microdomains potentiate Met receptor tyrosine kinase signaling and down-regulation. *J Biol Chem*. 285:24956-24967.

Antoku, S., and B.J. Mayer. 2009. Distinct roles for Crk adaptor isoforms in actin reorganization induced by extracellular signals. *J Cell Sci*. 122:4228-4238.

Artym, V.V., S. Swatkoski, K. Matsumoto, C.B. Campbell, R.J. Petrie, E.K. Dimitriadis, X. Li, S.C. Mueller, T.H. Bugge, M. Gucek, and K.M. Yamada. 2015. Dense fibrillar collagen is a potent inducer of invadopodia via a specific signaling network. *J Cell Biol*. 208:331-350.

Azimifar, S.B., R.T. Bottcher, S. Zanivan, C. Grashoff, M. Kruger, K.R. Legate, M. Mann, and R. Fassler. 2012. Induction of membrane circular dorsal ruffles requires co-signalling of integrin-ILK-complex and EGF receptor. *J Cell Sci*. 125:435-448.

Boissan, M., G. Montagnac, Q. Shen, L. Griparic, J. Guitton, M. Romao, N. Sauvonnet, T. Lagache, I. Lascu, G. Raposo, C. Desbourdes, U. Schlattner, M.L. Lacombe, S. Polo, A.M. van der Bliek, A. Roux, and P. Chavrier. 2014. Membrane trafficking. Nucleoside diphosphate kinases fuel dynamin superfamily proteins with GTP for membrane remodeling. *Science*. 344:1510-1515.

Boissan, M., U. Schlattner, and M.L. Lacombe. 2018. The NDPK/NME superfamily: state of the art. *Lab Invest*. 98:164-174.

Bottcher, R.T., M. Veelders, P. Rombaut, J. Faix, M. Theodosiou, T.E. Stradal, K. Rottner, R. Zent, F. Herzog, and R. Fassler. 2017. Kindlin-2 recruits paxillin and Arp2/3 to promote membrane protrusions during initial cell spreading. *J Cell Biol*. 216:3785-3798.

Bouaouina, M., B.T. Goult, C. Huet-Calderwood, N. Bate, N.N. Brahme, I.L. Barsukov, D.R. Critchley, and D.A. Calderwood. 2012. A conserved lipid-binding loop in the kindlin FERM F1 domain is required for kindlin-mediated alphaIIbbeta3 integrin coactivation. *J Biol Chem*. 287:6979-6990.

Boyle, S.N., G.A. Michaud, B. Schweitzer, P.F. Predki, and A.J. Koleske. 2007. A critical role for cortactin phosphorylation by Abl-family kinases in PDGF-induced dorsal-wave formation. *Curr Biol*. 17:445-451.

Buccione, R., J.D. Orth, and M.A. McNiven. 2004. Foot and mouth: podosomes, invadopodia and circular dorsal ruffles. *Nat Rev Mol Cell Biol*. 5:647-657.

Burke, R.D. 1999. Invertebrate integrins: structure, function, and evolution. *Int Rev Cytol*. 191:257-284.

Cooper, J.A., T. Kaneko, and S.S. Li. 2015. Cell regulation by phosphotyrosine-targeted ubiquitin ligases. *Mol Cell Biol*. 35:1886-1897.

Cox, J., M.Y. Hein, C.A. Luber, I. Paron, N. Nagaraj, and M. Mann. 2014. Accurate proteome-wide label-free quantification by delayed normalization and maximal peptide ratio extraction, termed MaxLFQ. *Mol Cell Proteomics*. 13:2513-2526.

Cox, J., and M. Mann. 2008. MaxQuant enables high peptide identification rates, individualized p.p.b.-range mass accuracies and proteome-wide protein quantification. *Nat Biotechnol*. 26:1367-1372.

Dharmawardhane, S., A. Schurmann, M.A. Sells, J. Chernoff, S.L. Schmid, and G.M. Bokoch. 2000. Regulation of macropinocytosis by p21-activated kinase-1. *Mol Biol Cell*. 11:3341-3352.

Finn, A.J., G. Feng, and A.M. Pendergast. 2003. Postsynaptic requirement for Abl kinases in assembly of the neuromuscular junction. *Nat Neurosci*. 6:717-723.

Fournier, H.N., S. Dupe-Manet, D. Bouvard, M.L. Lacombe, C. Marie, M.R. Block, and C. Albiges-Rizo. 2002. Integrin cytoplasmic domain-associated protein 1alpha (ICAP-1alpha) interacts directly with the metastasis suppressor nm23-H2, and both proteins are targeted to newly formed cell adhesion sites upon integrin engagement. *J Biol Chem*. 277:20895-20902.

Fuhs, S.R., and T. Hunter. 2017. pHisphorylation: the emergence of histidine phosphorylation as a reversible regulatory modification. *Curr Opin Cell Biol*. 45:8-16.

Giancotti, F.G., and E. Ruoslahti. 1999. Integrin signaling. *Science*. 285:1028-1032.

Gourley, S.L., A.J. Koleske, and J.R. Taylor. 2009. Loss of dendrite stabilization by the Abl-related gene (Arg) kinase regulates behavioral flexibility and sensitivity to cocaine. *Proc Natl Acad Sci U S A*. 106:16859-16864.

Gu, Z., E.H. Noss, V.W. Hsu, and M.B. Brenner. 2011. Integrins traffic rapidly via circular dorsal ruffles and macropinocytosis during stimulated cell migration. *J Cell Biol*. 193:61-70.

Hensley, K., K. Venkova, A. Christov, W. Gunning, and J. Park. 2011. Collapsin response mediator protein-2: an emerging pathologic feature and therapeutic target for neurodisease indications. *Mol Neurobiol*. 43:180-191.

Hernandez, S.E., M. Krishnaswami, A.L. Miller, and A.J. Koleske. 2004. How do Abl family kinases regulate cell shape and movement? *Trends Cell Biol*. 14:36-44.

Hoon, J.L., W.K. Wong, and C.G. Koh. 2012. Functions and regulation of circular dorsal ruffles. *Mol Cell Biol*. 32:4246-4257.

Hynes, R.O. 2002. Integrins: bidirectional, allosteric signaling machines. *Cell*. 110:673-687.

Inagaki, N., K. Chihara, N. Arimura, C. Menager, Y. Kawano, N. Matsuo, T. Nishimura, M. Amano, and K. Kaibuchi. 2001. CRMP-2 induces axons in cultured hippocampal neurons. *Nat Neurosci*. 4:781-782.

Itoh, T., and J. Hasegawa. 2013. Mechanistic insights into the regulation of circular dorsal ruffle formation. *J Biochem*. 153:21-29.

King, S.J., D.C. Worth, T.M. Scales, J. Monypenny, G.E. Jones, and M. Parsons. 2011. beta1 integrins regulate fibroblast chemotaxis through control of N-WASP stability. *EMBO J*. 30:1705-1718.

Koleske, A.J., A.M. Gifford, M.L. Scott, M. Nee, R.T. Bronson, K.A. Miczek, and D. Baltimore. 1998. Essential roles for the Abl and Arg tyrosine kinases in neurulation. *Neuron*. 21:1259-1272.

Krueger, E.W., J.D. Orth, H. Cao, and M.A. McNiven. 2003. A dynamin-cortactin-Arp2/3 complex mediates actin reorganization in growth factor-stimulated cells. *Mol Biol Cell*. 14:1085-1096.

Kua, H.Y., H. Liu, W.F. Leong, L. Li, D. Jia, G. Ma, Y. Hu, X. Wang, J.F. Chau, Y.G. Chen, Y. Mishina, S. Boast, J. Yeh, L. Xia, G.Q. Chen, L. He, S.P. Goff, and B. Li. 2012. c-Abl promotes osteoblast expansion by differentially regulating canonical and non-canonical BMP pathways and p16INK4a expression. *Nat Cell Biol*. 14:727-737.

Legate, K.R., S.A. Wickstrom, and R. Fassler. 2009. Genetic and cell biological analysis of integrin outside-in signaling. *Genes Dev*. 23:397-418.

Lewis, J.M., R. Baskaran, S. Taagepera, M.A. Schwartz, and J.Y. Wang. 1996. Integrin regulation of c-Abl tyrosine kinase activity and cytoplasmic-nuclear transport. *Proc Natl Acad Sci U S A*. 93:15174-15179.

Li, B., S. Boast, K. de los Santos, I. Schieren, M. Quiroz, S.L. Teitelbaum, M.M. Tondravi, and S.P. Goff. 2000. Mice deficient in Abl are osteoporotic and have defects in osteoblast maturation. *Nat Genet*. 24:304-308.

Li, H., Y. Deng, K. Sun, H. Yang, J. Liu, M. Wang, Z. Zhang, J. Lin, C. Wu, Z. Wei, and C. Yu. 2017. Structural basis of kindlin-mediated integrin recognition and activation. *Proc Natl Acad Sci U S A*. 114:9349-9354.

Liu, J., K. Fukuda, Z. Xu, Y.Q. Ma, J. Hirbawi, X. Mao, C. Wu, E.F. Plow, and J. Qin. 2011. Structural basis of phosphoinositide binding to kindlin-2 protein pleckstrin homology domain in regulating integrin activation. *J Biol Chem*. 286:43334-43342.

Liu, Z., D. Lu, X. Wang, J. Wan, C. Liu, and H. Zhang. 2015. Kindlin-2 phosphorylation by Src at Y193 enhances Src activity and is involved in Migfilin recruitment to the focal adhesions. *FEBS Lett*. 589:2001-2010.

McCorkle, J.R., M.K. Leonard, S.D. Kraner, E.M. Blalock, D. Ma, S.G. Zimmer, and D.M. Kaetzel. 2014. The metastasis suppressor NME1 regulates expression of genes linked to metastasis and patient outcome in melanoma and breast carcinoma. *Cancer Genomics Proteomics*. 11:175-194.

Montanez, E., S. Ussar, M. Schifferer, M. Bosl, R. Zent, M. Moser, and R. Fassler. 2008. Kindlin-2 controls bidirectional signaling of integrins. *Genes Dev*. 22:1325-1330.

Moresco, E.M., S. Donaldson, A. Williamson, and A.J. Koleske. 2005. Integrin-mediated dendrite branch maintenance requires Abelson (Abl) family kinases. *J Neurosci*. 25:6105-6118.

Moser, M., B. Nieswandt, S. Ussar, M. Pozgajova, and R. Fassler. 2008. Kindlin-3 is essential for integrin activation and platelet aggregation. *Nat Med*. 14:325-330.

Myllykoski, M., A. Baumann, K. Hensley, and P. Kursula. 2017. Collapsin response mediator protein 2: high-resolution crystal structure sheds light on small-molecule binding, post-translational modifications, and conformational flexibility. *Amino Acids*. 49:747-759.

Orth, J.D., E.W. Krueger, S.G. Weller, and M.A. McNiven. 2006. A novel endocytic mechanism of epidermal growth factor receptor sequestration and internalization. *Cancer Res*. 66:3603-3610.

Parsons, J.T., A.R. Horwitz, and M.A. Schwartz. 2010. Cell adhesion: integrating cytoskeletal dynamics and cellular tension. *Nat Rev Mol Cell Biol*. 11:633-643.

Perera, H.D., Y.Q. Ma, J. Yang, J. Hirbawi, E.F. Plow, and J. Qin. 2011. Membrane binding of the N-terminal ubiquitin-like domain of kindlin-2 is crucial for its regulation of integrin activation. *Structure*. 19:1664-1671.

Plattner, R., L. Kadlec, K.A. DeMali, A. Kazlauskas, and A.M. Pendergast. 1999. c-Abl is activated by growth factors and Src family kinases and has a role in the cellular response to PDGF. *Genes Dev*. 13:2400-2411.

Polanski, R., M. Maguire, P.C. Nield, R.E. Jenkins, B.K. Park, K. Krawczynska, T. Devling, A. Ray-Sinha, C.P. Rubbi, N. Vlatkovic, and M.T. Boyd. 2011. MDM2 interacts with NME2 (non-metastatic cells 2, protein) and suppresses the ability of NME2 to negatively regulate cell motility. *Carcinogenesis*. 32:1133-1142.

Qu, H., Y. Tu, J.L. Guan, G. Xiao, and C. Wu. 2014. Kindlin-2 tyrosine phosphorylation and interaction with Src serve as a regulatable switch in the integrin outside-in signaling circuit. *J Biol Chem*. 289:31001-31013.

Rappsilber, J., M. Mann, and Y. Ishihama. 2007. Protocol for micro-purification, enrichment, pre-fractionation and storage of peptides for proteomics using StageTips. *Nat Protoc*. 2:1896-1906.

Robinson, D.R., Y.M. Wu, and S.F. Lin. 2000. The protein tyrosine kinase family of the human genome. *Oncogene*. 19:5548-5557.

Sarhan, A.R., J. Szyroka, S. Begum, M.G. Tomlinson, N.A. Hotchin, J.K. Heath, and D.L. Cunningham. 2017. Quantitative Phosphoproteomics Reveals a Role for Collapsin Response Mediator Protein 2 in PDGF-Induced Cell Migration. *Sci Rep*. 7:3970.

Schwartzberg, P.L., A.M. Stall, J.D. Hardin, K.S. Bowdish, T. Humaran, S. Boast, M.L. Harbison, E.J. Robertson, and S.P. Goff. 1991. Mice homozygous for the ablm1 mutation show poor viability and depletion of selected B and T cell populations. *Cell*. 65:1165-1175.

Sero, J.E., C.K. Thodeti, A. Mammoto, C. Bakal, S. Thomas, and D.E. Ingber. 2011. Paxillin mediates sensing of physical cues and regulates directional cell motility by controlling lamellipodia positioning. *PLoS One*. 6:e28303.

Shevchenko, A., H. Tomas, J. Havlis, J.V. Olsen, and M. Mann. 2006. In-gel digestion for mass spectrometric characterization of proteins and proteomes. *Nat Protoc*. 1:2856-2860.

Sini, P., A. Cannas, A.J. Koleske, P.P. Di Fiore, and G. Scita. 2004. Abl-dependent tyrosine phosphorylation of Sos-1 mediates growth-factor-induced Rac activation. *Nat Cell Biol*. 6:268-274.

Stuart, J.R., F.H. Gonzalez, H. Kawai, and Z.M. Yuan. 2006. c-Abl interacts with the WAVE2 signaling complex to induce membrane ruffling and cell spreading. *J Biol Chem*. 281:31290-31297.

Suetsugu, S., D. Yamazaki, S. Kurisu, and T. Takenawa. 2003. Differential roles of WAVE1 and WAVE2 in dorsal and peripheral ruffle formation for fibroblast cell migration. *Dev Cell*. 5:595-609.

Tan, F., C.J. Thiele, and Z. Li. 2014. Collapsin response mediator proteins: Potential diagnostic and prognostic biomarkers in cancers (Review). *Oncol Lett*. 7:1333-1340.

Thakur, R.K., V.K. Yadav, P. Kumar, and S. Chowdhury. 2011. Mechanisms of non-metastatic 2 (NME2)-mediated control of metastasis across tumor types. *Naunyn Schmiedebergs Arch Pharmacol*. 384:397-406.

Theodosiou, M., M. Widmaier, R.T. Bottcher, E. Rognoni, M. Veelders, M. Bharadwaj, A. Lambacher, K. Austen, D.J. Muller, R. Zent, and R. Fassler. 2016. Kindlin-2 cooperates with talin to activate integrins and induces cell spreading by directly binding paxillin. *Elife*. 5:e10130.

Tybulewicz, V.L., C.E. Crawford, P.K. Jackson, R.T. Bronson, and R.C. Mulligan. 1991. Neonatal lethality and lymphopenia in mice with a homozygous disruption of the c-abl proto-oncogene. *Cell*. 65:1153-1163.

Ussar, S., M. Moser, M. Widmaier, E. Rognoni, C. Harrer, O. Genzel-Boroviczeny, and R. Fassler. 2008. Loss of Kindlin-1 causes skin atrophy and lethal neonatal intestinal epithelial dysfunction. *PLoS Genet*. 4:e1000289.

van der Flier, A., and A. Sonnenberg. 2001. Function and interactions of integrins. *Cell Tissue Res*. 305:285-298.

Wei, X., X. Wang, Y. Xia, Y. Tang, F. Li, W. Fang, and H. Zhang. 2014. Kindlin-2 regulates renal tubular cell plasticity by activation of Ras and its downstream signaling. *Am J Physiol Renal Physiol*. 306:F271-278.

Wei, X., Y. Xia, F. Li, Y. Tang, J. Nie, Y. Liu, Z. Zhou, H. Zhang, and F.F. Hou. 2013. Kindlin-2 mediates activation of TGF-beta/Smad signaling and renal fibrosis. *J Am Soc Nephrol*. 24:1387-1398.

Winograd-Katz, S.E., R. Fassler, B. Geiger, and K.R. Legate. 2014. The integrin adhesome: from genes and proteins to human disease. *Nat Rev Mol Cell Biol*. 15:273-288.

Woodring, P.J., E.D. Litwack, D.D. O'Leary, G.R. Lucero, J.Y. Wang, and T. Hunter. 2002. Modulation of the F-actin cytoskeleton by c-Abl tyrosine kinase in cell spreading and neurite extension. *J Cell Biol*. 156:879-892.

Wu, C., H. Jiao, Y. Lai, W. Zheng, K. Chen, H. Qu, W. Deng, P. Song, K. Zhu, H. Cao, D.L. Galson, J. Fan, H.J. Im, Y. Liu, J. Chen, D. Chen, and G. Xiao. 2015. Kindlin-2 controls TGF-beta signalling and Sox9 expression to regulate chondrogenesis. *Nat Commun*. 6:7531.

Yoneda, A., M. Morgan-Fisher, R. Wait, J.R. Couchman, and U.M. Wewer. 2012. A collapsin response mediator protein 2 isoform controls myosin II-mediated cell migration and matrix assembly by trapping ROCK II. *Mol Cell Biol*. 32:1788-1804.

Yu, Y., J. Wu, Y. Wang, T. Zhao, B. Ma, Y. Liu, W. Fang, W.G. Zhu, and H. Zhang. 2012. Kindlin 2 forms a transcriptional complex with beta-catenin and TCF4 to enhance Wnt signalling. *EMBO Rep*. 13:750-758.

Zhang, H., E. Kang, Y. Wang, C. Yang, H. Yu, Q. Wang, Z. Chen, C. Zhang, K.M. Christian, H. Song, G.L. Ming, and Z. Xu. 2016. Brain-specific Crmp2 deletion leads to neuronal development deficits and behavioural impairments in mice. *Nat Commun*. 7.

Figure 1

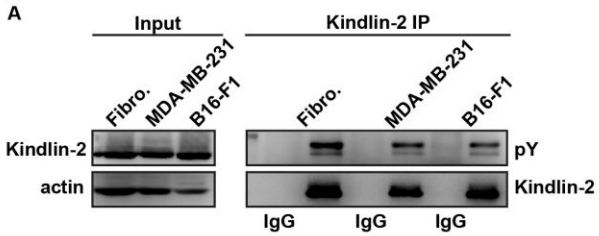

B

Kinase	Activity Ratio (cpm)
Abl1	11.82
Abl2	2.69

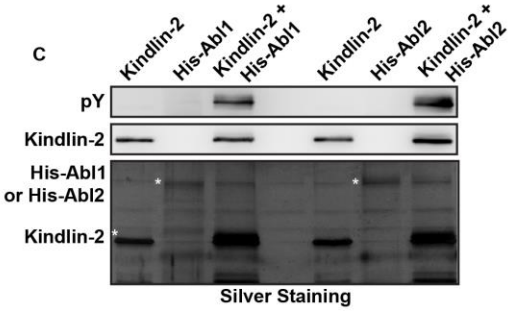

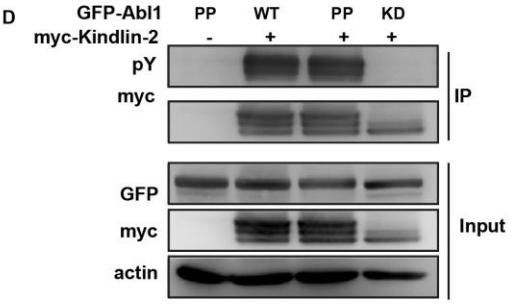

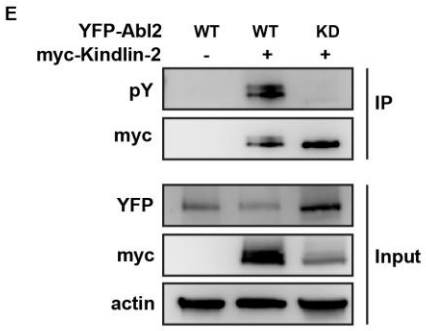

Figure 2

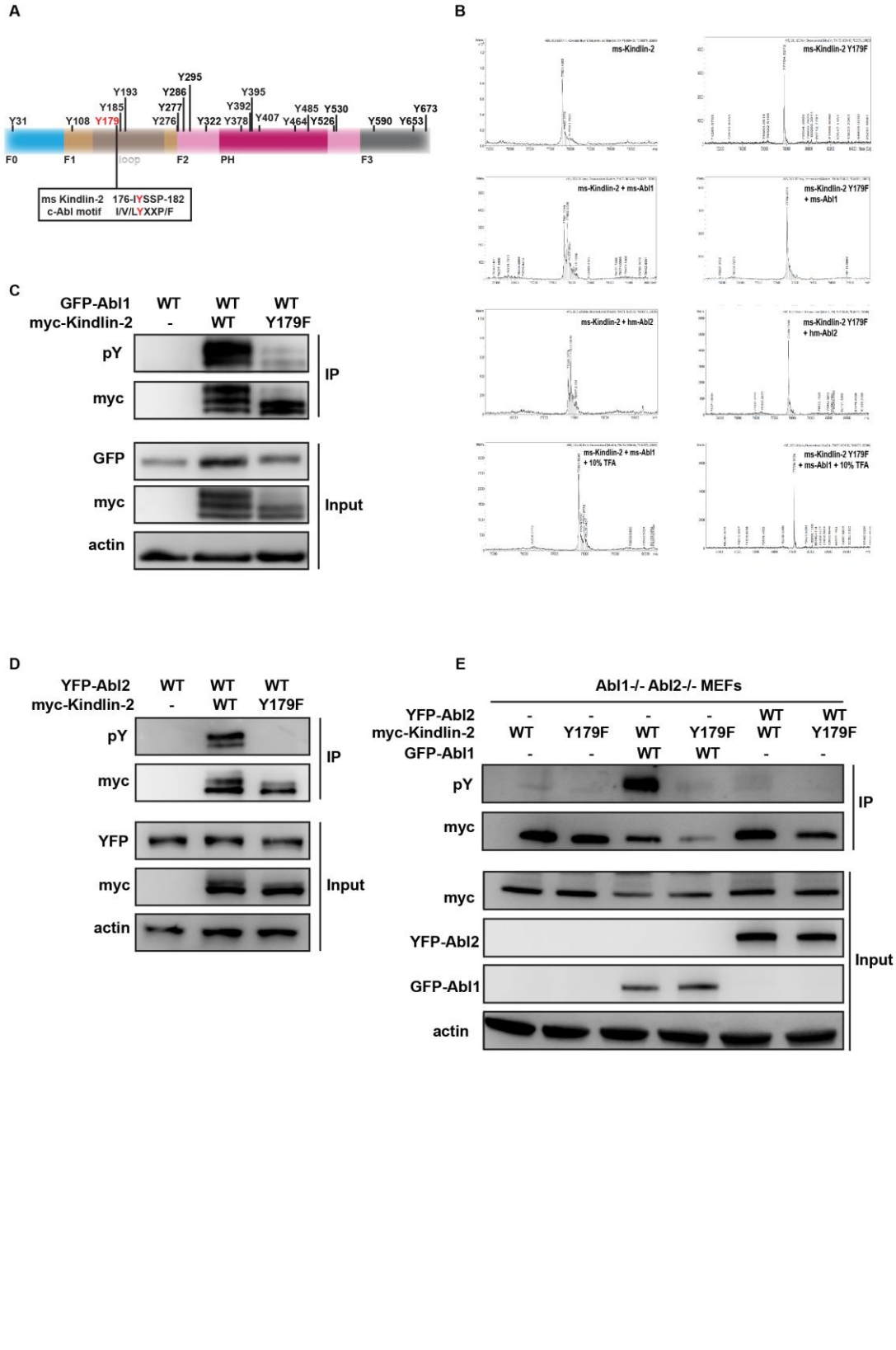
A
Y295
Y193
Y286
Y395
Y185
Y277
Y392
Y485
Y530
Y673
Y31
Y108
Y179
Y276
Y322
Y378
Y407
Y464
Y526
Y590
Y653
F0
F1
loop
F2
PH
F3
ms Kindlin-2 176-IYSSP-182
c-Abl motif I/V/LYXXP/F
B
ms-Kindlin-2
ms-Kindlin-2 Y179F
ms-Kindlin-2 + ms-Abl1
ms-Kindlin-2 Y179F + ms-Abl1
ms-Kindlin-2 + hm-Abl2
ms-Kindlin-2 Y179F + hm-Abl2
ms-Kindlin-2 + ms-Abl1 + 10% TFA
ms-Kindlin-2 Y179F + ms-Abl1 + 10% TFA
C
GFP-Abl1 WT WT WT
myc-Kindlin-2 - WT Y179F
pY
myc
IP
GFP
myc
actin
Input
D
YFP-Abl2 WT WT WT
myc-Kindlin-2 - WT Y179F
pY
myc
IP
YFP
myc
actin
Input
E
Abl1-/- Abl2-/- MEFs
YFP-Abl2 - - - - WT WT
myc-Kindlin-2 WT Y179F WT Y179F WT Y179F
GFP-Abl1 - - WT WT - -
pY
myc
IP
myc
YFP-Abl2
GFP-Abl1
actin
Input

Figure 3

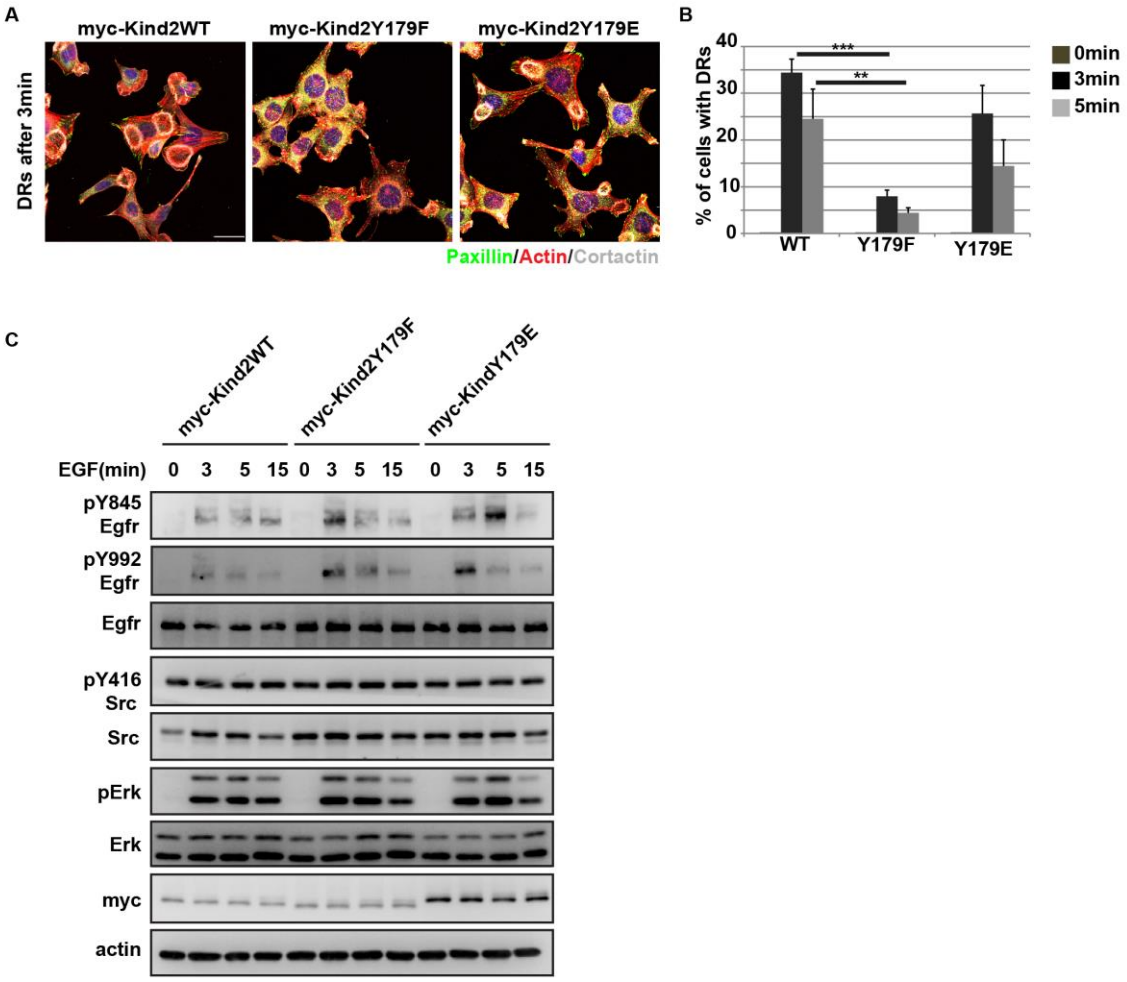
A
myc-Kind2WT
myc-Kind2Y179F
myc-Kind2Y179E
DRs after 3min
Paxillin/Actin/Cortactin
B
% of cells with DRs
40
30
20
10
0
***
**
WT
Y179F
Y179E
0min
3min
5min
C
myc-Kind2WT
myc-Kind2Y179F
myc-KindY179E
EGF(min) 0 3 5 15 0 3 5 15 0 3 5 15
pY845 Egfr
pY992 Egfr
Egfr
pY416 Src
Src
pErk
Erk
myc
actin

Figure 4

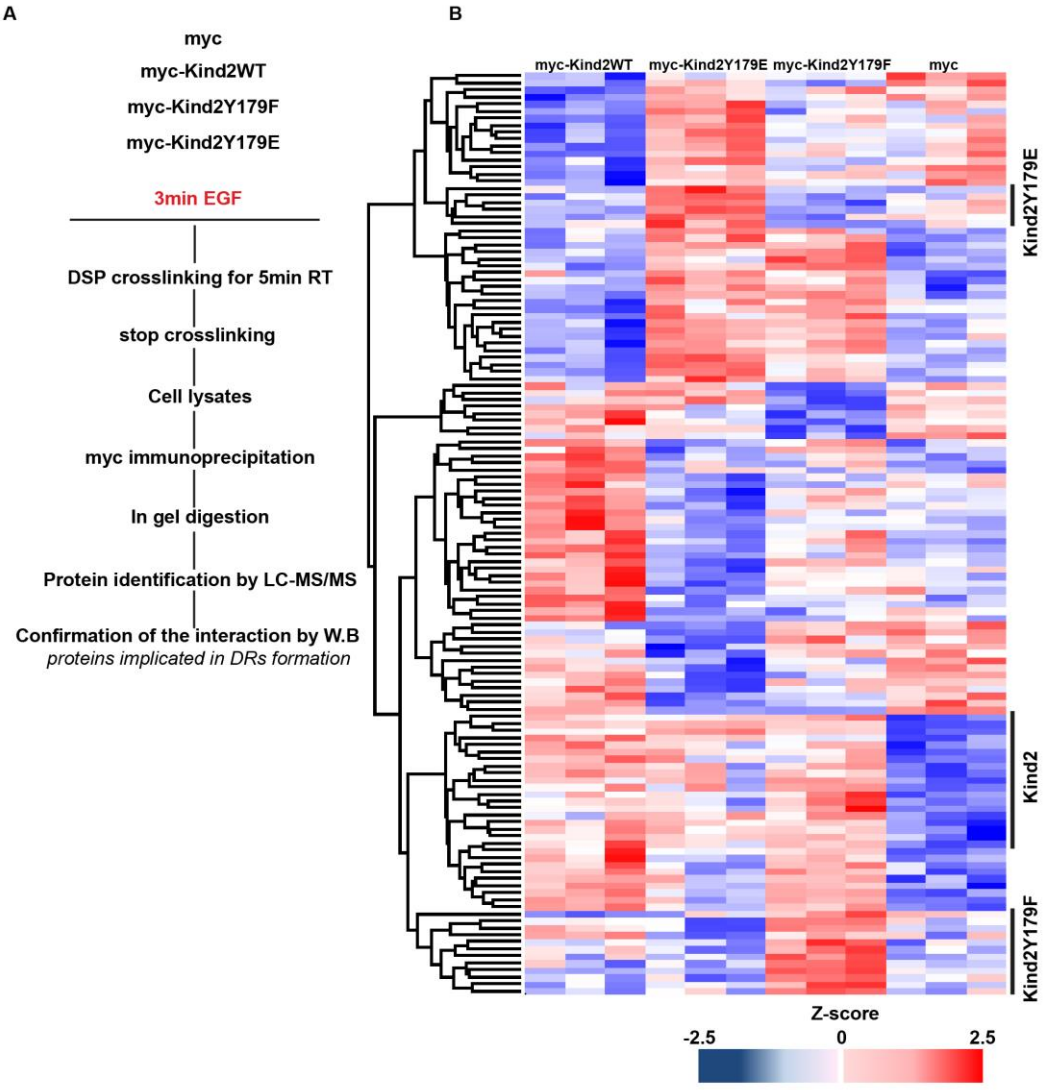
A
myc
myc-Kind2WT
myc-Kind2Y179F
myc-Kind2Y179E
3min EGF
DSP crosslinking for 5min RT
stop crosslinking
Cell lysates
myc immunoprecipitation
In gel digestion
Protein identification by LC-MS/MS
Confirmation of the interaction by W.B
proteins implicated in DRs formation
B
myc-Kind2WT
myc-Kind2Y179E
myc-Kind2Y179F
myc
Kind2Y179E
Kind2
Kind2Y179F
Z-score
-2.5
0
2.5

Figure S1

A

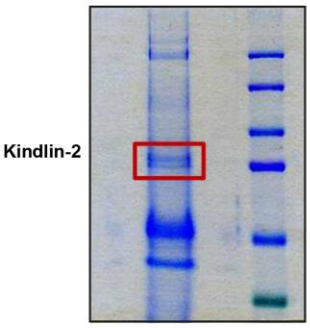

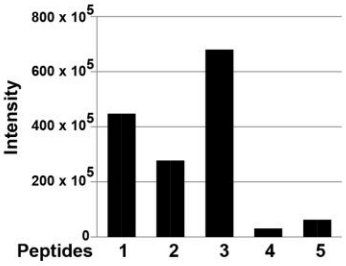

1- DQNE**S**LDEEMFYK (S666)

2- EVDEVDAAL**S**DLEITLEGGK (S351)

3- KLDDQ**S**EDEALELEGPLIMPGSGSIYSSPGLYSK (S159)

4- KLDDQSEDEALELEGPLIMPGSGSIYS**S**PGLYSK (S181)

5- KLDDQSEDEALELEGPLIMPGSGSIY**S**SPGLYSK (s180)

B

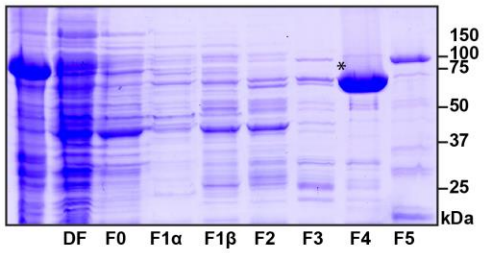

C

Kinase	Activity Ratio (cpm)
FLT3 D835Y	15.59
TXK	14.14
ABL1 wt	11.81
BLK	11.10
FER	10.00
MET M1250T	8.84
CSF1-R	8.63
TYRO3	8.63
HCK	7.55
MERTK	7.15
FGF-R1 V561M	5.73
EPHB4	5.67
LYN	5.07
TRK-B	4.48
ABL1 T315I	4.45
ALK	3.97
RON	3.94
KIT D816V	3.93
ROS	3.87
KIT wt	3.67
EPHA8	3.66
BRK	3.56
FES	3.54
YES	3.44
ALK L1196M	3.29
EPHA1	3.25
KIT T670I	3.18
INS-R	3.11
TRK-C	2.80
MET	2.80
ABL2	2.69
LCK	2.66

Figure S2

A

	Site	Location
F0	Y13	
	Y108	surface
F1	Y179	accesible
	Y185	accesible
	Y193	accesible
	Y276	inside
F2	Y277	surface
	Y286	surface
	Y295	inside
	Y322	surface
	Y378	surface
	Y392	surface
	Y395	surface
	Y407	surface
	Y464	inside
	Y485	surface
	Y526	surface
	Y530	surface
F3	Y590	surface
	Y653	inside
	Y673	surface

B

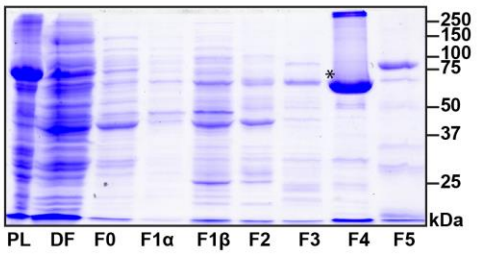

C

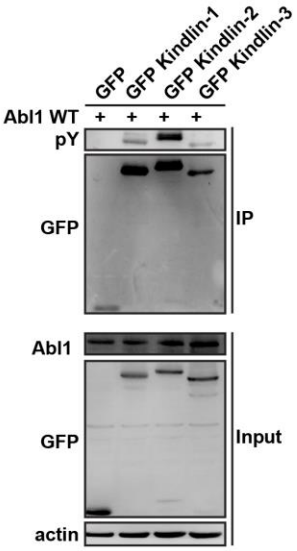

D

```
Kindlin-1  GSP---VSPGL
Kindlin-2  GSGSIYSSPGL
Kindlin-3  GVA-----PTL
           *       * *
```

Figure S3

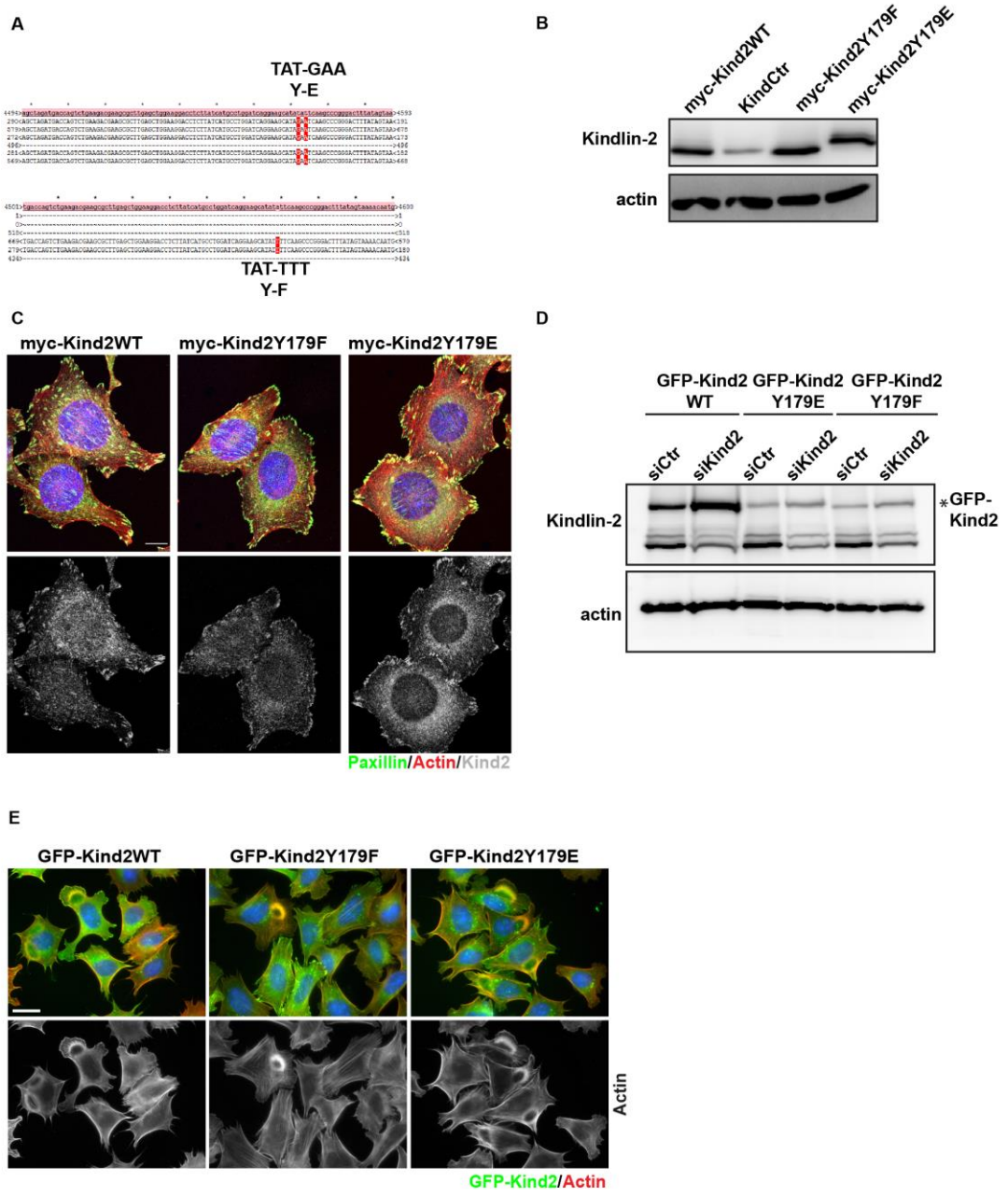
A
TAT-GAA
Y-E
TAT-TTT
Y-F
B
myc-Kind2WT
KindCtr
myc-Kind2Y179F
myc-Kind2Y179E
Kindlin-2
actin
C
myc-Kind2WT
myc-Kind2Y179F
myc-Kind2Y179E
Paxillin/Actin/Kind2
D
GFP-Kind2 WT
GFP-Kind2 Y179E
GFP-Kind2 Y179F
siCtr
siKind2
siCtr
siKind2
siCtr
siKind2
Kindlin-2
*GFP-Kind2
actin
E
GFP-Kind2WT
GFP-Kind2Y179F
GFP-Kind2Y179E
Actin
GFP-Kind2/Actin

Figure S4

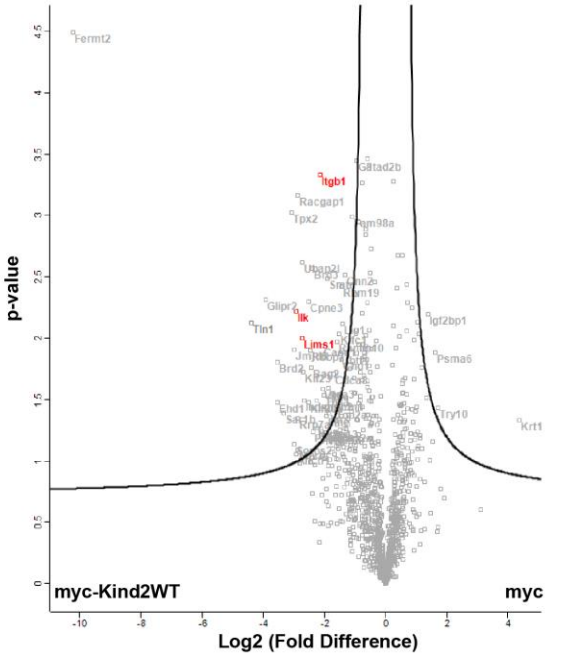
Fermt2
Itgb1
Racgap1
Tpx2
Arhgap19
Glipr2
Cpne3
Tln1
Ilk
Lims1
Brd2
Igf2bp1
Psma6
Try10
Krt1
p-value
myc-Kind2WT
myc
Log2 (Fold Difference)

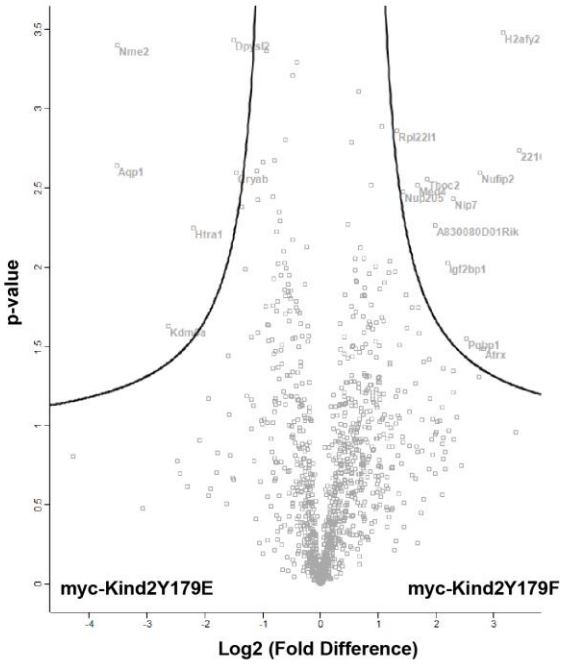
Nme2
Dpysl2
H2afy2
Rpl22l1
Aqp1
Cryab
Nufip2
Nip7
Htra1
A830080D01Rik
Igf2bp1
Kdm5a
Pqbp1
Atrx
p-value
myc-Kind2Y179E
myc-Kind2Y179F
Log2 (Fold Difference)

eLIFE elifesciences.org

RESEARCH ARTICLE

Kindlin-2 cooperates with talin to activate integrins and induces cell spreading by directly binding paxillin

Marina Theodosiou[1], Moritz Widmaier[1], Ralph T Böttcher[1], Emanuel Rognoni[1], Maik Veelders[1], Mitasha Bharadwaj[2], Armin Lambacher[1], Katharina Austen[1], Daniel J Müller[2], Roy Zent[3,4], Reinhard Fässler[1]*

[1]Department of Molecular Medicine, Max Planck Institute of Biochemistry, Martinsried, Germany; [2]Department of Biosystems Science and Engineering, Eidgenössische Technische Hochschule Zürich, Basel, Switzerland; [3]Division of Nephrology, Department of Medicine, Vanderbilt University, Nashville, United States; [4]Department of Medicine, Veterans Affairs Medical Center, Nashville, United States

Abstract Integrins require an activation step prior to ligand binding and signaling. How talin and kindlin contribute to these events in non-hematopoietic cells is poorly understood. Here we report that fibroblasts lacking either talin or kindlin failed to activate β1 integrins, adhere to fibronectin (FN) or maintain their integrins in a high affinity conformation induced by Mn^{2+}. Despite compromised integrin activation and adhesion, Mn^{2+} enabled talin- but not kindlin-deficient cells to initiate spreading on FN. This isotropic spreading was induced by the ability of kindlin to directly bind paxillin, which in turn bound focal adhesion kinase (FAK) resulting in FAK activation and the formation of lamellipodia. Our findings show that talin and kindlin cooperatively activate integrins leading to FN binding and adhesion, and that kindlin subsequently assembles an essential signaling node at newly formed adhesion sites in a talin-independent manner.
DOI: 10.7554/eLife.10130.001

***For correspondence:** faessler@biochem.mpg.de

Competing interests: The authors declare that no competing interests exist.

Funding: See page 21

Received: 15 July 2015
Accepted: 19 December 2015
Published: 28 January 2016

Reviewing editor: Vivek Malhotra, The Barcelona Institute of Science and Technology, Barcelona, Spain

Introduction

Integrins are heterodimeric transmembrane receptors that mediate cell adhesion to the extracellular matrix (ECM) and to other cells (***Hynes, 2002***). The consequence of integrin-mediated adhesion is the assembly of a large molecular network that induces various signaling pathways, resulting in cell migration, proliferation, survival and differentiation (***Winograd-Katz et al., 2014***). The quality and strength of integrin signaling is controlled by the interaction between integrins and substrate-attached ligands, which is, in turn, regulated by the on- and off-rates of the integrin–ligand binding process. The on-rate of the integrin–ligand binding reaction (also called integrin activation or inside-out signaling) is characterized by switching the unbound form of integrins from an inactive (low affinity) to an active (high affinity) conformation. The affinity switch proceeds from a bent and clasped low affinity conformation to an extended and unclasped high affinity conformation with an open ligand-binding pocket (***Askari et al., 2010***; ***Springer and Dustin, 2012***). This change in affinity is believed to be induced through the binding of talin and kindlin to the β integrin cytoplasmic domain (***Moser et al., 2009***; ***Shattil et al., 2010***) and divalent cations to distinct sites close to the ligand-binding pocket (***Gailit and Ruoslahti, 1988***; ***Mould et al., 1995***; ***Xia and Springer, 2014***; ***Mould et al., 2003***).

The stabilisation of integrin–ligand complexes is mediated by integrin clustering and catch bond formation between integrin and bound ligand. The stabilizing effect of clustered integrins is

eLife digest A meshwork of proteins called the extracellular matrix surrounds the cells that make up our tissues. Integrins are adhesion proteins that sit on the membrane surrounding each cell and bind to the matrix proteins. These adhesive interactions control many aspects of cell behavior such as their ability to divide, move and survive.

Before integrins can bind to the extracellular matrix they must be activated. Previous research has shown that in certain types of blood cells, proteins called talins and kindlins perform this activation. These proteins bind to the part of the integrin that extends into the cell, causing shape changes to the integrin that allow binding to the extracellular matrix. However, it is not clear whether talin and kindlin also activate integrins in other cell types.

Fibroblasts are cells that help to make extracellular matrix proteins, and are an important part of connective tissue. Theodosiou et al. engineered mouse fibroblast cells to lack either talin or kindlin, and found that both of these mutant cell types were unable to activate their integrins and as a result failed to bind to an extracellular matrix protein called fibronectin.

Even when cells were artificially induced to activate integrins by treating them with manganese ions, cells lacking talin or kindlin failed to fully activate integrins and hence did not adhere well to fibronectin. This suggests that talin and kindlin work together to activate integrins and to maintain them in this activated state.

When treated with manganese ions, cells that lacked talin were able to flatten and spread out, whereas cells that lacked kindlin were unable to undergo this shape change. Theodosiou et al. found that this cell shape is dependent on kindlin and its ability to bind to and recruit a protein called paxillin to "adhesion sites", where integrins connect the cell surface with the extracellular matrix. Kindlin and paxillin then work together to activate other signaling molecules to induce the cell spreading.

The next challenge is to understand how talin and kindlin are activated in non-blood cells and how they maintain integrins in an active state.

DOI: 10.7554/eLife.10130.002

achieved by the ability of dissociated integrin–ligand complexes to rebind before they leave the adhesion site (***van Kooyk and Figdor, 2000***; ***Roca-Cusachs et al., 2009***), while catch bonds are receptor–ligand bonds whose lifetime increases with mechanical force (***Kong et al., 2009***; ***Chen et al., 2010***; ***Kong et al., 2013***). Both mechanisms extend the duration and increase the strength of integrin-mediated adhesion and signaling (also called outside-in signaling) (***Koo et al., 2002***; ***van Kooyk and Figdor, 2000***; ***Maheshwari et al., 2000***; ***Roca-Cusachs et al., 2009***; ***Coussen et al., 2002***), and depend on the association of integrins with the actin cytoskeleton via talin (***Roca-Cusachs et al., 2009***; ***Friedland et al., 2009***), and probably kindlin (***Ye et al., 2013***).

The talin family consists of two (talin-1 and -2) and the kindlin family of three isoforms (kindlin-1-3), which show tissue-specific expression patterns (***Calderwood et al., 2013***; ***Moser et al., 2009***; ***Shattil et al., 2010***). The majority of studies that defined integrin affinity regulation by talin and kindlin were performed on αIIbβ3 and β2-class integrins expressed by platelets and leukocytes, respectively. These cells circulate in the blood and hold their integrins in an inactive state until they encounter soluble or membrane-bound agonists (***Evans et al., 2009***, ***Bennett, 2005***). The prevailing view is that agonist-induced signaling pathways activate talin-1 and the hematopoietic cell-specific kindlin-3, which cooperate to induce integrin activation (***Moser et al., 2008***; ***Han et al., 2006***) and clustering (***Cluzel et al., 2005***; ***Ye et al., 2013***).

Integrin affinity regulation in non-hematopoietic cells such as fibroblasts and epithelial cells is poorly understood. It is not known how integrin activation is induced on these cells (no integrin-activating agonists have been identified) and it is also controversial whether talin and kindlin are required to shift their integrins into the high affinity state. While there are reports showing that talin and kindlin are required for integrin activation in epithelial cells (***Montanez et al., 2008***; ***Margadant et al., 2012***), it was also shown that in myoblasts and mammary epithelial cells activation of β1 integrins, adhesion and spreading on multiple ECM substrates can proceed in the absence of talin (***Conti et al., 2009***; ***Wang et al., 2011***). Likewise, it was reported that focal adhesion

kinase (FAK)-deficient fibroblasts develop small, nascent adhesions (NAs) at the edge of membrane protrusions without visible talin and that integrins carrying a mutation in the talin-binding site can still nucleate and stabilize NAs (**Lawson et al., 2012**). Also fibroblasts lacking talin-1 and -2 were shown to adhere to fibronectin (FN) and initiate isotropic spreading (**Zhang et al., 2008**). Another intriguing study demonstrated that overexpression of kindlin-2 in Chinese hamster ovary (CHO) cells inhibits rather than promotes talin head-induced α5β1 integrin activation (**Harburger et al., 2009**). Given the fundamental importance of talin and kindlin for integrin activation in hematopoietic cells, the findings of these studies are unexpected and imply that either integrin affinity regulation is substantially different in fibroblasts and epithelial cells or the experimental approaches used to manipulate protein expression and localization were imperfect.

To directly evaluate the functions of talin and kindlins for FN-binding integrins on fibroblasts, we used a genetic approach and derived fibroblasts from mice lacking either the *Tln1* and *-2* or the *Fermt1* and *-2* genes. We show that integrin affinity regulation depends on both talin and kindlin, and that kindlin has the additional function of triggering cell spreading by binding directly to paxillin in a talin-independent manner.

Results

Kindlins and talins control cell morphology, adhesion and integrin expression

To obtain cells lacking the expression of talin-1 and kindlin-2, we intercrossed mice carrying *loxP* flanked (floxed; fl) *Tln1* or *Fermt2* alleles (**Figure 1A**), isolated kidney fibroblasts and immortalized them with the SV40 large T antigen (parental fibroblasts). The floxed alleles were deleted by adenoviral *Cre* recombinase transduction resulting in $T1^{Ko}$ and $K2^{Ko}$ fibroblasts. Loss of talin-1 or kindlin-2 expression in fibroblasts was compensated by talin-2 or the de novo expression of kindlin-1, respectively, allowing adhesion and spreading, although to a lesser extent compared with control cells (**Figure 1—figure supplement 1A,B**). To prevent this compensation, we generated mice with floxed *Tln1* and nullizygous *Tln2* alleles or with floxed *Fermt1* and *-2* alleles (Tln^{Ctr}; $Kind^{Ctr}$) from which we isolated, immortalized and cloned kidney fibroblasts with comparable integrin surface levels (**Figure 1A** and **Figure 1—figure supplement 2**). The floxed alleles were deleted by transducing *Cre* resulting in talin-1, -2 (Tln^{Ko}) and kindlin-1, -2 ($Kind^{Ko}$) deficient cells, respectively (**Figure 1A–C**). Since the Tln^{Ctr} and $Kind^{Ctr}$ control cells showed similar morphologies and behaviour in our experiments, we display one control cell line in several result panels. *Cre*-mediated deletion of the floxed *Tln1* or floxed *Fermt1/2* genes was efficient (**Figure 1B**) and resulted in cell rounding, weak adhesion of a few cells, and reduced cell proliferation despite the immortalisation with the oncogenic large T antigen (**Figure 1C** and **Figure 1—figure supplement 3**). To minimize cell passage-induced abnormalities, we used cells only up to 12 passages after *Cre*-mediated gene deletions.

To define the adhesion defect, we performed plate and wash assays for 30 min on defined substrates and found that neither Tln^{Ko} nor $Kind^{Ko}$ cells adhered to FN, laminin-111 (LN), type I collagen (COL) and vitronectin (VN) (**Figure 1D**). To test whether the inability of Tln^{Ko} and $Kind^{Ko}$ cells to adhere to ECM proteins is due to an integrin activation defect, we bypassed inside-out activation by treating cells with Mn^{2+}, which binds to the integrin ectodomain and induces unbending and unclasping of integrin heterodimers (**Mould et al., 1995**). Treatment with Mn^{2+} induced partial adhesion of Tln^{Ko} and $Kind^{Ko}$ cells to FN, while partial adhesion to LN and VN was only induced in Tln^{Ko} cells (**Figure 1D**). Time course experiments revealed that Mn^{2+}-induced adhesion of Tln^{Ko} and $Kind^{Ko}$ cells to FN was already significantly lower 2.5 min after plating and remained significantly lower compared with control cells (**Figure 1E**), suggesting that talin and kindlin cooperate to initiate and maintain normal Mn^{2+}-induced adhesion to FN. In line with these findings, dose-response profiles showed that Tln^{Ko} and $Kind^{Ko}$ cells have severe adhesion defects at low (1.25 μg ml^{-1}) as well as high (20 μg ml^{-1}) substrate concentrations (**Figure 1—figure supplement 4**).

These findings indicate that talin and kindlin promote integrin-mediated adhesion to FN and proliferation, and that the integrin-activating compound Mn^{2+} can only partially substitute for the adhesion promoting roles that talin and kindlin accomplish together.

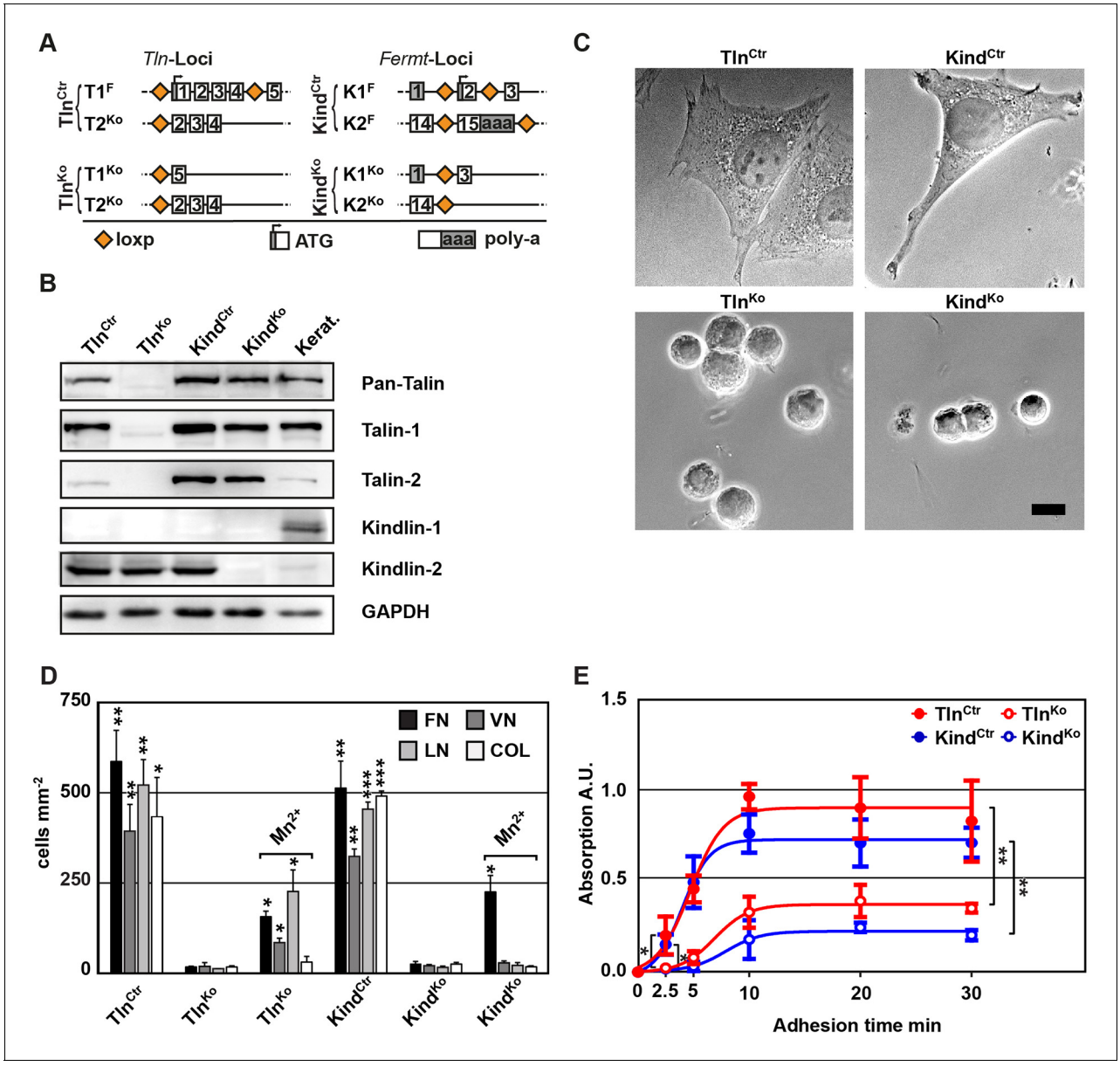

Figure 1. Kindlin and talin are required for integrin-mediated cell adhesion. (**A**) Scheme showing gene loci before and after ablation of the *Tln1, -2* and *Fermt1, -2* genes. Orange diamonds indicate *loxP* sites and rectangles exons; untranslated regions are marked grey. (**B**) Western blot of Tln^{Ko} and $Kind^{Ko}$ cells. Keratinocyte lysates (Kerat.) served to control kindlin-1 expression. (**C**) Bright field images of Tln^{Ctr}, $Kind^{Ctr}$, Tln^{Ko} and $Kind^{Ko}$ cells. (**D**) Quantification of cell adhesion on indicated substrates 30 min after seeding by counting DAPI stained cells; n=3 independent experiments, error bars indicate standard error of the mean; t-test significances are calculated between untreated Tln^{Ko} or $Kind^{Ko}$ cells and the corresponding Tln^{Ctr} and $Kind^{Ctr}$ or Mn^{2+}-treated Tln^{Ko} or $Kind^{Ko}$ cell lines on same substrates; only significant differences are shown. (**E**) Quantification of Mn^{2+}-stimulated cell adhesion for indicated times on FN; cells were quantified by absorbance measurement of crystal violet staining; n=3 independent experiments; lines represent sigmoidal curve fit; error bars indicate standard deviation; significances for indicated pairs after 2.5 min were calculated by two-tailed t-test and significances for indicated pairs of the overall kinetics were calculated by two-way RM ANOVA. Bar, 10 µm. COL, collagen; DAPI, 4',6-diamidino-2-phenylindole; FN, fibronectin; GAPDH, glyceraldehyde-3-phosphate dehydrogenase; LN, laminin-111; RM ANOVA, repeated measures analysis of variance; VN, vitronectin.

DOI: 10.7554/eLife.10130.003

The following figure supplements are available for figure 1:

Figure supplement 1. Talin-1- and kindlin-2-deficient fibroblasts.

DOI: 10.7554/eLife.10130.004

Figure supplement 2. Integrin expression profiles of Tln^{Ctr} and $Kind^{Ctr}$ cells.

DOI: 10.7554/eLife.10130.005

Figure 1 continued on next page

Figure 1 continued

Figure supplement 3. Cell proliferation of Tln^{Ko} and $Kind^{Ko}$ cells.

DOI: 10.7554/eLife.10130.006

Figure supplement 4. Cell adhesion of Tln^{Ko} and $Kind^{Ko}$ cells on different FN concentrations.

DOI: 10.7554/eLife.10130.007

Integrin activation and binding to FN requires talin and kindlin-2

The inability of Mn^{2+} to fully rescue the adhesion defect of Tln^{Ko} and $Kind^{Ko}$ cells raised the question whether integrin surface levels change after deletion of the *Tln1/2* and *Fermt1/2* genes. We quantified integrin surface levels by flow cytometry and found that the levels of β1 and β3 were significantly reduced in $Kind^{Ko}$ and unaffected in Tln^{Ko} cells (***Figure 2A*** and ***Figure 2—figure supplement 1***). The levels of α2 and α3 integrin were reduced in both cell lines, α6 was elevated in Tln^{Ko} and decreased in $Kind^{Ko}$ cells, and the α3 levels were significantly more decreased in $Kind^{Ko}$ than in Tln^{Ko} cells (***Figure 2A***) explaining the absent adhesion of both cell lines to COL and their differential adhesion behaviour on LN (***Figure 1D***). The β5 levels were similarly up-regulated in $Kind^{Ko}$ and Tln^{Ko} cells, and the α5 and αv integrin levels were slightly reduced but not significantly different between Tln^{Ko} and $Kind^{Ko}$ cells (***Figure 2A***). The differential adhesion of Mn^{2+}-treated Tln^{Ko} and $Kind^{Ko}$ cells to VN (***Figure 1D***), despite similar surface levels of αv integrins, points to particularly important role(s) for kindlin-2 in αv integrins-VN adhesion and signaling (***Liao et al., 2015***). Serendipitously, the reduced expression of β1-associating α2, α3 and α6 subunits in $Kind^{Ko}$ cells, which impairs adhesion to LN and COL enables α5 to associate with the remaining β1 subunits and leads to comparable α5β1 levels on Tln^{Ko} and $Kind^{Ko}$ cells (***Figure 2—figure supplement 2***) explaining their similar adhesion to FN (***Figure 1D,E*** and ***Figure 1—figure supplement 4***). Therefore, we performed all further experiments with FN.

Since we excluded different surface levels of FN-binding integrins as a cause for the severely compromised adhesion of Tln^{Ko} and $Kind^{Ko}$ cells to FN, we tested whether talin and kindlin are required to activate FN-binding α5β1 integrins. To directly assess integrin activation, we made use of an antibody against the 9EG7 epitope, which specifically recognizes Mn^{2+} and/or ligand activated β1 integrins (***Bazzoni et al., 1995***). The amount of 9EG7 epitope exposure relative to total β1 integrin exposure corresponds to the integrin activation index, which can be measured by flow cytometry using 9EG7 and anti-total β1 integrin antibodies. These measurements revealed that Tln^{Ctr} and $Kind^{Ctr}$ cells bound 9EG7 antibodies, while Tln^{Ko} and $Kind^{Ko}$ cells lacked 9EG7 binding in the absence of Mn^{2+} (***Figure 2—figure supplement 3A***). Mn^{2+} treatment significantly increased 9EG7 binding by Tln^{Ctr} and $Kind^{Ctr}$ cells, which was further elevated in the presence of FN-Arg-Gly-Asp (RGD) ligand known to stabilize the high affinity state of integrins (***Figure 2—figure supplement 3A***). Mn^{2+}-treated Tln^{Ko} and $Kind^{Ko}$ cells bound significantly less 9EG7 antibodies than control cells, which marginally increased with FN-RGD (***Figure 2—figure supplement 3A***). Moreover, the normalization of the 9EG7 binding to the total β1 integrin surface levels also indicated a significantly lower influence of Mn^{2+} and FN-RGD on the integrin activation index of $Kind^{Ko}$ as compared to Tln^{Ko} cells (***Figure 2—figure supplement 3A***). These findings confirm that both, talin and kindlin are required for β1 integrin activation and to stabilize Mn^{2+}-induced unbending/unclasping of α5β1 integrins.

Our findings so far suggest that talin and kindlin are required to activate FN-binding integrins and maintain Mn^{2+}-induced activation of FN-binding integrins. To further analyze whether ligand-induced stabilisation of high-affinity integrin conformations (also termed 'ligand-induced integrin activation; ***Du et al., 1991***) can form in the absence of talin or kindlin, we used atomic force microscopy (AFM)-based single cell force spectroscopy (SCFS). We attached control, Tln^{Ko} or $Kind^{Ko}$ cells to Concanavalin A (ConA)-coated cantilevers, allowed the cells to contact surfaces coated with either wild type $FN\text{-}III_{7\text{-}10}$ (FN-RGD) or an integrin-binding-deficient $FN\text{-}III_{7\text{-}10}$ fragment lacking the RGD binding motif (FN-ΔRGD) for increasing contact times, either in the absence or presence of Mn^{2+} and then detached them from the substrate by lifting the cantilever (***Figure 2B,C***). In the absence of Mn^{2+} Tln^{Ctr} and $Kind^{Ctr}$ cells developed significant adhesion to FN-RGD within 5 s contact time. After a contact time of 20 s around 2 nN force was required to disrupt adhesion to FN-RGD, and after 50 and 120 s, respectively, 3 and 6 nN were required (***Figure 2B***). Tln^{Ko} and $Kind^{Ko}$ cells failed to develop measurable adhesions to FN-RGD after contact times of 5, 20, 50 and 120 s (***Figure 2B***). Treatment with Mn^{2+} induced a slight and similar increase of force required to disrupt adhesion of

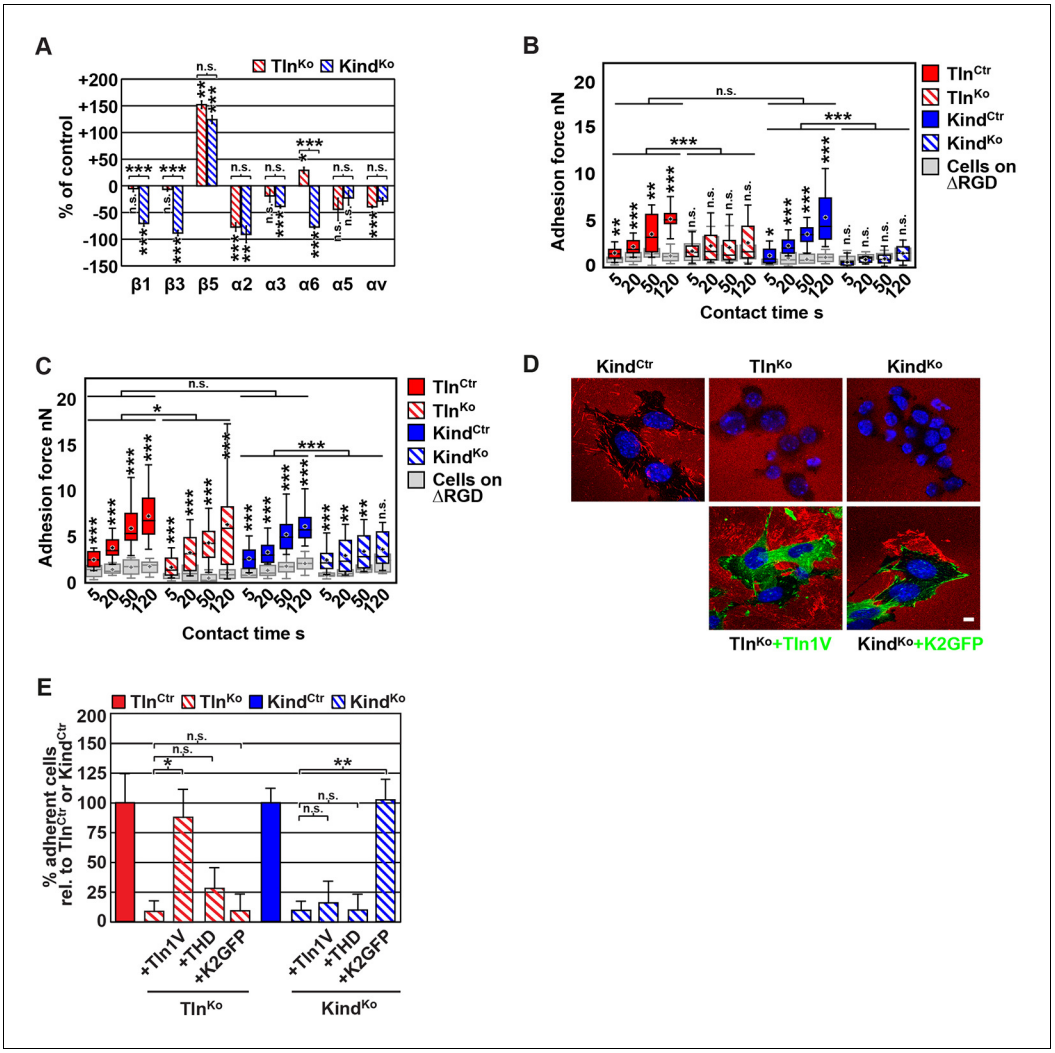

Figure 2. FN binding by Tln^{Ko} and $Kind^{Ko}$ cells. (**A**) Quantification of integrin surface expression levels relative to the Tln^{Ctr} and $Kind^{Ctr}$ cell lines; independent experiments: n=10 for β1; n=4 for β3, α5, αv; n=3 for remaining integrin subunits; error bars indicate standard error of the mean; significances are calculated between Tln^{Ko} and $Kind^{Ko}$ cells indicated by brackets, or between Tln^{Ko} or $Kind^{Ko}$ cells and corresponding control cells indicated by the significances above or below bars. (**B**, **C**) Box plot representation of adhesion forces generated by cells interacting with surface immobilized FN fragments. Cells were immobilized on ConA-coated AFM cantilevers and pressed onto surfaces coated with the FN-RGD or integrin-binding deficient FN-ΔRGD fragments for varying contact times, either in the absence (**B**) or presence of Mn^{2+} (**C**). Coloured and grey boxplots represent adhesion forces from at least 10–15 independent experiments with single cells; + signs represent mean; the significance between adhesion on FN-RGD versus FN-ΔRGD is given on top of each boxplot and was calculated with a Mann–Whitney U test; brackets indicate two-way RM ANOVA comparisons of the whole adhesion kinetics. (**D**) FN staining after plating cells on a FN-coated dish for 24 hr. (**E**) Quantification of cell adhesion on FN 30 min after seeding; values are normalized to Tln^{Ctr} and $Kind^{Ctr}$; n=3 independent experiments; error bars indicate standard error of the mean. Bar, 10 μm. AFM, atomic force microscopy; ConA, Concanavalin A; FN, fibronectin; K2GFP, green fluorescent protein-tagged kindlin-2; RGD, Arg-Gly-Asp; RM ANOVA, repeated measures analysis of variance; THD, talin-1 head domain; Tln1V, Venus-tagged full length talin-1.

DOI: 10.7554/eLife.10130.008

The following figure supplements are available for figure 2:

Figure supplement 1. Integrin expression profiles of Tln^{Ctr}, Tln^{Ko}, $Kind^{Ctr}$ and $Kind^{Ko}$ cells.

DOI: 10.7554/eLife.10130.009

Figure supplement 2. Tln^{Ko} and $Kind^{Ko}$ cells display comparable $\alpha 5\beta 1$ integrin cell surface levels.

DOI: 10.7554/eLife.10130.010

Figure supplement 3. $\beta 1$ i ntegrin activation in Tln^{Ctr}, Tln^{Ko}, $Kind^{Ctr}$, $Kind^{Ko}$ cells.

DOI: 10.7554/eLife.10130.011

Figure supplement 4. Re-expression of talin-1 or kindlin-2 in Tln^{Ko} and $Kind^{Ko}$ cells.

DOI: 10.7554/eLife.10130.012

control, Tln^{Ko} and $Kind^{Ko}$ cells to FN-RGD after 5 s contact time (***Figure 2C***). However, with increasing contact times, the AFM profiles of Tln^{Ko} and $Kind^{Ko}$ cells differ in the presence of Mn^{2+}. While the adhesion force increased concomitantly with longer contact times in Tln^{Ctr}, $Kind^{Ctr}$ and Tln^{Ko} cells, adhesion forces of $Kind^{Ko}$ cells plateaued after 50 s and showed no further increase towards 120 s contact time. The latter finding suggests that kindlin stabilizes integrin–ligand complexes with time, by inducing integrin clustering and/or by modulating the off-rate of integrin ligand bonds, for example, through associating with the integrin-linked kinase (ILK)-Pinch-Parvin (IPP) complex that links kindlin to the F-actin cytoskeleton (***Cluzel et al., 2005***; ***Ye et al., 2013***; ***Montanez et al., 2008***; ***Fukuda et al., 2014***).

We next tested whether their impaired integrin function affects the assembly of FN into fibrils, which requires association of active α5β1 integrin with the actin cytoskeleton (***Pankov et al., 2000***), and whether re-expression of talin and kindlin reverts the defects of Tln^{Ko} and $Kind^{Ko}$ cells. While neither Tln^{Ko} nor $Kind^{Ko}$ cells were able to assemble FN fibrils, re-expression of full-length Venus-tagged talin-1 (Tln1V) in Tln^{Ko} or GFP-tagged kindlin-2 (K2GFP) in $Kind^{Ko}$ cells (***Figure 2—figure supplement 4***) rescued FN fibril assembly and adhesion to FN (***Figure 2D,E***). Furthermore, neither overexpression of the talin-1 head (THD) nor K2GFP in Tln^{Ko} cells, nor Tln1V or THD in $Kind^{Ko}$ cells rescued adhesion to FN or 9EG7 binding (***Figure 2E*** and ***Figure 2—figure supplement 3B***).

Altogether, our results demonstrate that both talin and kindlin are required (1) for ligand-induced stabilisation of integrin-ligand complexes, (2) to stabilize Mn^{2+}-activated α5β1 integrins, and (3) to induce integrin-mediated FN fibril formation.

Tln^{Ko} cells initiate spreading and assemble β1 integrins at protruding membranes

It has been reported that a significant number of talin-2 small interfering RNA (siRNA)-expressing talin-$1^{-/-}$ fibroblasts adhere to FN and initiate isotropic cells spreading (***Zhang et al., 2008***). To test whether spreading can also be induced in adherent Tln^{Ko} and $Kind^{Ko}$ cells, we bypassed their adhesion defect with Mn^{2+}, seeded them for 30 min on FN and stained with an antibody against total β1 integrin and the β1 integrin activation epitope-reporting 9EG7 antibody. As expected, Tln^{Ctr} or $Kind^{Ctr}$ cells clustered 9EG7-positive β1 integrins in NAs and focal adhesions (FAs), whose frequency and size increased upon Mn^{2+} treatment (***Figure 3A,B***). In contrast, the sporadic and very weakly adherent Tln^{Ko} and $Kind^{Ko}$ cells were small, round and formed small and finely dispersed β1 integrin aggregates over the entire cell (***Figure 3A***) and lacked 9EG7-positive signals (***Figure 3B***) in the absence of Mn^{2+} treatment. Upon Mn^{2+} treatment 37 ± 1% (n=684, mean ± standard deviation of three independent experiments) of the Tln^{Ko} cells showed isotropic membrane protrusions (circumferential lamellipodia) with small, dot-like aggregates of β1 integrin, kindlin-2, paxillin and ILK at the membrane periphery (***Figure 3A*** and ***Figure 3—figure supplement 1***), which eventually detached from the substrate leading to the collapse of the protruded membrane (***Video 1***). Furthermore, 9EG7-positive β1 integrins accumulated along the lamellipodial edge and beneath the nucleus of Tln^{Ko} cells (***Figure 3B***). The remaining cells were spheroid, with half of them showing short, finger-like protrusions, which were motile due to their poor anchorage to the substrate. In the case of $Kind^{Ko}$ cells, we analysed 652 cells in three independent experiments and found that only 7 ± 1% (mean ± standard deviation) of the cells established lamellipodia, which formed around the entire circumference in 2 ± 0.4% (mean ± standard deviation) of the cells. Around 93 ± 1% of the $Kind^{Ko}$ cells were spheroid (mean ± standard deviation) and frequently had finger-like, motile protrusions with small dot-like signals containing β1 integrin and talin but rarely paxillin or ILK (***Figure 3A*** and ***Figure 3—figure supplement 1***). Importantly, re-expression of Tln1V in Tln^{Ko} cells or K2GFP in $Kind^{Ko}$ cells normalized FA formation and spreading on FN (***Figure 3—figure supplement 2***). These findings indicate that kindlin-2 expressing Tln^{Ko} cells can initiate the formation of large lamellipodia and assemble β1 integrins in lamellipodial edges.

To further characterize the distribution of β1 integrins in the lamellipodial edges of Tln^{Ko} cells, we visualized them by combining direct stochastic optical reconstruction microscopy (dSTORM) and total internal reflection fluorescence microscopy (TIRFM). Mn^{2+}-treated and non-permeablized cells were seeded on FN, stained with anti-total β1 integrin antibodies, and then permeabilized, immunostained for paxillin and imaged with normal resolution TIRFM and dSTORM (***Figure 3C***). Each localization detected by dSTORM was plotted as a Gaussian distribution around its centre with an average spatial accuracy of ~20 nm (resolution limit of dSTORM imaging). Since two or more

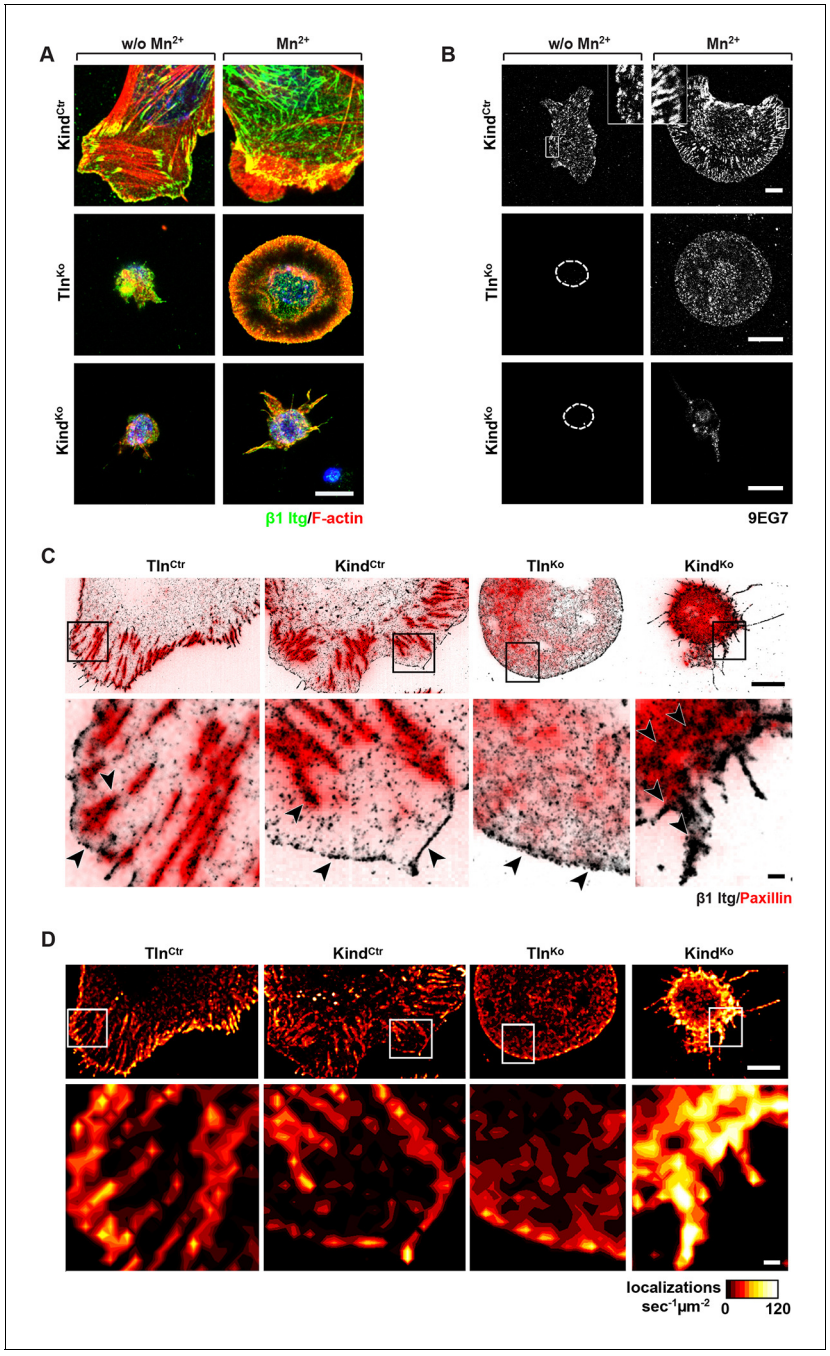

Figure 3. Integrin distribution in Tln^{Ko} and $Kind^{Ko}$ cells. (**A**) Confocal images of the ventral side of adherent cells stained for β1 integrin and F-actin in the absence or presence of Mn^{2+} stimulation. Notice the increase in the spreading area (w/o Mn^{2+}: 1696 ± 360 μm^2, Mn^{2+}: 2676 ± 466 μm^2) and in the average size (w/o Mn^{2+}: 0.64 ± 0.1 μm^2, Mn^{2+}: 0.89 ± 0.1 μm^2) and number (w/o Mn^{2+}: 105 ± 38, Mn^{2+}: 246 ± 8) of focal adhesions in $Kind^{Ctr}$ cells after Mn^{2+} stimulation and the increase of spreading area in the Tln^{Ko} (w/o Mn^{2+}: 77 ± 1 μm^2, Mn^{2+}: 572 ± 37 μm^2) and $Kind^{Ko}$ cells (w/o Mn^{2+}: 76 ± 27 μm^2, Mn^{2+}: 152 ± 8 μm^2) (n=3, mean ± standard deviation). (**B**) Confocal images from the ventral side of adherent cells stained for the 9EG7 epitope in the absence or presence of Mn^{2+} stimulation. (**C**) TIRF-dSTORM images of β1 integrin (grey scale image) obtained from immunostaining of non-permeabilized cells overlaid with anti-paxillin staining following permeabilization (red, normal resolution). Boxed areas are displayed in a five-fold magnification. (**D**) Images show heat map representations of dSTORM localizations per μm^2 and sec, indicative for integrin clustering defined by local integrin densities. The colour range indicates localizations s^{-1} μm^{-2} with low values shown in dark red colours and high densities from yellow to white colours. Bars, 10 µm (A,B); 5 µm (C,D); 500 nm (for the magnification in C,D). TIRF, total internal reflection fluourescence; dSTORM, direct stochastic optical reconstruction microscopy.

DOI: 10.7554/eLife.10130.014

The following figure supplements are available for figure 3:

Figure 3 continued on next page

Figure 3 continued

Figure supplement 1. Localization of FAs proteins in Mn^{2+}-treated $Kind^{Ctr}$, Tln^{Ko} and $Kind^{Ko}$ cells.
DOI: 10.7554/eLife.10130.015

Figure supplement 2. Rescue of FA formation and spreading after expression of Tln1V in Tln^{Ko} cells or K2GFP in $Kind^{Ko}$ cells.
DOI: 10.7554/eLife.10130.016

Figure supplement 3. Distribution of $\beta 1$ integrins in spheroid-shaped Tln^{Ko} cells.
DOI: 10.7554/eLife.10130.017

localizations from single or multiple dyes in close proximity cannot be distinguished, the number of localizations does not directly reflect integrin numbers. However, all antibody molecules display the same average behaviour with respect to the number of localizations per second in all areas of the cell. This allowed to average the number of localizations per second and μm^2 and to plot them in a heat map representation (***Figure 3D***), which directly reflects the density of stained β1 integrin molecules and thus the degree of integrin clustering. The β1 integrin staining of Tln^{Ctr} and $Kind^{Ctr}$ cells revealed small round structures of ~50 nm diameter indicating clusters of integrins larger than the resolution limit (***Figure 3C***; high magnification; see arrowheads). Furthermore, high numbers of localizations were enriched in paxillin-positive FAs and in NAs at the lamellipodial edge (***Figure 3C***; see arrowheads). In these areas, we observed a high average density of 60–120 localizations s^{-1} μm^{-2}, while outside of the adhesion sites ~0–20 localizations s^{-1} μm^{-2} were detected, indicating a high degree of β1 integrin clustering within and a low degree of clustering outside of adhesion sites (***Figure 3D***). Tln^{Ko} cells with circumferential lamellipodia showed a high density of blinking with up to 100 localizations s^{-1} μm^{-2} at lamellipodial edges (***Figure 3C,D***; see arrowheads), which appeared less compact than in control cells. $Kind^{Ko}$ cells showed >120 localizations s^{-1} μm^{-2} in the periphery and finger-like membrane protrusions (***Figure 3C,D***; see arrowheads), which were also observed in Tln^{Ko} cells that adopted a spheroid rather than an isotropic spread shape (***Figure 3—figure supplement 3***). The exclusive presence of these large and entangled β1 integrin aggregates on Tln^{Ko} and $Kind^{Ko}$ cells with small, spheroid shapes and protrusions suggests that they were induced by spatial constraints rather than specific signaling.

These findings demonstrate that, in contrast to $Kind^{Ko}$ cells, Mn^{2+}-treated kindlin-2-expressing Tln^{Ko} cells induce circumferential membrane protrusions with β1 integrins at the protrusive edges.

Kindlin-2 binds and recruits paxillin to NAs

Our data so far indicate that the expression of kindlin-2 enables initial, isotropic spreading and the accumulation of integrins in lamellipodia of Mn^{2+}-treated Tln^{Ko} cells. To identify binding partner(s) of kindlin-2 that transduce this function to downstream effectors, we performed yeast-two-hybrid assays with kindlin-2 as bait using a human complementary DNA (cDNA) library containing all possible open reading frames and a human keratinocyte-derived cDNA library. Among the 124 cDNAs identified from both screenings, 17 coded for leupaxin and 11 for Hic-5. Immunoprecipitation of overexpressed green fluorescent protein (GFP)-tagged paxillin family members, paxillin, Hic-5 and leupaxin in HEK-293 cells with an anti-GFP antibody efficiently co-precipitated FLAG-tagged kindlin-2 (K2flag) (***Figure 4A***). Conversely, overexpressed GFP-tagged kindlin family members (kindlin-1, kindlin-2, kindlin-3) co-precipitated Cherry-paxillin (***Figure 4—figure supplement 1***). Since fibroblasts express high levels of paxillin (***Figure 4—figure supplement 2***), we performed all further interaction analysis with paxillin. Immunoprecipitations of GFP-tagged paxillin or kindlin-2 truncation mutants (***Figure 4—figure supplement 3A***) revealed that

Video 1. Spreading $Kind^{Ctr}$, Tln^{Ko} and $Kind^{Ko}$ cells on FN. Assembled time lapse movies of $Kind^{Ctr}$, Tln^{Ko} and $Kind^{Ko}$ cells. Cell spreading was recorded 5 min after seeding on FN. $Kind^{Ctr}$ cells were already well spread and only a minor size increase was observed over the following minutes. The Tln^{Ko} cells formed a circumferential lamellipodium that rapidly collapsed and subsequently the cells formed finger-like protrusions of varying size and failed to reestablish a fully formed circular lamellipodium. The $Kind^{Ko}$ cells failed to form a lamellipodium and formed finger-like protrusions that were not always adherent. Bar, 10 μm. FN, fibronectin.
DOI: 10.7554/eLife.10130.013

the interaction between kindlin-2 and paxillin was dramatically reduced in the absence of the Lin-11, Isl-1 and Mec-3 (LIM)1-4, LIM2-4 or LIM3-4 domains of paxillin (***Figure 4B***), or the pleckstrin homology (PH) domain (K2ΔPHGFP; lacking amino acids 380-477) or the N-terminus of kindlin-2 including the F0, F1, and the N-terminal part of the F2 domains (K2NTGFP; terminating at the end of F1; spanning amino acids 1-229) (***Figure 4C***). As expected, the interaction between kindlin-2 and ILK (***Montanez et al., 2008***), which is mediated via a recently identified sequence in the linker domain between the end of the N-terminal F2 and the beginning of the PH domain (amino acids 353–357) (***Fukuda et al., 2014***; ***Huet-Calderwood et al., 2014***), was abolished by the K2NTGFP truncation but unaffected by the deletion of the PH domain (K2ΔPHGFP) or the deletion of the N-terminal F0 and F1 domains (K2CTGFP, spanning amino acids 244-680) (***Figure 4C***). Importantly, immunoprecipitation of $Kind^{Ctr}$ lysates with antibodies against paxillin co-precipitated kindlin-2 (***Figure 4D***), confirming interactions between the endogenous proteins. Pull down experiments with recombinant full-length paxillin or paxillin-LIM3 domain and recombinant kindlin-2 demonstrated that binding to LIM3 and full-length paxillin is direct, Zn^{2+}-dependent and abrogated with ethylenediaminetetraacetic acid (EDTA) (***Figure 4E*** and ***Figure 4—figure supplement 3B***). $Kind^{Ko}$ cells were transduced with K2GFP or K2ΔPHGFP expression constructs, seeded on FN for different times and stained for β1 integrin, paxillin and F-actin. The experiments revealed that the expression of K2GFP in $Kind^{Ko}$ cells rescued spreading and induced robust paxillin recruitment to β1 integrin-positive NAs (***Figure 4F, G***). In contrast, expression of K2ΔPHGFP failed to recruit paxillin to β1 integrin-positive adhesion sites at the rim of membrane protrusions (***Figure 4F,G***) and induce normal cell spreading (***Figure 4—figure supplement 4A***) despite proper, although weaker, localisation to β1 integrin-positive adhesion sites (***Figure 4—figure supplement 4B,C***). Interestingly, mature FAs in K2ΔPHGFP-expressing cells were prominent after 30 min and contained significant amounts of paxillin, indicating that paxillin is recruited to mature FAs in a kindlin-2-independent manner (***Figure 4F***).

These findings indicate that the PH domain of kindlin-2 directly binds the LIM3 domain of paxillin and recruits paxillin into NAs but not into mature FAs.

The kindlin-2/paxillin complex promotes FAK-mediated cell spreading

Our findings revealed that kindlin-2 is required to recruit paxillin to NAs. Paxillin in turn, was shown to bind, cluster and activate FAK in NAs, which leads to the recruitment of p130Cas, Crk and Dock followed by the activation of Rac1 and the induction of cell spreading, and, in concert with growth factor signals, to the activation of Akt-1 followed by the induction of cell proliferation and survival (***Schlaepfer et al., 2004***; ***Bouchard et al., 2007***; ***Zhang et al., 2014***; ***Brami-Cherrier et al., 2014***). We therefore hypothesized that the recruitment of paxillin and FAK by kindlin-2 triggers the isotropic spreading and expansion of Tln^{Ko} cells. To test this hypothesis, we seeded our cell lines on FN or poly-L-lysine (PLL) in the presence or absence of epidermal growth factor (EGF) and Mn^{2+}. We found that EGF induced similar phosphorylation of tyrosine-992 (Y992) of the epidermal growth factor receptor (pY992-EGFR) in control, Tln^{Ko} and $Kind^{Ko}$ cells. The phosphorylation of tyrosine-397 of FAK (pY379-FAK) in $Kind^{Ctr}$ cells was strongly induced after the adhesion of control cells on FN and was not further elevated after the addition of EGF and Mn^{2+} (***Figure 5A*** and ***Figure 5—figure supplement 1***). Tln^{Ko} cells also increased pY397-FAK as well as pY31-Pxn and pY118-Pxn levels upon adhesion to FN, however, significantly less compared to control cells (***Figure 5A*** and ***Figure 5—figure supplement 1A-C***). Furthermore, EGF and Mn^{2+} treatments further increased pY397-FAK levels in Tln^{Ko} cells and localized pY397-FAK to peripheral NA-like adhesions (***Figure 5A,B*** and ***Figure 5—figure supplement 1A-C***). In sharp contrast, $Kind^{Ko}$ cells seeded on FN or treated with EGF and Mn^{2+} failed to induce pY397-FAK, pY31-Pxn, pY118-Pxn (***Figure 5A*** and ***Figure 5—figure supplement 1A-C***) and localize pY397-FAK to peripheral membrane regions (***Figure 5B***). Importantly, re-expression of Talin1-Venus in Tln^{Ko} and Kindlin2-GFP and $Kind^{Ko}$ cells fully rescued these signaling defects (***Figure 5—figure supplement 1B,C***). Furthermore, stable expression of K2GFP in $Kind^{Ko}$ cells rescued pY397-FAK and pS473-Akt levels (***Figure 5C***) and co-precipitated paxillin and FAK with K2GFP (***Figure 5—figure supplement 2***). In contrast, stable expression of K2ΔPHGFP in $Kind^{Ko}$ cells failed to co-precipitate paxillin and FAK (***Figure 5—figure supplement 2***) and induce pY397-FAK and pS473-Akt (***Figure 5C***).

In line with previous reports showing that the paxillin/FAK complex can trigger the activation of p130Cas (***Zhang et al., 2014***) and, in cooperation with EGFR signaling, the activation of Akt (***Sulzmaier et al., 2014***, ***Deakin et al., 2012***), we observed Y410-p130Cas, pT308-Akt, S473-Akt and

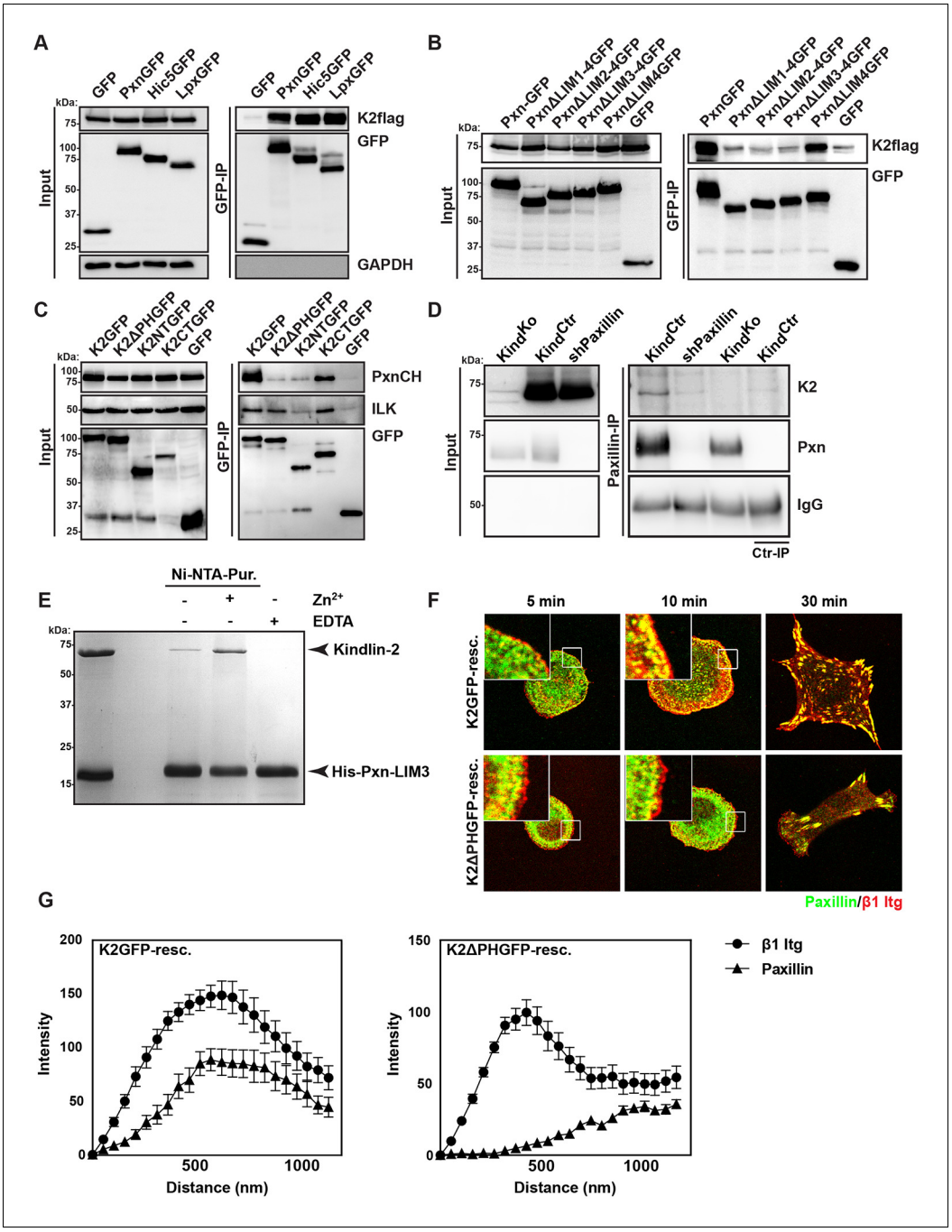

Figure 4. Kindlin binds and recruits paxillin to NAs. (**A**) GFP-IP of lysates from HEK 293T cells overexpressing GFP-tagged paxillin, Hic5 and leupaxin constructs (Pxn, paxillin; Hic5; Lpx, leupaxin) and K2flag reveal interaction of kindlin-2 with all three paxillin family members. (**B**) GFP-IP of lysates from HEK 293T cells overexpressing GFP-tagged paxillin truncation mutants and K2flag identifies the paxillin LIM3 domain as kindlin-2-binding domain. (**C**) GFP-IP of lysates from HEK 293T cells overexpressing GFP-tagged kindlin-2 truncation/deletion mutants and Cherry-tagged paxillin (PxnCH) identifies the kindlin-2 PH domain as paxillin binding domain. (**D**) Co-IP of endogenous paxillin and kindlin-2 from Kind^{Ctr} cells. (**E**) Purified His-tagged paxillin-LIM3 domain pulls down recombinant kindlin-2 in a Zn^{2+}-dependent manner. (**F**) K2GFP and K2ΔPHGFP expressing Kind^{Ko} cells seeded on FN for the indicated times and stained for paxillin and β1 integrin. (**G**) Fluorescence intensity line scans from K2GFP- (n=11 cells) and K2ΔPHGFP- (n=17 cells) expressing Kind^{Ko} cells cultured on FN for 10 min and stained for paxillin and β1 integrin; error bars indicate standard error of the mean. Bar, 10 μm. EDTA, ethylenediaminetetraacetic acid; FN, fibronection; GAPDH, glyceraldehyde-3-phosphate dehydrogenase; GFP, green fluorescent protein; ILK, integrin-linked kinase; IP, immunoprecipitation; K2GFP, green fluorescent protein-tagged kindlin-2; LIM, Lin-11, Isl-1 and Mec-3; NAs, nascent adhesions; PH, pleckstrin homology.

DOI: 10.7554/eLife.10130.018

Figure 4 continued on next page

Figure 4 continued

The following figure supplements are available for figure 4:

Figure supplement 1. Kindlin-1, -2 and -3 interact with paxillin.

DOI: 10.7554/eLife.10130.019

Figure supplement 2. Expression of paxillin family members in different cell lines.

DOI: 10.7554/eLife.10130.020

Figure supplement 3. Direct interaction between paxillin and kindlin-2.

DOI: 10.7554/eLife.10130.021

Figure supplement 4. K2ΔPHGFP fails to recruit paxillin to β1 integrin-positive adhesions in Kind^{Ko} cells.

DOI: 10.7554/eLife.10130.022

pT202/pY204 Erk1/2 phosphorylation after Mn^{2+} and/or EGF treatment of FN-seeded control and rescued cells, and to a slightly lesser extent Tln^{Ko} cells (***Figure 5D***, ***Figure 5— figure supplement 3A,B***). In contrast, FN-seeded Kind^{Ko} cells failed to activate p130Cas and showed reduced Akt and Erk1/2 phosphorylation in response to EGF (***Figure 5D***, ***Figure 5—figure supplement 3A,B***).

Finally, we tested whether the impaired activity of FAK contributed to the spreading defect of Kind^{Ko} cells by chemically inhibiting FAK activity in Tln^{Ko} cells or by overexpressing FAK in Kind^{Ko} cells (***Figure 5E–G***). The experiments revealed that inhibiting FAK reduced lamellipodia formation of Tln^{Ko} cells to an extent that was similar to untreated Kind^{Ko} cells (***Figure 5E***). Conversely, overexpression of FAKGFP in Kind^{Ko} cells resulted in high active FAK, increased lamellipodial formation and increased cell spreading in Tln^{Ko} and Kind^{Ko} cells (***Figure 5F,G*** and ***Figure 5—figure supplement 4A,B***).

Altogether, these findings show that the kindlin-2/paxillin complex in NAs recruits and activates FAK to induce cell spreading and increase the strength of Akt signaling.

Discussion

While the functions of talin and kindlin for integrin activation, adhesion and integrin-dependent signaling in hematopoietic cells are firmly established, their roles for these processes in non-hematopoietic cells are less clear. To clarify this issue, we established mouse fibroblast cell lines that lacked either talin-1/2 (Tln^{Ko}) or kindlin-1/2 (Kind^{Ko}) and tested whether they were able to activate integrins and mediate substrate adhesion and signaling. In line with previous reports (***Bottcher et al., 2012***; ***Margadant et al., 2012***), the deletion of *Tln1/2* or *Fermt1/2* genes changed the surface levels of laminin- and collagen-binding integrins. Since surface levels of α5 and αv integrins remained unchanged between Tln^{Ko} and Kind^{Ko} cells, we were able to establish the specific roles of talin and kindlin for the function of FN-binding integrins under identical conditions.

A major finding of our study demonstrates that integrin affinity regulation (activation) is essential for fibroblast adhesion and depends on both talin and kindlin-2 (***Figure 6A,D***). The unambiguity of this finding was unexpected in light of several reports showing that integrin activation and integrin-mediated adhesion still occurs in talin-depleted cells, or is inhibited when kindlin-2 is overexpressed (***Harburger et al., 2009***; ***Wang et al., 2011***; ***Lawson et al., 2012***). The previous studies that addressed the functional properties of talin used siRNA-mediated protein depletion, a combination of gene ablation and siRNA technology, or approaches to interfere with talin recruitment to NAs either by ablating the talin upstream protein FAK or by expressing an integrin that harbors a mutation in the talin binding site. Since the majority of approaches deplete rather than eliminate proteins from cells and adhesion sites, the respective cells were most likely recruiting sufficient residual protein to adhesion sites to allow integrin activation, cell adhesion and spreading, and the assembly of adhesion- and signaling-competent NAs. It is possible that not all integrin molecules have to be occupied by talin and therefore low levels of talin suffice, particularly in NAs that were shown by fluorescence correlation spectroscopy to contain only half the number of talin relative to α5β1 integrin and kindlin-2 molecules (***Bachir et al., 2014***). However, when the entire pool of talin is lost or decreased below certain thresholds (***Margadant et al., 2012***) integrins remain inactivate and consequently adhesion sites do not form. With respect to kindlin, it was reported that overexpressed kindlin-2 in CHO cells inhibits rather than promotes talin head domain-induced α5β1 integrin activation (***Harburger et al., 2009***). An integrin inhibiting effect of kindlin-2 is inconsistent with our study,

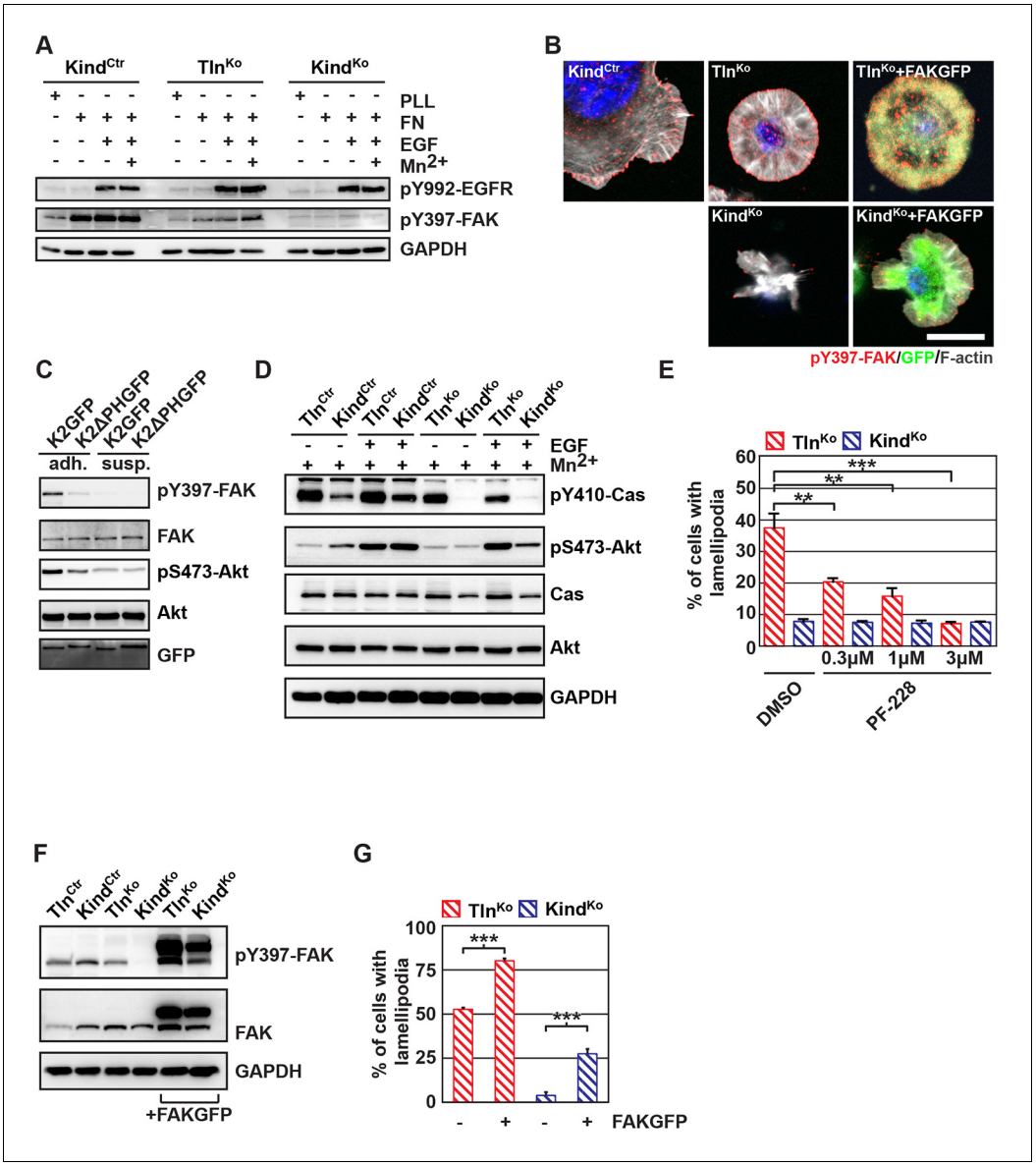

Figure 5. The kindlin/paxillin complex induces FAK signaling and cell spreading. (**A**) FAK and EGFR activation after seeding serum-starved Kind^{Ctr}, Tln^{Ko} and Kind^{Ko} cells on PLL or FN and treating them with or without EGF and Mn^{2+}. (**B**) Immunofluorescence staining of activated (Tyr-397 phosphorylated) FAK and F-actin in cells seeded on FN and treated with Mn^{2+} for 30 min (FAKGFP indicates exogenous expression of FAKGFP fusion protein). (**C**) FAK and Akt activation in Kind^{Ko} cells stably transduced with K2GFP or K2ΔPHGFP either seeded on FN or kept in suspension. GFP indicates similar expression of transduced GFP-tagged constructs. GAPDH levels served to control loading. (**D**) Levels of phosphorylated signaling mediators downstream of FAK in Mn^{2+}-treated, serum-starved or EGF-treated Kind^{Ctr}, Tln^{Ko} and Kind^{Ko} cells. GAPDH levels served to control loading. (**E**) Quantification of lamellipodia formation of FN-seeded Tln^{Ko} and Kind^{Ko} cells treated with Mn^{2+} and either DMSO or the FAK inhibitor PF-228 (n=3 independent repeats; >100 cells/condition; error bars indicate standard error of the mean; significances are given in comparison to the DMSO control). (**F**) FAK activity in Tln^{Ko} and Kind^{Ko} cells stably transduced with FAKGFP (n=3 independent experiments). (**G**) Quantification of lamellipodia formation in Tln^{Ko} and Kind^{Ko} cells stably transduced with FAKGFP (n=3 independent experiments; significances are given in comparison to untreated control; error bars indicate standard error of the mean). Bar, 10 μm. DMSO, dimethyl sulfoxide; EGF, epidermal growth factor; EGFR, epidermal growth factor receptor; FAK, focal adhesion kinase; FAKGFP, green fluorescent protein-tagged FAK; FN, fibronectin; GAPDH, glyceraldehyde-3-phosphate dehydrogenase; GFP, green fluorescent protein; PLL, poly-L-lysine.

DOI: 10.7554/eLife.10130.023

The following figure supplements are available for figure 5:

Figure supplement 1. FAK phosphorylation in Tln^{Ctr}, Tln^{Ko}, Tln^{Ko+T1V}, Kind^{Ctr}, Kind^{Ko} and Kind$^{Ko+K2GFP}$ cells.

DOI: 10.7554/eLife.10130.024

Figure supplement 2. Kindlin-2 forms a ternary complex with paxillin and FAK.

Figure 5 continued on next page

Figure 5 continued

DOI: 10.7554/eLife.10130.025

Figure supplement 3. Activity of signaling mediators downstream of FAK in Tln^{Ctr}, Tln^{Ko}, Tln^{Ko+T1V}, $Kind^{Ctr}$, $Kind^{Ko}$ and $Kind^{Ko+K2GFP}$ cells.

DOI: 10.7554/eLife.10130.026

Figure supplement 4. Cell spreading of FAK overexpressing Tln^{Ko} and $Kind^{Ko}$ cells.

DOI: 10.7554/eLife.10130.027

which identified a crucial role for kindlin in integrin activation, as well as with other studies also demonstrating that kindlin-2 promotes integrin functions (***Montanez et al., 2008***). It could well be that the reported inhibition of α5β1 by kindlin-2 represents an artifact that arose from protein overexpression.

Integrin activation can be induced with Mn^{2+}, whose binding to the ectodomain of β subunits directly shifts integrins into the high affinity state without the requirement for inside-out signals (***Mould et al., 1995***). We observed that Mn^{2+}-treated Tln^{Ko} and $Kind^{Ko}$ cells expressed the activation-dependent epitope 9EG7 and adhered to FN, albeit at significantly lower levels and efficiencies than the normal parental or rescued cells (***Figure 6B,C***). This observation strongly indicates that talin and kindlin also cooperate to maintain the extended and unclasped conformation of active integrins. Although it is not known how talin and kindlin keep integrins in an active state, it is possible that they stabilize this conformation by linking the unclasped β integrin cytoplasmic domain to the plasma membrane and/or to cortical actin, which may firmly hold separated integrin α/β subunits apart from each other. The expression of mutant talins and kindlins in our cells should allow us to examine these possibilities in future.

Finally, our study also revealed that Mn^{2+}-treated Tln^{Ko} cells began to form large, circumferential lamellipodia that eventually detached from FN, leading to the collapse of the protruded membrane. This initial isotropic spreading was significantly less frequent in $Kind^{Ko}$ cells, and has also been observed in talin-2-depleted talin-$1^{-/-}$ cells on FN, although these cells did not require Mn^{2+} for inducing spreading, which is likely due to the presence of residual talin-2 that escaped siRNA-mediated depletion (***Zhang et al., 2008***; ***Zhang et al., 2014***). These findings strongly suggest that integrin binding to FN enables kindlin-2 in Tln^{Ko} cells to cluster β1 integrins (as shown for αIIbβ3 by kindlin-3 in ***Ye et al., 2013***) and to trigger a signaling process that initiates spreading.

To find a mechanistic explanation for the kindlin-2-mediated cell spreading, we used the yeast-two-hybrid technology to identify paxillin as a novel and direct binding partner of kindlin-2. The interaction of the two proteins occurs through the LIM3 domain of paxillin, which was previously identified as integrin adhesion-targeting site (***Brown et al., 1996***), and the PH domain of kindlin-2. It is not unusual that PH domains fulfill dual roles by binding phospholipids and proteins, either simultaneously or consecutively (***Scheffzek and Welti, 2012***). The expression of a PH domain-deficient kindlin-2 in $Kind^{Ko}$ cells rescues adhesion to FN and FA maturation, however, significantly impairs spreading and plasma membrane protrusions. This finding together with the observations that paxillin-null fibroblasts and embryonic stem cells have defects in spreading, adhesion site remodeling and formation of lamellipodia (***Hagel et al., 2002***, ***Wade et al., 2002***) indicates that the kindlin-2/paxillin complex induces the elusive signaling process, leading to initial spreading of Tln^{Ko} and talin-depleted cells (***Zhang et al., 2008***). Indeed, the kindlin-2/paxillin complex in NAs recruits FAK (***Deramaudt et al., 2014***, ***Thwaites et al., 2014***; ***Choi et al., 2011***), which cooperates with growth factor receptors (such as EGFR) to induce signaling pathways that activate Erk and Akt to promote proliferation and survival, as well as Arp2/3 and Rac1 to induce actin polymerization and membrane protrusions (***Figure 6B,E***). Kindlin-2 also recruits ILK, which binds in the vicinity of the kindlin-2 PH domain and links integrins to actin and additional signaling pathways (***Figure 6E***). The short-lived nature of the initial spreading of Tln^{Ko} and talin-depleted (***Zhang et al., 2008***) cells shows that talin concludes the integrin-mediated adhesion process in NAs (***Figure 6F***) and induces the maturation of FAs. The formation of paxillin-positive FAs in cells expressing the PH domain-deficient kindlin-2 suggests that the recruitment of paxillin to FAs occurs either in a kindlin-independent manner or through a modification of kindlin in a second binding motif.

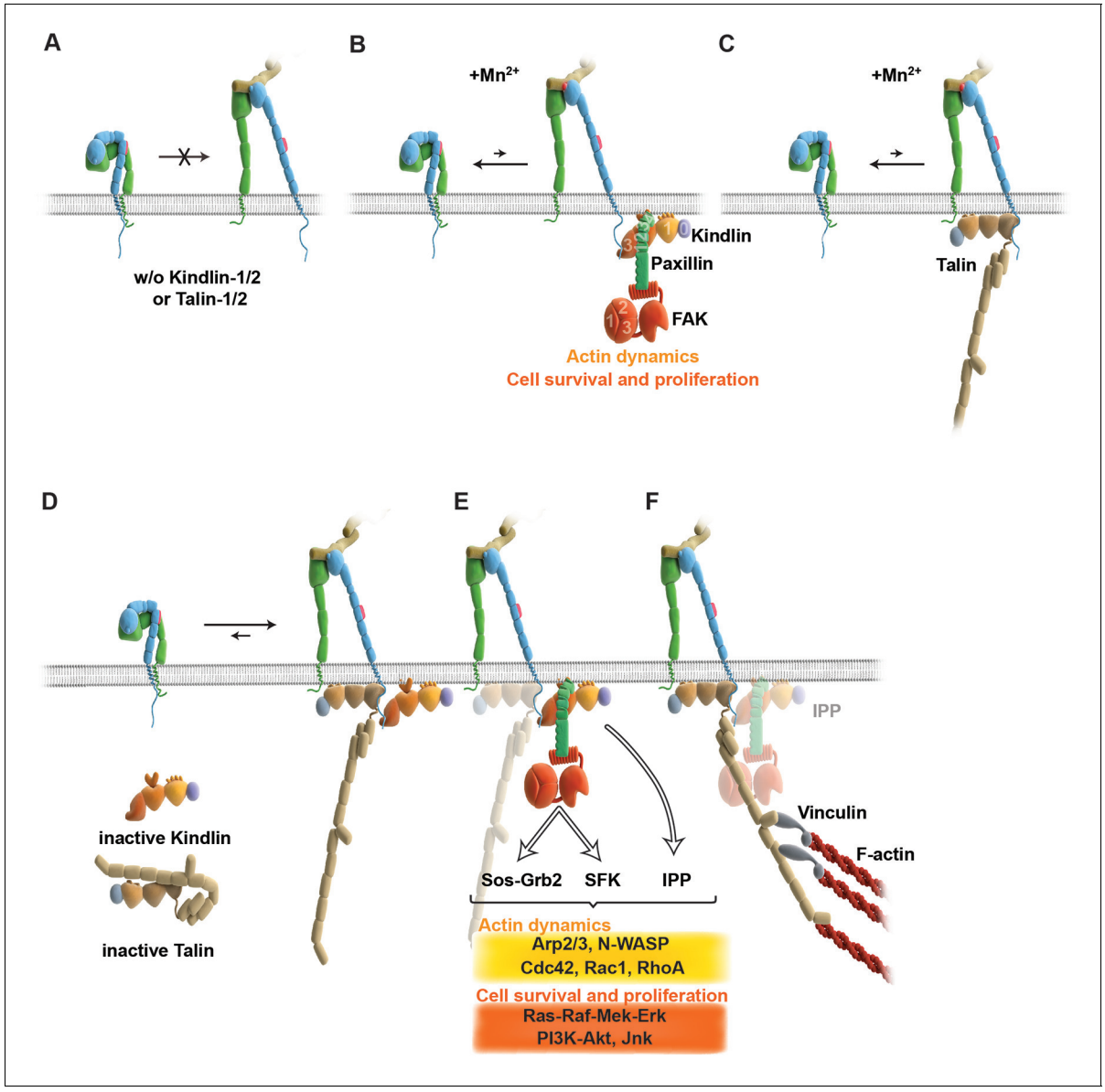

Figure 6. Model for the roles of talin and kindlin during inside-out and outside-in signaling of $\alpha 5\beta 1$ integrin. Integrin subunits are modelled according to ***Zhu et al. (2008)***, with the α5 subunit in green and the β1 subunit in blue showing the bent and clasped low affinity and the extended and unclasped high affinity conformations; the 9EG7 epitope is marked as red dot at the β1 leg and the FN ligand as beige dimers. (**A**) α5β1 integrin fails to shift from a bent to an extended/unclasped, high affinity state in the absence of talin-1/2 or kindlin-1/2; the bent/clasped conformation brings the EGF-2 domain of the β subunit in close contact with the calf domain of the α5 subunit and prevents exposure of the 9EG7 epitope. (**B**) In the absence of talin (Tln^{Ko}) and presence of Mn^{2+}, kindlin-2 allows adhesion by stabilizing the high affinity conformation of a low number of integrins and the direct binding of paxillin, leading to nucleation of integrins, recruitment of FAK, FAK-dependent signaling and lamellipodia formation. (**C**) In the absence of kindlins ($Kind^{Ko}$), talin stabilizes the high affinity conformation of a low number of integrins but does not enable paxillin recruitment and lamellipodia formation. (**D**) In normal fibroblasts, binding of kindlin and talin to the β1 tail is associated with the stabilisation of the unclasped α5β1 heterodimer and 9EG7 epitope exposure. (**E**) Kindlin recruits paxillin and FAK through the kindlin-PH domain and ILK/Pinch/Parvin (IPP; not shown) in a talin-independent manner and induces cell spreading, proliferation and survival. (**F**) The high affinity conformation of α5β1 integrin is stabilized by linkage of the β1 tail to the actin cytoskeleton through talin (and potentially the IPP complex; not shown). The arrow length indicates integrin conformations existing at equilibrium. EGF, epidermal growth factor; FAK, focal adhesion kinase; FN, fibronectin; ILK, integrin-linked kinase; IPP, integrin-linked kinase-Pinch-Parvin; SFK, src family kinases.

DOI: 10.7554/eLife.10130.028

Materials and methods

Mouse strains and cell lines and cell culture

The floxed kindlin-1 (*Fermt1*$^{flox/flox}$), floxed talin-1 (*Tln1*$^{flox/flox}$) and the constitutive talin-2-null (*Tln2*$^{-/-}$) mouse strains have been described (**Rognoni et al., 2014**; **Nieswandt et al., 2007**; **Conti et al., 2009**). The floxed kindlin-2 (*Fermt2*$^{flox/flox}$) mouse strain generated via recombinant recombination in embryonic stem cells (**Fassler and Meyer, 1995**) carries *loxP* sites flanking exon 15, which contains the stop codon and the polyadenylation signal of the murine *Fermt2* gene. Homologous recombination and germ line transmission were verified by Southern blots, and the *frt*-flanked neo cassette was removed with a transgenic mouse strain carrying a *deleter-flipase* gene. Floxed talin-1 and talin-2-null mice, and floxed kindlin-1 and kindlin-2 mice were intercrossed to generate *Tln1*$^{flox/flox}$ *Tln2*$^{-/-}$ and *Fermt1*$^{flox/flox}$ *Fermt2*$^{flox/flox}$ mice.

The cell lines used in this study are mouse fibroblasts derived from the kidneys of 21 d old mice, immortalized by retrovirally transducing the SV40 large T antigen, cloned (Tln^{Ctr} and Kind^{Ctr}) and finally infected with an adenovirus to transduce the *Cre* recombinase resulting in talin-null (Tln^{Ko}) and kindlin-null (Kind^{Ko}) cells. The parental cell lines were authenticated based on morphological criteria and the surface experession of specific integrins. All cells were cultured under standard cell culture conditions using Dulbecco's modified Eagle's medium (DMEM) supplemented with 8% fetal calf serum (FCS) and Penicillin/Streptomycin but not subjected to mycoplasma contamination testing.

Flow cytometry

Flow cytometry was carried out with a FACSCantoTMII cytometer (BD Biosciences, Franklin Lakes, NJ, USA) equipped with FACS DiVa software (BD Biosciences) using standard procedures. Data analysis was carried out with the FlowJo program (version 9.4.10). Fibroblasts were incubated with primary antibodies diluted in FACS-Tris buffered saline (FACS-TBS; 30 mM Tris, pH 7.4, 180 mM NaCl, 3.5 mM KCl, supplemented with 1 mM $CaCl_2$, 1 mM $MgCl_2$, 3% BSA, 0,02% NaN_3) for 1 hr on ice, washed twice with cold FACS-TBS and finally incubated with the secondary antibody for 45 min on ice.

Real-time polymerase chain reaction

Total RNA was extracted with the RNeasy Mini extraction kit (Qiagen, Germany) from cultured cells, cDNAs were prepared with an iScript cDNA Synthesis Kit (BioRad, Germany) and real-time polymerase chain reaction (PCR) was performed with an iCycler (BioRad). Each sample was measured in triplicate and values were normalized to *Gapdh*. Primer sequences for Lpxn and Pxn were from PrimerBank (**Spandidos et al., 2010**) (Lpxn: 26080416a1; aPxn: 114326500c2; bPxn: 22902122a1), GAPDH primers were described before (**Rognoni et al., 2014**) and Hic5 primers were newly designed (Hic5-fwd: 5′-ttcctttgcagcggttgttcc-3′; Hic5-rev: 5′-ggttacagaagccacatcgtggg-3′).

Antibodies and inhibitors

The following antibodies or molecular probes were used at indicated concentrations for western blot (WB), immunofluorescence (IF) or flow cytometry (FACS): kindlin-1 (home made), (**Ussar et al., 2008**) WB: 1:5000, IF: 1:1000; kindlin-2 (MAB2617 from Millipore, Germany) WB: 1:1000, IF: 1:500; talin (8D4 from Sigma, Germany) WB: 1:1000; talin (sc-7534 from Santa Cruz, Germany) IF: 1:500; talin-1 (ab57758 from Abcam, UK) WB: 1:2000; talin-2 (ab105458 from Abcam) WB: 1:2000; GAPDH (6C5 from Calbiochem, Billerica, MA, USA) WB: 1:10,000; Paxillin (610051 from BD Transduction Laboratories, Franklin Lakes, NJ, USA) WB: 1:1000, IF: 1:400; integrin β1-488 (102211 from Biolegend, San Diego, CA, USA) IF: 1:400, FACS: 1:200; integrin β1 (MAB1997 from Chemicon, Billerica, MA, USA) FACS: 1:400; integrin β1-647 (102213 from Biolegend) IF: 1:200; integrin β1 (home-made), (**Azimifar et al., 2012**) IF: 1:400; integrin β3-biotin (553345 from PharMingen, Franklin Lakes, NJ, USA) FACS: 1:200; integrin β3 (M031-0 from Emfret, Germany) IF: 1:200; integrin α2-FITC (554999 from BD Biosciences) FACS: 1:100; integrin α3 (AF2787 from R&D, Germany) FACS: 1:200; integrin α5-biotin (557446 from Pharmingen) FACS: 1:200, IP 1μg; integrin α5 (4705 from Cell Signaling, Germany) WB: 1:1000; integrin α6-FITC (555735 from Pharmingen) FACS 1:100; integrin αv-biotin (551380 from Pharmingen) FACS: 1:200; β1-integrin 9EG7 (550531 from BD Biosciences, San Diego, CA, USA) IF: 1:200; FACS: 1:200;

fibronectin (AB2033 from Millipore) IF: 1:500; IgG2a rat isotype control (13-4321 from eBioscience, Germany) FACS: 1:200; IP 1μg; Tritc-Phalloidin (P1951 from Sigma) IF: 1:400; Flag-tag-HRP (8592 from Sigma) WB: 1:10,000; GFP (A11122 from Invitrogen, Germany) WB: 1:2000; Cherry (PM005 from MBL, Woburn, MA, USA) WB:1:1000; Myc (05-724 from Millipore) WB 1:2000; FAK (06-543 from Upstate, Billerica, MA, USA) WB: 1:1000; FAK (3285 from Cell Signaling) WB (1:1000); phospho-Y397 FAK (3283 from Cell Signaling) WB: 1:1000; phospho-Y397 FAK (44624G from Biosource, Waltham, MA, USA) WB: 1:1000, IF: 1:400; ILK (611803 from Transduction Labs) WB: 1:5000; IF: 1:500; phospho-Y992 EGFR (2235 from Cell Signaling) WB: 1:2000; phospho-Y31 Paxillin (44720G from Invitrogen) WB: 1:1000; phospho-Y118 Paxillin (44722G from Invitrogen) WB: 1:1000; p130Cas (P27820 Transduction Labs) WB: 1:1000; phospho-Y410 p130 Cas (4011S from Cell Signaling) WB: 1:1000; Akt (9272 from Cell Signaling) WB: 1:1000; phospho-S473 Akt (4060 from Cell Signaling) WB: 1:1000; phosho-T308 Akt (9275 from Cell Signaling) WB: 1:1000; Erk1/2 (9102 from Cell Signaling) WB: 1:1000; Erk1/2 phosphorylated T202 Y204 (4376 Cell Signaling) WB: 1:1000.

The following secondary antibodies were used: goat anti-rabbit Alexa 488 (A11008), goat anti-mouse Alexa 488 (A11029), goat anti-rat Alexa 488 (A11006), goat anti-mouse Alexa 546 (A11003), donkey anti-mouse Alexa 647 (A31571), goat anti-rabbit Alexa 647 (A21244), (all from Invitrogen) FACS: 1:500, IF: 1:500; streptavidin-Cy5 (016170084) FACS: 1:400; goat anti-rat horseradish peroxidase (HRP) (712035150) (both from Dianova, Germany) WB: 1:10,000, donkey anti-rabbit Cy3 (711-165-152) (from Jackson ImmunoResearch, West Grove, PA, USA) IF: 1:500, goat anti-mouse HRP (172-1011) and goat anti-rabbit HRP (172-1019) (both from BioRad) WB: 1:10,000.

The FAK inhibitor PF-228 (PZ0117 from Sigma) was dissolved in dimethyl sulfoxide at 10 mM and used at 1:2000.

Expression and purification of recombinant proteins

The recombinant expression of kindlin-2, full-length paxillin (paxillin-FL) and paxillin-LIM3 in *Escherichia coli* Rosetta cells (Merck Millipore) was induced with 1 mM or 0.2 mM IPTG, respectively, at 18°C for 22 hr. After cell lysis and clarification of the supernatant, kindlin-2 was purified by Ni-NTA affinity chromatography (Qiagen). Eluate fractions containing kindlin-2 were pooled, cleaved with SenP2 protease and purified by size-exclusion chromatography (Superdex 200 26/600, GE Healthcare, UK) yielding unmodified murine kindlin-2. The paxillin constructs were purified by Ni-NTA affinity chromatography (Qiagen), and subsequent size-exclusion chromatography (SEC650, BioRad) to obtain N-terminally tagged His10-SUMO3-paxillin-FL and His10-SUMO3-paxillin-LIM3 domain, respectively.

Immunostaining

For immunostaining, cells were cultured on plastic ibidi-μ-slides (80826 from Ibidi, Germany) coated with 20 μg ml^{-1} FN (Calbiochem). Cells were routinely fixed with 4% paraformaldehyde (PFA) (w/v) in phosphate buffered saline (PBS; 180 mM NaCl, 3.5 mM KCl, 10 mM Na_2HPO_4, 1.8 mM $K_2H_2PO_4$) for 10 min at room temperature (RT) or with –20°C cold acetone–methanol when indicated. If necessary, cells were solubilized with staining buffer (PBS supplemented with 0.1% Triton X-100 (v/v) and 3% BSA (w/v)) or with –20°C cold methanol for kindlin-2 staining. Background signals were blocked by incubating cells for 1 hr at RT in staining buffer. Subsequently, they were incubated in the dark with primary and secondary antibodies diluted in staining buffer. Fluorescent images were aquired with a LSM 780 confocal microscope (Zeiss, Germany) equiped with a 100×/NA 1.46 oil objective and with a DMIRE2-SP5 confocal microscope (Leica, Germany) equiped with a 40×/NA 1.25 or 63×/NA 1.4 oil objective using Leica Confocal software (version 2.5 build 1227). Brightfield images were aquired with an Axioskop (Carl Zeiss) 40×/NA 0.75 objective and DC500 camera with IM50 software (Leica). Z-stack projection and contrast adjustments ImageJ (v1.47) were used for further image analysis.

Super-resolution imaging was carried out by direct stochastic optical reconstruction microscopy (dSTORM) (***van de Linde et al., 2011***), which is based on precise emitter localization. To induce reversible switching of the Alexa 647 label and reduce photobleaching, imaging was performed in imaging solution (50% Vectashield (v/v) (H-1000; Vector Laboratories, Burlingame, CA, USA), 50% TBS (v/v), pH=8.0) supplemented with 50 mM β-mercaptoethylamine (Sigma-Aldrich; M9768).

dSTORM was implemented on a custom built total internal reflection fluourescence (TIRF) system (Visitron Systems, Germany) based on a Zeiss Axiovert 200M with fiber-coupled lasers. Sample were

excited with a 640 nm laser in a TIRF mode using a Zeiss α Plan-Fluar 100×/NA 1.45 oil objective. The emitted light was detected in the spectral range 660–710 nm through a Semrock FF02-685/40-25 bandpass filter (Semrock Inc., Rochester, NY, USA). Images were recorded with a Photometrics Evolve Delta emCCD camera (Photometrics, Huntington Beach, CA, USA), with its EM gain set to 250. Additional magnification by a factor of 1.6 resulted in a pixel size of 100 nm. For each final image, a total of 20,000 frames with an exposure time of 14 ms were recorded.

A standard TIRF imaging of the same sample in the green channel (anti-paxillin) was achieved by illumination with a 488 nm laser and detection in the spectral range 500–550 nm through a Chroma Et 525/50 bandpass filter (Chroma Technology Corporation, Bellows Falls, VT, USA). Simultaneous dual-colour imaging of both the green and the red channel was realized with a Hamamatsu W-View Gemini image splitter (Hamamatsu Photonics, Bridgewater, NJ, USA) mounted between the microscope and the camera. Image analysis was carried out with the ImageJ plugin ThunderSTORM (***Ovesny et al., 2014***) and standard tools of ImageJ. Heat maps of density of blink events were created using the 2D-Frequency Count/Binning module of OriginPro 9.1 (OriginLab Corporation, Northampton, MA, USA).

AFM-based single-cell force spectroscopy

Tipless, 200 μm long V-shaped cantilevers (spring constants of 0.06 N m^{-1}; NP-O, Bruker, Billerica, MA, USA) were prepared for cell attachment as described (***Friedrichs et al., 2010***). Briefly, plasma cleaned cantilevers were incubated in 2 mg ml^{-1} ConA (Sigma) in PBS at 4°C overnight. Polydimethylsiloxan (PDMS) masks were overlaid on glass bottoms of Petri dishes (35 mm FluoroDish, World Precision Instruments, Sarasota, FL, USA) to allow different coatings of the glass surface (***Te Riet et al., 2014***). PDMS-framed glass surfaces were incubated overnight with 50 μg ml^{-1} FN-RGD and 50 μg ml^{-1} FN-ΔRGD in PBS at 4°C. Overnight serum-starved fibroblasts (Tln^{Ctr}, $Kind^{Ctr}$, Tln^{Ko}, $Kind^{Ko}$) grown on FN-coated (Calbiochem) 24 well plates (Thermo Scientific, Denmark) to confluency of ~ 80% were washed with PBS and detached with 0.25% (w/v) trypsin/EDTA (Sigma). Detached cells were suspended in single-cell force spectroscopy (SCFS) medium (DMEM supplemented with 20 mM HEPES) containing 1% (v/v) FCS, pelleted and further resuspended in serum-free SCFS medium. Detached cells were left suspended in SCFS media to recover from detachment for ~1 hr (***Schubert et al., 2014***). For the activation or chelation assay, the detached cells were incubated in SCFS media supplemented with 0.5 mM Mn^{2+} or 5 mM EDTA, respectively, for ~1 hr and SCFS was performed in the presence of the indicated supplement. SCFS was performed using an AFM (NanoWizard II, JPK Instruments, Germany) equipped with a CellHesion module (JPK Instruments) mounted on an inverted optical microscope (Zeiss Axiovert 200M). Measurements were performed at 37°C, controlled by a PetriDish Heater (JPK Instruments). Cantilevers were calibrated using the equipartition theorem (***Hutter and Bechhoefer, 1993***).

To attach a single cell to the cantilever, cell suspensions were pipetted to the region containing the FN-ΔRGD coating. The ConA functionalized cantilever was lowered onto a single cell with a velocity of 10 μm s^{-1} until reaching a contact force of 5 nN. After 5 s contact, the cantilever was retracted from the Petri dish by 50 μm and the cantilever-bound cell was left for incubation for >10 min. For adhesion experiments, the cantilever-bound cell was brought into contact with the FN-ΔRGD coated support at a contact force of ~2 nN for 5, 20, 50 and 120 s and then retracted while measuring the cantilever deflection and the distance travelled. Subsequently, the cell adhesion to the FN-RGD coated support was characterized as described. In case cantilever attached cells showed morphological changes (e.g. spreading) they were discarded. The approach and retract velocity of the cantilever was 5 μm s^{-1}. The deflection of the cantilever was recorded as force-distance curves. Adhesion forces were extracted from retraction force-distance curves using the AFM data processing software (JPK Instruments).

Immunoprecipitations and recombinant protein pulldown

GFP-IPs were performed using μ-MACS anti-GFP magnetic beads (130-091-288 from Miltenyi, Germany). To pulldown recombinant kindlin-2 35 μg of purified His10-LIM3 or 10 μg of purified His10-paxillin-FL were incubated with 100 μl of 50% Ni-NTA-Agarose slurry (Qiagen) in pulldown buffer (20 mM Tris, pH 7.5, 200 mM NaCl, 1 mM TCEP, 0.05% Tween20) for 1 hr at 4°C. After a first wash with 20 column volumes (CV) of pulldown buffer supplemented with 1 mM $ZnCl_2$ and a second wash with

20 CV of pulldown buffer, 14 µg of purified kindlin-2 were added to 100 µl of Ni-NTA-agarose slurry and incubated for 30 min at 4˚C. Subsequently, the Ni-NTA beads were washed three times with 20 CV of pulldown buffer supplemented with 25 mM imidazole and either 1 mM $ZnCl_2$ or 1 mM EDTA. The beads were eluted with 50 µl pulldown buffer supplemented with 500 mM imidazole and analysed on a 12% sodium dodecyl sulfate polyacrylamide gel electrophoresis (SDS-PAGE).

For immunoprecipitation of kindlin-2 or paxillin, control fibroblasts were lysed in lysis buffer (50 mM Tris, pH 8.0, 150 mM NaCl, 1% Triton X-100, 0.05% sodium deoxycholate, 10 mM EDTA). Lysates were incubated with kindlin-2 or paxillin antibodies for 2 hr at 4˚C while rotating. Isotype-matched IgG was used as a negative control. After this, lysates were incubated with 50 µl protein A/G Plus Agarose (Santa Cruz) for 2 hr at 4˚C. Following repeated washes with lysis buffer, proteins were eluted from the beads using Laemmli buffer and analyzed by western blotting.

For the immunoprecipitation of α5 integrin from the cell surface of live cells, α5 integrins were labeled with a biotinylated anti-α5 integrin antibody (PharMingen #557446) or an isotype control (eBioscience # 13-4321) for 1 hr on ice. After two washes in ice-cold PBS to remove unbound antibody, cells were lysed in IP buffer (50 mM Tris, pH 7.5, 150 mM NaCl, 1% Triton X-100, 0.1% sodium deoxycholate, 1mM EDTA, and protease inhibitors) and cleared by centrifugation. α5 integrin immuno-complexes were pulled-down by incubation with streptavidin-sepharose (GE Healthcare) overnight at 4˚C with gentle agitation. After several washes with lysis buffer, proteins were subjected to SDS-PAGE and western blot analysis with antibodies against α5 and β1 integrin.

Spreading and adhesion assays

Cells were grown to 70% confluency and then detached using trypsin/EDTA. Suspended cells were serum starved for 1 hr in adhesion assay medium (10 mM HEPES, pH 7.4; 137 mM NaCl; 1 mM $MgCl_2$; 1 mM $CaCl_2$; 2.7 mM KCl; 4.5 g L^{-1} glucose; 3% BSA (w/v)) before 40,000 cells per well were plated out in the same medium supplemented with 8% FCS, and 5 mM Mn^{2+} if indicated. Plastic ibidi-µ-slides (Ibidi; 80826) were coated with 10 µg ml^{-1} FN (Calbiochem) for adhesion or 20 µg ml^{-1} FN for spreading assays, 10 µg ml^{-1} LN (11243217001 from Roche, Germany), 10 µg ml^{-1} COL (5005B from Advanced Bio Matrix, Carlsbad, CA, USA), 10 µg ml^{-1} VN (07180 from StemCell, Canada) or 0.1% PLL (w/v) (Sigma; P4707) diluted in PBS. Seeded cells were centrifuged at 600 rpm in a Beckman centrifuge for 30 min at 37˚C before they were fixed with 4% PFA (w/v) in PBS and stained with Phalloidin-TRITC and DAPI. For cell adhesion assays, nuclear staining of the whole well was imaged using a 2.5x objective and cell numbers were counted using ITCN plugin for imageJ (***Byun et al., 2006***). For cell spreading assays, 12 confocal images of different regions of Phalloidin and DAPI stained cells were aquired using a Leica confocal microscope, cell spreading was quantified using imageJ.

For time dependent and ligand concentration dependent adhesion on FN, 40,000 cells were plated on 96-well plates, vigorously washed after the indicated timepoints with PBS and fixed with 4% PFA. Cell attachment was meassured by crystal violet staining (0.1% in 20% methanol) of cells in a absorbance plate reader at the wavelength of 570 nm.

Live cell imaging

A hole of 15 mm diameter was drilled into the bottom of a 35 mm falcon tissue culture dish (353001, Becton Dickinson) and a coverslip (Ø 25 mm, Menzel-Gläser, Germany), rinsed with ethanol, was glued to the dish with silicon glue (Elastosil E43, Wacker, Germany). After coating coverslips with 20 µg ml^{-1} FN (Calbiochem) overnight at 4˚C, cells were plated and imaged in an inverted transmission light microscope (Zeiss Axiovert 200 M, Carl Zeiss) equipped with a climate chamber. Phase contrast images were taken with a ProEM 1024 EMCCD camera (Princeton Instruments, Acton, MA, USA) through a Zeiss Plan Neofluar 100x objective (NA 1.3, Ph3). Frames were acquired at 30 sec or 1 min intervals and converted to time lapse movies using ImageJ.

Constructs and transfections

K2ΔPHGFP was cloned by PCR using the K2GFP cDNA (***Ussar et al., 2006***) as template and the Kind2fwd (5'-ctcgaggaggtatggctctggacgggataag -3', Kind2PHrev 5'-**tggtcttgcctttaatatag**tcagcaagtt -3'), Kind2PHfwd (5'-**ctatattaaaggcaa**gaccatggcagacag -3') and Kind2rev (5'- tctagatcacacccaac-cactggtga-3') primers. The two fragments containing homologous regions (indicated with bold

letters in the primer sequences) were fused by another round of amplification using the most 5′ and 3′ primers (Kind2fwd and Kind2rev). The resulting PCR product was cloned into the K2GFP vector. The N- and C-terminal truncation constructs of kindlin-2 were cloned by PCR using K2GFP as template. The primer sequences were: Kind2-NT-fwd 5′-ctgtacaagtccggactc-3′, Kind2-NT-rev 5′-gcggccgcctattttgctttatcaagaagagc-3′, Kind2-CT-fwd 5′-ctcgagctatggataaagcaaaaaccaaccaag-3′, Kind2-CT-rev 5′-gttatctagagcggccgc-3′. Stable expression of K2ΔPHGFP and FAKGFP- or Myc-FAK (a gift from Dr. Ambra Pozzi; Vanderbilt University, Nashville, USA) cDNAs was achieved with the sleeping beauty transposase system (***Bottcher et al., 2012***). Kindlin-1-GFP and Kindlin-3-GFP constructs have been described (***Ussar et al., 2008***; ***Moser et al., 2008***).

For stable expression of murine talin-1 and THD (amino acids1-443), the corresponding cDNAs were N-terminally tagged with Venus and cloned into the retroviral pLPCX vector. The constructs for GFP-tagged paxillin-LIM truncation mutants were generated by PCR from GFP- and Cherry-tagged α-paxillin (***Moik et al., 2013***) and cloned into the retroviral pLPCX vector. The primer sequences were: stop codon in bold: ΔLIM1-4fwd 5′- caccgttgccaaa**tga**gggtctgtggagcc -′3, ΔLIM1-4rev 5′-ggctccacagaccc**tca**tttggcaacggtg -′3, ΔLIM2-4fwd 5′- cagcctcttctcccca**tga**cgctgctactactg -′3, ΔLIM2-4rev 5′- cagtagtagcagcg**tca**tggggagaagaggctg -′3, ΔLIM3-4fwd 5′- aagattacttcgacatgtttgct**tga**cccaagtgcggc -′3, ΔLIM3-4rev 5′- gccgcacttggg**tca**agcaaacatgtcgaagtaatctt -′3, ΔLIM4fwd 5′-ggcgcggctcg**tga**ctgtgctccgg -′3, ΔLIM4rev 5′- ccggagcacag**tca**cgagccgcgcc -′3). The cDNA of murine Hic5 was amplified from a cDNA derived from murine vascular smooth muscle cells, cloned into pCR2.1-TOPO (Invitrogen) and subcloned into pEGFP-C1 vector. Murine leupaxin cDNA (cloneID: 5065405 from Thermo Scientific, Germany) was PCR-amplified (Lpxn-fwd: 5′- ctcgagcaatggaagagctggatgccttattg -3′; Lpxn-rev 5′- gaattcctactgtgaaaagagcttagtgaagc -3′) and subcloned into the pEGFP-C1 vector.

To express recombinant murine kindlin-2 and paxillin-LIM3 (A473-S533) cDNAs were fused with N-terminal tandem tags consisting of 10x-Histidine followed by a SUMO3-tag and cloned into pCoofy17. The primer sequences for amplifying the paxillin-LIM3 domain were: LIM3fwd 5′-aaccggtggagctcccaagtgc-3′ and LIM3rev 5′-ttctcgagttacgagccgcgcc-3′. The plasmid carrying $FNIII_{7-10}$ cDNA has been described previously (***Takahashi et al., 2007***). For Y2H analysis, the kindlin-2 cDNA was PCR amplified using the primers K2-Bamfw: 5′-gggatcccactgggcctaatggctctggacgggataagg-3′ and K2-Salrev: 5′-gtgtcgacgtcacacccaaccactggtgagtttg-3′ and cloned into the pGBKT7 plasmid to obtain a kindlin-2 version that was N-terminally fused with the Gal4-DNA binding domain. Screening of this construct against a human full ORF library was conducted by the Y2H protein interaction screening service of the German Cancer Research Center in Heidelberg, Germany.

Statistical analysis

Experiments were routinely repeated at least three times and the repeat number was increased according to the effect size or sample variation. Unless stated differently, all statistical significances (*P<0.05; **P<0.01; ***P<0.001; n.s., not significant) were determined by two-tailed unpaired *t*-test. In the boxplots, the middle line represents the median, the box ends represent the 25th and 75th percentiles and the whisker ends show the 5th and 95th percentiles. Statistical analysis were performed with Prism (GraphPad, La Jolla, CA, USA).

Acknowledgements

We thank Ursula Kuhn for expert technical help. The work was supported by RO1-DK083187, RO1-DK075594, R01-DK069221 and VA Merit Award 1I01BX002196 (to RZ), by the Deutsches Zentrum für Herz-Kreislauf-Forschung, partner site Munich Heart Alliance (to RTB and RF) and by the European Research Council (Grant Agreement no. 322652), Deutsche Forschungsgemeinschaft (SFB-863) and the Max Planck Society (to RF).

Additional information

Funding

Funder	Grant reference number	Author
Veterans Affair Merit Award	1I01BX002196	Roy Zent
NIH Office of the Director	RO1-DK083187	Roy Zent
NIH Office of the Director	RO1-DK075594	Roy Zent
NIH Office of the Director	R01-DK069221	Roy Zent
European Research Council	322652	Reinhard Fässler
Deutsche Forschungsgemeinschaft	SFB-863	Reinhard Fässler
Max-Planck-Gesellschaft		Reinhard Fässler

The funders had no role in study design, data collection and interpretation, or the decision to submit the work for publication.

Author contributions

MT, MW, Carried out most experiments and data analysis, evaluated and interpreted the data.; RTB, Tested integrin activation, paxillin recruitment and the kindlin-2 interaction with paxillin in vivo, evaluated and interpreted the data.; ER, Performed immunoblottings and PCR experiments; MV, Produced recombinant kindlin-2 and paxillin.; MB, Performed AFM experiments; AL, Performed dSTORM; KA, Analyzed FN assembly; DJM, Evaluated and interpreted the data; RZ, Crossed talin mice, established cell lines, evaluated and interpreted the data.; RF, Initiated, conceived and directed the project, evaluated and interpreted the data and wrote the manuscript.

Ethics

Animal experimentation: Housing and use of laboratory animals at the Max Planck Institute of Biochemistry are fully compliant with all German (e.g. German Animal Welfare Act) and EU (e.g. Annex III of Directive 2010/63/EU on the protection of animals used for scientific purposes) applicable laws and regulations concerning care and use of laboratory animals. All of the animals were handled according to approved license (No.5.1-568- rural districts office). The animal experiments using the talin mice were performed with the approval of the Vanderbilt Institute Animal Care and Use Committee under protocol M09/374.

References

Askari JA, Tynan CJ, Webb SED, Martin-Fernandez ML, Ballestrem C, Humphries MJ. 2010. Focal adhesions are sites of integrin extension. *The Journal of Cell Biology* **188**:891–903. doi: 10.1083/jcb.200907174

Azimifar SB, Bottcher RT, Zanivan S, Grashoff C, Kruger M, Legate KR, Mann M, Fassler R. 2012. Induction of membrane circular dorsal ruffles requires co-signalling of integrin-ILK-complex and EGF receptor. *Journal of Cell Science* **125**:435–448. doi: 10.1242/jcs.091652

Bachir AI, Zareno J, Moissoglu K, Plow EF, Gratton E, Horwitz AR. 2014. Integrin-associated complexes form hierarchically with variable stoichiometry in nascent adhesions. *Current Biology* **24**:1845–1853. doi: 10.1016/j.cub.2014.07.011

Bazzoni G, Shih D-T, Buck CA, Hemler ME. 1995. Monoclonal antibody 9EG7 defines a novel 1 integrin epitope induced by soluble ligand and manganese, but inhibited by calcium. *Journal of Biological Chemistry* **270**:25570–25577. doi: 10.1074/jbc.270.43.25570

Bennett JS. 2005. Structure and function of the platelet integrin IIb 3. *Journal of Clinical Investigation* **115**:3363–3369. doi: 10.1172/JCI26989

Böttcher RT, Stremmel C, Meves A, Meyer H, Widmaier M, Tseng H-Y, Fässler R. 2012. Sorting nexin 17 prevents lysosomal degradation of β1 integrins by binding to the β1-integrin tail. *Nature Cell Biology* **14**:584–592. doi: 10.1038/ncb2501

Bouchard V, Demers M-J, Thibodeau S, Laquerre V, Fujita N, Tsuruo T, Beaulieu J-F, Gauthier R, Vézina A, Villeneuve L, Vachon PH. 2007. Fak/Src signaling in human intestinal epithelial cell survival and anoikis: differentiation state-specific uncoupling with the PI3-K/Akt-1 and MEK/Erk pathways. *Journal of Cellular Physiology* **212**:717–728. doi: 10.1002/jcp.21096

Brami-Cherrier K, Gervasi N, Arsenieva D, Walkiewicz K, Boutterin M-C, Ortega A, Leonard PG, Seantier B, Gasmi L, Bouceba T, Kadare G, Girault J-A, Arold ST. 2014. FAK dimerization controls its kinase-dependent functions at focal adhesions. *The EMBO Journal* **33**:356–370. doi: 10.1002/embj.201386399

Brown MC, Perrotta JA, Turner CE. 1996. Identification of LIM3 as the principal determinant of paxillin focal adhesion localization and characterization of a novel motif on paxillin directing vinculin and focal adhesion kinase binding. *The Journal of Cell Biology* **135**:1109–1123. doi: 10.1083/jcb.135.4.1109

Byun J, Verardo MR, Sumengen B, Lewis GP, Manjunath BS, Fisher SK. 2006. Automated tool for the detection of cell nuclei in digital microscopic images: application to retinal images. *Molecular Vision* **12**:949–960.

Calderwood DA, Campbell ID, Critchley DR. 2013. Talins and kindlins: partners in integrin-mediated adhesion. *Nature Reviews Molecular Cell Biology* **14**:503–517. doi: 10.1038/nrm3624

Chen W, Lou J, Zhu C. 2010. Forcing switch from short- to intermediate- and long-lived states of the a domain generates LFA-1/ICAM-1 catch bonds. *Journal of Biological Chemistry* **285**:35967–35978. doi: 10.1074/jbc.M110.155770

Choi CK, Zareno J, Digman MA, Gratton E, Horwitz AR. 2011. Cross-correlated fluctuation analysis reveals phosphorylation-regulated paxillin-FAK complexes in nascent adhesions. *Biophysical Journal* **100**:583–592. doi: 10.1016/j.bpj.2010.12.3719

Cluzel C, Saltel F, Lussi J, Paulhe F, Imhof BA, Wehrle-Haller B. 2005. The mechanisms and dynamics of v 3 integrin clustering in living cells. *The Journal of Cell Biology* **171**:383–392. doi: 10.1083/jcb.200503017

Conti FJ, Monkley SJ, Wood MR, Critchley DR, Muller U. 2009. Talin 1 and 2 are required for myoblast fusion, sarcomere assembly and the maintenance of myotendinous junctions. *Development* **136**:3597–3606. doi: 10.1242/dev.035857

Coussen F, Choquet D, Sheetz MP, Erickson HP. 2002. Trimers of the fibronectin cell adhesion domain localize to actin filament bundles and undergo rearward translocation. *Journal of Cell Science* **115**:2581–2590.

Deakin NO, Pignatelli J, Turner CE. 2012. Diverse roles for the paxillin family of proteins in cancer. *Genes & Cancer* **3**:362–370. doi: 10.1177/1947601912458582

Deramaudt TB, Dujardin D, Noulet F, Martin S, Vauchelles R, Takeda K, Rondé P, Parsons M. 2014. Altering FAK-paxillin interactions reduces adhesion, migration and invasion processes. *PLoS ONE* **9**:e92059. doi: 10.1371/journal.pone.0092059

Du X, Plow EF, Frelinger AL, O'Toole TE, Loftus JC, Ginsberg MH. 1991. Ligands 'activate' integrin αIIbβ3 (platelet GPIIb-IIIa). *Cell* **65**:409–416. doi: 10.1016/0092-8674(91)90458-B

Evans R, Patzak I, Svensson L, De Filippo K, Jones K, McDowall A, Hogg N. 2009. Integrins in immunity. *Journal of Cell Science* **122**:215–225. doi: 10.1242/jcs.019117

Fassler R, Meyer M. 1995. Consequences of lack of beta 1 integrin gene expression in mice. *Genes & Development* **9**:1896–1908. doi: 10.1101/gad.9.15.1896

Friedland JC, Lee MH, Boettiger D. 2009. Mechanically activated integrin switch controls 5 1 function. *Science* **323**:642–644. doi: 10.1126/science.1168441

Friedrichs J, Helenius J, Muller DJ. 2010. Quantifying cellular adhesion to extracellular matrix components by single-cell force spectroscopy. *Nature Protocols* **5**:1353–1361. doi: 10.1038/nprot.2010.89

Fukuda K, Bledzka K, Yang J, Perera HD, Plow EF, Qin J. 2014. Molecular basis of kindlin-2 binding to integrin-linked kinase pseudokinase for regulating cell adhesion. *Journal of Biological Chemistry* **289**:28363–28375. doi: 10.1074/jbc.M114.596692

Gailit J, Ruoslahti E. 1988. Regulation of the fibronectin receptor affinity by divalent cations. *The Journal of Biological Chemistry* **263**:12927–12932.

Hagel M, George EL, Kim A, Tamimi R, Opitz SL, Turner CE, Imamoto A, Thomas SM. 2002. The adaptor protein paxillin is essential for normal development in the mouse and is a critical transducer of fibronectin signaling. *Molecular and Cellular Biology* **22**:901–915. doi: 10.1128/MCB.22.3.901-915.2002

Han J, Lim CJ, Watanabe N, Soriani A, Ratnikov B, Calderwood DA, Puzon-McLaughlin W, Lafuente EM, Boussiotis VA, Shattil SJ, Ginsberg MH. 2006. Reconstructing and deconstructing agonist-induced activation of integrin αIIbβ3. *Current Biology* **16**:1796–1806. doi: 10.1016/j.cub.2006.08.035

Harburger DS, Bouaouina M, Calderwood DA. 2009. Kindlin-1 and -2 directly bind the c-terminal region of integrin cytoplasmic tails and exert integrin-specific activation effects. *Journal of Biological Chemistry* **284**:11485–11497. doi: 10.1074/jbc.M809233200

Huet-Calderwood C, Brahme NN, Kumar N, Stiegler AL, Raghavan S, Boggon TJ, Calderwood DA. 2014. Differences in binding to the ILK complex determines kindlin isoform adhesion localization and integrin activation. *Journal of Cell Science* **127**:4308–4321. doi: 10.1242/jcs.155879

Hutter JL, Bechhoefer J. 1993. Calibration of atomic-force microscope tips. *Review of Scientific Instruments* **64**:1868–1873. doi: 10.1063/1.1143970

Hynes RO. 2002. Integrins. *Cell* **110**:673–687. doi: 10.1016/S0092-8674(02)00971-6

Kong F, Garcia AJ, Mould AP, Humphries MJ, Zhu C. 2009. Demonstration of catch bonds between an integrin and its ligand. *The Journal of Cell Biology* **185**:1275–1284. doi: 10.1083/jcb.200810002

Kong F, Li Z, Parks WM, Dumbauld DW, García AJ, Mould AP, Humphries MJ, Zhu C. 2013. Cyclic mechanical reinforcement of integrin–ligand interactions. *Molecular Cell* **49**:1060–1068. doi: 10.1016/j.molcel.2013.01.015

Koo LY, Irvine DJ, Mayes AM, Lauffenburger DA, Griffith LG. 2002. Co-regulation of cell adhesion by nanoscale RGD organization and mechanical stimulus. *Journal of Cell Science* **115**:1423–1433.

Lawson C, Lim S-T, Uryu S, Chen XL, Calderwood DA, Schlaepfer DD. 2012. FAK promotes recruitment of talin to nascent adhesions to control cell motility. *The Journal of Cell Biology* **196**:223–232. doi: 10.1083/jcb.201108078

Liao Z, Kato H, Pandey M, Cantor JM, Ablooglu AJ, Ginsberg MH, Shattil SJ. 2015. Interaction of kindlin-2 with integrin 3 promotes outside-in signaling responses by the v 3 vitronectin receptor. *Blood* **125**:1995–2004. doi: 10.1182/blood-2014-09-603035

Maheshwari G, Brown G, Lauffenburger DA, Wells A, Griffith LG. 2000. Cell adhesion and motility depend on nanoscale RGD clustering. *Journal of Cell Science* **113** :1677–1686.

Margadant C, Kreft M, de Groot D-J, Norman JC, Sonnenberg A. 2012. Distinct roles of talin and kindlin in regulating integrin $\alpha 5\beta 1$ function and trafficking. *Current Biology* **22**:1554–1563. doi: 10.1016/j.cub.2012.06.060

Moik D, Bottcher A, Makhina T, Grashoff C, Bulus N, Zent R, Fassler R. 2013. Mutations in the paxillin-binding site of integrin-linked kinase (iLK) destabilize the pseudokinase domain and cause embryonic lethality in mice. *Journal of Biological Chemistry* **288**:18863–18871. doi: 10.1074/jbc.M113.470476

Montanez E, Ussar S, Schifferer M, Bosl M, Zent R, Moser M, Fassler R. 2008. Kindlin-2 controls bidirectional signaling of integrins. *Genes & Development* **22**:1325–1330. doi: 10.1101/gad.469408

Moser M, Nieswandt B, Ussar S, Pozgajova M, Fässler R. 2008. Kindlin-3 is essential for integrin activation and platelet aggregation. *Nature Medicine* **14**:325–330. doi: 10.1038/nm1722

Moser M, Legate KR, Zent R, Fassler R. 2009. The tail of integrins, talin, and kindlins. *Science* **324**:895–899. doi: 10.1126/science.1163865

Mould AP, Akiyama SK, Humphries MJ. 1995. Regulation of integrin 5 1-fibronectin interactions by divalent cations: evidence for distinct classes of binding sites for Mn2+, Mg2+, and Ca2+. *Journal of Biological Chemistry* **270**:26270–26277. doi: 10.1074/jbc.270.44.26270

Mould AP, Barton SJ, Askari JA, Craig SE, Humphries MJ. 2003. Role of ADMIDAS cation-binding site in ligand recognition by integrin 5 1. *Journal of Biological Chemistry* **278**:51622–51629. doi: 10.1074/jbc.M306655200

Nieswandt B, Moser M, Pleines I, Varga-Szabo D, Monkley S, Critchley D, Fassler R. 2007. Loss of talin1 in platelets abrogates integrin activation, platelet aggregation, and thrombus formation in vitro and in vivo. *Journal of Experimental Medicine* **204**:3113–3118. doi: 10.1084/jem.20071827

Ovesny M, K i ek P, Borkovec J, vindrych Z, Hagen GM. 2014. ThunderSTORM: a comprehensive ImageJ plug-in for PALM and STORM data analysis and super-resolution imaging. *Bioinformatics* **30**:2389–2390. doi: 10.1093/bioinformatics/btu202

Pankov R, Cukierman E, Katz BZ, Matsumoto K, Lin DC, Lin S, Hahn C, Yamada KM. 2000. Integrin dynamics and matrix assembly: tensin-dependent translocation of alpha5beta1 integrins promotes early fibronectin fibrillogenesis. *The Journal of Cell Biology* **148**:1075–1090. doi: 10.1083/jcb.148.5.1075

Roca-Cusachs P, Gauthier NC, del Rio A, Sheetz MP. 2009. Clustering of 5 1 integrins determines adhesion strength whereas v 3 and talin enable mechanotransduction. *Proceedings of the National Academy of Sciences of the United States of America* **106**:16245–16250. doi: 10.1073/pnas.0902818106

Rognoni E, Widmaier M, Jakobson M, Ruppert R, Ussar S, Katsougkri D, Böttcher RT, Lai-Cheong JE, Rifkin DB, McGrath JA, Fässler R. 2014. Kindlin-1 controls wnt and TGF-β availability to regulate cutaneous stem cell proliferation. *Nature Medicine* **20**:350–359. doi: 10.1038/nm.3490

Scheffzek K, Welti S. 2012. Pleckstrin homology (pH) like domains – versatile modules in protein–protein interaction platforms. *FEBS Letters* **586**:2662–2673. doi: 10.1016/j.febslet.2012.06.006

Schlaepfer DD, Mitra SK, Ilic D. 2004. Control of motile and invasive cell phenotypes by focal adhesion kinase. *Biochimica Et Biophysica Acta (BBA) - Molecular Cell Research* **1692**:77–102. doi: 10.1016/j.bbamcr.2004.04.008

Schubert R, Strohmeyer N, Bharadwaj M, Ramanathan SP, Krieg M, Friedrichs J, Franz CM, Muller DJ. 2014. Assay for characterizing the recovery of vertebrate cells for adhesion measurements by single-cell force spectroscopy. *FEBS Letters* **588**:3639–3648. doi: 10.1016/j.febslet.2014.06.012

Shattil SJ, Kim C, Ginsberg MH. 2010. The final steps of integrin activation: the end game. *Nature Reviews Molecular Cell Biology* **11**:288–300. doi: 10.1038/nrm2871

Spandidos A, Wang X, Wang H, Seed B. 2010. PrimerBank: a resource of human and mouse PCR primer pairs for gene expression detection and quantification. *Nucleic Acids Research* **38**:D792–D799. doi: 10.1093/nar/gkp1005

Springer TA, Dustin ML. 2012. Integrin inside-out signaling and the immunological synapse. *Current Opinion in Cell Biology* **24**:107–115. doi: 10.1016/j.ceb.2011.10.004

Sulzmaier FJ, Jean C, Schlaepfer DD. 2014. FAK in cancer: mechanistic findings and clinical applications. *Nature Reviews Cancer* **14**:598–610. doi: 10.1038/nrc3792

Takahashi S, Leiss M, Moser M, Ohashi T, Kitao T, Heckmann D, Pfeifer A, Kessler H, Takagi J, Erickson HP, Fassler R. 2007. The RGD motif in fibronectin is essential for development but dispensable for fibril assembly. *The Journal of Cell Biology* **178**:167–178. doi: 10.1083/jcb.200703021

te Riet J, Helenius J, Strohmeyer N, Cambi A, Figdor CG, Muller DJ. 2014. Dynamic coupling of ALCAM to the actin cortex strengthens cell adhesion to CD6. *Journal of Cell Science* **127**:1595–1606. doi: 10.1242/jcs.141077

Thwaites T, Nogueira AT, Campeotto I, Silva AP, Grieshaber SS, Carabeo RA. 2014. The *chlamydia* effector TarP mimics the mammalian leucine-aspartic acid motif of paxillin to subvert the focal adhesion kinase during invasion. *Journal of Biological Chemistry* **289**:30426–30442. doi: 10.1074/jbc.M114.604876

Ussar S, Wang H-V, Linder S, Fässler R, Moser M. 2006. The kindlins: subcellular localization and expression during murine development. *Experimental Cell Research* **312**:3142–3151. doi: 10.1016/j.yexcr.2006.06.030

Ussar S, Moser M, Widmaier M, Rognoni E, Harrer C, Genzel-Boroviczeny O, Fässler R, van Heyningen V. 2008. Loss of kindlin-1 causes skin atrophy and lethal neonatal intestinal epithelial dysfunction. *PLoS Genetics* **4**:e1000289. doi: 10.1371/journal.pgen.1000289

van Kooyk Y, Figdor CG. 2000. Avidity regulation of integrins: the driving force in leukocyte adhesion. *Current Opinion in Cell Biology* **12**:542–547. doi: 10.1016/S0955-0674(00)00129-0

van de Linde S, Löschberger A, Klein T, Heidbreder M, Wolter S, Heilemann M, Sauer M. 2011. Direct stochastic optical reconstruction microscopy with standard fluorescent probes. *Nature Protocols* **6**:991–1009. doi: 10.1038/nprot.2011.336

Wade R, Bohl J, Vande Pol S. 2002. Paxillin null embryonic stem cells are impaired in cell spreading and tyrosine phosphorylation of focal adhesion kinase. *Oncogene* **21**:96–107. doi: 10.1038/sj.onc.1205013

Wang P, Ballestrem C, Streuli CH. 2011. The c terminus of talin links integrins to cell cycle progression. *The Journal of Cell Biology* **195**:499–513. doi: 10.1083/jcb.201104128

Winograd-Katz SE, Fässler R, Geiger B, Legate KR. 2014. The integrin adhesome: from genes and proteins to human disease. *Nature Reviews Molecular Cell Biology* **15**:273–288. doi: 10.1038/nrm3769

Xia W, Springer TA. 2014. Metal ion and ligand binding of integrin $\alpha_5\beta_1$. *Proceedings of the National Academy of Sciences of the United States of America* **111**:17863–17868. doi: 10.1073/pnas.1420645111

Ye F, Petrich BG, Anekal P, Lefort CT, Kasirer-Friede A, Shattil SJ, Ruppert R, Moser M, Fässler R, Ginsberg MH. 2013. The mechanism of kindlin-mediated activation of integrin αIIbβ3. *Current Biology* **23**:2288–2295. doi: 10.1016/j.cub.2013.09.050

Zhang X, Jiang G, Cai Y, Monkley SJ, Critchley DR, Sheetz MP. 2008. Talin depletion reveals independence of initial cell spreading from integrin activation and traction. *Nature Cell Biology* **10**:1062–1068. doi: 10.1038/ncb1765

Zhang X, Moore SW, Iskratsch T, Sheetz MP. 2014. N-WASP-directed actin polymerization activates cas phosphorylation and lamellipodium spreading. *Journal of Cell Science* **127**:1394–1405. doi: 10.1242/jcs.134692

Zhu J, Luo B-H, Xiao T, Zhang C, Nishida N, Springer TA. 2008. Structure of a complete integrin ectodomain in a physiologic resting state and activation and deactivation by applied forces. *Molecular Cell* **32**:849–861. doi: 10.1016/j.molcel.2008.11.018

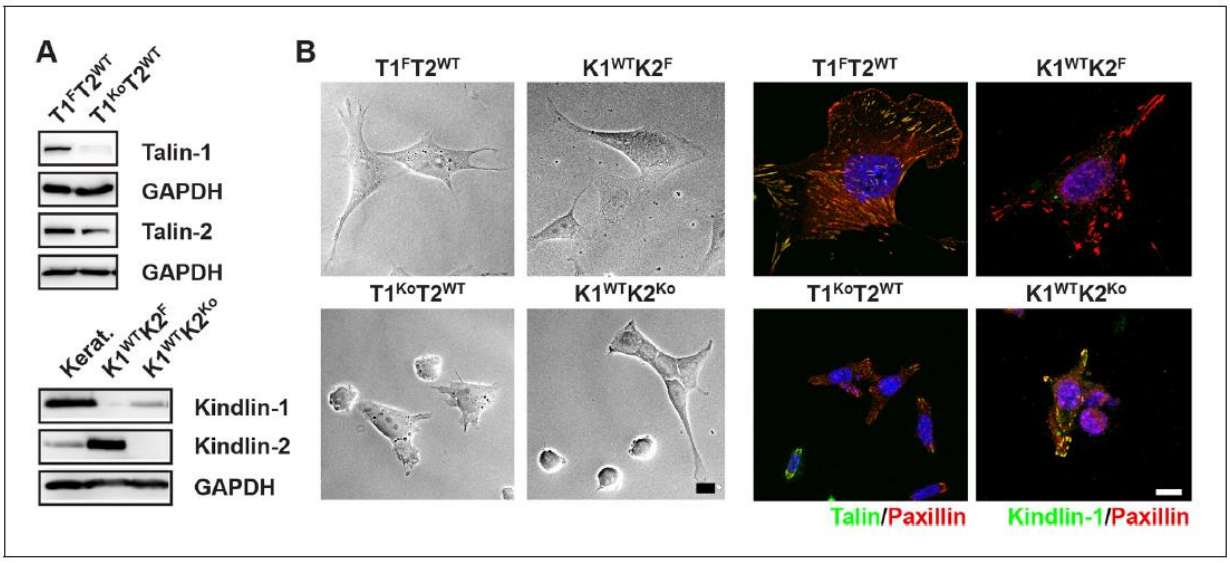

Figure 1—figure supplement 1. Talin-1- and kindlin-2-deficient fibroblasts. (**A**) Western blots showing talin-2 expression in floxed talin-1 ($T1^{F}$) and $T1^{Ko}$ fibroblasts and de novo expression of the *Fermt1* gene in kindlin-2-null ($K2^{Ko}$) fibroblasts. Keratinocytes (Kerat.) expressing high levels of kindlin-1 served as control for the anti-kindlin-1 antibody. GAPDH served as loading control. (**B**) Talin-1- and kindlin-2-deficient fibroblasts partially spread (bright field imaging, left panels) and form paxillin-positive adhesion sites (immunostaining, right panels). Bars, 10 µm. GAPDH, glyceraldehyde-3-phosphate dehydrogenase.

DOI: http://dx.doi.org/10.7554/eLife.10130.004

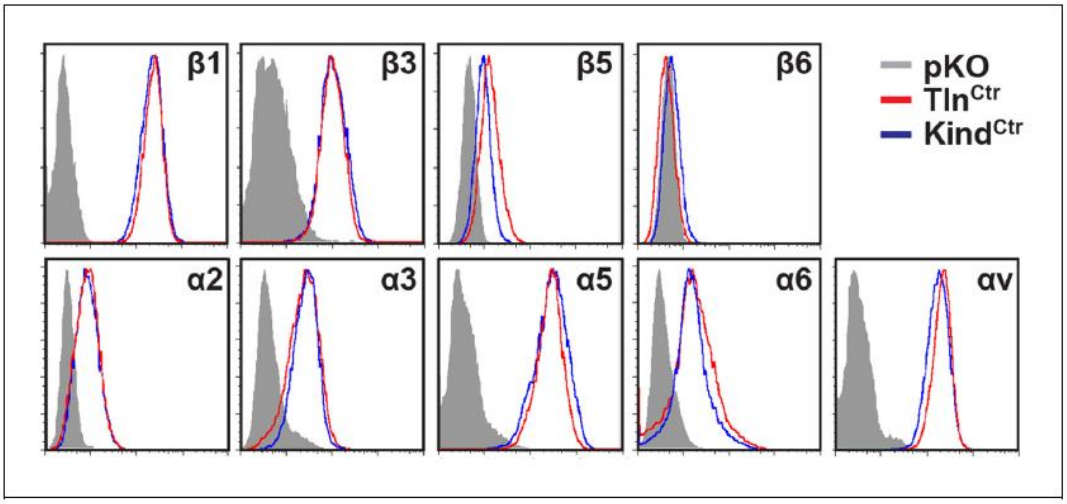

Figure 1—figure supplement 2. Integrin expression profiles of Tln^{Ctr} and $Kind^{Ctr}$ cells. Cell surface expression of different integrin subunits on Tln^{Ctr} and $Kind^{Ctr}$ cells was measured by flow cytometry and presented as histograms. Fluorescence-activated cell sorting histograms of cells lacking expression of all integrins (pKO) served as negative control and are shown in grey.

DOI: http://dx.doi.org/10.7554/eLife.10130.005

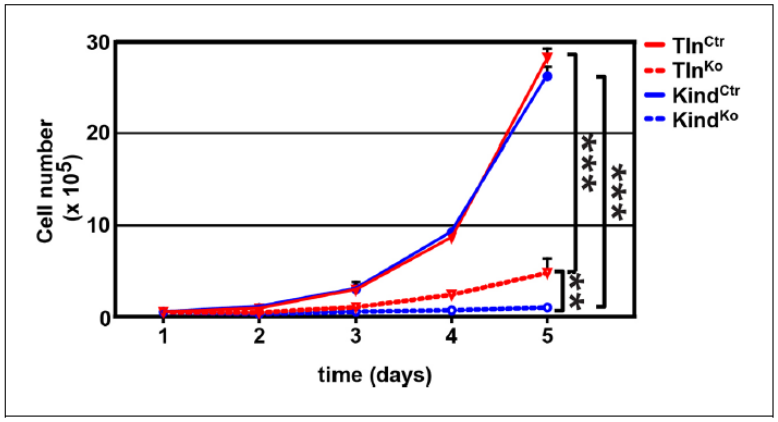

Figure 1—figure supplement 3. Cell proliferation of Tln^{Ko} and $Kind^{Ko}$ cells. Tln^{Ko} and $Kind^{Ko}$ cells show a significantly reduced increase in cell numbers, which were determined by cell counting at indicated time points (error bars indicate standard deviation; significances are given for indicated pairs and were calculated by two-way ANOVA). ANOVA, analysis of variance.

DOI: http://dx.doi.org/10.7554/eLife.10130.006

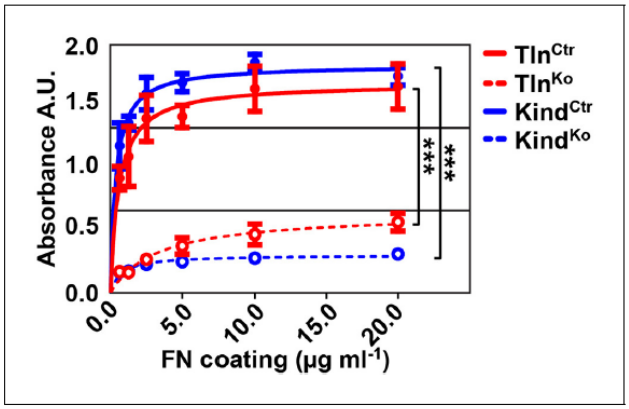

Figure 1—figure supplement 4. Cell adhesion of Tln^{Ko} and $Kind^{Ko}$ cells on different FN concentrations. Cell adhesion was measured 20 min after seeding the indicated cell lines on plastic surfaces coated with the indicated FN concentrations. Cells were PFA fixed and quantified by absorbance measurement of crystal violet staining (n=3 independent experiments; lines represent hyperbolic curve fits; error bars indicate standard deviation; significances for indicated pairs of the overall kinetics were calculated by two-way RM ANOVA). FN, fibronectin, PFA, paraformaldehyde; RM ANOVA, repeated measures analysis of variance.

DOI: http://dx.doi.org/10.7554/eLife.10130.007

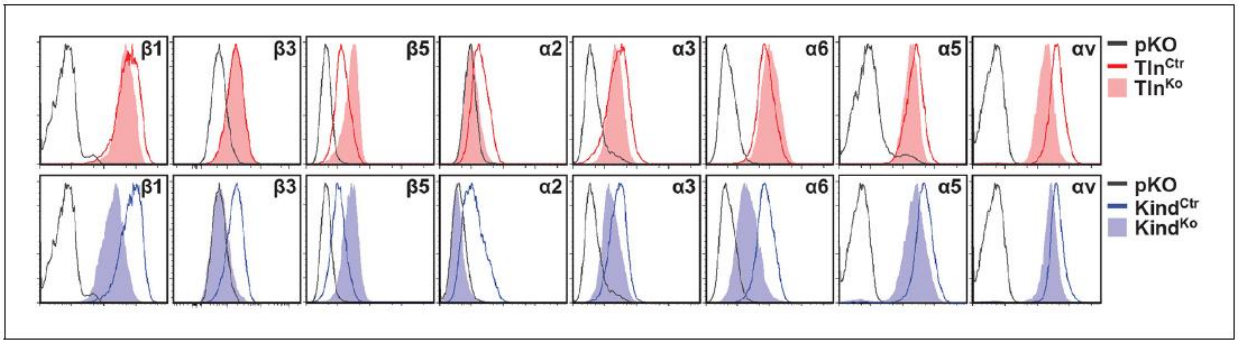

Figure 2—figure supplement 1. Integrin expression profiles of Tln^{Ctr}, Tln^{Ko}, $Kind^{Ctr}$ and $Kind^{Ko}$ cells. Representative FACS histograms of different integrin subunits expressed on Tln^{Ctr}, Tln^{Ko}, $Kind^{Ctr}$ and $Kind^{Ko}$ cells are shown. FACS histograms of cells lacking expression of all integrins (pKO) served as negative control and are shown in grey. FACS, fluorescence-activated cell sorting.

DOI: http://dx.doi.org/10.7554/eLife.10130.009

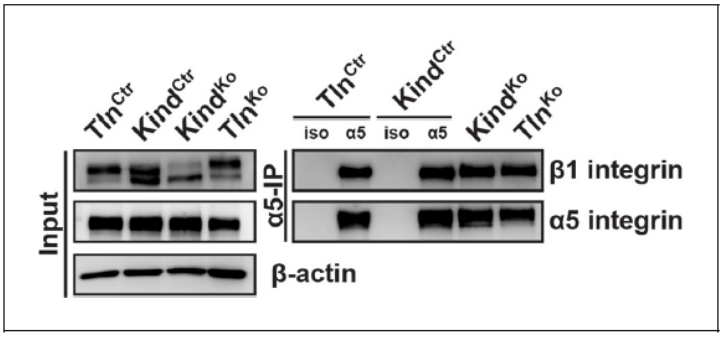

Figure 2—figure supplement 2. Tln^{Ko} and $Kind^{Ko}$ cells display comparable $\alpha5\beta1$ integrin cell surface levels. Live Tln^{Ctr}, $Kind^{Ctr}$, Tln^{Ko} and $Kind^{Ko}$ cells were incubated with antibodies against α5 integrin (α5) or with an unrelated isotype control (iso) on ice to immunoprecipitate α5 integrin from their cell surface. Following immunoprecipitation, the proteins were analyzed by western blotting to determine the levels of β1 and α5 integrin.

DOI: http://dx.doi.org/10.7554/eLife.10130.010

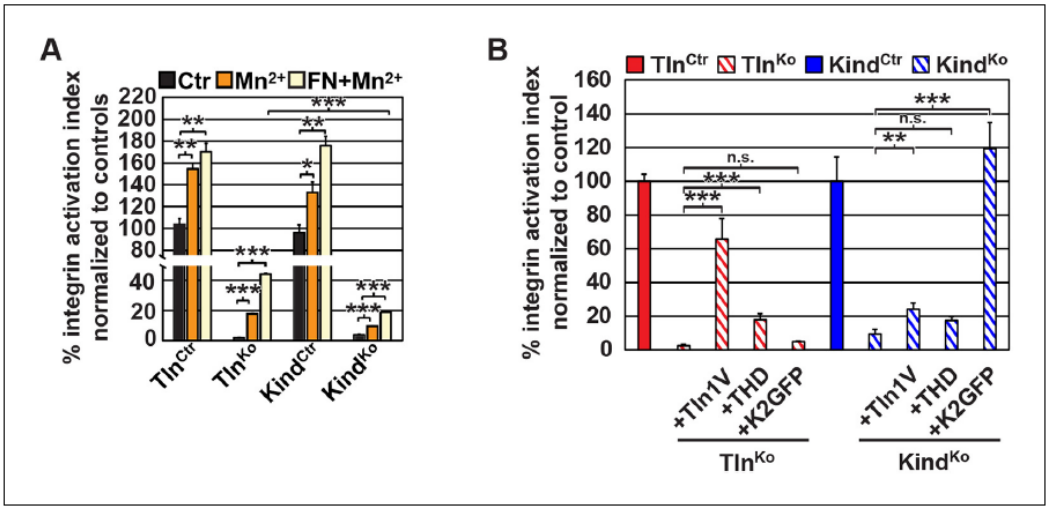

Figure 2—figure supplement 3. β1 i ntegrin activation in Tln^{Ctr}, Tln^{Ko}, $Kind^{Ctr}$, $Kind^{Ko}$ cells. (**A**) FACS quantification of 9EG7 antibody binding to the indicated cell lines in the presence of 0.3 µM FN (FN) or 5 mM $MnCl_2$ and 0.3 µM FN ($FN+Mn^{2+}$) (n=3 independent experiments; 9EG7 binding was normalized to total-β1 surface levels and 100% represents the average of Tln^{Ctr} and $Kind^{Ctr}$ under control buffer condition; error bars indicate standard error of the mean; significances are calculated between Ctr and indicated condition). (**B**) FACS quantification of total β1-antibody and 9EG7-antibody binding to Tln^{Ctr} and $Kind^{Ctr}$ cells and cells reconstituted with Tln1V, K2GFP or THD. 9EG7 binding was normalized to total β1 surface levels and control cell lines were set to 100% (n>3 independent experiments; significances are given for indicated pairs; error bars indicate standard error of the mean). FACS, fluorescence-activated cell sorting; FN, fibronectin; K2GFP, green fluorescent protein-tagged kindlin-2; THD, talin-1 head domain; Tln1V, Venus-tagged full length talin-1.

DOI: http://dx.doi.org/10.7554/eLife.10130.011

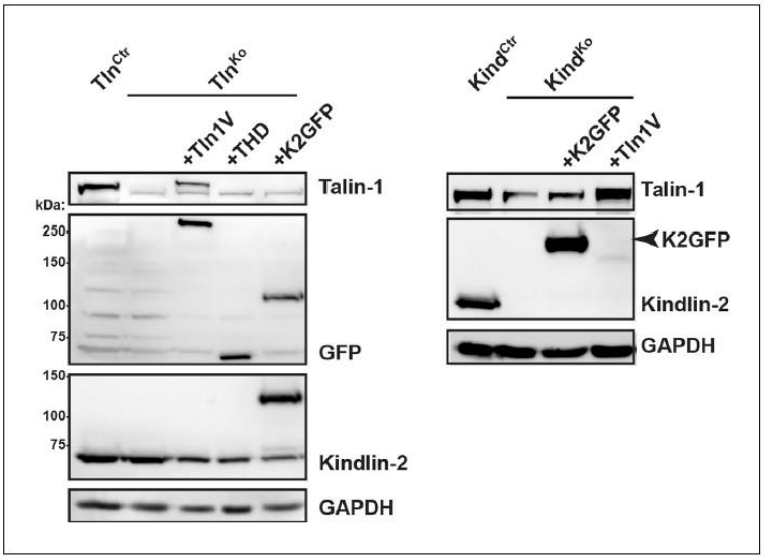

Figure 2—figure supplement 4. Re-expression of talin-1 or kindlin-2 in Tln^{Ko} and $Kind^{Ko}$ cells. Western blot analysis of cell lysates from Tln^{Ko} and $Kind^{Ko}$ cells reconstituted with Tln1V, THD or K2GFP expression plasmids. GAPDH, glyceraldehyde-3-phosphate dehydrogenase; K2GFP, green fluorescent protein-tagged kindlin-2; THD, talin-1 head domain; Tln1V, Venus-tagged full length talin-1.

DOI: http://dx.doi.org/10.7554/eLife.10130.012

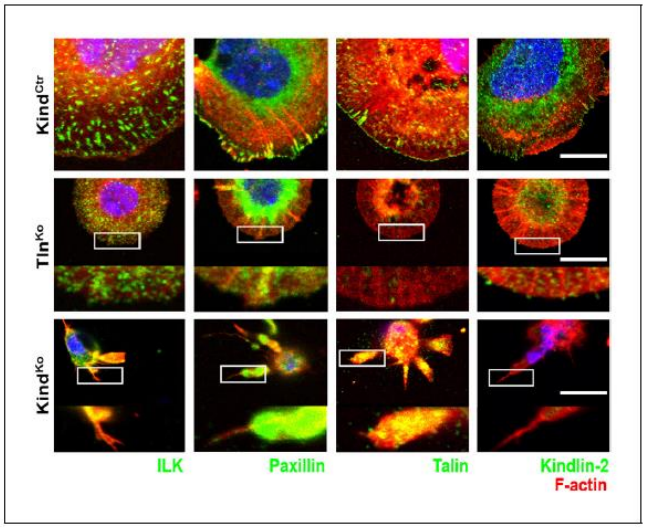

Figure 3—figure supplement 1. Localization of FAs proteins in Mn^{2+}-treated $Kind^{Ctr}$, Tln^{Ko} and $Kind^{Ko}$ cells. Confocal images of the ventral plasma membrane of adherent, Mn^{2+}-treated $Kind^{Ctr}$, Tln^{Ko} and $Kind^{Ko}$ cells stained for ILK, paxillin, talin, and kindlin-2 (green), always together with phalloidin to visualize F-actin (red). For Tln^{Ko} and $Kind^{Ko}$, three-fold magnifications of indicated areas are shown. For kindlin-2 staining, acetone-methanol fixation was used. Bar, 10 μm. FAs, focal adhesions; ILK, integrin-linked kinase.
DOI: http://dx.doi.org/10.7554/eLife.10130.015

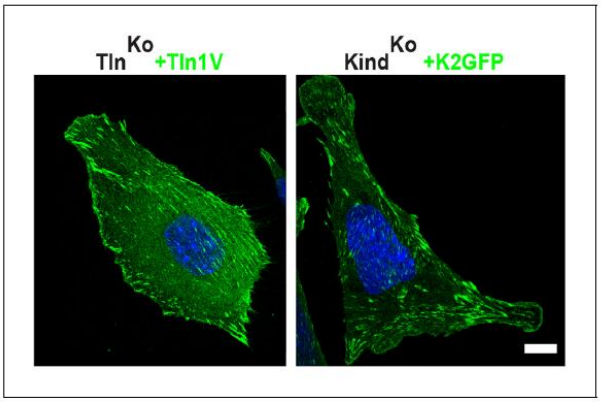

Figure 3—figure supplement 2. Rescue of FA formation and spreading after expression of Tln1V in Tln^{Ko} cells or K2GFP in $Kind^{Ko}$ cells. Confocal images of $Kind^{Ko}$ and Tln^{Ko} cells reconstituted with K2GFP or Tln1V expression plasmids, respectively. Bar, 10 μm. FA, focal adhesion; K2GFP, green fluorescent protein-tagged kindlin-2; Tln1V, Venus-tagged full length talin-1.
DOI: http://dx.doi.org/10.7554/eLife.10130.016

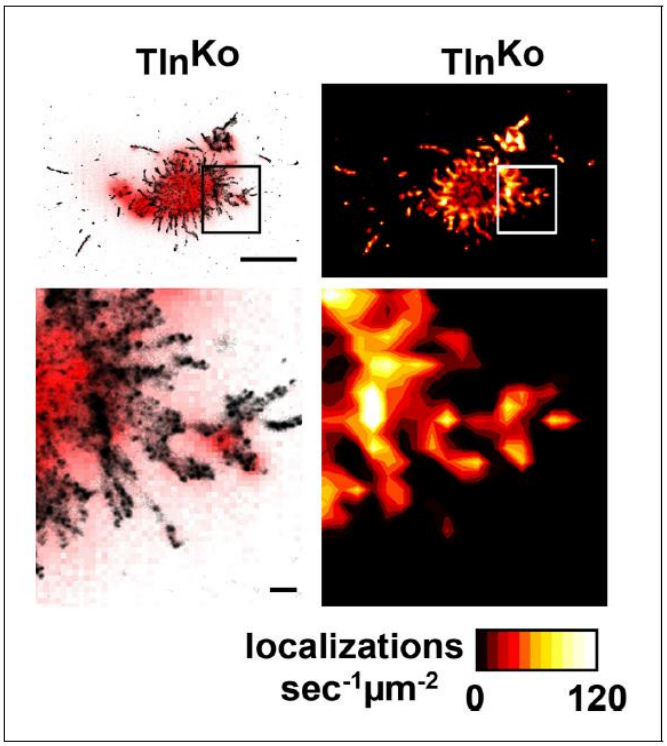

Figure 3—figure supplement 3. Distribution of β1 integrins in spheroid-shaped Tln^{Ko} cells. dSTORM image and density map of β1 integrins in non-spread, spheroid-shaped Tln^{Ko} cells shows aggregation of integrin in the cell body and finger-like protrusions. Bars, 5 µm and 500 nm (for high magnification). dSTORM, direct stochastic optical reconstruction microscopy.

DOI: http://dx.doi.org/10.7554/eLife.10130.017

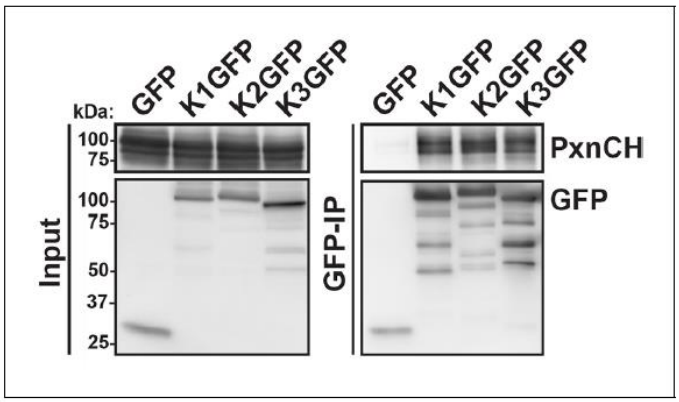

Figure 4—figure supplement 1. Kindlin-1, -2 and -3 interact with paxillin. GFP-IP of lysates from HEK293T cells expressing GFP, K1GFP, K2GFP and K3GFP followed by western blotting for Cherry-tagged paxillin (PxnCH) and GFP. GFP, green fluorescent protein; IP, immunoprecipitation; K1GFP, green fluorescent protein-tagged kindlin-1; K2GFP, green fluorescent protein-tagged kindlin-2; K3GFP, green fluorescent protein-tagged kindlin-3.
DOI: http://dx.doi.org/10.7554/eLife.10130.019

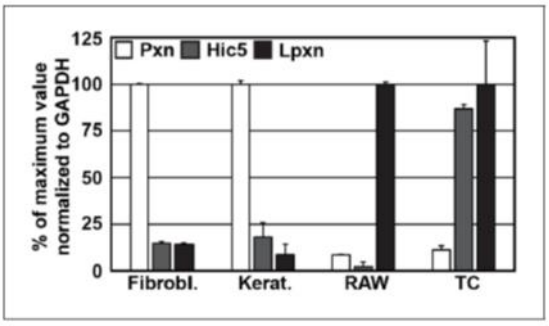

Figure 4—figure supplement 2. Expression of paxillin family members in different cell lines. qPCR of paxillin (Pxn), Hic5, and leupaxin (Lpxn) from cDNAs generated from wild type fibroblasts (Fibrobl.), keratinocytes (Kerat.), RAW 264.7 macrophages (RAW) and T cells (TC). Results are normalized to the isoform with highest expression in the respective cell types (n=3 independent repeats; error bars show standard error of the mean). cDNA, complementary DNA; GAPDH, glyceraldehyde-3-phosphate dehydrogenase; qPCR, quantitative polychromase chain reaction.
DOI: http://dx.doi.org/10.7554/eLife.10130.020

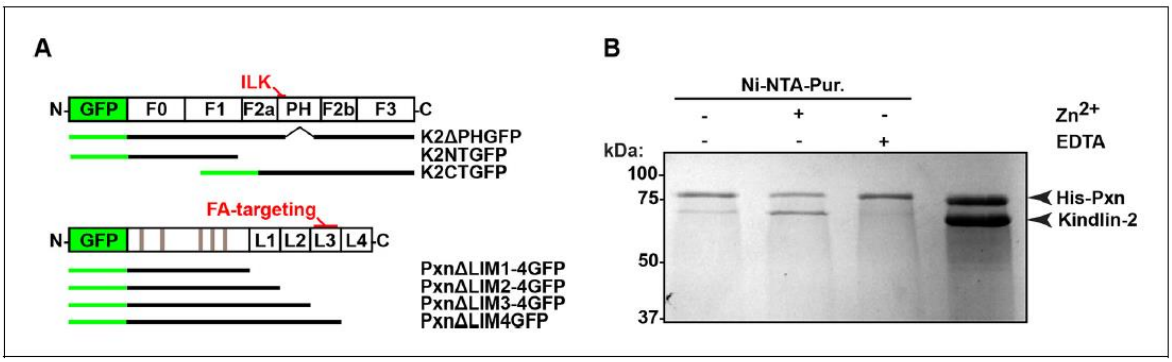

Figure 4—figure supplement 3. Direct interaction between paxillin and kindlin-2. (**A**) Domain organization of kindlin-2 (F0,1,3: FERM domains 0,1,3; F2a,F2b: N-terminal (F2a) and C-terminal (F2b) halves of FERM domain 2 connected by a PH domain and small linkers on each side of the PH domain), and paxillin (L1-4: LIM domains 1-4; grey stripes represent LD-rich motifs). The ILK interaction site in kindlin-2 (N-terminal linker region located before the PH domain) and the FA-targeting region of paxillin (LIM3 domain) are indicated in red; the black lines show the length of the truncation mutants. (**B**) Full-length paxillin pulls down recombinant kindlin-2 in a Zn^{2+}-dependent manner. FERM, Four-point-one, ezrin, radixin, moesin; ILK, integrin-linked kinase; LD, leucine-aspartate repeat; LIM, Lin-11, Isl-1 and Mec-3; PH, pleckstrin homology.

DOI: http://dx.doi.org/10.7554/eLife.10130.021

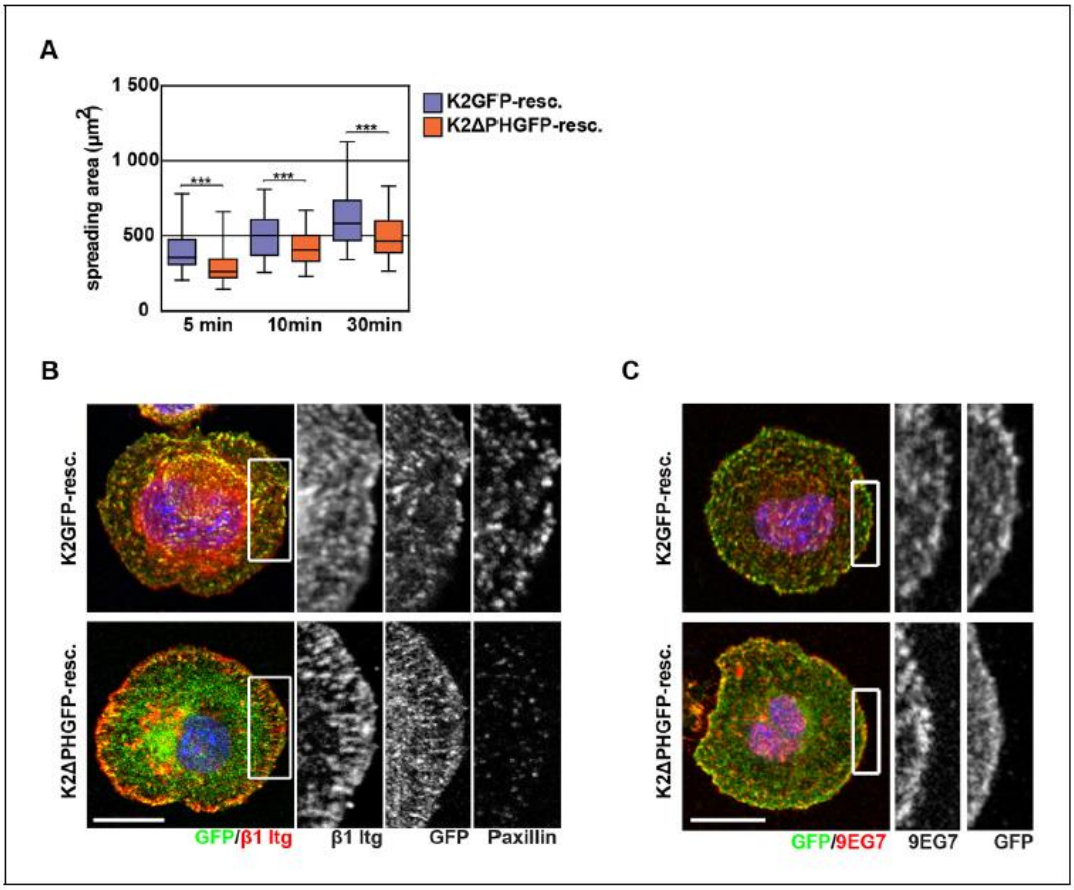

Figure 4—figure supplement 4. K2ΔPHGFP fails to recruit paxillin to β1 integrin-positive adhesions in $Kind^{Ko}$ cells. (**A**) Boxplots show the distribution of spreading areas for K2GFP and K2ΔPHGFP seeded on FN for the indicated times (n> 65 cells per time point). Significances for indicated pairs were calculated by a Mann–Whitney U test. (**B**) Confocal images of K2GFP- and K2ΔPHGFP-expressing $Kind^{Ko}$ cells seeded on FN for 10 min and stained for total β1 integrin and paxillin. (**C**) Confocal images of K2GFP- and K2ΔPHGFP-expressing $Kind^{Ko}$ cells seeded on FN for 10 min and stained for 9EG7. Bars, 10 μm. GFP, green fluorescent protein; FN, fibronectin; K2GFP, green fluorescent protein-tagged kindlin-2.

DOI: http://dx.doi.org/10.7554/eLife.10130.022

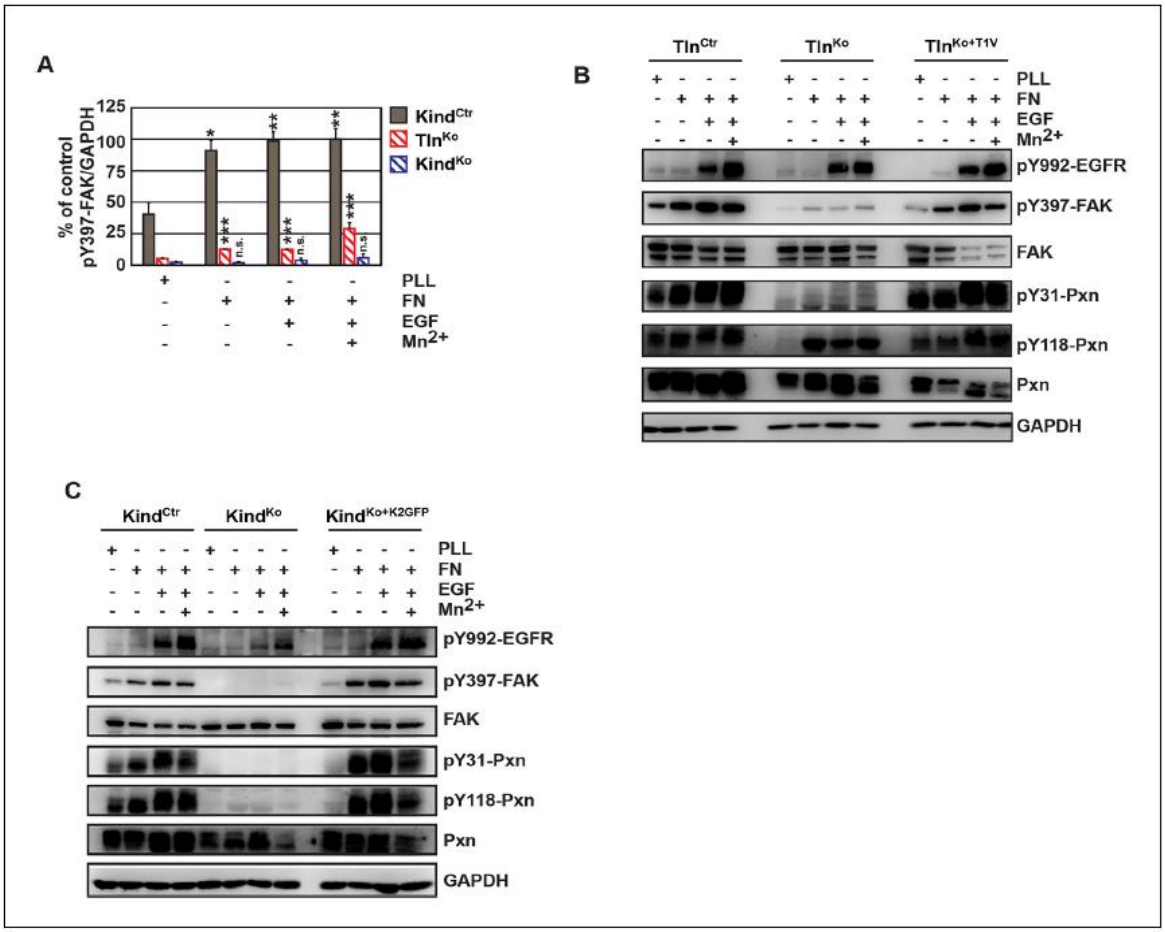

Figure 5—figure supplement 1. FAK phosphorylation in Tln^{Ctr}, Tln^{Ko}, Tln^{Ko+T1V}, $Kind^{Ctr}$, $Kind^{Ko}$ and $Kind^{Ko+K2GFP}$ cells. (**A**) Densitometric quantification of western blot signals of lysates from untreated, EGF- and Mn^{2+}-treated $Kind^{Ctr}$, Tln^{Ko} and $Kind^{Ko}$ cells seeded either on FN or PLL and probed with anti-Tyr-397 phosphorylated FAK (pY397-FAK) antibodies (n=3 independent repeats; significances are calculated with respect to PLL adherent cells; error bars indicate standard error of the mean). (**B**,**C**) Western blotting of indicated signaling proteins in untreated, EGF- and Mn^{2+}-treated Tln^{Ctr}, Tln^{Ko} and Tln^{Ko} cells re-expressing Venus-tagged talin-1 (Tln^{Ko+T1V}) (**B**), and $Kind^{Ctr}$, $Kind^{Ko}$ and $Kind^{Ko}$ cells re-expressing GFP-tagged kindlin-2 ($Kind^{Ko+K2GFP}$) (**C**) seeded either on FN or PLL. EGF, epidermal growth factor; FAK, focal adhesion kinase; K2GFP, green fluorescent protein-tagged kindlin-2; FN, fibronectin; GFP, green fluorescent protein; PLL, poly-L-lysine; T1V, Venus-tagged full length talin-1.

DOI: http://dx.doi.org/10.7554/eLife.10130.024

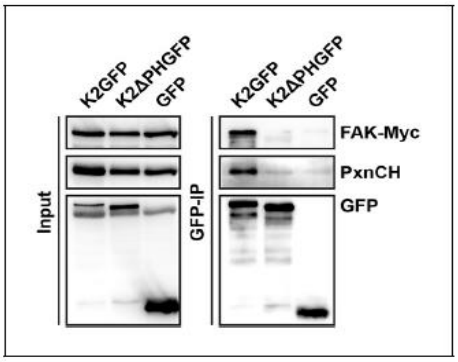

Figure 5—figure supplement 2. Kindlin-2 forms a ternary complex with paxillin and FAK. GFP-IP in lysates of K2GFP-, K2ΔPHGFP- or GFP-reconstituted $Kind^{Ko}$ cells overexpressing Myc-tagged FAK (FAK-Myc) and Cherry-tagged paxillin (PxnCH). K2GFP but not K2ΔPHGFP forms a ternary complex with paxillin and FAK. FAK, focal adhesion kinase; GFP, green fluorescent protein; IP, immunoprecipitation; K2GFP, green fluorescent protein-tagged kindlin-2.
DOI: http://dx.doi.org/10.7554/eLife.10130.025

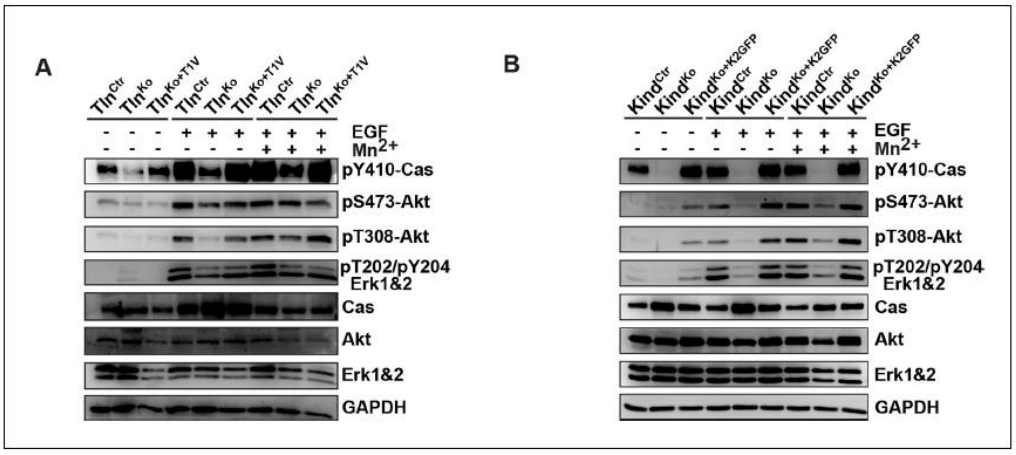

Figure 5—figure supplement 3. Activity of signaling mediators downstream of FAK in Tln^{Ctr}, Tln^{Ko}, Tln^{Ko+T1V}, $Kind^{Ctr}$, $Kind^{Ko}$ and $Kind^{Ko+K2GFP}$ cells. (**A**,**B**) Western blotting of indicated signaling proteins in untreated (first three lanes), EGF- and Mn^{2+}-treated Tln^{Ctr}, Tln^{Ko} and Tln^{Ko} cells re-expressing Venus-tagged talin-1 (Tln^{Ko+T1V}) (**A**), and $Kind^{Ctr}$, $Kind^{Ko}$ and $Kind^{Ko}$ cells re-expressing GFP-tagged kindlin-2 ($Kind^{Ko+K2GFP}$) (**B**) seeded on FN. EGF, epidermal growth factor; FN, fibronectin; GAPDH, glyceraldehyde-3-phosphate dehydrogenase; GFP, green fluorescent protein; K2GFP, green fluorescent protein-tagged kindlin-2; T1V, Venus-tagged full length talin-1.
DOI: http://dx.doi.org/10.7554/eLife.10130.026

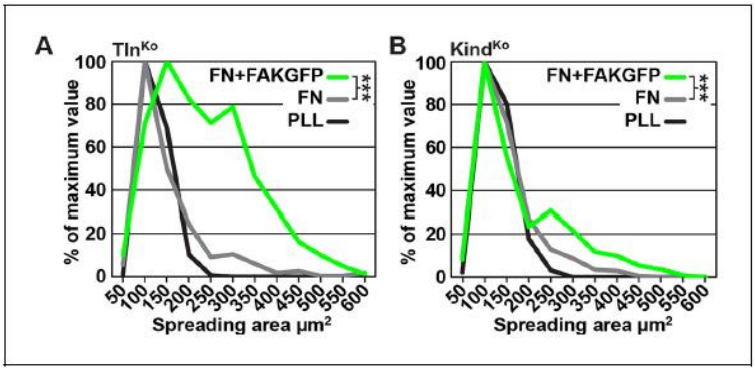

Figure 5—figure supplement 4. Cell spreading of FAK overexpressing Tln^{Ko} and $Kind^{Ko}$ cells. (**A**,**B**) Cell spreading area of Tln^{Ko} (**A**) and $Kind^{Ko}$ cells (**B**) seeded on PLL, FN or on FN after FAKGFP overexpression measured by image quantification (n=3; independent repeats are pooled; >100 cells/condition and repeat; resulting areas are shown as binning histograms; significances are calculated between non-transfected cells and FAKGFP expressing cells plated on FN). FAK, focal adhesion kinase; FAKGFP, green fluorescent protein-tagged FAK; FN, fibronectin; GFP, green fluorescent protein; PLL, poly-L-lysine.

DOI: http://dx.doi.org/10.7554/eLife.10130.027

Published Online: 14 September, 2017 | Supp Info: http://doi.org/10.1083/jcb.201701176

Kindlin-2 recruits paxillin and Arp2/3 to promote membrane protrusions during initial cell spreading

Ralph T. Böttcher,[1,2] Maik Veelders,[1] Pascaline Rombaut,[3] Jan Faix,[4] Marina Theodosiou,[1] Theresa E. Stradal,[5] Klemens Rottner,[5,6] Roy Zent,[7,8] Franz Herzog,[3] and Reinhard Fässler[1,2]

[1]Department of Molecular Medicine, Max Planck Institute of Biochemistry, Martinsried, Germany
[2]German Centre for Cardiovascular Research (DZHK), partner site Munich Heart Alliance, Munich, Germany
[3]Gene Center Munich, Ludwig Maximilians University Munich, Munich, Germany
[4]Institute for Biophysical Chemistry, Hannover Medical School, Hannover, Germany
[5]Helmholtz Centre for Infection Research, Braunschweig, Germany
[6]Zoological Institute, Technische Universität Braunschweig, Braunschweig, Germany
[7]Division of Nephrology, Department of Medicine, Vanderbilt University, Nashville, TN
[8]Department of Medicine, Veterans Affairs Medical Center, Nashville, TN

Cell spreading requires the coupling of actin-driven membrane protrusion and integrin-mediated adhesion to the extracellular matrix. The integrin-activating adaptor protein kindlin-2 plays a central role for cell adhesion and membrane protrusion by directly binding and recruiting paxillin to nascent adhesions. Here, we report that kindlin-2 has a dual role during initial cell spreading: it binds paxillin via the pleckstrin homology and F0 domains to activate Rac1, and it directly associates with the Arp2/3 complex to induce Rac1-mediated membrane protrusions. Consistently, abrogation of kindlin-2 binding to Arp2/3 impairs lamellipodia formation and cell spreading. Our findings identify kindlin-2 as a key protein that couples cell adhesion by activating integrins and the induction of membrane protrusions by activating Rac1 and supplying Rac1 with the Arp2/3 complex.

Introduction

Cell migration and cell spreading are multistep processes involving protrusion of the plasma membrane, induction of new adhesions to the underlying substratum, and maturation and turnover of adhesion sites (Petrie et al., 2009; Devreotes and Horwitz, 2015). The different processes critically rely on the coordinated and dynamic regulation of integrin-mediated adhesions and actin structures, e.g., the formation of nascent adhesions (NAs) and branched actin networks in lamellipodia, and the assembly of stress fibers that connect focal adhesions (FAs) further toward the middle and rear of spread cells. Lamellipodia are smooth and narrow projections of the plasma membrane that extend along the cell edges and are initiated by the actin nucleation activity of the Arp2/3 complex (Pollard and Borisy, 2003). The canonical Arp2/3 complex consists of seven subunits (Machesky et al., 1994; Welch et al., 1997; Winter et al., 1997; Bugyi and Carlier, 2010), binds to the sides of already existing actin filaments, and triggers the growth of new actin branches. The actin nucleation activity of the Arp2/3 complex is induced by members of the Wiskott–Aldrich syndrome protein family, including WASP and WAVE (Mullins et al., 1998; Rohatgi et al., 1999; Winter et al., 1999; Rouiller et al., 2008), whose activity in turn is controlled by small Rho-like GTPases, including Rac1 and Cdc42 (Takenawa and Suetsugu, 2007).

The physical coupling of the branched actin network to the ECM occurring in lamellipodia and membrane protrusions of isotropically spreading cells is achieved by integrin-mediated adhesions that initially form as small, short-lived NAs at or near the edge of protruding membranes. Once formed, they either disassemble or mature in an actomyosin-dependent manner into large and long-lived FAs (Vicente-Manzanares and Horwitz, 2011). The induction of integrin-mediated adhesions requires an integrin-activation step characterized by the conformational shift of the unbound, low-affinity (inactive) state to the bound, high-affinity (active) state, which is followed by integrin clustering to stabilize integrin–ligand complexes and the assembly of a large multiprotein network that enables signaling. The two cytosolic adaptor proteins talin and kindlin bind to β integrin cytoplasmic domains and induce and/or maintain integrin-mediated cell–extracellular matrix adhesion. The prevalent view is that talin and kindlin cooperate to induce integrin activation (Han et al., 2006; Moser et al., 2008; Theodosiou et al., 2016) and clustering (Cluzel et al., 2005; Ye et al., 2013). An additional function of kindlin is to induce membrane protrusions during early, isotropic cell spreading by directly binding

Correspondence to Ralph T. Böttcher: rboettch@biochem.mpg.de

Abbreviations used: co-IP, coimmunoprecipitation; FA, focal adhesion; FN, fibronectin; IF, immunofluorescence; ITC, isothermal titration calorimetry; KO, knockout; MS, mass spectrometry; NA, nascent adhesion; PH, pleckstrin homology; PLL, poly-L-lysine; qKO, quadruple knockout; TCEP, tris(2-carboxyethyl) phosphine; VN, vitronectin; XL-MS, cross-linking mass spectrometry.

and recruiting paxillin to NAs, which in turn leads to FAK and Rac1 activation (Theodosiou et al., 2016).

Arp2/3–driven membrane protrusion and integrin-mediated adhesion to the ECM in NAs are tightly coupled and depend on each other. It has been shown that Arp2/3 can be recruited to adhesion sites through transient interactions with vinculin (DeMali et al., 2002; Chorev et al., 2014) and FAK (Serrels et al., 2007; Swaminathan et al., 2016).

Talin is unable to induce circumferential membrane protrusions during isotropic spreading in the absence of kindlin-2 (Theodosiou et al., 2016). Because kindlin-2 recruits paxillin and FAK, which in turn was shown to induce Rac1 activation and membrane protrusion, we hypothesized that by circumventing the Rac1 activation defect in kindlin-deficient cells, cell spreading should efficiently be induced. In this study, we tested this hypothesis and further characterized the kindlin-2–paxillin complex using cross-linking proteomics. The findings of our studies are discussed here.

Results

Kindlin-2 directly binds paxillin through the PH and F0 domains

In a previous study, we reported a direct, Zn^{2+}-dependent interaction between the pleckstrin homology (PH) domain of kindlin-2 and the Lin-11, Isl-1, and Mec-3 (LIM3) domain of paxillin by size-exclusion chromatography and pull-down experiments (Theodosiou et al., 2016). Furthermore, we found that the absence of the PH domain in kindlin-2 leads to low levels of paxillin in NAs but to normal levels in mature FAs of fibroblasts (Theodosiou et al., 2016), indicating that paxillin recruitment to FAs occurs either in a kindlin-independent manner or through additional, unrecognized paxillin-binding sites in kindlin. To test the latter possibility, we performed cross-linking mass spectrometry (XL-MS) experiments of recombinant kindlin-2–paxillin complexes by cross-linking the amine groups of lysine side chains with an isotopically coded bis-sulfosuccinimidyl suberate (Leitner et al., 2010). Cross-linked peptides were identified by tandem mass spectrometry (MS) and used to assemble a map of the inter- and intraprotein cross-links of the kindlin-2–paxillin complex (Figs. 1 A and S1 A and Supplemental dataset). We identified cross-links between the N-terminal LD motifs of paxillin and the PH domain of kindlin-2. In addition, we also observed multiple cross-links between the F0 domain of kindlin-2 and the LIM3/4 domains and the LD motifs of paxillin, suggesting that the PH as well as the F0 domains contribute to kindlin-2 binding to paxillin.

We verified the XL-MS results by analytical ultracentrifugation, in which fluorescent labeling of one of the two interaction partners was used at a time to detect the corresponding absorption wavelengths. The in vitro reconstituted kindlin-2–paxillin complex sedimented at 4.3 S, whereas recombinant kindlin-2 lacking the F0 and PH domains failed to form a detectable complex with paxillin (Fig. 1 B). Recombinant F0 and PH domains and a hybrid F0–PH domain of kindlin-2 were able to bind paxillin (Fig. 1 C). Interestingly, the sedimentation coefficients of paxillin associated with the F0 or PH domain of kindlin-2 were lower than the sedimentation coefficient of paxillin alone, indicating that the impact of the weight increase on the sedimentation coefficient is compensated by an induced compaction of paxillin upon complex formation with either the F0 or PH domain.

Next, we performed affinity measurements using isothermal titration calorimetry (ITC). The affinity of paxillin for full-length kindlin-2 was 205 ± 59 nM, whereas the affinities of paxillin to the F0 or the PH domain alone were lower and ranged between 1,920 ± 628 and 1,080 ± 320 nM, respectively (Fig. 1, D–F). Addition of EDTA abolished the interactions with paxillin, indicating that not only binding of full-length kindlin-2 but also binding of the isolated F0 or PH domain is Zn^{2+} ion dependent (Fig. S1, B–D). Altogether, these data point to the existence of a second, previously unnoticed paxillin-binding domain in kindlin-2 and suggest that both domains bind concurrently to increase the affinity of kindlin-2 to paxillin.

The kindlin-2 PH and F0 domains are required for cell adhesion and spreading

To characterize kindlin-2–paxillin binding in cells, we isolated, immortalized and cloned kidney fibroblasts from mice carrying floxed kindlin-1 (*Fermt1*$^{flox/flox}$), kindlin-2 (*Fermt2*$^{flox/flox}$), *Tln1* alleles, and nullizygous *Tln2* alleles (Flox cells; Fig. 2 A). To directly compare kindlin-2 and talin-1 functions in the same cellular background, the floxed alleles were deleted by adenoviral expression of *Cre* recombinase, resulting in kindlin-1, kindlin-2, talin-1, and talin-2–deficient (quadruple knockout [qKO]) cells, and reconstituted with C-terminally mCherry-tagged talin-1 (T1-mCherry), N-terminally EGFP-tagged kindlin-2 (EGFP-K2), or a combination of both (T1-mCherry + EGFP-K2).

Cre treatment deleted the floxed *Tln1* and floxed *Fermt1/2* genes (Fig. 2 B), resulted in cell rounding (Fig. 2 C), and abolished adhesion of the resulting qKO cells to fibronectin (FN) and vitronectin (VN; Fig. 2, D and E). Reexpression of T1-mCherry or EGFP-K2 did not rescue the severe adhesion defects of qKO cells when plated on FN or VN, whereas coexpression of T1-mCherry together with EGFP-K2 rescued cell adhesion and spreading (Fig. 2, B–E). Importantly, loss of endogenous talin and/or kindlin as well as reexpression of T1-mCherry and/or EGFP-K2 did not change surface levels of the FN-binding integrins α5β1 and αvβ3. In fact, α5, αv and β3 levels were increased in qKO and single reconstituted cells (Fig. 2 F).

Next, we expressed either EGFP-K2 or EGFP-tagged kindlin-2 truncation mutants that lacked either the F0 (EGFP-K2ΔF0) or the PH domain (EGFP-K2ΔPH) or both domains (EGFP-K2ΔF0ΔPH) in T1-mCherry cells (Fig. 3 A) and performed coimmunoprecipitation (co-IP) assays. The experiments revealed that paxillin coprecipitated EGFP-K2, whereas the co-IP of EGFP-K2ΔF0 or EGFP-K2ΔPH were reduced and of the K2ΔF0ΔPH abolished (Fig. 3 B), confirming that both the F0 and PH domains of kindlin-2 contribute to paxillin binding.

In line with our previous finding (Theodosiou et al., 2016), qKO cells expressing either T1-mCherry or EGFP-K2 failed to adhere to FN (Fig. 2 D). Reexpression of EGFP-K2 in T1-mCherry expressing cells fully rescued adhesion to FN, whereas reexpression of EGFP-K2ΔF0 or EGFP-K2ΔPH only partially rescued adhesion and reexpression of EGFP-K2ΔF0ΔPH almost completely abolished cell adhesion and spreading (Fig. 3, C and D, gray bars without Mn^{2+}). Furthermore, EGFP-K2, EGFP-K2ΔF0, and EGFP-K2ΔPH localized to FAs in kindlin-2–deficient T1-mCherry cells, whereas the few adhering EGFP-K2ΔF0ΔPH expressing T1-mCherry cells remained round and failed to form discernable FAs (Fig. S2).

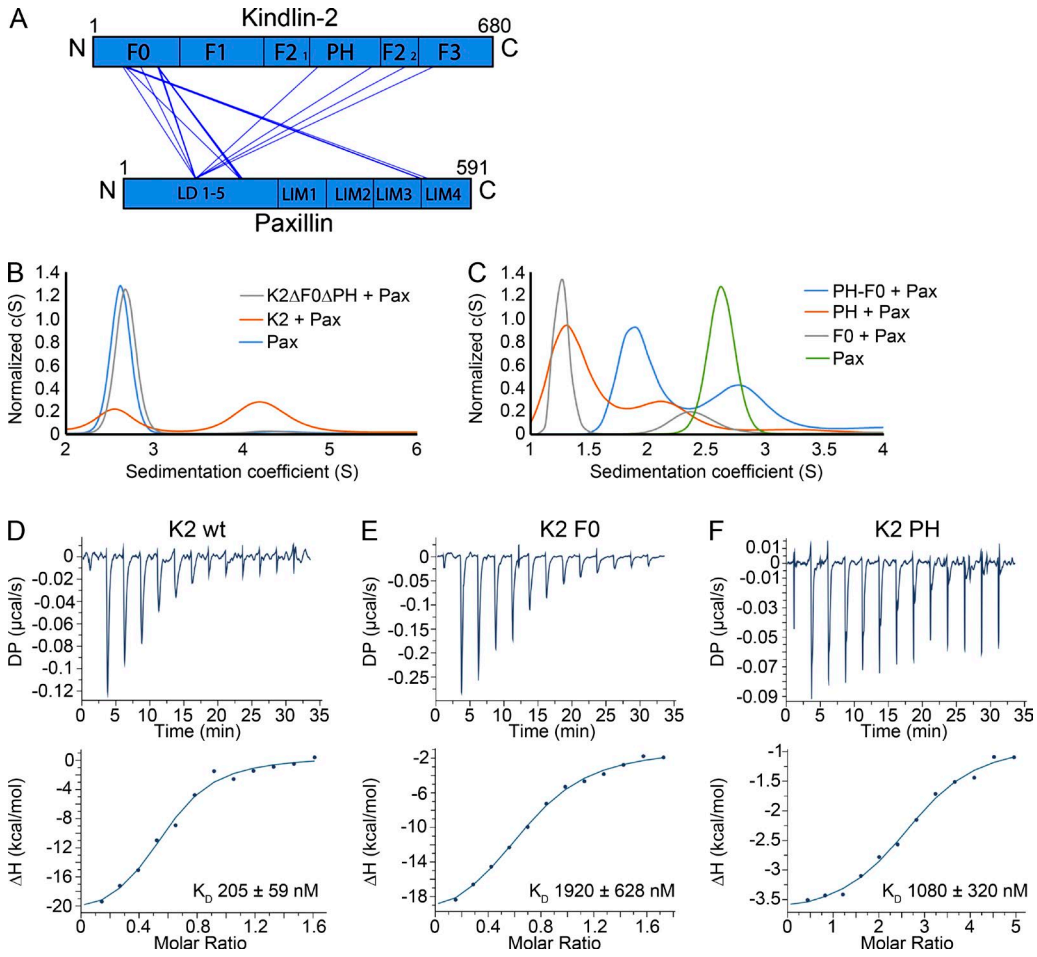

Figure 1. **Cross-linking identifies two distinct kindlin-2–paxillin interaction sites.** (A) Cross-link map of the kindlin-2–paxillin interaction. Cross-links are detected between the kindlin-2 PH domain and the paxillin LD motifs and between the kindlin-2 F0 domain and paxillin LD motifs and LIM3-domain region. Intraprotein cross-links are not depicted for clarity. F0, F1, F2, and F3 part of the FERM domain; C, C terminus; LD, LD motifs; LIM, Lin-11, Isl-1 and Mec-3 domain; N, N terminus. (B) Analytical ultracentrifugation profiles of Atto520-labeled paxillin (Pax) in complex with wild-type kindlin-2 and K2ΔF0ΔPH. (C) Complex formation of paxillin with different Atto520-labeled kindlin-2 subdomains determined by analytical ultracentrifugation. (D–F) Isothermal titration calorimetry measurements of paxillin bound to K2 wild type (D), K2 F0 (E), or K2 PH (F). c(S), continuous sedimentation coefficient distribution; DP, differential power.

To bypass integrin activation, we treated cells with Mn^{2+}, which binds to the integrin ectodomain and induces the conformational changes of activated integrins (Mould et al., 1995). The experiments revealed that expression of EGFP-K2ΔF0 and EGFP-K2ΔPH almost completely rescued adhesion of T1-mCherry–expressing cells to FN. In contrast, EGFP-K2ΔF0ΔPH expression only slightly increased adhesion in the presence of Mn^{2+} (Fig. 3 D).

To test whether the EGFP-K2ΔF0ΔPH expressing cells also exhibit defects in integrin outside-in signaling, we analyzed spreading of cells seeded for 30 min on FN in the presence or absence of Mn^{2+}. In the absence of Mn^{2+}, T1-mCherry cells expressing EGFP-K2ΔF0 or EGFP-K2ΔPH spread less compared with T1-mCherry cells expressing EGFP-K2 (Fig. 3 E). Expression of EGFP-K2ΔF0ΔPH in T1-mCherry cells increased the spreading area much less efficiently than expression of EGFP-K2ΔF0 or EGFP-K2ΔPH in T1-mCherry (Fig. 3 E). Altogether, these findings indicate that the absence of either the F0 or PH domain of kindlin-2 impairs cell spreading, whereas the lack of both domains further curbs spreading.

Active Rac1 requires kindlin-2 to induce cell spreading

We previously reported that expression of kindlin-2, but not talin-1, enables isotropic cell spreading in the presence of Mn^{2+} and serum (Theodosiou et al., 2016). Our findings so far revealed that binding of the F0 and PH domains of kindlin-2 to paxillin is required for normal adhesion and spreading of T1-mCherry–expressing cells. Moreover, the absence of F0 and PH domains in kindlin-2 abrogated activation of FAK (Fig. 4 A), which in turn assembles the FAK–Src–p130Cas–Dock180 complex to induce Rac1-mediated cell spreading (Schlaepfer et al., 2004; Brami-Cherrier et al., 2014; Zhang et al., 2014). In line with this finding, the levels of active, GTP-bound Rac1 did not increase in Mn^{2+}-treated T1-mCherry cells adhering to FN and expressing EGFP-K2ΔF0ΔPH (Fig. 4 B).

Next, we tested whether a constitutively active myc-tagged Rac1 Q61L is able to induce spreading of T1-mCherry or K2-EGFP cells. To this end, we retrovirally transduced the cells with Rac1 Q61L (Fig. 4 C) and seeded them on FN without serum or growth factors and in the presence or absence of Mn^{2+}. In the absence of Mn^{2+}, the sporadic and very weakly

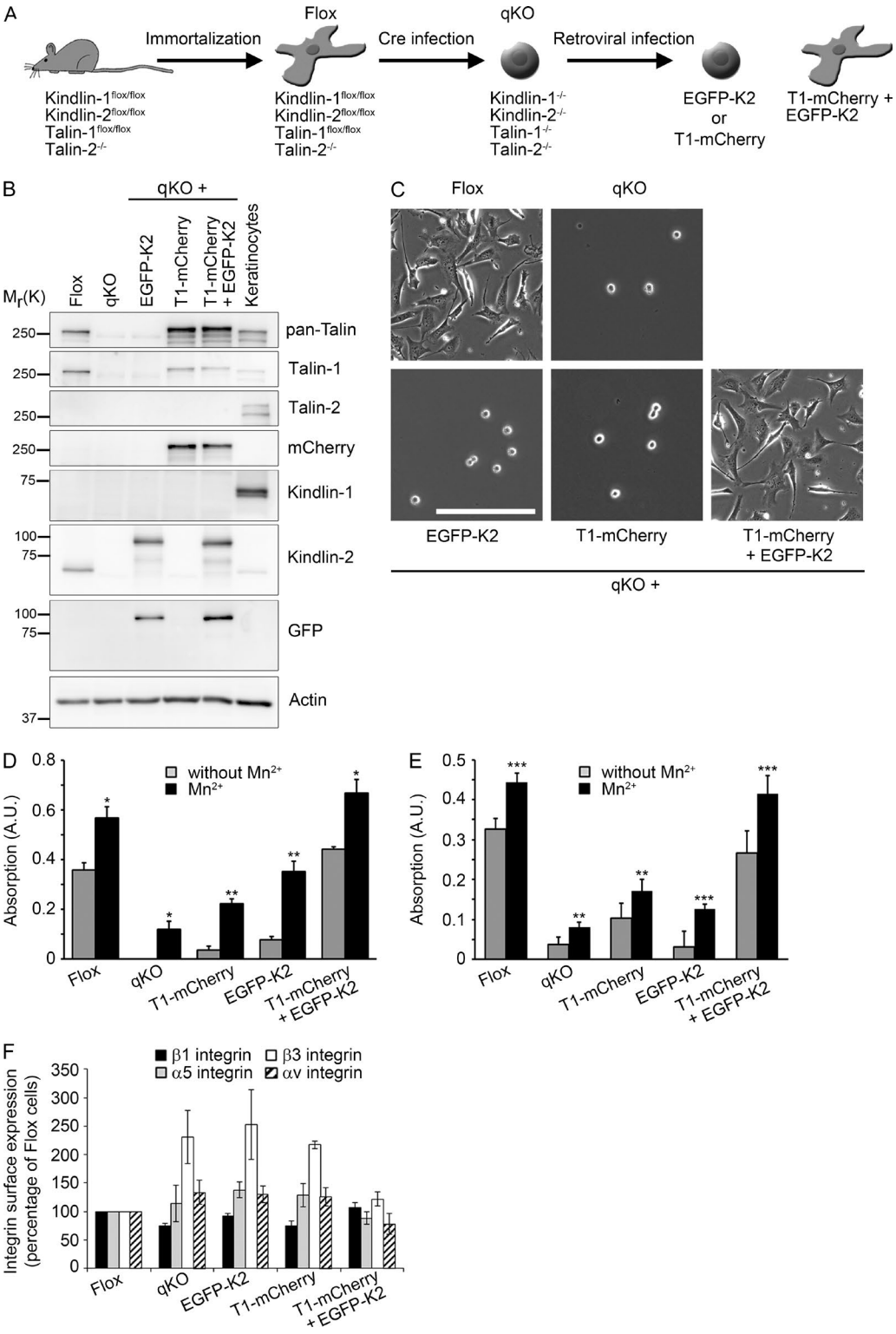

Figure 2. **Kindlin and talin cooperate to establish cell adhesion.** (A) Scheme for the generation of qKO cells from mouse kidney lacking talin-1/-2 as well as kindlin-1/-2. qKO fibroblasts were retrovirally transduced with EGFP-kindlin-2 (EGFP-K2), talin-1-mCherry (T1-mCherry), or a combination of both. (B) Western blot of Flox, qKO, and EGFP-K2, T1-mCherry–expressing cells. Keratinocyte lysates served to control kindlin-1 and talin-2 expression. (C) Phase contrast images of the indicated cell lines. Bar, 200 µm. (D) Quantification of cell adhesion on FN 30 min after seeding in the absence or presence of 5 mM Mn^{2+} (n = 3 independent experiments). Error bars indicate SEM; significance was calculated between untreated cells and the corresponding Mn^{2+}-treated cells (t test). (E) Quantification of cell adhesion on VN 30 min after seeding in the absence or presence of 5 mM Mn^{2+} (n = 4 independent experiments). Error bars indicate SEM; significance was calculated between untreated cells and the corresponding Mn^{2+}-treated cells (t test). *, P < 0.05; **, P < 0.01; ***, P < 0.001. (F) Quantification of cell surface expression of different integrin subunits on Flox, qKO, and EGFP-K2, T1-mCherry–reexpressing cells measured by flow cytometry. The integrin levels were normalized to the levels on Flox cells (n = 3 independent experiments). Error bars indicate SD.

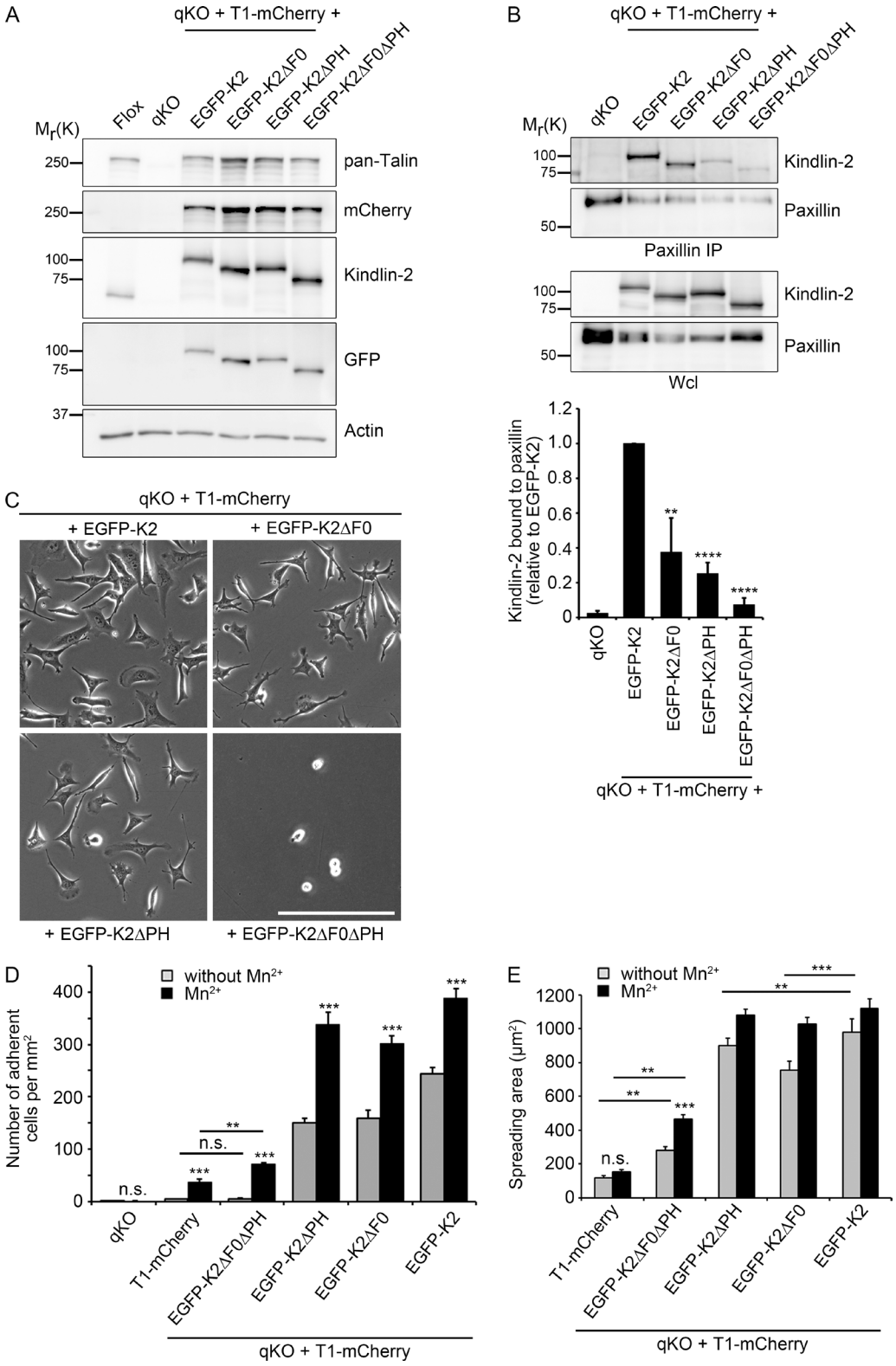

Figure 3. **Kindlin-2 requires paxillin binding to induce cell adhesion and spreading.** (A) Western blot of parental Flox cells, qKO cells, and qKO cells expressing T1-mCherry and EGFP-tagged kindlin-2 (K2), K2ΔF0, K2ΔPH, or K2ΔF0ΔPH. (B) Co-IP of endogenous paxillin and densitometric analysis of Western blots to determine paxillin binding to EGFP-tagged kindlin-2 (K2), K2ΔF0, K2ΔPH, or K2ΔF0ΔPH. Graph shows kindlin-2 binding to paxillin relative to EGFP-K2. Wcl, whole cell lysate (n = 3 independent experiments). Error bars indicate SD; significance was calculated between EGFP-K2 and the kindlin-2 deletion variants (t test). (C) Phase contrast images of indicated cell lines. Bar, 200 µm. (D) Quantification of adhesion to FN of qKO cells expressing T1-mCherry alone or in combination with EGFP-tagged kindlin-2 (K2), K2ΔF0, K2ΔPH, or K2ΔF0ΔPH for 30 min in the absence or presence of 5 mM Mn^{2+} (n = 4 independent experiments). Error bars indicate SEM; significance was calculated between untreated cells and the corresponding Mn^{2+}-treated cells (t test). (E) Quantification of the cell area after spreading on FN for 30 min in the absence and presence of 5 mM Mn^{2+} (>50 cells counted in two independent experiments). Error bars indicate SEM; significance is indicated (t test). **, P < 0.01; ***, P < 0.001; ****, P < 0.0001; n.s., not significant.

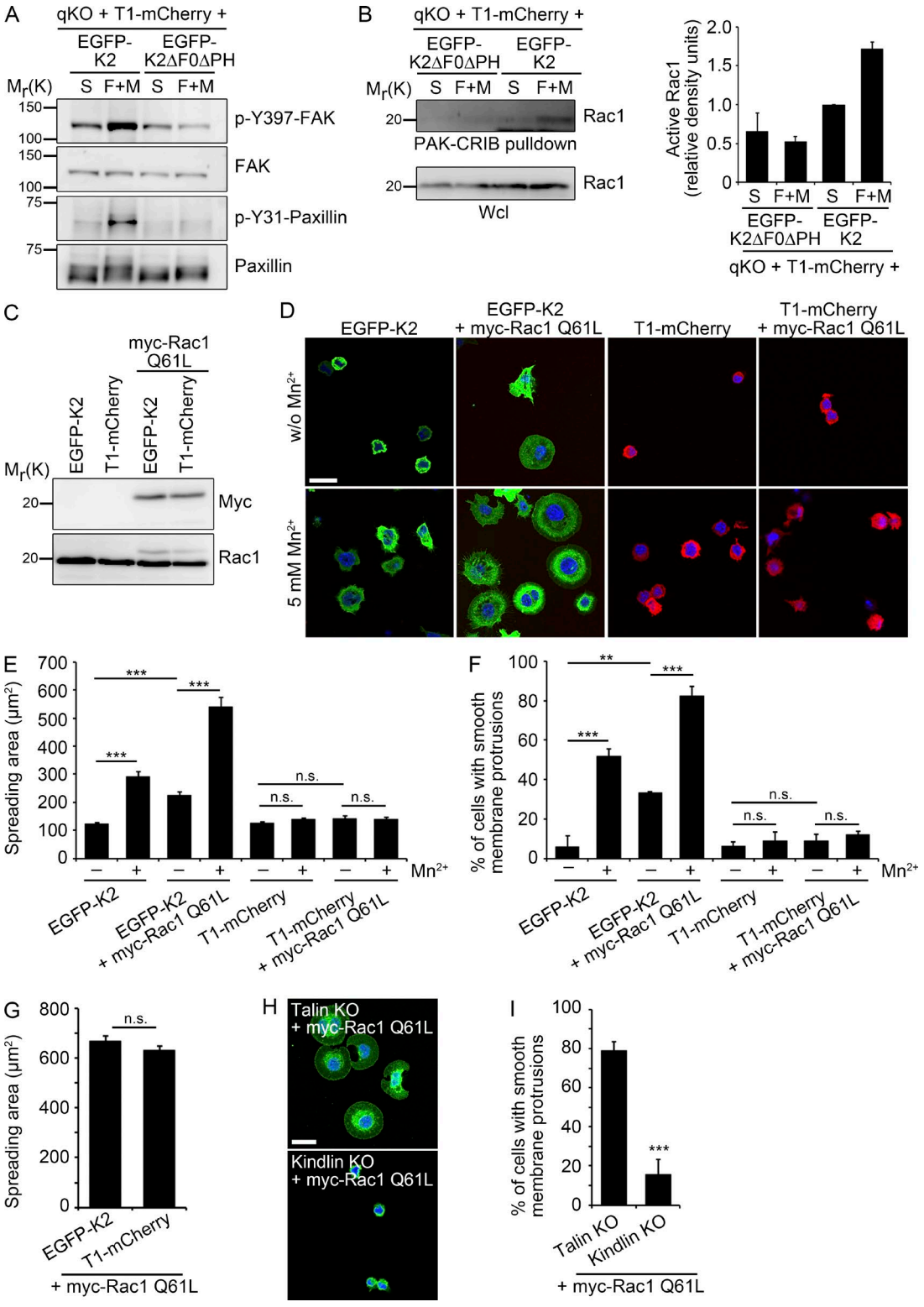

Figure 4. **The kindlin–paxillin complex induces Rac1 activation and cell spreading.** (A) Levels of phosphorylated FAK and paxillin in cell lines kept in suspension (S) or seeded on FN for 30 min in the presence of Mn^{2+} and serum (F+M). (B) Western blot and densitometric analysis (n = 2) of Rac1 activation in cell lines kept in suspension (S) or seeded on FN for 15 min in the presence of Mn^{2+} and serum (F+M). The bar chart shows results that were quantified and normalized against total Rac1 levels. (C) Western blot of T1-mCherry and EGFP-K2 cells expressing constitutively active myc-tagged Rac1 (myc-Rac1 Q61L). (D) Fluorescence images of T1-mCherry and EGFP-K2 cells transduced with or without myc-Rac1 Q61L and allowed to spread for 30 min on FN in the absence or presence of 5 mM Mn^{2+}. DAPI was used to stain nuclei. Bar, 25 µm. (E and F) Quantification of spreading area (E) and membrane protrusions (F) of FN-seeded T1-mCherry and EGFP-K2 cells expressing myc-Rac1 Q61L and treated with or without 5 mM Mn^{2+} 30 min after seeding the cells on FN (n = 3 independent experiments; >90 cells/condition). Error bars indicate SEM; n.s., not significant. (G) Quantification of spreading area 30 min after plating of PLL-seeded T1-mCherry and EGFP-K2 cells expressing myc-Rac1 Q61L (n = 3 independent experiments; >130 cells/condition). Error bars indicate SEM; n.s., not significant. (H) Immunofluorescence images of talin KO and kindlin KO cells transduced with myc-Rac1 Q61L and allowed to

adherent EGFP-K2 cells remained small and lacked membrane protrusions, whereas Mn^{2+} treatment improved cell adhesion and induced circumferential membrane protrusions, which further increased upon expression of Rac1 Q61L (Fig. 4, D–F). Interestingly, T1-mCherry–expressing cells failed to form large membrane protrusions on FN and upon expression of Rac1 Q61L, irrespective of whether Mn^{2+} was absent or present in the culture medium (Fig. 4, D–F), whereas integrin-independent spreading on poly-L-lysine (PLL) was not affected by the absence of kindlin-2 (Fig. 4 G). Importantly, similar results were obtained upon expression of Rac1 Q61L in our previously published talin knockout (KO) cells that express kindlin-2 and kindlin KO cells that express talin-1 (Theodosiou et al., 2016), excluding clonal effects as cause for the absent membrane protrusions in cells co-expressing talin and Rac Q61L (Fig. 4, H and I). Altogether these findings suggest that kindlin-2, aside from operating upstream of Rac1, also provides an additional function to initiate Rac1-induced membrane protrusions, which is lacking in talin-1–expressing T1-mCherry cells.

Kindlin-2 associates with the Arp2/3 complex

Because kindlin-2, but not talin-1, was able to induce stable membrane protrusions upon expression of Rac1 Q61L, we hypothesized that kindlin-2 harbors an additional functional feature that operates in parallel to the activation of FAK/Rac1. To identify new functional properties of kindlin-2, we screened for novel interaction partners by immunoprecipitation of GFP-tagged kindlin-2 followed by MS. Among proteins that were precipitated with kindlin-2 were subunits of the Arp2/3 complex (Fig. 5 A), which triggers the circumferential membrane protrusion with the characteristic smooth rim during early cell spreading (Suraneni et al., 2012, 2015). Although Western blots revealed similar levels of Arp2/3 and Arp2/3–activating WAVE2 protein in EGFP-K2 and T1-mCherry cells (Fig. 5 B), chemical inhibition of Arp2/3 (Nolen et al., 2009) strongly reduced the formation of lamellipodial protrusions in Mn^{2+}-treated EGFP-K2 cells (Fig. S3 A), highlighting the crucial role of Arp2/3 for kindlin-2–mediated formation of membrane protrusions. Hence, we decided to further analyze the relationship of the two proteins.

Consistent with the proteomic data, in vitro pull-down assays revealed that recombinant His-tagged kindlin-2 (His-K2) bound the purified Arp2/3 protein complex (Fig. 5 C). Furthermore, GFP-K2 coimmunoprecipitated the Arp2/3 complex (Fig. 5 D), and conversely, Arp2/3 complex members were able to coimmunoprecipitate endogenous kindlin-2 (Fig. 5 E). Finally, kindlin-2 colocalized with the Arp2/3 complex and the WAVE complex component Abi1 in membrane protrusions of spreading cells, but not in FAs (Fig. 5, F and G).

Next, we determined the kinetics of the interaction between kindlin-2 and the Arp2/3 complex before and after plating T1-mCherry + EGFP-K2–expressing cells on FN. The co-IP experiments revealed that the interaction of kindlin-2 with Arp3 was highest in suspended, nonadherent cells and in the first 5 min after seeding and sharply decreased ∼10 min after seeding (Fig. 5 H). Interestingly, neither vinculin nor FAK coimmunoprecipitated with kindlin in suspended and early spreading cells (Fig. 5 H). Furthermore, the association of kindlin-2 and Arp2/3 remained unaffected in vinculin-deficient and FAK-depleted cells (Fig. S3, B and C), which altogether suggests that kindlin-2–Arp2/3 complexes exist independently of vinculin–Arp2/3 (DeMali et al., 2002; Chorev et al., 2014) and FAK–Arp2/3 complexes (Serrels et al., 2007; Swaminathan et al., 2016) to induce membrane protrusions from newly assembled adhesion sites at the periphery of the plasma membrane.

The integrity of the Arp2/3-kindlin-2 complex is required for cell spreading

The interaction between FAK and Arp2/3 is mediated by lysine-38 and arginine-86 located in the F1 subdomain of the four-point-one, ezrin, radixin, moesin (FERM) domain of FAK and the Arp2/3 complex (Serrels et al., 2007). We also observed that the F1 subdomain of kindlin-2 was required to efficiently coimmunoprecipitate Arp3 (Fig. 6 A). A superposition of the FAK FERM F1 domain and a model of the mouse kindlin-2 F1 domain suggested that arginine-100 and leucine-141 of kindlin-2 occupy the positions of lysine-38 and arginine-86 in FAK (Fig. 6 B). To test this hypothesis, we generated qKO cells stably expressing T1-mCherry and an EGFP-tagged kindlin-2, in which arginine-100 and leucine-141 were substituted with alanine residues (EGFP-K2 RL/AA). Although EGFP-K2 RL/AA localized to talin-1–containing adhesion structures and allowed cell adhesion (Fig. 6 C), EGFP-K2 RL/AA coimmunoprecipitated less Arp3 than EGFP-K2 (Fig. 6 D).

A time course analysis of cell spreading showed that 30 min after cell seeding, only approximately half of EGFP-K2 RL/AA–expressing cells were spread (Fig. 6, E and F; and Fig. S4, A and B), and only 22% formed ArpC5A-positive, protrusive membranes (22% ± 5%, n = 162) compared with 80% spread EGFP-K2 expressing cells, of which 70% displayed ArpC5A-positive membrane protrusions (70% ± 4%, n = 93; Fig. 6, F and G). A similar spreading defect was observed upon expression of EGFP-K2 RL/AA in an independent kindlin KO cell line (Theodosiou et al., 2016), although the differences were less pronounced (Fig. 6 H). Altogether, these findings indicate that the Arp2/3–kindlin-2 complex promotes the production of protrusive membranes during early cell spreading and lamellipodia formation.

Discussion

In the present study, we report two major findings. First, we identified a previously unrecognized interaction between the kindlin-2 F0 domain and the LIM3/4 domains as well as the LD motifs of paxillin using cross-linking proteomics. A deletion mutant of kindlin-2 lacking the F0 and PH domain failed to bind paxillin and localize to adhesion sites, suggesting that both sites contribute to paxillin binding and integrin-ligand binding, possibly through the recruitment of proteins to the kindlin-2–paxillin complex.

Second, we observed that constitutively active Rac1 (Rac1 Q61L) induced isotropic spreading with circumferential

spread for 20 min on FN in the presence of 5 mM Mn^{2+}. Cells were stained with an antibody against β1 integrin. DAPI was used to stain nuclei. Bar, 20 µm. (I) Quantification of membrane protrusions of FN-seeded talin KO and kindlin KO cells expressing myc-Rac1 Q61L and treated with 5 mM Mn^{2+} 20 min after plating (n = 3 independent repeats; >250 cells/condition). Error bars indicate SD. **, P < 0.01; ***, P < 0.001; n.s., not significant.

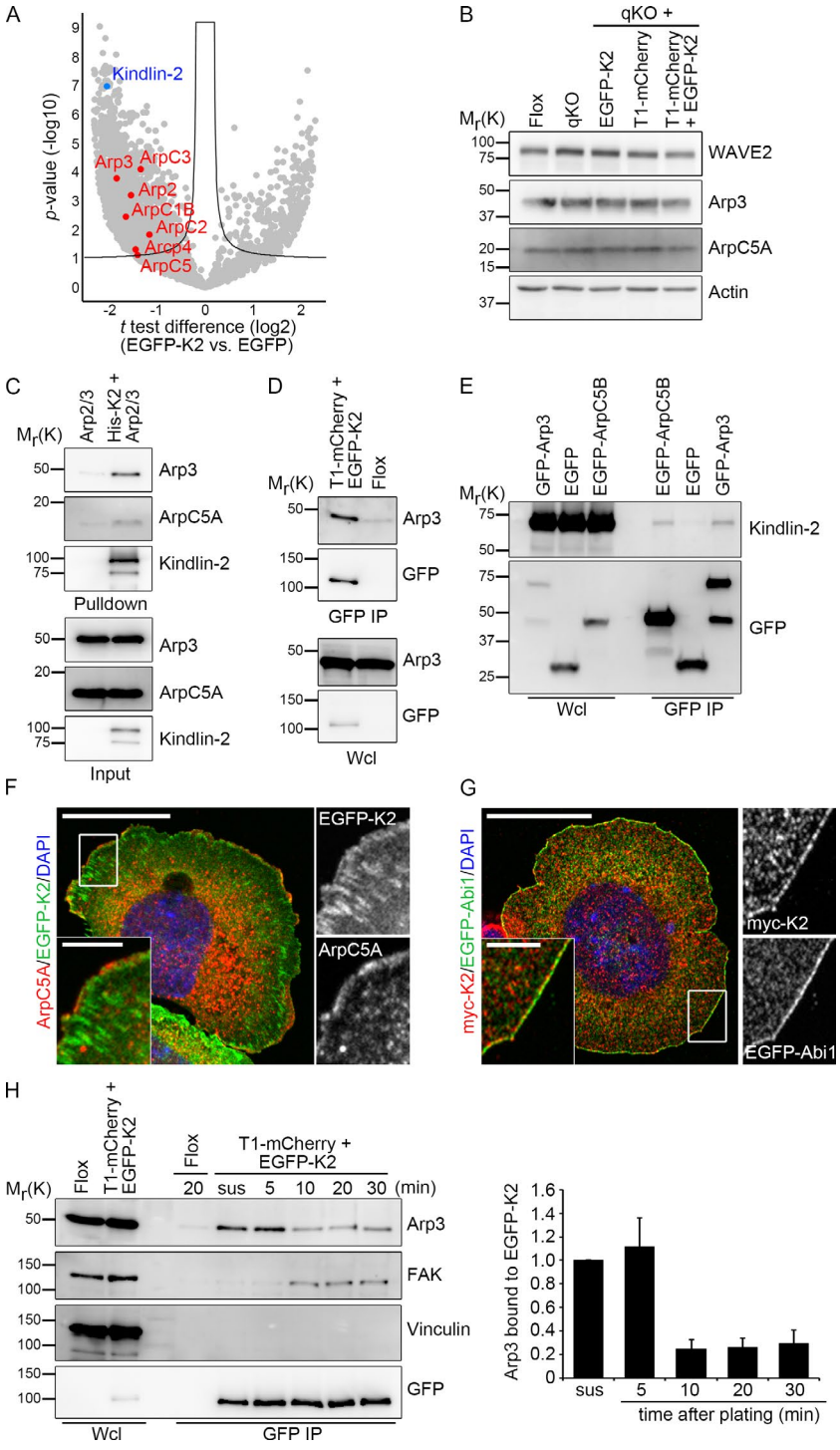

Figure 5. **Kindlin-2 binds and recruits the Arp2/3 complex to NAs.** (A) Volcano plot showing the *t* test difference of label-free MS quantification of protein LFQ intensity (log2) of EGFP-K2 versus GFP (control) immunoprecipitates plotted against the p-value (−log10) resulting from a one-sided *t* test (n = 3 independent experiments for both groups). Kindlin-2 is highlighted in blue and components of the Arp2/3 complex in red. The black curve indicates the significance cutoff (false discovery rate, 0.05; S0:1). (B) Protein levels of WAVE2 and Arp2/3 complex subunits in the indicated cell lines. (C) Ni-NTA pull down of His-tagged K2 incubated with purified Arp2/3 complex followed by Western blot for kindlin-2 and the Arp2/3 complex components Arp3 and ArpC5A. (D) Immunoprecipitation of GFP-kindlin-2 to determine binding to Arp3. (E) Coimmunoprecipitation of Arp2/3 complex subunits and endogenous kindlin-2 from Flox cells. (F) Immunostaining of ArpC5A (red) in T1-mCherry + EGFP-K2–expressing cells seeded on FN-coated coverslips for 20 min before immunostaining. DAPI was used to stain nuclei. Bars: (main) 20 µm; (insets) 4 µm. (G) Colocalization of myc-tagged kindlin-2 and EGFP-Abi1 in cells seeded on FN-coated coverslips for 12 min before fixation and immunostaining with antibodies against myc (red). DAPI was used to stain the nuclei. Bars: (main) 20 µm; (insets) 4 µm. (H) Western blot and densitometric analysis of GFP-immunoprecipitations from EGFP-K2 cells kept in suspension (sus) or seeded into FN-coated dishes for indicated time points (in minutes). Graph shows Arp3 binding to EGFP-K2 relative to suspension cells (n = 3 independent experiments). Error bars indicate SD.

membrane protrusions in Mn^{2+}-treated kindlin/talin–null cells solely reexpressing fluorescently tagged kindlin-2 (EGFP-K2), but not talin-1 (T1-mCherry), cells. This finding strongly suggests that kindlin-2 provides an essential function in addition to Rac1 activation that is not provided by talin-1. MS-based interactome screening revealed that kindlin-2 associates with the Arp2/3 complex, and coimmunostaining revealed colocalization of the two proteins in the smooth rim of the protruding membrane. The accumulation of a functional Arp2/3 complex at the periphery of spreading cells requires a direct association of kindlin-2 with the Arp2/3 complex. Consistently, disruption of this interaction by introducing point mutations into the F1 subdomain of kindlin-2 caused impaired membrane protrusion. The kindlin-2 structure (Kammerer et al., 2017; Li et al., 2017) supports the model in which arginine-100 and leucine-141 of kindlin-2 occupy the positions of lysine-38 and arginine-86 in FAK with respect to Arp2/3 binding. Of note, however, the experimental structure indicates that leucine-141 in kindlin-2 is partly masked by a flexible loop within the kindlin-2 F1 module that locates into a groove between the F1 and F3 modules. It is therefore possible that although the K2 RL/AA substitutions do not diminish binding to β1 integrin tails and ILK,

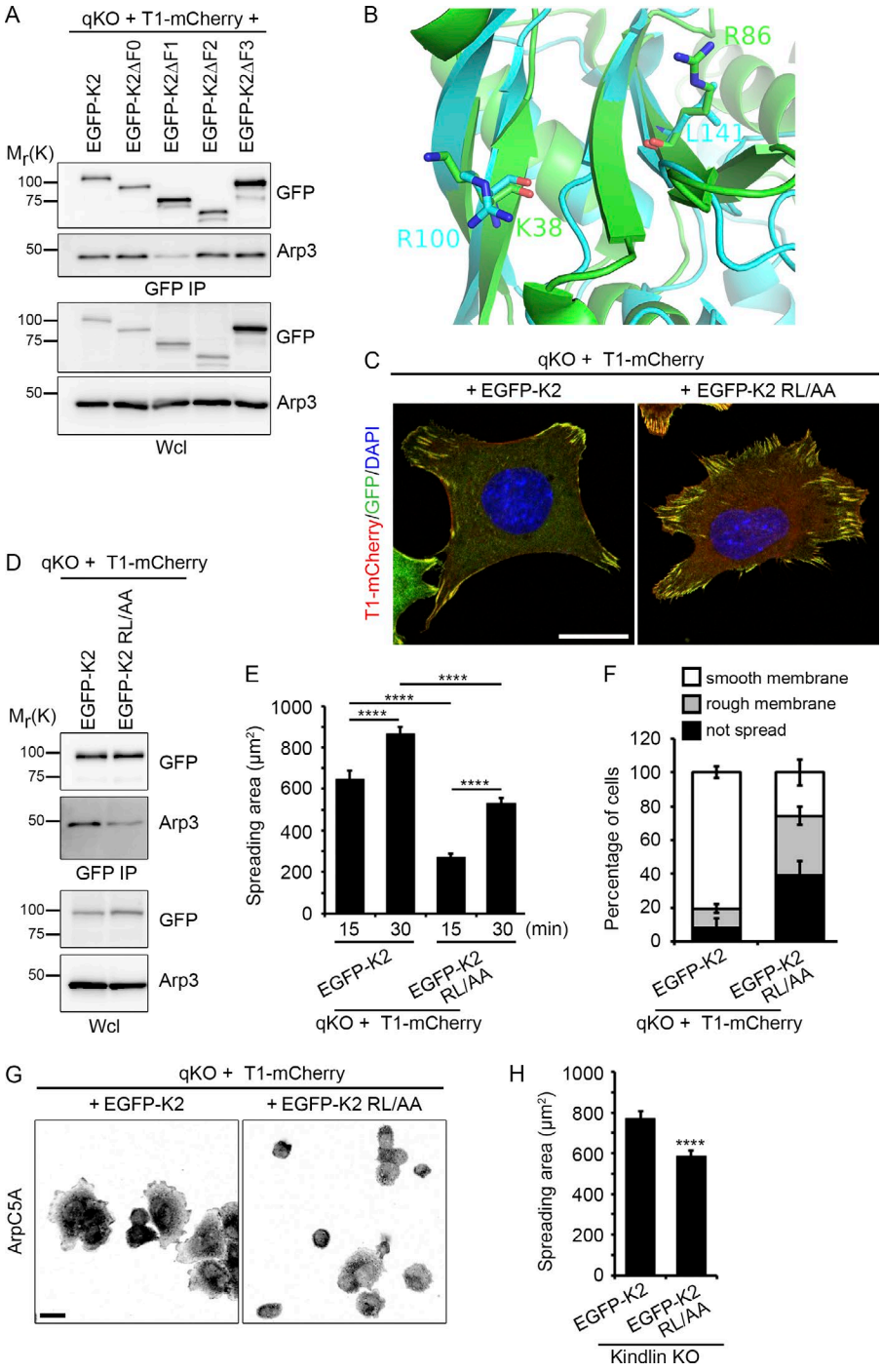

Figure 6. **Lamellipodia formation and cell spreading requires kindlin-2 binding to Arp2/3.** (A) Western blot of GFP immunoprecipitates from the indicated EGFP-K2 mutant–expressing cell lines kept in suspension. (B) Superposition of in silico–modeled murine kindlin-2 F1 domain (cyan) and the FERM domain of avian FAK (PDB: 4CYE, green). The residues K38 and R86 responsible for Arp2/3 interaction in the F1 domain of FAK correspond to residues R100 and L141 in the kindlin-2 F1 domain, as indicated. (C) Localization of T1-mCherry and EGFP-tagged kindlin-2 variants in T1-mCherry–expressing cells seeded for 2 h on FN. DAPI was used to stain nuclei. Bar, 20 µm. (D) Western blot of GFP immunoprecipitates from EGFP-K2 and EGFP-K2 RL/AA cell lines kept in suspension. (E) Quantification of spreading area of T1-mCherry cells expressing EGFP-K2 or EGFP-K2 RL/AA seeded for 15 min or 30 min on FN (n = 3 independent experiments; >90 cells/condition). Error bars indicate SEM. (F) Classification into nonspreading or spreading cells with smooth or rough membrane protrusions of T1-mCherry cells expressing either EGFP-K2 or EGFP-K2 RL/AA and seeded for 30 min on FN. (G) T1-mCherry cells expressing either EGFP-K2 or EGFP-K2 RL/AA were plated for 30 min on FN and then fixed and stained with antibodies against Arpc5A. Bar, 20 µm. (H) Quantification of spreading area of kindlin KO cells expressing either EGFP-K2 or EGFP-K2 RL/AA and seeded for 15 min onto FN (n = 2 independent experiments; 89 cells per condition). Error bars indicate SEM. ****, P < 0.0001.

they may destabilize the structure of the Arp2/3 interaction site and hence contribute to the decreased Arp2/3 binding observed in our experiments.

The kinetic interaction studies suggest that kindlin-2–Arp2/3 complexes are preassembled in the cytoplasm and recruited to nascent integrin adhesion sites where the kindlin-2–paxillin complex induces Rac1-WAVE–mediated activation of the Arp2/3 complex and the formation of smooth membrane protrusions. Although Arp2/3 levels were unchanged in T1-mCherry cells and Arp2/3 was previously shown to associate with vinculin and FAK (DeMali et al., 2002; Serrels et al., 2007; Chorev et al., 2014; Swaminathan et al., 2016), which both bind talin, the expression of Rac1 Q61L in T1-mCherry–expressing cells was not sufficient to induce cell spreading and Arp2/3–mediated formation of lamellipodia. It is therefore possible that talin-1 requires a signal (e.g., from kindlin-2 or kindlin-2–bound paxillin) to become functionalized and contribute to cell spreading with Arp2/3 bound to vinculin or FAK. Clearly, the cross talk between kindlin-2 and talin-1 during adhesion and initial spreading requires further cell biological and biochemical investigations.

It is conceivable that kindlin-2 contributes to cell spreading with additional signals or properties. Such a function of kindlin-2 could be clustering of active Rac1 GTPases at the plasma membrane. Phagocytosis was shown to require localized actin polymerization and membrane remodeling, which

critically depends on Rac1 activation and Rac1 recruitment to and clustering at the plasma membrane (Castellano et al., 2000). Kindlin-3 has recently been shown to induce clustering of ligand-occupied integrins (Ye et al., 2013). If this function is conserved among all kindlins, then kindlin-2 may aggregate Rac1, helping Rac1 to exceed a threshold required for inducing lamellipodia-driven cell spreading.

In summary, our findings suggest that the preassembled kindlin-2–Arp2/3 complex is recruited to early adhesion sites in the cell periphery to induce initial cell spreading. As soon as the task is accomplished, other FA proteins, including FAK and vinculin, control Arp2/3 activity. It is possible that each FA protein assembles a specific Arp2/3 complex equipped with specific properties (Chorev et al., 2014; Abella et al., 2016) that are determined by subunit isoform compositions and/or additional proteins present in the different complexes (Serrels et al., 2007; Chorev et al., 2014; Abella et al., 2016; Swaminathan et al., 2016). Future studies are required to define whether kindlin-2 associates with the canonical Arp2/3 complex or whether kindlin-2 assembles a specific Arp2/3 complex that initiates but does not complete cell spreading.

Materials and methods

Mouse strains and cell lines

The floxed kindlin-1 (*Fermt1*$^{flox/flox}$), kindlin-2 (*Fermt2*$^{flox/flox}$), and talin-1 (*Tln1*$^{flox/flox}$) mouse strains and the constitutive talin-2–null (*Tln2*$^{-/-}$) mouse strain (Nieswandt et al., 2007; Conti et al., 2009; Rognoni et al., 2014; Theodosiou et al., 2016) were intercrossed to isolate kidney fibroblasts from 21-d-old mice. Cells were immortalized by retroviral transduction of the SV40 large T antigen and then cloned (Flox cells). To obtain cells lacking talin-1 and talin-2 as well as kindlin-1 and kindlin-2 (qKO cells) the parental Flox cells with similar integrin surface profiles were adenovirally transduced with Cre. To generate talin and kindlin rescue cell lines, the qKO cells were retrovirally transduced with cDNAs coding for mCherry-tagged talin-1 (T1-mCherry) and EGFP-tagged full-length kindlin-2 (EGFP-K2) or EGFP-tagged kindlin-2 truncation mutants that lacked the F0 domain (EGFP-K2ΔF0), PH domain (EGFP-K2ΔPH), or both domains (EGFP-K2ΔF0ΔPH). Fibroblasts lacking either talins (talin KO) or kindlins (kindlin KO) and myc-kindlin-2 (myc-K2)–reexpressing cells have been described previously (Theodosiou et al., 2016). Vinculin flox (Vinc$^{fl/fl}$) and vinculin-deficient (Vinc$^{-/-}$) fibroblasts were a gift from C. Grashoff (Max Planck Institute of Biochemistry, Martinsried, Germany; Austen et al., 2015). For stably depleting FAK expression, qKO cells were retrovirally transduced with shRNA target sequences against mouse FAK (5′-GTCCAACTATGAAGTATTA-3′ and 5′-GGTCCAATGACAAGGTATA-3′). All cell lines were cultured in DMEM supplemented with 10% FCS and penicillin/streptomycin.

Transient and stable transfection/transduction

To generate stable cell lines, vesicular stomatitis virus G pseudotyped retroviral vectors were produced by transient transfection of 293T (human embryonic kidney) cells. 48 and 72 h after transfection of the viral packaging plasmids, viral particles were harvested by collecting the cell culture medium. After filtering the collected medium through 0.45-µm filters, viral particles were pelleted by ultracentrifugation at 20,300 rpm for 2 h with a SW 32 Ti rotor (Beckman Coulter) and resuspended in 45 µl cold Hank's balanced salt solution (14175046; Thermo Fisher Scientific) per 15-cm dish. Cells were transiently transfected with Lipofectamine 2000 (Thermo Fisher Scientific) according to the manufacturer's protocol.

Flow cytometry

Flow cytometry was performed with a FACSCanto TMII cytometer (BD Biosciences) equipped with FACS DiVa software (BD Biosciences). Fibroblasts were incubated with primary antibodies diluted in PBS + 1% BSA for 1 h on ice and washed with cold PBS + 1% BSA before incubation with the secondary antibody for 45 min on ice. Data analysis was performed with the FlowJo program (version 9.4.10).

Antibodies and inhibitors

The following antibodies or molecular probes were used at indicated concentrations for Western blot, immunofluorescence (IF), or flow cytometry (FACS): rabbit anti–kindlin-1 (homemade; Ussar et al., 2008) Western blot: 1:5,000; mouse anti–kindlin-2 (MAB2617; Millipore) Western blot: 1:1,000; mouse anti-talin (8D4; Sigma) Western blot: 1:1,000; mouse anti–talin-1 (ab57758; Abcam) Western blot: 1:2,000; mouse anti–talin-2 (ab105458; Abcam) Western blot: 1:2,000; mouse anti-paxillin (610051; BD Transduction Laboratories) Western blot: 1:1,000; rabbit anti-actin (A-2066; Sigma) Western blot: 1:1,000; mouse anti-Arp3 (A5979; Sigma) Western blot: 1:1,000; mouse anti-ArpC5 (Olazabal et al., 2002) Western blot: 1:10, IF 1:2; hamster anti–integrin β1-488 (102211; BioLegend) FACS: 1:200; rat anti–integrin β1 (MAB1997; Chemicon) FACS: 1:400; rabbit anti–integrin β1 (homemade; Azimifar et al., 2012) IF: 1:400, hamster anti–integrin β3-biotin (553345; PharMingen) FACS: 1:200; rat anti–integrin α5-biotin (557446; PharMingen) FACS: 1:200; rat anti–integrin αv-biotin (551380; PharMingen) FACS: 1:200; rat IgG2a isotype control (13-4321; eBioscience) FACS: 1:200; rabbit anti-GFP (A11122; Invitrogen) Western blot: 1:2,000; rabbit anti-Cherry (PM005; MBL International) Western blot: 1:1,000; mouse anti-myc (4A6; Millipore) Western blot: 1:1,000, IF 1:300; mouse anti–Rac1 (R56220; BD Biosciences) Western blot: 1:1,000; and rabbit anti-WAVE2 (3659; Cell Signaling) Western blot: 1:1,000.

The following secondary antibodies were used: goat anti–rabbit Alexa Fluor 488 (A11008), goat anti–mouse Alexa Fluor 488 (A11029), goat anti–rat Alexa Fluor 488 (A11006), goat anti–mouse Alexa Fluor 546 (A11003), donkey anti–mouse Alexa Fluor 647 (A31571), goat anti–rabbit Alexa Fluor 647 (A21244; all from Thermo Fisher Scientific) FACS: 1:500, IF: 1:500; streptavidin-Cy5 (016170084) FACS: 1:400; goat anti–rat HRP (712035150; both from Dianova) Western blot: 1:10,000, donkey anti–rabbit Cy3 (711-165-152; Jackson ImmunoResearch) IF: 1:500, goat anti–mouse HRP (172-1011), and goat anti–rabbit HRP (172-1019; both from Bio-Rad) Western blot: 1:10,000.

Phalloidin–Alexa Fluor 647 (A22287; Thermo Fisher Scientific) and DAPI (Sigma) were used to stain F-actin and nuclei, respectively. The Arp2/3 complex inhibitors CK-666 (SML0006; Sigma) and CK-869 (C9125; Sigma) were dissolved in dimethyl sulfoxide at 50 mg/ml.

Plasmids, constructs, and expression and purification of recombinant proteins

Mouse *kindlin-2* complementary DNAs (full length: amino acids 1–680, K2ΔF0: deletion of amino acids 1–91, K2ΔF1: deletion of amino acids 96–272, K2ΔF2: deletion of amino acids 271–559, K2ΔF3: deletion of amino acids 571–680, K2ΔPH: deletion of amino acids 381–476, K2ΔF0ΔPH: deletions of amino acids 1–91 and 381–476, and K2 RL/AA, in which R100 and L141 were substituted with alanine) were cloned into pEGFP-C1 vector (Clontech) using XhoI and BamHI sites. For retrovirus-mediated expression, cDNAs of EGFP-K2, EGFP-K2ΔF0, EGFP-K2ΔF1, EGFP-K2ΔF2, EGFP-K2ΔF3, EGFP-K2ΔPH, EGFP-K2ΔF0ΔPH, and EGFP-K2 RL/AA were inserted between NheI and BamHI sites of the pRetroQ-AcGFP-C1 (Clontech) vector. Stable expression of myc-Kindlin2 cDNA was achieved with

the sleeping beauty transposase system using ITR-Puro (+) plasmid containing the mouse kindlin-2 cDNA. Myc-tagged Rac1 Q61L was cloned into the retroviral vector pCLMFG to generate stable cell lines. EGFP-tagged variants of Abi1 and the Arp2/3 complex subunit ArpC5B were as described previously (Lai et al., 2008). Constructs of murine paxillin (full length: amino acids 1–557) and kindlin-2 (full length: amino acids 1–680, K2 F0: amino acids 1–97, K2 PH: amino acids 386–496, K2ΔPH: deletion of amino acids 372–500, K2ΔF0ΔPH: deletions of amino acids 1–97 and 372–500 and K2 F0-PH: amino acids 1–97 and 386–496 fused by a flexible linker [SGGGGTSGGGG]) were cloned into the AgeI–XhoI site of pCoofy17 (Max Planck Institute of Biochemistry core facility), yielding proteins N-terminally tagged with a 10× histidine tag followed by a SUMO3 tag. Production of recombinant proteins in *Escherichia coli Rosetta* cells (Millipore) was induced by addition of IPTG to a final concentration of 0.2 mM at 18°C for 24 h. After cell lysis and clarification of the supernatant, the proteins were purified by Ni-NTA affinity chromatography (Qiagen). Eluate fractions containing the protein of interest were pooled, cleaved with SenP2 protease, and subsequently purified by size exclusion chromatography (Superdex 200 16/60; GE Healthcare).

The Arp2/3 complex was affinity purified from pig brain as described previously (Block et al., 2012). In brief, the brain was homogenized with a blender in the presence of a fivefold excess (vol/vol) of ice-cold extraction buffer containing 20 mM Tris-HCl, pH 7.5, 25 mM KCl, 2 mM DTT, 1 mM $MgCl_2$, 0.5 mM EDTA, and 0.1 mM ATP and the homogenate centrifuged at 20,000 *g* for 45 min. The cleared supernatant was loaded on a GST-WAVE1-VCA (amino acids 492–559) glutathione Sepharose column, and after extensive washing of the column with extraction buffer, the remaining non–Arp2/3 proteins were eluted by 0.2 M KCl in extraction buffer. The Arp2/3 complex was subsequently eluted with 0.2 M $MgCl_2$ in extraction buffer and further purified by size exclusion chromatography using an Äkta Purifier System equipped with a HiLoad 26/600 Superdex 200 column (GE Healthcare) equilibrated with elution buffer. Fractions containing the Arp2/3 complex were pooled, dialyzed against a storage buffer (150 mM KCl, 1 mM DTT, 55% glycerol, and 20 mM Hepes, pH 7.4), and stored at −20°C.

Chemical cross-linking and MS of the kindlin-2–paxillin complex

The kindlin-2–paxillin complex was purified on a size exclusion column (SEC650; Bio-Rad) equilibrated with XL buffer (25 mM Hepes, pH 8, 300 mM NaCl, 5% glycerol, 0.05% Tween 20, 1 mM tris[2-carboxyethyl]phosphine [TCEP], and 10 µM $ZnCl_2$). The used fraction showed a 1:1 stoichiometry of kindlin-2 and paxillin and a concentration of 60 µg/ml. This solution was supplemented with 10 µM of isotopically light (d0)– and heavy (d12)–labeled bissulfosuccinimidyl suberate cross-linker (Creative Molecules Inc.) and allowed to react on ice for 18 h before stopping the cross-linking reaction with 5 mM ammonium bicarbonate. Cross-linked proteins were enzymatically digested, and cross-linked peptides were identified by tandem MS as reported previously (Herzog et al., 2012). In brief, cross-linked proteins were denatured by adding two sample volumes of 8 M urea and reduced by incubating with 5 mM TCEP (Thermo Fisher Scientific) at 35°C for 15 min. Proteins were alkylated with 10 mM iodoacetamide (Sigma-Aldrich) for 35 min at RT in the dark. Proteins were proteolytically digested by adding lysyl endopeptidase (1/50 [wt/wt]; Wako) for 2 h at 35°C followed by the addition of trypsin (1/50 [wt/wt]; Promega) overnight at a final concentration of 1 M urea. Proteolysis was stopped by the addition of 1% (vol/vol) trifluoroacetic acid. Acidified peptides were purified by reversed-phase chromatography on C18 columns (Sep-Pak, Waters). Eluates were dried and reconstituted in 20 µl of mobile phase (water/acetonitrile/trifluoroacetic acid, 75:25:0.1) and cross-linked peptides were enriched on a Superdex Peptide PC 3.2/30 column (GE Healthcare) at a flow rate of 25 µl/min. Fractions of the cross-linked peptides were dried and reconstituted in 20 µl 2% acetonitrile and 0.2% formic acid and analyzed by liquid chromatography coupled to tandem MS using a LTQ Orbitrap Elite (Thermo Fisher Scientific) instrument. The cross-link fragment ion spectra were searched and the peptides identified by the open-source software xQuest (Walzthoeni et al., 2012). False discovery rates calculated by xProphet were ≤0.05, and results were filtered according to the following parameters: delta score ≤0.85, MS1 tolerance window of −4 to 4 ppm, and score >22.

Analytical ultracentrifugation

To qualitatively determine the binding of different kindlin-2 constructs to paxillin, the proteins of interest were labeled using Atto520-NHS-ester (ATTOTec) according to the manufacturer's instructions. The measurements were conducted using an analytical Optima XL-I centrifuge (Beckman-Coulter) at 14°C and 50,000 rpm/201,600 *g*, and sedimentation data were recorded at the wavelength of maximum absorption of the dye. The data were analyzed using SedFit (Schuck, 2000) in continuous sedimentation coefficient distribution mode.

ITC

Quantitative ITC measurements were conducted using a PeaqITC instrument (Malvern) at a constant jacket temperature of 14°C. Proteins were rebuffered in 20 mM Tris, pH 7.5, 200 mM NaCl, 1 mM TCEP, and 10 µM $ZnCl_2$. 12 × 3 µl of the respective kindlin-2 construct was injected into the measurement cell containing paxillin. To show the Zn^{2+} dependence of the interaction, 5 mM EDTA was added to the sample cell. All data were analyzed using MicroCal PeaqITC Analysis software.

Modeling of the kindlin-2 F1 structure

A kindlin-2 structural model was generated by I-tasser (Roy et al., 2010) using the talin-head FERM domain (Protein Data Bank [PDB]: 3IVF; Elliott et al., 2010) as search model. A version of the kindlin-2 F1 domain structure obtained by this approach was aligned to a structure of avian FAK (PDB: 4CYE) using PyMol (Molecular Graphics System, Version 1.6; Schrodinger, LLC). The obtained structural root mean square deviations were 2.259 Å for one molecule in the asymmetric unit and 2.106 Å for the second molecule in the asymmetric unit of 4CYE, respectively.

Immunostaining

For immunostaining, cells were cultured on plastic ibidi µ-Slides (80826) or glass coverslips coated with 10 µg/ml FN (Calbiochem). Cells were routinely fixed with 4% PFA (wt/vol) in PBS (180 mM NaCl, 3.5 mM KCl, 10 mM Na_2HPO_4, and 1.8 mM $K_2H_2PO_4$) for 10 min at RT and permeabilized for 10 min with 0.1% Triton X-100/PBS on ice. Background signals were blocked by incubating cells for 1 h at RT in 3% BSA/PBS. Subsequently, they were incubated in the dark with primary and secondary antibodies diluted in 3% BSA/PBS, stained with DAPI, and mounted with Elvanol. Fluorescent images were acquired with a LSM 780 confocal microscope (Zeiss) equipped with 100×/NA 1.46 and 40×/NA 1.4 oil objectives and operated by Zen software (version 2.1; Zeiss). Image acquisition was performed at ambient temperature. Images were processed and analyzed with ImageJ (National Institutes of Health) or Photoshop (Adobe).

Immunoprecipitations and pull-down assays

For immunoprecipitation of paxillin, cells were lysed in β1 lysis buffer (50 mM Tris-HCl, pH 8.0, 150 mM NaCl, 1% Triton X-100, 0.05% sodium deoxycholate, and 10 mM EDTA) and incubated with paxillin antibodies for 2 h at 4°C while rotating. Subsequently, lysates were

incubated with 50 µl protein A/G Plus Agarose (Santa Cruz Biotechnology) for 2 h at 4°C. After repeated washes with lysis buffer, proteins were eluted from the beads using Laemmli buffer, separated on a 10% SDS-PAGE, and analyzed by Western blotting.

For immunoprecipitation of GFP-tagged proteins, cells were lysed in M-PER (78501; Thermo Fisher Scientific) or β1 lysis buffer (50 mM Tris-HCl, pH 8.0, 150 mM NaCl, 1% Triton X-100, 0.05% sodium deoxycholate, and 10 mM EDTA) and proteins were immunoprecipitated using the µMACS GFP Isolation kit (130-091-288; Miltenyi Biotec) for 20 min on ice following the manufacturer's protocol.

For the Ni pull down, 10 µg recombinant His–kindlin-2 was bound to 30 µl Ni Sepharose (GE Healthcare) in 0.5 ml M-PER buffer (78501; Thermo Fisher Scientific) for 1–2 h at 4°C under rotation. After several washes, the beads were incubated with 12.5 µg purified Arp2/3 complex in 0.5 ml M-PER buffer containing 80 mM imidazole for 2 h at 4°C under rotation. After three washes with M-PER buffer containing 80 mM imidazole, proteins were eluted by boiling the samples for 7 min at 95°C in Laemmli sample buffer and analyzed by Western blot using antibodies against kindlin-2, ArpC5A, and Arp3.

Kindlin-2 interactome analysis by MS

qKO cells expressing T1-mCherry and EGFP-K2 or EGFP were kept in suspension for 20 min at 37°C. Cells were washed in PBS and lysed in M-PER before incubation with 50 µl magnetic beads coupled to monoclonal mouse anti-GFP antibody (130-091-288; Miltenyi Biotec) for 20 min on ice. Cell lysates were added to magnetic columns and washed four times with M-PER buffer and once with wash buffer II containing 20 mM Tris, pH 7.5 (Miltenyi Biotec). Purified proteins were predigested on-column by adding 25 µl 2 M urea in 50 mM Tris, pH 7.5, 1 mM dithiothreitol, and 150 ng Trypsin for 30 min at RT and eluted by adding two times 50 µl 2 M urea in 50 mM Tris, pH 7.5, and 5 mM chloroacetamide. After overnight incubation at RT, the digestion was stopped by adding 1 µl trifluoroacetic acid, and the peptides were purified using C18 stage tips (Rappsilber et al., 2007). The samples were loaded on a 15-cm column packed with 1.9-µm C18 beads (Dr Maisch GmbH) via the nanoLC-1200 autosampler (Thermo Fisher Scientific) and sprayed directly into Q Exactive HF mass spectrometer (Thermo Fisher Scientific). The mass spectrometer was operated in data-dependent mode with the Top N acquisition method. The raw data were processed using the MaxQuant computational platform (Cox and Mann, 2008). The peak lists generated were searched with initial precursor and fragment mass tolerance of 7 and 20 ppm, respectively. Carbamidomethylation of cysteine was used as static modification, and oxidation of methionine and protein N-terminal acetylation was used as variable modification. The peak lists were searched against the UniProt Mouse database, and the proteins and peptides were filtered at a 1% false discovery rate. Proteins were quantified using the MaxLFQ algorithm in MaxQuant (Cox et al., 2014).

Spreading and adhesion assays

Cells were grown to 70% confluence followed by overnight incubation in DMEM containing 0.2% FCS. After detaching with trypsin/EDTA, cells were serum starved for 1 h in adhesion assay medium (10 mM Hepes, pH 7.4, 137 mM NaCl, 1 mM $MgCl_2$, 1 mM $CaCl_2$, 2.7 mM KCl, 4.5 g/l glucose, and 3% BSA [wt/vol]) in bacterial dishes. Flat-bottom 96-well plates were coated with 10 µg/ml FN (Calbiochem), 1 µg/ml VN (07180; StemCell), or 5% BSA diluted in PBS. Cells were then plated (40,000 per well) in adhesion buffer supplemented with 8% FCS and 5 mM Mn^{2+} where indicated and incubated for 30 min at 37°C. After vigorous washing with PBS, cell attachment was measured by fixing and staining with crystal violet staining (0.1% in 20% methanol) in an absorbance plate reader at a wavelength of 570 nm.

For cell spreading, 40,000 cells were seeded on 10 µg/ml FN or PLL (0.01% wt/vol)–coated coverslips, cultured for the indicated time points at 37°C, fixed with 4% PFA (wt/vol) in PBS, and stained with phalloidin–Alexa Fluor 647 and DAPI. At least 10 images were taken using a Zeiss AxioImager Z1 microscope equipped with a 63×/NA 1.4 oil objective, and cell spreading area was measured using AxioVision software (release 4.8.2; Zeiss).

For phase contrast analysis of spreading cells, 50,000 cells were seeded on 10 µg/ml FN-coated six-well plates and cultured at 37°C. Living cells were imaged with an EVOS FL Auto Cell Imaging System (Thermo Fisher Scientific) equipped with an EVOS Onstage Incubator using a 20×/NA 0.4 objective at 37°C. Images were analyzed with ImageJ (National Institutes of Health).

Rac1 GTPase activity

Cells were grown in DMEM containing 0.2% FCS overnight, detached with trypsin–EDTA, and starved for 1 h in adhesion assay medium in bacterial dishes. Cells were then plated on 10 µg/ml FN–coated dishes in serum-free medium containing 5 mM Mn^{2+}. Cell lysis and active Rac1-GTPase pull-down was performed using the active Rac1 Pull-Down and Detection kit (16118; Thermo Fisher Scientific) according to manufacturer's instructions. The active Rac1 signal was normalized to the total protein level of the GTPase.

Statistical analysis

All experiments were repeated at least three times (as indicated in figure legends). Statistical significance (*, $P < 0.05$; **, $P < 0.01$; ***, $P < 0.001$; ****, $P < 0.0001$; n.s., not significant) was determined by two-tailed unpaired *t* test and performed with Prism (GraphPad).

Online supplemental material

Fig. S1 shows the intra- and interprotein cross-links between kindlin-2 and paxillin as well as the Zn^{2+} dependence of kindlin–paxillin binding. Fig. S2 shows the FA recruitment of different kindlin-2 deletions. Fig. S3 displays the kindlin-2–Arp2/3 interaction in the absence of either vinculin or FAK. Fig. S4 shows the spreading behavior of kindlin-2 RL/AA–expressing cells. Supplemental data 1 is a detailed overview of the high-confidence lysine–lysine cross-links of the kindlin-2–paxillin complex.

Acknowledgments

We thank Hildegard Reiter for expert technical help and Carsten Grashoff for providing the vinculin KO cells.

This work was supported by the Deutsche Forschungsgemeinschaft (SFB 914, project A05), the European Research Council (grant 322652), and the Max Planck Society (R. Fässler).

The authors declare no competing financial interests.

Author contributions: R.T. Böttcher and M. Veldeers carried out the experiments and analyzed the data. P. Rombaut and F. Herzog performed the cross-linking proteomics. R. Zent and M. Theodosiou generated the flox and qKO fibroblasts. J. Faix, T.E. Stradal, and K. Rottner provided tools and analyzed the data. R.T. Böttcher and R. Fässler initiated, supervised, and designed the present study and wrote the manuscript. The manuscript was read and approved by all authors.

Submitted: 27 January 2017
Revised: 14 July 2017
Accepted: 8 August 2017

References

Abella, J.V.G., C. Galloni, J. Pernier, D.J. Barry, S. Kjær, M.-F. Carlier, and M. Way. 2016. Isoform diversity in the Arp2/3 complex determines actin filament dynamics. *Nat. Cell Biol.* 18:76–86. http://dx.doi.org/10.1038/ncb3286

Austen, K., P. Ringer, A. Mehlich, A. Chrostek-Grashoff, C. Kluger, C. Klingner, B. Sabass, R. Zent, M. Rief, and C. Grashoff. 2015. Extracellular rigidity sensing by talin isoform-specific mechanical linkages. *Nat. Cell Biol.* 17:1597–1606. http://dx.doi.org/10.1038/ncb3268

Azimifar, S.B., R.T. Böttcher, S. Zanivan, C. Grashoff, M. Krüger, K.R. Legate, M. Mann, and R. Fässler. 2012. Induction of membrane circular dorsal ruffles requires co-signalling of integrin-ILK-complex and EGF receptor. *J. Cell Sci.* 125:435–448. http://dx.doi.org/10.1242/jcs.091652

Block, J., D. Breitsprecher, S. Kühn, M. Winterhoff, F. Kage, R. Geffers, P. Duwe, J.L. Rohn, B. Baum, C. Brakebusch, et al. 2012. FMNL2 drives actin-based protrusion and migration downstream of Cdc42. *Curr. Biol.* 22:1005–1012. http://dx.doi.org/10.1016/j.cub.2012.03.064

Brami-Cherrier, K., N. Gervasi, D. Arsenieva, K. Walkiewicz, M.-C. Boutterin, A. Ortega, P.G. Leonard, B. Seantier, L. Gasmi, T. Bouceba, et al. 2014. FAK dimerization controls its kinase-dependent functions at focal adhesions. *EMBO J.* 33:356–370. http://dx.doi.org/10.1002/embj.201386399

Bugyi, B., and M.-F. Carlier. 2010. Control of actin filament treadmilling in cell motility. *Annu. Rev. Biophys.* 39:449–470. http://dx.doi.org/10.1146/annurev-biophys-051309-103849

Castellano, F., P. Montcourrier, and P. Chavrier. 2000. Membrane recruitment of Rac1 triggers phagocytosis. *J. Cell Sci.* 113:2955–2961.

Chorev, D.S., O. Moscovitz, B. Geiger, and M. Sharon. 2014. Regulation of focal adhesion formation by a vinculin-Arp2/3 hybrid complex. *Nat. Commun.* 5:3758. http://dx.doi.org/10.1038/ncomms4758

Cluzel, C., F. Saltel, J. Lussi, F. Paulhe, B.A. Imhof, and B. Wehrle-Haller. 2005. The mechanisms and dynamics of (α)v(β)3 integrin clustering in living cells. *J. Cell Biol.* 171:383–392. http://dx.doi.org/10.1083/jcb.200503017

Conti, F.J., S.J. Monkley, M.R. Wood, D.R. Critchley, and U. Müller. 2009. Talin 1 and 2 are required for myoblast fusion, sarcomere assembly and the maintenance of myotendinous junctions. *Development.* 136:3597–3606. http://dx.doi.org/10.1242/dev.035857

Cox, J., and M. Mann. 2008. MaxQuant enables high peptide identification rates, individualized p.p.b.-range mass accuracies and proteome-wide protein quantification. *Nat. Biotechnol.* 26:1367–1372. http://dx.doi.org/10.1038/nbt.1511

Cox, J., M.Y. Hein, C.A. Luber, I. Paron, N. Nagaraj, and M. Mann. 2014. Accurate proteome-wide label-free quantification by delayed normalization and maximal peptide ratio extraction, termed MaxLFQ. *Mol. Cell. Proteomics.* 13:2513–2526. http://dx.doi.org/10.1074/mcp.M113.031591

DeMali, K.A., C.A. Barlow, and K. Burridge. 2002. Recruitment of the Arp2/3 complex to vinculin: Coupling membrane protrusion to matrix adhesion. *J. Cell Biol.* 159:881–891. http://dx.doi.org/10.1083/jcb.200206043

Devreotes, P., and A.R. Horwitz. 2015. Signaling networks that regulate cell migration. *Cold Spring Harb. Perspect. Biol.* 7:a005959. http://dx.doi.org/10.1101/cshperspect.a005959

Elliott, P.R., B.T. Goult, P.M. Kopp, N. Bate, J.G. Grossmann, G.C.K. Roberts, D.R. Critchley, and I.L. Barsukov. 2010. The Structure of the talin head reveals a novel extended conformation of the FERM domain. *Structure.* 18:1289–1299. http://dx.doi.org/10.1016/j.str.2010.07.011

Han, J., C.J. Lim, N. Watanabe, A. Soriani, B. Ratnikov, D.A. Calderwood, W. Puzon-McLaughlin, E.M. Lafuente, V.A. Boussiotis, S.J. Shattil, and M.H. Ginsberg. 2006. Reconstructing and deconstructing agonist-induced activation of integrin αIIbβ3. *Curr. Biol.* 16:1796–1806. http://dx.doi.org/10.1016/j.cub.2006.08.035

Herzog, F., A. Kahraman, D. Boehringer, R. Mak, A. Bracher, T. Walzthoeni, A. Leitner, M. Beck, F.-U. Hartl, N. Ban, et al. 2012. Structural probing of a protein phosphatase 2A network by chemical cross-linking and mass spectrometry. *Science.* 337:1348–1352. http://dx.doi.org/10.1126/science.1221483

Kammerer, P., J. Aretz, and R. Fässler. 2017. Lucky kindlin: A cloverleaf at the integrin tail. *Proc. Natl. Acad. Sci. USA*. 114:9234–9236. http://dx.doi.org/10.1073/pnas.1712471114

Lai, F.P.L., M. Szczodrak, J. Block, J. Faix, D. Breitsprecher, H.G. Mannherz, T.E.B. Stradal, G.A. Dunn, J.V. Small, and K. Rottner. 2008. Arp2/3 complex interactions and actin network turnover in lamellipodia. *EMBO J.* 27:982–992. http://dx.doi.org/10.1038/emboj.2008.34

Leitner, A., T. Walzthoeni, A. Kahraman, F. Herzog, O. Rinner, M. Beck, and R. Aebersold. 2010. Probing native protein structures by chemical cross-linking, mass spectrometry, and bioinformatics. *Mol. Cell. Proteomics.* 9:1634–1649. http://dx.doi.org/10.1074/mcp.R000001-MCP201

Li, H., Y. Deng, K. Sun, H. Yang, J. Liu, M. Wang, Z. Zhang, J. Lin, C. Wu, Z. Wei, and C. Yu. 2017. Structural basis of kindlin-mediated integrin recognition and activation. *Proc. Natl. Acad. Sci. USA.* 114:9349–9354. http://dx.doi.org/10.1073/pnas.1703064114

Machesky, L.M., S.J. Atkinson, C. Ampe, J. Vandekerckhove, and T.D. Pollard. 1994. Purification of a cortical complex containing two unconventional actins from Acanthamoeba by affinity chromatography on profilin-agarose. *J. Cell Biol.* 127:107–115. http://dx.doi.org/10.1083/jcb.127.1.107

Moser, M., B. Nieswandt, S. Ussar, M. Pozgajova, and R. Fässler. 2008. Kindlin-3 is essential for integrin activation and platelet aggregation. *Nat. Med.* 14:325–330. http://dx.doi.org/10.1038/nm1722

Mould, A.P., S.K. Akiyama, and M.J. Humphries. 1995. Regulation of integrin α 5 β 1-fibronectin interactions by divalent cations. Evidence for distinct classes of binding sites for Mn2+, Mg2+, and Ca2+. *J. Biol. Chem.* 270:26270–26277. http://dx.doi.org/10.1074/jbc.270.44.26270

Mullins, R.D., J.A. Heuser, and T.D. Pollard. 1998. The interaction of Arp2/3 complex with actin: nucleation, high affinity pointed end capping, and formation of branching networks of filaments. *Proc. Natl. Acad. Sci. USA.* 95:6181–6186. http://dx.doi.org/10.1073/pnas.95.11.6181

Nieswandt, B., M. Moser, I. Pleines, D. Varga-Szabo, S. Monkley, D. Critchley, and R. Fässler. 2007. Loss of talin1 in platelets abrogates integrin activation, platelet aggregation, and thrombus formation in vitro and in vivo. *J. Exp. Med.* 204:3113–3118. http://dx.doi.org/10.1084/jem.20071827

Nolen, B.J., N. Tomasevic, A. Russell, D.W. Pierce, Z. Jia, C.D. McCormick, J. Hartman, R. Sakowicz, and T.D. Pollard. 2009. Characterization of two classes of small molecule inhibitors of Arp2/3 complex. *Nature.* 460:1031–1034. http://dx.doi.org/10.1038/nature08231

Olazabal, I.M., E. Caron, R.C. May, K. Schilling, D.A. Knecht, and L.M. Machesky. 2002. Rho-kinase and myosin-II control phagocytic cup formation during CR, but not FcγR, phagocytosis. *Curr. Biol.* 12:1413–1418. http://dx.doi.org/10.1016/S0960-9822(02)01069-2

Petrie, R.J., A.D. Doyle, and K.M. Yamada. 2009. Random versus directionally persistent cell migration. *Nat. Rev. Mol. Cell Biol.* 10:538–549. http://dx.doi.org/10.1038/nrm2729

Pollard, T.D., and G.G. Borisy. 2003. Cellular motility driven by assembly and disassembly of actin filaments. *Cell.* 112:453–465. http://dx.doi.org/10.1016/S0092-8674(03)00120-X

Rappsilber, J., M. Mann, and Y. Ishihama. 2007. Protocol for micro-purification, enrichment, pre-fractionation and storage of peptides for proteomics using StageTips. *Nat. Protoc.* 2:1896–1906. http://dx.doi.org/10.1038/nprot.2007.261

Rognoni, E., M. Widmaier, M. Jakobson, R. Ruppert, S. Ussar, D. Katsougkri, R.T. Böttcher, J.E. Lai-Cheong, D.B. Rifkin, J.A. McGrath, and R. Fässler. 2014. Kindlin-1 controls Wnt and TGF-β availability to regulate cutaneous stem cell proliferation. *Nat. Med.* 20:350–359. http://dx.doi.org/10.1038/nm.3490

Rohatgi, R., L. Ma, H. Miki, M. Lopez, T. Kirchhausen, T. Takenawa, and M.W. Kirschner. 1999. The interaction between N-WASP and the Arp2/3 complex links Cdc42-dependent signals to actin assembly. *Cell.* 97:221–231. http://dx.doi.org/10.1016/S0092-8674(00)80732-1

Rouiller, I., X.-P. Xu, K.J. Amann, C. Egile, S. Nickell, D. Nicastro, R. Li, T.D. Pollard, N. Volkmann, and D. Hanein. 2008. The structural basis of actin filament branching by the Arp2/3 complex. *J. Cell Biol.* 180:887–895. http://dx.doi.org/10.1083/jcb.200709092

Roy, A., A. Kucukural, and Y. Zhang. 2010. I-TASSER: a unified platform for automated protein structure and function prediction. *Nat. Protoc.* 5:725–738. http://dx.doi.org/10.1038/nprot.2010.5

Schlaepfer, D.D., S.K. Mitra, and D. Ilic. 2004. Control of motile and invasive cell phenotypes by focal adhesion kinase. *Biochim. Biophys. Acta.* 1692:77–102. http://dx.doi.org/10.1016/j.bbamcr.2004.04.008

Schuck, P. 2000. Size-distribution analysis of macromolecules by sedimentation velocity ultracentrifugation and lamm equation modeling. *Biophys. J.* 78:1606–1619. http://dx.doi.org/10.1016/S0006-3495(00)76713-0

Serrels, B., A. Serrels, V.G. Brunton, M. Holt, G.W. McLean, C.H. Gray, G.E. Jones, and M.C. Frame. 2007. Focal adhesion kinase controls actin assembly via a FERM-mediated interaction with the Arp2/3 complex. *Nat. Cell Biol.* 9:1046–1056. http://dx.doi.org/10.1038/ncb1626

Suraneni, P., B. Rubinstein, J.R. Unruh, M. Durnin, D. Hanein, and R. Li. 2012. The Arp2/3 complex is required for lamellipodia extension and

directional fibroblast cell migration. *J. Cell Biol.* 197:239–251. http://dx.doi.org/10.1083/jcb.201112113

Suraneni, P., B. Fogelson, B. Rubinstein, P. Noguera, N. Volkmann, D. Hanein, A. Mogilner, and R. Li. 2015. A mechanism of leading-edge protrusion in the absence of Arp2/3 complex. *Mol. Biol. Cell.* 26:901–912. http://dx.doi.org/10.1091/mbc.E14-07-1250

Swaminathan, V., R.S. Fischer, and C.M. Waterman. 2016. The FAK-Arp2/3 interaction promotes leading edge advance and haptosensing by coupling nascent adhesions to lamellipodia actin. *Mol. Biol. Cell.* 27:1085–1100. http://dx.doi.org/10.1091/mbc.E15-08-0590

Takenawa, T., and S. Suetsugu. 2007. The WASP-WAVE protein network: Connecting the membrane to the cytoskeleton. *Nat. Rev. Mol. Cell Biol.* 8:37–48. http://dx.doi.org/10.1038/nrm2069

Theodosiou, M., M. Widmaier, R.T. Böttcher, E. Rognoni, M. Veelders, M. Bharadwaj, A. Lambacher, K. Austen, D.J. Müller, R. Zent, and R. Fässler. 2016. Kindlin-2 cooperates with talin to activate integrins and induces cell spreading by directly binding paxillin. *eLife.* 5:e10130. http://dx.doi.org/10.7554/eLife.10130

Ussar, S., M. Moser, M. Widmaier, E. Rognoni, C. Harrer, O. Genzel-Boroviczeny, and R. Fässler. 2008. Loss of Kindlin-1 causes skin atrophy and lethal neonatal intestinal epithelial dysfunction. *PLoS Genet.* 4:e1000289. http://dx.doi.org/10.1371/journal.pgen.1000289

Vicente-Manzanares, M., and A.R. Horwitz. 2011. Adhesion dynamics at a glance. *J. Cell Sci.* 124:3923–3927. http://dx.doi.org/10.1242/jcs.095653

Walzthoeni, T., M. Claassen, A. Leitner, F. Herzog, S. Bohn, F. Förster, M. Beck, and R. Aebersold. 2012. False discovery rate estimation for cross-linked peptides identified by mass spectrometry. *Nat. Methods.* 9:901–903. http://dx.doi.org/10.1038/nmeth.2103

Welch, M.D., A. Iwamatsu, and T.J. Mitchison. 1997. Actin polymerization is induced by Arp2/3 protein complex at the surface of *Listeria monocytogenes*. *Nature.* 385:265–269. http://dx.doi.org/10.1038/385265a0

Winter, D., A.V. Podtelejnikov, M. Mann, and R. Li. 1997. The complex containing actin-related proteins Arp2 and Arp3 is required for the motility and integrity of yeast actin patches. *Curr. Biol.* 7:519–529. http://dx.doi.org/10.1016/S0960-9822(06)00223-5

Winter, D., T. Lechler, and R. Li. 1999. Activation of the yeast Arp2/3 complex by Bee1p, a WASP-family protein. *Curr. Biol.* 9:501–504. http://dx.doi.org/10.1016/S0960-9822(99)80218-8

Ye, F., B.G. Petrich, P. Anekal, C.T. Lefort, A. Kasirer-Friede, S.J. Shattil, R. Ruppert, M. Moser, R. Fässler, and M.H. Ginsberg. 2013. The mechanism of kindlin-mediated activation of integrin αIIbβ3. *Curr. Biol.* 23:2288–2295. http://dx.doi.org/10.1016/j.cub.2013.09.050

Zhang, X., S.W. Moore, T. Iskratsch, and M.P. Sheetz. 2014. N-WASP-directed actin polymerization activates Cas phosphorylation and lamellipodium spreading. *J. Cell Sci.* 127:1394–1405. http://dx.doi.org/10.1242/jcs.134692

Böttcher et al., https://doi.org/10.1083/jcb.201701176

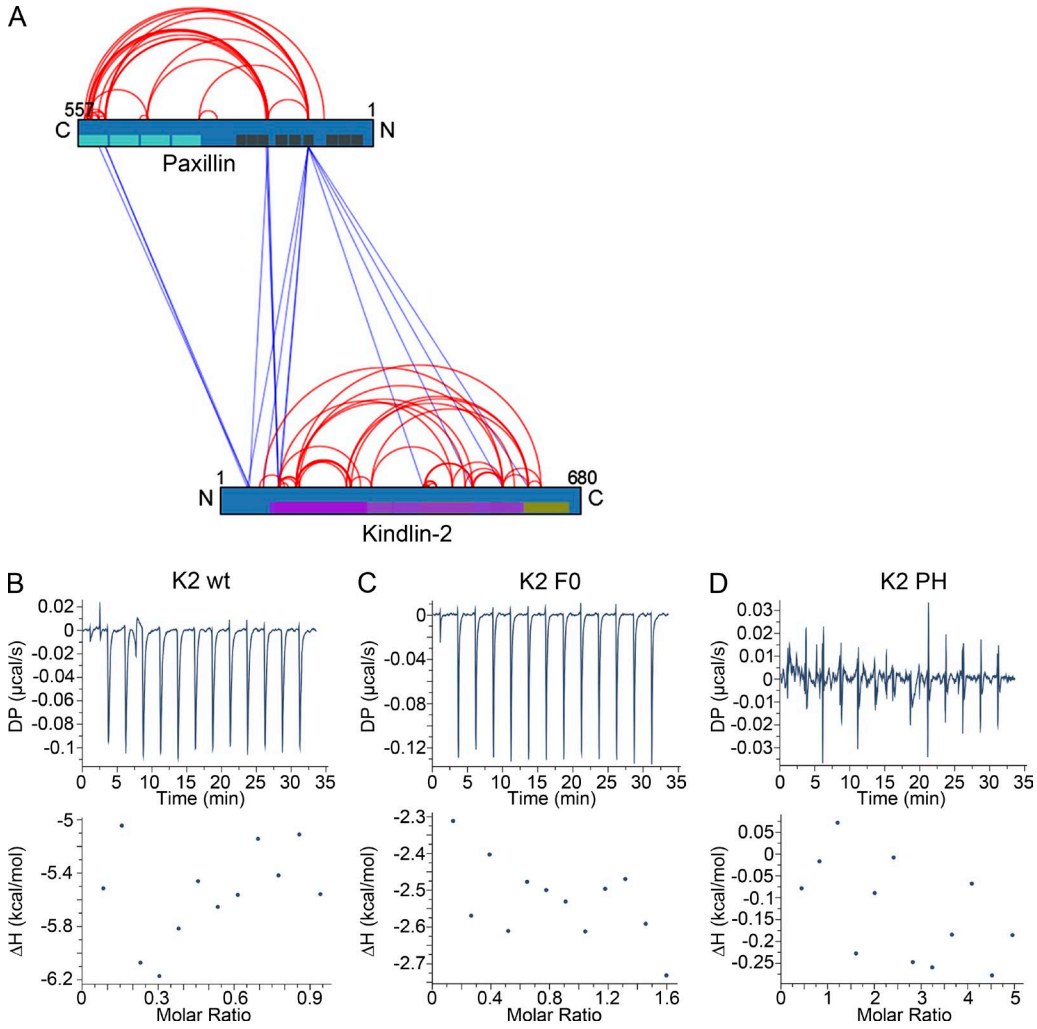

Figure S1. **Zn^{2+} dependence of kindlin–paxillin binding.** (A) Cross-link map of kindlin-2–paxillin with intraprotein cross-links in red and interprotein cross-links in blue. (B–D) ITC measurements of full-length paxillin bound to recombinant K2 wild type (B), K2 F0 (C), and K2 PH (D) in the presence of 5 mM EDTA. C, C terminus; DP, differential power; N, N terminus.

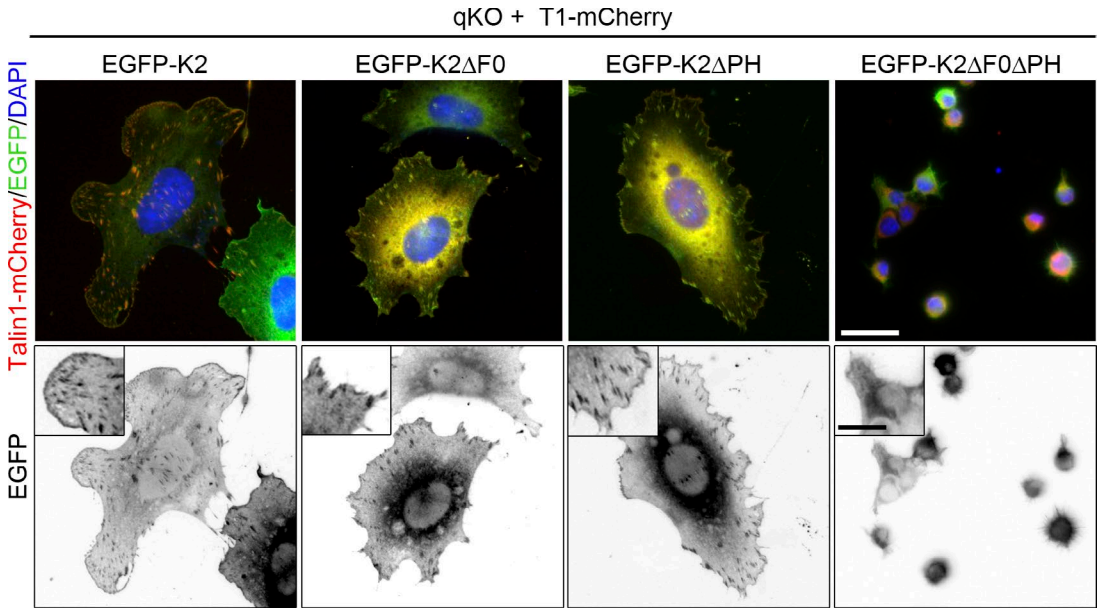

Figure S2. **FA recruitment of kindlin-2 deletions.** Localization of T1-mCherry and EGFP-tagged kindlin-2 mutants in T1-mCherry–expressing qKO cells seeded for 2 h on FN. DAPI was used to stain nuclei. Bar: 20 µm; (inset) 10 µm.

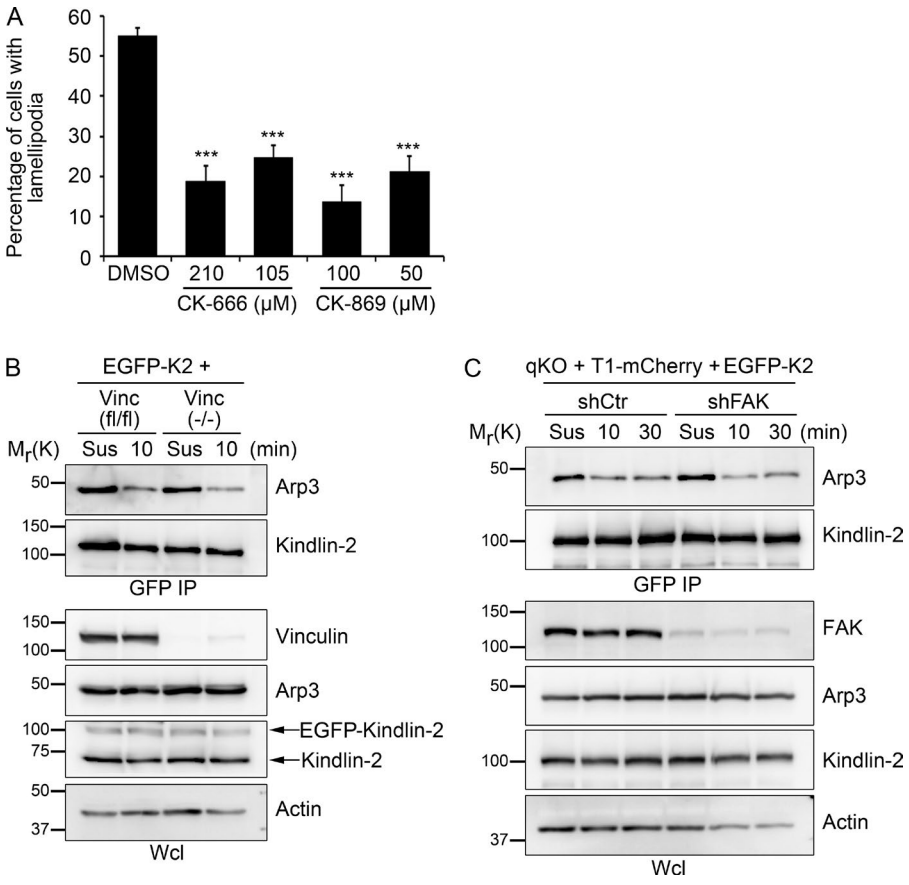

Figure S3. **Kindlin-2–Arp2/3 interaction.** (A) Quantification of membrane protrusions of FN-seeded EGFP-K2 cells 30 min after plating treated with 5 mM Mn^{2+} and either DMSO or the Arp2/3 inhibitors CS-666 and CD-869 (n = 6 independent repeats; >100 cells/condition; error bars indicate SEM, t test significances are calculated relative to DMSO-treated cells). ***, $P < 0.001$. (B and C) Western blot analysis of GFP-K2 immunoprecipitations from vinculin flox ($Vinc^{fl/fl}$) and knockout ($Vinc^{-/-}$) fibroblasts (B) or FAK-depleted cells (shFAK; C) kept in suspension (Sus) or seeded for the indicated times (in minutes) on FN.

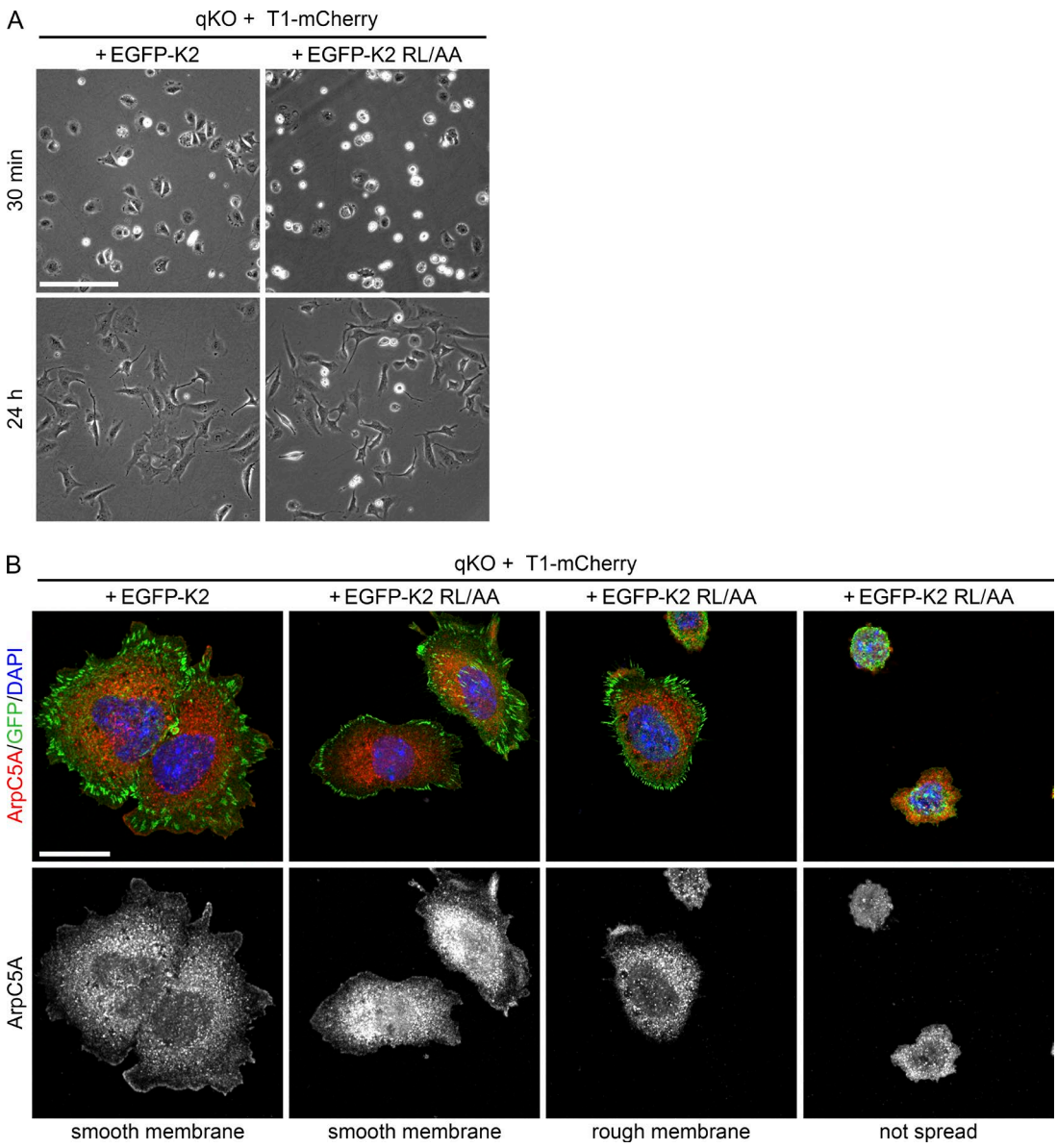

Figure S4. **Kindlin-2 RL/AA–expressing cells.** (A) Bright-field images of the indicated cell lines 30 min and 24 h after seeding on FN. Bar, 200 µm. (B) Localization of ArpC5A and EGFP-tagged kindlin-2 and kindlin-2 RL/AA in T1-mCherry cells seeded for 30 on FN. Note the different cell morphologies with smooth membranes to rough or spiky membrane protrusions and nonspreading cells. DAPI was used to stain nuclei. Bar, 20 µm.

Provided online is supplemental data in Excel, showing high-confidence lysine–lysine cross-links of the kindlin-2–paxillin complex.